TRANSLATIONAL EFFICIENCY OF HERPESVIRUS MESSENGER RIBONUCLEIC ACIDS

by

Eric S. Pringle

Submitted in partial fulfilment of the requirements
for the degree of Doctor of Philosophy

at

Dalhousie University
Halifax, Nova Scotia
March 2019

Table of Contents

List of Tables ..... **vi**

List of Figures ..... **vii**

Abstract ..... **ix**

List of Abbreviations Used ..... **x**

Acknowledgements ..... **xv**

Chapter One – Introduction **1**

1.1 Overview 1

1.2 Kaposi's Sarcoma-associated Herpesvirus 2

1.2.1 Herpesviridae 2

1.2.2 Discovery of KSHV in AIDS-related Malignancies 3

1.2.3. KSHV Replication 4

1.2.3.1 KSHV Latency 4

1.2.3.2 Reactivation from Latency and Lytic Replication 7

1.2.4 KSHV Promotes Tumourigenesis by Paracrine Action 10

1.3 eIF4F-dependent Translation Initiation 12

1.3.1 eIF4F-dependent Translation Initiation 12

1.3.2 Integrated Stress Response and eIF2 Phosphorylation 13

1.3.3 Herpesvirus mRNA Processing 14

1.4 Mechanistic Target of Rapamycin (mTOR) 16

1.4.1 mTOR Complex 1 (mTORC1) 16

1.4.2 Regulation of Translation Initiation by mTORC1 18

1.4.3 5' Tract of Oligopyrimidines (TOP) mRNA 20

1.4.4 Regulation of Autophagy by mTORC1 20

1.4.5 Regulation of mTORC1 by Herpesviruses 22

1.5 Non-eIF4F Mechanisms of Translation Initiation 25

1.5.1 Internal Ribosomal Entry Sites 25

1.5.2 eIF4G2-dependent Translation 26

1.5.3 Translation during Hypoxia 27

1.5.3.1 eIF4E2-dependent Translation 27

1.5.3.2 Hypoxia Response Elements in KSHV 29

1.5.4 eIF4E3 Translation during MNK1 Activation 29
1.5.5 Pioneer Translation 30
1.5.6 eIF3d-dependent Translation 31
1.5.7 N6-Methyladenosine (m^6A) 32
1.5.7.1 N6-Methyladenosine-dependent Translation 32
1.5.7.2 N6-Methyladenosine Modification of Viral Genomes and mRNA 34
1.5.8 Herpesvirus Control of Translation 35
1.6 Rationale and Overview 37
Chapter Two – Materials and Methods 45
2.1 Cell Lines 45
2.2 Fluorescent Imaging and Cell Counting 45
2.3 Chemical Inhibitors 46
2.4 Immunoblotting (IB) 46
2.5 Immunofluorescence (IFA) 47
2.6 Viral Genome Amplification and qRT-PCR 48
2.7 KSHV Titering and Infection 48
2.7.1 DNAse-protected Virion qPCR 48
2.7.2 KSHV Infection and Titering Flow Cytometry 48
2.8 Puromycin Translation Assay 49
2.9 m^7GTP Pulldown 49
2.10 Polysome Analysis 50
2.10.1 Polysome Isolation 50
2.10.2 RNA-Seq Analysis of Polysome Fractions 50
2.10.3 Polysome RT-qPCR 51
2.10.4 Polysome Immunoblot 52
2.11 Enzyme-linked Immunosorbent Assay (ELISA) 52
2.12 shRNA Gene-silencing 52
2.13 Nuclear-Cytoplasmic Fractionation 53
2.14 Proteomics 54
2.14.1 Sample Preparation for LC-MS3 54
2.14.2 Data Analysis 56

2.15 Statistical Analysis 56
2.16 Gene Ontology Analysis 56
Chapter Three – Requirement of mTORC1 for KSHV lytic replication 61
3.1 Introduction 61
3.2 Results 62
3.2.1 mTORC1 Is Dispensable for Genome Replication and Late Protein Synthesis 62
3.2.2 Infectious Virion Can be Produced with mTOR Inhibition 63
3.2.3 mTORC1 Inhibition Limits RTA Expression 65
3.2.4 mTORC1 Is Not Required to Inhibit Autophagy during Lytic Replication 66
3.2.5 Butyrate Removes the Requirement for mTOR during Lytic Reactivation 68
3.3 Discussion 69
Chapter Four – Translational Efficiency of Viral mRNA 81
4.1 Introduction 81
4.2 Results 82
4.2.1 mTOR Activity Promotes Bulk Protein Synthesis 82
4.2.2 mTOR Inhibition Does Not Affect Translational Efficiency of Viral mRNA 83
4.2.3 Translation of Cytokines 86
4.2.4 mTOR Inhibition in Lytic Replication Disrupts eIF4F Assembly 86
4.2.5 Non-eIF4F-dependent Accumulation of Viral Proteins 88
4.2.6 N6-methyladenosine Modification during Lytic Replication 90
4.3 Discussion 90
Chapter Five – Lytic Messenger Ribonucleoproteins 108
5.1 Introduction 108
5.2 Results 109
5.2.1 Proteome of Translating mRNP in Lytic Replication 109
5.2.2 Association of Viral Proteins with Translating mRNA 110
5.3 Discussion 112
5.3.1 Quality of the Polysome Proteome 112
5.3.2 Viral Proteins Associated with Polysomes 115
Chapter Six – Conclusions 126

6.1 Summary 126
6.2 mTORC1 Activation during KSHV Infection 127
6.3 A Second-Signal for KSHV Reactivation 128
6.4 Translation Initiation Without eIF4F 130
6.5 Future Investigations 131
References 134

List of Tables

Table 2.1 Antibodies used in this study 58

Table 2.2 Sequences of oligonucleotides 60

Table 5.1 Viral proteins detected in polysomes 125

List of Figures

Fig 1.1 KSHV replication cycle and temporal classes. 40

Fig 1.2 eIF4F-dependent translation initiation. 41

Fig 1.3 mTORC1 regulation. 43

Fig 1.4 Non-eIF4F translation initiation complexes. 44

Fig 3.2 mTOR is required for reactivation from latency, but not progression from early to late replication 73

Fig 3.3 mTOR is not required for production of infectious virions after KSHV reactivation 74

Fig 3.4 Effects of mTOR inhibition on RTA-transgene expression from iSLK and TREx-BCBL1-RTA cells 75

Fig 3.5 mTOR inhibition does not enhance autophagic flux during lytic replication 77

Fig 3.6 ATG14 is required for inhibitory effects of Torin on reactivation and virion production 78

Fig 3.7 ATG14 is not required for mTORC1 kinase activity, or dephosphorylation of target proteins 79

Fig 3.8 Butyrate overcomes the mTORC1 requirement for lytic reactivation 80

Fig 4.1 mTORC1 promotes bulk protein synthesis during lytic replication 96

Fig 4.2 Effect of Torin treatment on translational efficiencies of viral mRNA 97

Fig 4.3 Distribution of viral and cellular mRNA in polysome fractions 99

Fig 4.4 VEGF-A release is restricted by mTORC1 inhibition during latency 101

Fig 4.5 mTOR inhibition disrupts eIF4F formation during latency and lytic replication 102

Fig 4.6 Association of translation initiation factors during viral latency and lytic replication 103

Fig 4.7 Silencing of translation initiation factors that are not displaced from the polysomes by Torin does not restrict virion production 104

Fig 4.8 eIF3d silencing does not affect viral protein accumulation 105

Fig 4.9 eIF4F inhibitors 4EGi and 4E1RCat inhibit virus replication 106

Fig 4.10 METTL3 is required for virion production 107

Fig 5.1 Changes in whole cell proteome over lytic replication 120

Fig 5.2 Quantitative proteomics of polysomes during latency and 24 hpi 121

Fig 5.3 Unscaled Abundance of quantified viral proteins detected in lytic polysomes.. 123
Fig 5.4 Cytoplasmic localization of ORF59 and ORF57..... 124

Abstract

Kaposi's sarcoma-associated herpesvirus (KSHV) is the causative agent of Kaposi's sarcoma and primary effusion lymphoma. Herpesvirus genomes are decoded by host RNA polymerase enzymes, generating messenger ribonucleotides (mRNA) that are post-transcriptionally modified and exported to the cytoplasm through the combined work of host and viral factors. These viral mRNA bear 5′-m^{7}GTP caps and poly(A) tails that should permit assembly of canonical host eIF4F cap-binding complexes to initiate protein synthesis. However, the precise mechanisms of translation initiation remain to be investigated for KSHV and other herpesviruses. Mechanistic target of rapamycin complex 1 (mTORC1) normally promotes eIF4F assembly in response to sufficient growth signals and nutrient abundance, while simultaneously suppressing autophagy, an important mechanism of cellular catabolism. Here I demonstrate that mTORC1 activity supports viral reactivation from latency, but this requirement can be relieved by silencing the essential autophagy gene *ATG14*. I show that mTORC1 is activated during KSHV lytic replication, but unresponsive to normal inhibitory signals. mTORC1 activity is required for eIF4F assembly during viral latency and lytic replication, but dispensable for suppression of autophagy. eIF4F contributes to bulk protein synthesis during lytic replication, but it is dispensable for the efficient synthesis of viral proteins and subsequent release of infectious progeny virions. KSHV virions also accumulate normally when known non-eIF4F translation initiation factors are depleted. To identify proteins required to support viral protein synthesis, I isolated and characterized actively-translating messenger ribonucleoprotein (mRNP) complexes by ultracentrifugation and sucrose-gradient fractionation followed by quantitative mass spectrometry. This analysis revealed the presence of viral proteins in mRNP complexes that had not previously been shown to play roles in viral protein synthesis. This work demonstrates that KSHV can disrupt cellular mTORC1 regulation to ensure efficient viral protein synthesis and evasion of autophagy during lytic replication.

List of Abbreviations Used

^{o}C	degree Celsius
%	percent
ΔTE	difference in translational efficiency, or efficiencies
ΔΔCt	delta-delta threshold cycle
γHV68	murine gammaherpesvirus 68
µg	microgram
µL	microliter
µM	micromolar
1x	one-times
2x	two-times
4x	four-times
A	adenosine
A_{260}	absorbance at 260 nanometers
AA	amino acids
ACN	acetonitrile
AIDS	acquired immunodeficiency syndrome
ANOVA	analysis of variance
AP-1	activator-protein 1
BEC	blood endothelial cell
BCBL	body cavity B lymphoma
C	cytosine
C-terminal	carboxy-terminal
CD	cluster of differentiation
CDS	coding sequence
circRNA	circular ribonucleic acid
CHX	cycloheximide
CITE	cap-independent translation-enhancer
cpm	counts per million
CQ	chloroquine
CR1	clustered-repeat 1

CRISPR	clustered regulatory interspaced short palindromic repeats
Ct	threshold cycle
dsDNA	double-stranded deoxyribonucleic acid
dsRNA	double-stranded ribonucleic acid
dT	deoxythymidine
DAPI	4′,6-diamidino-2-phenylindole
DMEM	Dulbecco's modified Eagle's medium
DMSO	dimethyl sulfoxide
DNA	deoxyribonucleic acid
dPBS	Dulbecco's phosphate-buffered saline
dox	doxycycline
DR	direct-repeat
DTT	dithiothreitol
EBV	Epstein-Barr virus
eIF2	eukaryotic initiation factor 2
eIF3	eukaryotic initiation factor 3
eIF4F	eukaryotic initiation factor 4F
$eIF4F_H$	eukaryotic initiation factor 4F, hypoxic
FA	formic acid
FC	fold-change
FDR	False discovery rate
G	guanine
GAP	guanosine triphosphate activating protein
GATOR	guanosine triphosphate activating protein towards Rags
GEF	guanosine triphosphate exchange factor
GO	gene-ontology
Glu	glutamic acid
GTP	guanosine triphosphate
GTPase	guanosine triphosphate hydrolase
h	hour, or hours
HCMV	human cytomegalovirus

HDAC	histone deacetylase
HHV	human herpesvirus
HIF	hypoxia inducible factor
hpi	hours-post-induction
HSV 1	Herpes Simplex virus 1
HSV 2	Herpes Simplex virus 2
HRE	hypoxia-response element
IE	immediate-early gene
IFN	interferon
IRES	internal ribosome entry site
ISG	interferon-stimulated gene
ISR	integrated-stress response
IU	international units
KS	Kaposi's sarcoma
KSHV	Kaposi's Sarcoma-associated herpesvirus
LC-MS3	liquid chromatography with three mass spectrometric scans
LEC	lymphatic endothelial cell
m^6A	N6-methyladenosine
m^7GTP	N7-methylguanosine triphosphate
MAM	mitochondria-associated-membrane
min	minutes
miRNA	micro-ribonucleic acid
MIF4G	middle domain of eIF4G
mL	milliliter
mm	millimeter
mM	millimolar
mRNA	messenger ribonucleic acid
mRNP	messenger ribonucleoprotein
Mta	messenger ribonucleic acid transcript accumulation protein
mTORC1	mechanistic target of rapamycin complex 1
mTORC2	mechanistic target of rapamycin complex 2

N-terminal	amino-terminal
NaB	sodium butyrate
NF-κB	nuclear factor -κB
nm	nanometer
nM	nanomolar
NMD	nonsense-mediated decay
OIS	oncogene-induced senescence
ORF`	open-reading frame
PAA	phosphonoacetic acid
PABP	polyadenosine-binding protein
PAS	phagophore assembly site
PBS	phosphate-buffered saline
PCR	polymerase chain reaction
PEL	primary effusion lymphoma
PFA	paraformaldehyde
Pol-Seq	polysome sequencing
Phe	phenylalanine
PI3K	pphosphoinositide 3-kinase
PIC	pre-initiation complex
Ppm	part-per-million
Pro	proline
psi	pounds-per-square-inch
qPCR	quantitative polymerase chain reaction
RBP	ribonucleic acid binding-protein
RNA	ribonucleic acid
RNA-Seq	ribonucleic acid sequencing
rpm	revolutions per minute
RPMI	Roswell Park Memorial Institute
RQC	ribosome quality control
rRNA	ribosomal ribonucleic acid
RT	room temperature

RT-qPCR	reverse transcription quantitative polymerase chain reaction
RTA	replication and transcriptional activator
SD	standard deviation
SDS	sodium dodecyl sulfate
SDS-PAGE	sodium dodecyl sulfate polyacrylamide gel electrophoresis
SEM	standard-error measurement
Ser	serine
shRNA	short-hairpin ribonucleic acid
TE	translational efficiency, or efficiencies
Thr	threonine
TIF	translation initiation factor, or factors
TOP	5’ tract of oligopyrimidine
Torin	Torin-1
TMT	tandem-mass tag
TPA	12-O-Tetradecanoylphorbol-13-acetate
TREx	Tet-regulated expressed, or expression
tRNA	transfer ribonucleic acid
U	uracil
uORF	upstream open-reading frame
UTR	untranslated gene
v	viral
v/v	volume per volume
w/v	weight per volume
WCL	whole-cell lysate
x *g*	force of gravity

Acknowledgements

None of the work here would have been possible without the support of my supervisor, Dr. Craig McCormick. I am grateful for the opportunity to study with him and for the significant intellectual freedom he provided. He encouraged me to travel widely, develop new assays, and to pursue my curiosity. I learned a lot from him and I'm sure he'll have more to show me as my career progresses. I want to thank my supervisory committee, Dr. Zhenyu Cheng, Dr. Roy Duncan, Dr. Patrick Lee, and Dr. Chris Richardson. They were always supportive in their comments and helpful in their suggestions. I would also like to thank my external examiner Dr. Andrew Mehle for agreeing to serve and for his constructive feedback. Generous training support throughout my degree was provided by the Beatrice Hunter Cancer Research Institute and the Nova Scotia Health Research Foundation.

I received significant support from several scientists without whose help this project would have been difficult to complete. Dr. Jim Uniacke hosted me in his lab at the University of Guelph for training in polysome isolation and analysis. Dr. Stephan Lewis and Dr. Nicholas Crapoulet at the Atlantic Cancer Research Institute, and Dr. Daniel Gaston in the Department of Pathology, provided crucial help in performing RNA-Seq analysis. Dr. Alejandro Cohen guided me through many proteomics experiments and spent a lot of time teaching me the inner workings of the instruments at the Proteomics Core Facility. The lab has always been a great source of support over the years, but I would like to specifically thank Carolyn Robinson, Andrea Monjo, and Katrina Bouzanis for their technical assistance during this project.

Finally, I'd like to thank my parents for all of their love and support over the years. Thank you to my partner Dr. Anna Greenshields, I'm not sure what I'd do without you. And none of this would have been possible without Dr. Patricia Shewen who started me down this path all those years ago. It's been a lot of work, but it's been fun.

Chapter One – Introduction

1.1 Overview

All viruses require access to host protein synthesis machinery to translate viral messenger ribonucleic acid (mRNAs) into proteins and generate progeny virions. These viral mRNAs have features that enable efficient recruitment of host translation initiation factors (TIFs) and ribosomes. Translation is energetically expensive and subject to multiple levels of regulation. A variety of stresses can disrupt bulk translation; this blockade excludes a subset of mRNAs with that encode stress-mitigating proteins. This stress-dependent translation program can resolve stress and enable resumption of bulk translation. Viruses must reconcile the high metabolic demands of virion production and the stress of replication with continued access to translation machinery.

Viral transcripts are in constant competition with host cell mRNA for TIFs and ribosomes. Herpesviruses, which replicate in the nucleus of the host cell, generate mRNAs that are structurally similar to cellular mRNA. By adopting the general features of host cell mRNAs, viral mRNAs can be efficiently post-transcriptionally processed by host enzymes, exported from the nucleus, and bound to TIFs. This mimicry also reduces the generation of deleterious pathogen-associated molecular patterns that can be recognized by host pattern recognition receptors. However, this creates a challenge for the virus that needs to specifically ensure translation of its own mRNA. The translational environment of a stressed cell is distinct from that of an unstressed cell. This produces distinct translatomes where the translational efficiency (TE) of some mRNA is enhanced or suppressed. This regulation is poorly understood, but seems to be based on the engagement of distinct sets of TIF that engage with specific sets of mRNA. Little is known about how stress affects herpesvirus protein synthesis, or whether these viruses have adapted to optimal gene expression in stressful environments.

In this work, I examine how the regulation of mTORC1, the master regulator of nutrient abundance and protein synthesis, affects the translation of viral mRNA from a gammaherpesvirus, Kaposi's Sarcoma-associated herpesvirus (KSHV). This section provides a summary of KSHV replication, mTORC1 signalling, and cap-dependent translation, and alternative mechanisms of translation initiation during stress. Special

attention is provided to how KSHV and other herpesviruses seize these processes when stress is high and resources are scarce.

1.2 Kaposi's Sarcoma-associated Herpesvirus

1.2.1 Herpesviridae

Herpesviruses are ubiquitous, enveloped, large dsDNA viruses (Moustafa et al., 2017). All herpesviruses can establish a quiescent form of infection known as latency in which viral gene expression is severely restricted and the genome is maintained in an extra-chromosomal episome. An essential feature of latency is reversibility, which is required for viral replication and production of viral progeny. Reactivation from latency requires expression of a viral lytic switch protein, which initiates an ordered cascade of viral gene expression resulting in the production of infectious virions. The authentic *in vivo* stimuli for reactivation from latency is largely unknown, but cellular stress is likely important as this can stimulate reactivation in cell culture. The loss of adaptive immune surveillance may directly contribute to, or simply reveal, lytic reactivation.

There are eight human herpesviruses that represent three viral sub-families: the alpha herpesviruses (alphaherpesvirinae) herpes simplex virus 1, and 2 (HSV-1, HSV-2) and varicella zoster virus (VZV); the beta herpesviruses (betaherpesvirinae) cytomegalovirus (HCMV), HHV-6A/B, HHV-7; and the gamma herpesviruses (gammaherpesvirinae) Epstein-Barr virus (EBV) and Kaposi's Sarcoma-associated virus (KSHV). Alpha herpesviruses establish latency in sensory neural ganglia. On reactivation, virions bud from neuronal axons and infect epithelial cells, where alphaherpesviruses undergo only the lytic program. The betaherpesvirus HCMV establishes latency in CD34+ haematopoietic progenitor cells (Pantry and Medveczky, 2017). HHV 6A/B and 7 can also establish latency in these cells, but CD4+ seem to be the site of latent infection in humans. HHV-6A/B and HHV-7 latency is exceptional as the viral genome does not persist as an episome, but instead directly integrates into telomeric host DNA (Pantry and Medveczky, 2017). The gammaherpesviruses, or lymphocrytoviruses, establish latency in B lymphocytes. EBV infection drives B lymphocyte differentiation towards a CD27+ memory phenotype. It is unclear what B lymphocyte population contains the KSHV reservoir. B lymphocytes can be co-infected

with EBV and KSHV leading to co-establishment of latency in the same cell, which is advantageous for long-term KSHV latent infection (Bigi et al., 2018). Both of the human gammaherpesviruses are oncoviruses that can promote lymphoproliferative diseases, including lymphomas and cancer in other cell types. EBV is also a potential causative agent for some gastric cancer; KSHV is the causative agent for Kaposi's sarcoma (Y. Chang et al., 1994; Cho et al., 2016).

1.2.2 Discovery of KSHV in AIDS-related Malignancies

Kaposi's sarcoma (KS) is an acquired immunodeficiency syndrome (AIDS)-defining malignancy. KS is a multicentric, endothelial cell cancer. Lesions are highly inflamed and resemble a leaky, poorly structured mass of highly spindled endothelial cells (Ganem, 2010; Mesri et al., 2014). Yuan Chang and Patrick Moore's group discovered KSHV by detecting herpesvirus DNA sequences in Kaposi's sarcoma lesions using a subtractive hybridization technique known as representational difference analysis (Chang et al., 1994). In this method, DNA is isolated from disease tissue and healthy adjacent tissues and digested with restriction endonucleases. The digested DNA from the disease sample was then ligated to universal primers sequences, then melted and combined with an excess of melted DNA from non-disease tissue. The pooled DNA is then hybridized before PCR is performed using the universal primers. Only hybridized sequences present with the disease condition should contain two primer binding sites; sequences present in both the diseased and non-diseased tissue will predominantly contain one or no ligated primer binding sites. This investigation yielded several DNA fragments with homology to gammaherpesviruses, most closely related to the squirrel monkey rhadinovirus herpesvirus saimiri (P. S. Moore et al., 1996). Soon after KSHV was also detected in cells from two AIDS-related lymphoproliferative diseases, primary effusion lymphoma (Cesarman et al., 1995) and multicentric Castleman's disease (Soulier et al., 1995). PEL cells proliferated efficiently in immunodeficient mouse models. These cells displayed clear evidence of a nuclear 110 nm icosahedral capsid and enveloped virions ultra-structurally consistent with herpesviruses (Said et al., 1996).

Complete sequencing of the KSHV genome revealed numerous viral homologues of cellular genes including several genes that suggested a role in cell transformation.

Homologues included viral (v) cyclin (v-cyclin, a viral Cyclin D), vIL-6, vGPCR (an IL-8R homologue), vFLIP, vBcl2, vFAGARAT, vOX2, vMIPs (macrophage inhibitory protein), and vIRFs (interferon regulatory factors) (Arias et al., 2014; Russo et al., 1996). Murine gammaherpesvirus 68 (γHV68) was sequenced shortly after KSHV and had significant similarity in genome organization, including viral homologues of a cyclin, Bcl2 and IL-8R (Virgin et al., 1997).

While KSHV DNA could be detected in PEL-derived cell lines, Body Cavity B lymphoma (BCBL1) being the first, there was limited transcription from the viral episome, suggesting that KSHV was predominantly a latent infection in these cells. A circular viral episome was soon after observed by Southern blot and Gardella gel (Renne et al., 1996a). A Gardella gel is a variant of agarose electrophoresis where cells are lysed directly in the well of the agarose gel. Circular episomes generate fast-migrating bands while bulk DNA remains in the well (Gardella et al., 1984). Northern blot analysis similarly demonstrated the dominant mode of KSHV infection in KS lesions was latency (Zhong et al., 1996). However, a small proportion of cells produced lytic antigens, suggesting sporadic reactivation from latency in KS lesions (Ganem, 2010; Mesri et al., 2014).

1.2.3. KSHV Replication

1.2.3.1 KSHV Latency

KSHV latent infection is characterized by retention of a nuclear, circularized, chromatinized viral episome with restricted transcription from the viral genome. KSHV latency is somewhat more complex than in HSV-1/2, which is characterized by expression of a single long non-coding RNA lariat and miRNA expression (reviewed in Roizman and Whitley, 2013), and better resembles the latency program of EBV (reviewed in Speck and Ganem, 2010). The KSHV latent program consists of three viral proteins: LANA, v-cyclin and vFLIP; the Kaposin locus; and 12 pre-microRNA (miRNA), which are discussed below. In PEL cells, the latency program is supplemented by expression of two pirated genes, vIL-6 and vIRF3 (D. Chen et al., 2008; Rivas et al., 2001). KSHV latency in endothelial cells results in a spindle cell morphology, characterized by long, parallel actin stress fibers (Corcoran et al., 2015; Ganem, 2006).

Expression of either Kaposin B or v-FLIP is sufficient for spindle formation *in vitro* (Corcoran et al., 2015; Grossmann et al., 2006).

The episome is bound with the host chromatin by latency-associated nuclear antigen (LANA); LANA binds to host histones and non-specific contact with the episome (Toth et al., 2016). LANA also interacts with p53 and pRb, contributing to chromosome instability (Friborg et al., 1999; Radkov et al., 2000; Si and Robertson, 2005). LANA silences lytic promoters during latency by recruiting the Polycomb repressive complex to the episome, which deposits repressive chromatin marks (Toth et al., 2016).

v-cyclin is a viral homologue of cyclin D that drives G1 to S-phase transitions. v-cyclin binds to the cyclin-dependent kinase Cdk6 and can direct phosphorylation, but cannot complete inactivation of pRb. v-cyclin also expands the targeting repertoire of Cdk6 to include Cdk2 targets (reviewed in Verschuren et al., 2004). v-cyclin is a constitutively active cyclin in that it prevents CDK inhibition by canonical inhibitory proteins p21 and p27 (Swanton et al., 1997). v-cyclin causes a DNA-damage response in cells that can trigger oncogene-induced senescence (OIS) (Koopal et al., 2007; Leidal et al., 2012); however, this stress is managed during latency by the actions of another latent protein v-FLIP.

v-FLIP is co-cistronic with v-cyclin and is expressed by an IRES within the coding region of v-cyclin (discussed below; Bieleski and Talbot, 2001; Grundhoff and Ganem, 2001; Low et al., 2001). v-FLIP binds the essential autophagy protein ATG3, and strongly limits LC-3 lipidation, but the exact mechanism of this inhibition remains unclear. Autophagy restriction by v-FLIP inhibits OIS in part by limiting autophagy-dependent secretion of cytokines that enforce OIS by paracrine signalling (J.-S. Lee et al., 2009; Leidal et al., 2012). v-FLIP also stimulates constitutive NF-κB activity in latently infected cells by binding to NEMO of the inhibitor-of-kappa kinase complex and stimulating the phosphorylation and degradation of inhibitor of κB (IκB) alpha (Guasparri et al., 2004; L. Liu et al., 2002). NF-κB is thought to be important to gammaherpesvirus latency by limiting spontaneous lytic replication, inhibiting apoptosis, and elaboration of pro-inflammatory cytokines, and promoting survival (reviewed in Speck and Ganem, 2010). NF-κB is also required for the spindling phenotype of latency (Grossmann et al., 2006).

The Kaposin locus comprises a small AUG-initiated, transmembrane domain-containing ORF, preceded by two 5' guanine-cytosine-rich repeat regions consisting of 23-mer (DR1 and DR2). Only one mRNA is transcribed from a latent promoter, yet several protein products are produced from the locus from translation of non-canonical CUG- and GUG-initiation sites upstream of DR1 and DR2 (Sadler et al., 1999). These, at a minimum, consist of Kaposin B, which contains only the DR1 and DR2 repeats, Kaposin A, which is the small AUG-initiated transmembrane ORF, and Kaposin C which is DR1/2 repeats with Kaposin A. The coding sequence of the Kaposin locus is unusual as translation of the 23-mer repeats produce a -1 frameshift with each repeat, returning to the original reading frame after three repeats. Initiation at any of the three reading frames will produce permutations of the same amino acid (AA) sequence; Kaposin C is the same sequence of Kaposin B but the different reading frame allows read-through into Kaposin A. Kaposin B binds the p38 MAPK substrate kinase MAPKAP-kinase-2 (MK2) by the DR2 repeats and enhances phosphorylation of MK2 target proteins (McCormick and Ganem, 2005). One of the effects of this is stabilization of the normally labile mRNA with AU-rich elements in their 3'UTR that typically encode cytokines and other proteins that must be rapidly degraded during times of stress (McCormick and Ganem, 2005). During latency, Kaposin mRNA is processed to generate two miRNA, miR-K12-10, miR-K12-12, which restrict translation of Kaposin protein products. During lytic replication, the miRNA endonuclease Drosha is depleted and miRNA are no longer generated from Kaposin mRNA (Y.-T. Lin and Sullivan, 2011).

The KSHV miRNAs are generated from twelve pre-miRNAs transcribed from the latency locus. These are processed to generate 25 mature miRNA (two per pre-miRNA, and a 25th from and alternative hairpin formed from a pre-miRNA) (Qin et al., 2017). Some of these miRNAs are homologous to cellular miRNAs (Gottwein, 2012). KSHV miRNAs have complex effects on host gene expression. Several miRNAs can have some overlapping targets, and some mRNAs can be targeted by multiple miRNAs. Broadly, KSHV miRNAs limit the host immune response against, and modulate the metabolism of infected cells. KSHV miRNAs also support angiogenesis and dissemination of KSHV-infected endothelial cells (Gottwein, 2012; Qin et al., 2017).

KSHV readily establishes latency on infection in cell culture (Bechtel et al., 2003). Upon *de novo* infection in cell culture, there is a limited of expression of some KSHV lytic genes before the virus establishes its canonical latent program (Purushothaman et al., 2015). It is unclear whether this burst of lytic gene expression is required to reprogram host cells to accept the latent episome, but the silencing of lytic promoters is associated with accumulation of repressive chromatin marks on the viral genome (Toth et al., 2010). KSHV latency is leaky, and spontaneous expression of lytic antigens is observed in both *de novo* epithelial cell infections and in cultured PEL cells. This seems to be a cell-dependent property because sub-clones of latently infected populations can be isolated with tight control of latency and still remain permissive to lytic reactivation (Myoung and Ganem, 2011).

Latency is unstable in epithelial, fibroblast, and endothelial cells; the viral episome is rapidly lost over a few cell divisions. However, the episome can be efficiently maintained, and the copy number can be enhanced, in culture by selection with antibiotics (Grundhoff and Ganem, 2004; Vieira and O'Hearn, 2004; Myoung and Ganem, 2011). PEL cell lines efficiently maintain a high copy number of viral episomes in culture. It is unclear why this difference in episome retention exists. It has been suggested that sporadic lytic replication in a KS lesion might be required to repopulate transformed cells with KSHV by new infectious events (Grundhoff and Ganem, 2004). More likely is that the tumors cells have acquired a mutation that allows efficient retention of the viral episome. Such a cell line was derived by passaging KSHV-infected hTert-immortalized human umbilical cord endothelial cells through an immunodeficient mouse xenograft (Roy et al., 2013), yet only 50% of the cells retain the viral episome in culture. It is unclear what mutations these cells have acquired to sustain viral latency or if they are permissive for lytic replication.

1.2.3.2 Reactivation from Latency and Lytic Replication

The lytic program of KSHV was first investigated by treating cells with the phorbol ester 12-O-Tetradecanoylphorbol-13-acetate (TPA), which stimulated the release of infectious, enveloped virions in the supernatant (Renne et al., 1996b). The HDAC inhibitor butyrate was soon shown to stimulate lytic replication as well (Miller et al.,

1996). Both these chemicals stimulate transcription of the KSHV immediate-early (IE) protein replication and transcriptional activator (RTA) (ORF50), which initiates an ordered, temporal, cascade of gene expression (Lukac et al., 1998; Sun et al., 1998). While RTA is a sufficient and necessary to reactivate KSHV from latency, reactivation is relatively inefficient. RTA function is likely regulated by other cellular factors that will commit a cell to lytic replication (Guito and Lukac, 2012).

RTA trans-activates more than half of the viral genome, yet binds directly to only a few viral promoters including vIRF1, Mta, and SOX (Bu et al., 2008). Most RTA-responsive promoters require association with RTA and host transcription factor RBP-Jκ (Izumiya et al., 2009; Y. Liang et al., 2002; Toth et al., 2010). RTA also binds to the promoters of many host genes and modulates transcription; some of these gene products are required for virus replication. These seem to be largely dependent on RBP-Jκ binding to these cellular loci (Papp et al., 2018).

In addition to its role as a transactivator, RTA functions as a E3 ubiquitin ligase and can target proteins for ubiquitination and degradation. This property is shared by RTA homologues in alphaherpesvirus such as HSV-1 ICP0. RTA promotes degradation of innate immune modulators IRF-7 and MyD88 (Boutell and Everett, 2013; Y. Yu et al., 2005; Q. Zhao et al., 2015). Binding specificity of RTA is unclear, but RTA is directed to proteins modified by SUMOylation and targets them for degradation (Izumiya et al., 2013). A global analysis of proteins degraded by RTA has not been conducted.

After RTA expression, KSHV replication follows an orderly temporal cascade (Fig 1.1). Early genes include important regulators of viral and host gene expression that support genome replication and modulate the immune response. If early replication is successful and the viral genome replicates, late replication follows where virion components are synthesized (Arias et al., 2014). At least four viral proteins have been shown to play important roles in extending the host cell subversion initiated by RTA and ensuring efficient viral gene expression: the viral kinase ORF36, host shutoff endonuclease SOX, the viral RNA-binding protein (RBP) ORF57, and the multifunctional ORF45. Roles for ORF36 and ORF45 mRNA processing are discussed below.

ORF36 is a viral serine kinase and phosphorylates a range of cellular proteins and at least one viral protein. The catalytic domain of ORF36 has limited homology to p70 S6 kinase (p70 S6K); ORF36 can phosphorylate a subset of S6K target proteins (Bhatt et al., 2016). ORF36 phosphorylation of the histone acetyltransferase TIP60 stimulates its enzymatic activity and leads to chromatin remodelling that might support virus replication by exposing viral promoters. This action of ORF36 is conserved in homologous herpesvirus kinases and provokes a potent DNA damage response (R. Li et al., 2011). ORF36 also phosphorylates ORF59, which reduces its ability to interact with the origin of replication (McDowell et al., 2013). It is unclear if ORF36 is important for the function of other viral proteins, but its kinase activity is important for virus replication and the establishment of latency (Avey et al., 2016).

ORF45 is an early gene, and a tegument protein, suggesting a role early in *de novo* infection. It seems to act as a scaffolding protein that binds to proteins and alters their enzymatic activity or prevents their normal regulation. ORF45 forms a complex with both p90 S6 kinase (RSK) and ERK, which activates both kinases (Kuang et al., 2008; 2009). Formation of this complex is required for efficient late gene expression and virion production (B. Fu et al., 2015). During infection, this complex predominantly stimulates eIF4B Ser422 phosphorylation, but a broad array of proteins, including many transcriptional regulators are also phosphorylated (Avey et al., 2015). ORF45 also regulates the Type-I interferon (IFN) responses by binding to IRF-7 to prevent its phosphorylation and nuclear localization; ORF45 contains phosphorylation sites that mimic IRF-7 target residues and competitively inhibits IRF-7 kinases IKKε and TBK1 (Q. Liang et al., 2012; F. X. Zhu et al., 2002).

Both ORF36 and ORF45 support activation of cellular transcription factors through JNK and ERK phosphorylation (Hamza et al., 2004; X. Li et al., 2015). These mitogen-activated protein kinases lead to phosphorylation and stabilization of c-Fos and c-Jun, which form an AP-1 transcription complex and may support transcription of viral genes. ORF36 and ORF45 also directly associate, which stimulates the kinase activity of ORF36 (Avey et al., 2016).

During late replication, viral genome replication activates a virally encoded transcription complex on KSHV late promoters. This is regulated primarily by ORF24, a

viral TATA-box binding protein that binds to the variant TATT-box present in virus late promoters (Arias et al., 2014; Z. H. Davis et al., 2014). ORF24 coordinates the recruitment of five viral proteins (ORFs 18, 30, 31, 34, 66) to form a transcription complex required to recruit RNA polymerase II. Formation of this complex is essential for transcription of late genes (Brulois et al., 2015). A virus-specific transcription complex likely presents opportunities for KSHV to separately regulate its own transcription differently from the host. SOX-mediated host shutoff during early replication leads to the nuclear accumulation of RBPs, including the polyA-binding protein PABPC. Nuclear PABPC inhibits the RNA polymerase II function, which further represses transcription (Gilbertson et al., 2018). Viral late genes avoid this repression (Abernathy et al., 2015), likely due to the viral late gene transcription complex.

Late replication features synthesis of viral structural proteins, including capsid subunits, glycoproteins, and tegument components. The capsid assembles in the nucleus from four capsid proteins, (ORFs 25/26/62/65) around a core scaffolding protein (ORF17) (F. X. Zhu et al., 2004). The viral genome is loaded into the assembled capsids through a portal complex (ORF19/43) (Arias et al., 2014) at a capsid vertex, displacing ORF17 (Nealon et al., 2001). This requires the protease activity of N-terminal extension of ORF17, ORF17.5 that accumulates during late replication due to the utilization of an upstream late promoter (Arias et al., 2014; Unal et al., 1997). Packaging resolves linear genomes from sites of genome replication; four orientations of the genome are possible. KSHV capsids bud through the nuclear membrane by the actions of a viral nuclear egress complex (ORF67/69) after disruption of the nuclear lamina (Desai et al., 2011). The capsid then bud into the trans-Golgi network where glycoproteins are obtained, to bud via the secretory pathway (reviewed in Mettenleiter, 2002).

1.2.4 KSHV Promotes Tumourigenesis by Paracrine Action

Unlike EBV, KSHV latency is not sufficient to transform B cells or endothelial cells (Ganem, 2006; Mesri et al., 2014). KSHV infection has been sufficient to induce cellular transformation in only rat metanephric mesenchymal precursor cells (Jones et al., 2012). Without immune surveillance, KS emerges from a complex relationship between latently-infected, and lytically-replicating cells. Latently-infected spindle cells make up

the replicating bulk of the tumor, and a small proportion of lytic cells are thought to drive replication by cytokine secretion (Ganem, 2010; Mesri et al., 2014). Ganciclovir, an antiviral nucleoside analogue that inhibits lytic replication, dramatically reduces the risk of KS in untreated AIDS (Martin et al., 1999). Latent infection likely contributes to KS progression by promoting cell survival and dysregulating responses to pro-angiogenic cytokines (L. Wang and Damania, 2008). The action of v-cyclin and v-FLIP would contribute to cells poised to replicate without risk of OIS (Leidal et al., 2012). Inactivation of p53 and pRb by LANA likely contribute to genomic instability of replicating cells.

Paracrine stimulation of endothelial cell growth by VEGF-A appears to be the main driver of KS. Lytic replication is accompanied by expression of pro-inflammatory and pro-angiogenic cytokines from the host, in addition to viral cytokine homologues. Several lytic gene products enhance cytokine signalling from the host cell; both K1 and K15 stimulate NF-κB signalling (B. S. Lee et al., 2005; Pietrek et al., 2010). Kaposin B potentiates cytokine signalling by stabilizing liabile AU-rich element containing cytokine mRNA (McCormick and Ganem, 2005). One lytic protein, a constitutively active viral homologue of the human IL-8 receptor, vGPCR, is a potent activator of pro-angiogenic signalling (Bais et al., 1998). Ectopic vGPCR is sufficient for angiosarcoma formation in mouse xenografts. This is dependent on secretion of pro-angiogenic cytokines from vGPCR-expressing cells (Martin et al., 2013). vGPCR is also required for tumour formation in nude mouse xenografts of KSHV-infected endothelial cells; knockdown of vGPCR expression prevented VEGF-A accumulation as well (Mutlu et al., 2007). Paracrine growth promotion by lytic cells is sensitive to inhibition of the mechanistic target of rapamycin complex 1 (mTORC1), a master regulator of protein synthesis and degradation in cells (Martin et al., 2013; Sin et al., 2007; Stallone et al., 2005). mTORC1 upstream regulation and downstream effectors are discussed below.

It is unclear what progenitor cell forms the KS lesion. Identifying the progenitor cell is complicated by the reprogramming of blood or lymphatic endothelial cells (BEC or LEC) during latency. KSHV infection of BECs leads to upregulation of PROX1, the key transcriptional regulators of lymphatic cell identity. Conversely, KSHV infection of LECs down-regulates PROX1 expression. This results in infection of either cells type

moving to an intermediate cell phenotype, with expression of both LEC and BEC markers (Hong et al., 2004; H.-W. Wang et al., 2004). Further complicating this reprogramming is that KSHV infection in BEC establishes the normal latency program usually observed in PEL cells, but infection of LEC results in a more extensive latent program with expression of numerous lytic antigens (H. H. Chang et al., 2013).

1.3 eIF4F-dependent Translation Initiation

1.3.1 eIF4F-dependent Translation Initiation

Translation initiation is the major mode of control of protein synthesis. Cap-dependent translation canonically is initiated by eukaryotic initiation factor 4F (eIF4F), a heterotrimer comprising eIF4E, eIF4G, and eIF4A (Fig 1.2A). The methyl-7-guanoinse triphosphate (m^7GTP) cap at the 5'end of mRNA is bound with high affinity by eIF4E. eIF4G is a large scaffolding protein that recruits several other initiation factors. The N-terminal domain of eIF4G contains a YXXXXLϕ motif (where ϕ is any hydrophobic residue) with which it interacts with eIF4E. The middle domain of eIF4G (MIF4G) mediates association with eIF3, a large 13 subunit complex (eIF3a-m) that binds the small ribosomal subunit. This domain, together with the C-terminal domain contain contact sites for the eIF4A helicase, which is thought to reduce secondary structure in the 5' UTR of mRNA (Fig 1.2A; reviewed in Hinnebusch, 2014; Merrick, 2015).

Once bound to mRNA, eIF4F recruits additional factors that enhance the helicase activity of eIF4A, eIF4B and eIF4H. eIF4A helicase activity reduces the secondary structure of the 5'UTR, which likely aids in recruitment of the 43S pre-initiation complex (PIC) (Merrick, 2015). The 43S PIC, comprises the 40S small ribosomal subunit, eIF3, eIF1, eIF1A, and the ternary complex. The ternary complex consists of the heterotrimer eIF2, guanosine triphosphate, and initiator methionine tRNA (Met-$tRNA_i$). eIF1 and eIF1A hold the PIC in an "open" configuration to aid scanning. This complex scans the 5'UTR of the mRNA in a predominantly 5' to 3' direction until an AUG start codon base-pairs to the anti-codon of Met-$tRNA_i$. The large 60S ribosomal subunit is joined after hydrolysis of the eIF2-bound guanosine-triphosphate (GTP) by the guanosine-activating protein (GAP) action of eIF5, commencing peptide elongation (Hinnebusch, 2014). A polyA tail or circularization of the mRNA by polyA-binding protein (PABP) to

eIF4G is not required for initiation, but likely helps with reinitiating of freshly terminated ribosomes onto the same mRNA (Merrick, 2015). Multiple initiating, scanning, and elongation events can occur on the same mRNA. mRNA with multiple ribosomes are called polysomes.

Two small molecules disrupting eIF4F formation have also been described, 4EGi and 4E1RCat (Cencic et al., 2011b; Moerke et al., 2007). 4ER1Cat is predicted to directly interfere with YXXXXLϕ-dependent binding by both eIF4G1 and 4E-BP1 (Cencic et al., 2011b). 4EGi acts an allosteric inhibitor that binds eIF4E distant to the eIF4G1 binding site (Papadopoulos et al., 2014), this also stabilizes the association of unphosphorylated 4E-BP1 (discussed below) (Sekiyama et al., 2015). However, 4EGi also increases eIF2α Ser51 phosphorylation, which confuses interpretation of the effects of 4EGi on eIF4F-dependent initiation in cells (McMahon et al., 2010). This suggests that disruption of the eIF4F outside of its normal physiological control might lead to off target effects.

1.3.2 Integrated Stress Response and eIF2 Phosphorylation

Stress in the cell can stimulate the integrated-stress response (ISR), which potently limits protein synthesis, then attempts to mitigate the stress. The ISR is orchestrated by phosphorylation of the alpha subunit of eIF2 (eIF2α) at Ser51. This residue is phosphorylated by one of four eIF2α kinases that are activated by different stress stimuli: GCN2 responds to AA insufficiency or UV; PKR binds to dsRNA, which accumulates during virus infection; PERK is activated in the ER when chaperone proteins are depleted by high protein load; HRI responds to oxidative stress. When eIF2α is phosphorylated, it has greatly increased affinity for the ternary complex GEF, eIF2B. As eIF2B is limiting in the cell, the pool of GTP-bound eIF2 is rapidly depleted, inhibiting AUG-initiation (reviewed in Pakos Zebrucka et al., 2016). During ISR, enough mRNA cease translation during eIF2α phosphorylation that mRNA crashes out of solution and form stress granules. These granules may serve as sites of innate immune signalling, (McCormick and Khaperskyy, 2017; Van Treeck et al., 2018).

Even though nearly all bulk protein synthesis is lost during eIF2α Ser51 phosphorylation, translation of a subset of mRNA persists, or is enhanced. Transcripts containing non-AUG, near-cognate start codons, such as CUG or GUG, (Kearse and

Wilusz, 2017) are initiated by 43S complexes populated with eIF2 functional-homologues, such as eIF2A and eIF2D. This prevents their inhibition during eIF2α phosphorylation. Other transcripts include short, upstream ORFs, in the 5'UTR. Initiation of uORFs is predominant when eIF2α is not phosphorylated and Met-charged ternary complex is plentiful; however, when there is low eIF2 available, translation of the canonical downstream ORF is enhanced (Andreev et al., 2015). The mechanisms of uORF regulation are poorly understood, and likely to be transcript and translational environment-specific. Generally, it appears that uORFs are always preferentially translated (Andreev et al., 2015), but during stress, after the large ribosome disengages at the uORF stop codon, the 43S continues to scan and somehow reacquires another charged tRNA. This newly-acquired ternary complex could contain eIF2 and resemble a normal ternary complex (Young and Wek, 2016). Alternatively, an eIF2 functional homologue, such as the Denr-Mcts1 heterodimer may be acquired (Schleich et al., 2014). Further complicating this regulation is the presence of near cognate start codon uORFs in some transcripts (Kearse and Wilusz, 2017). Transcripts with increased translation during the ISR include key transcriptional activators (ATF4), chaperones (CHOP), and the regulatory subunit of the eIF2α phosphatase, GADD34.

Viruses encode proteins to limit the ISR. Herpesviruses in particular have several proteins that can bind to and limit the function of PKR. Host shutoff by viral endonucleases can also prevent PKR activation by depleting dsRNA (Burgess and Mohr, 2018). HSV-1 ICP34.5 limits eIF2α phosphorylation by acting as a viral mimic of GADD34 (Y. Li et al., 2011). Little is known about the regulation of the ISR in KSHV.

1.3.3 Herpesvirus mRNA Processing

Herpesviruses replicate in the cell nucleus where they can access host transcriptional machinery. Viral mRNA is transcribed by host RNA polymerase II and post-transcriptionally modified by host m^7GTP capping, poly-adenylation, and splicing. Many herpesvirus mRNAs are not spliced and therefore do not efficiently recruit nuclear export factors. Instead, nuclear export proteins Aly or Nxf1 are directly recruited to mRNA by a viral RBP, mRNA transcript accumulation (Mta). Mta is expressed by HSV1/2 (ICP27), KSHV (ORF57) and HCMV (UL69). Mta proteins bind to mRNA by

repetitive Arg-Gly-Gly motifs, or arginine-rich domains (Sandri-Goldin, 2011). Mta binding sites have been mapped throughout the viral genome, and most viral transcripts will contain at least one binding site (Sei et al., 2015; Sokolowski et al., 2003).

The sequence specificity of Mta recruitment remains unclear. ICP27 has a preference for GC-rich, unstructured RNA (Corbin-Lickfett et al., 2009). RNA crosslinking and immunoprecipitation analysis of ORF57 revealed that binding to cellular genes was generally near the first exon-intron boundary (Sei et al., 2015). While Mta makes direct contact with mRNA by an arginine and glycine-rich N-terminal domain (Sandri-Goldin, 2011), other RBPs could affect specificity of Mta binding. Mta makes direct, RNA-independent contact with hnRNPK, which is promoted by CK2-dependent phosphorylation of ORF57 (Malik and Clements, 2004) and likely ICP27 (Zhi and Sandri-Goldin, 1999). Mta post-translational modification could also alter transcript specificity.

Virus infection has limited effects on host mRNA processing as well. Ectopic ICP27, expressed outside of HSV-1 infection, inhibited intron splicing in <1% of human pre-mRNA. ICP27 also promoted usage of cryptic 5' donor sites and alternative poly-adenylation sites (Tang et al., 2016). Ectopic KSHV ORF57 seems to increase the abundance of some human pre-mRNA, which can also be observed during lytic replication (Sei et al., 2015). However, the RT-qPCR assay used for these measurements might not distinguish between increased stability of pre-mRNA or retention of introns in mature mRNA.

HSV-1 infection inhibits transcription termination, resulting in transcriptional run-off that extends tens of thousands of nucleotides into intragenic regions. The mechanism of termination inhibition is not clear, but ICP27 is not involved. The altered pre-mRNA structure can promote mis-splicing of transcripts by generating novel splice acceptor sites. Interestingly, this run-on transcription only occur on host transcripts and not on the viral episome (Rutkowski et al., 2015). While this may be due to mechanistic differences in RNA polymerase II function from human and viral promoters, it could also be a result from interference between transcription complexes from wide-spread transcription of both strands of the viral episome. Long read RNA or cDNA analysis by Nanopore sequencing could help address this issue.

Some transcripts are back-spliced where a donor site spliced to an acceptor site 5' of the donor site, generating a circular RNAs (circRNAs). circRNAs generally have lower expression than linear transcripts from the same gene, but they are broadly expressed from many genes and in many cell types. They can act as miRNA sponges, be translated, and serve as ligands for RBPs (X. Li et al., 2018). However, whether these are "functions" of circRNA or merely "effects" is unclear (Doolittle et al., 2014). Like the host mRNA, circRNAs are generated from both EBV and KSHV mRNA during both latency and lytic replication. At least for KSHV, there is currently no evidence for their translation (Tagawa et al., 2018; Toptan et al., 2018). Herpesviruses can also alter the expression of host circRNAs. KSHV latency leads to increased expression of some circRNAs. Some of the these circRNAs can limit establishment of latency after *de novo* infection. This suggests an anti-viral role for circRNAs, but induction of type-I IFN, or interferon-stimulated genes (ISG) was not observed (Tagawa et al., 2018). Whether circRNA are important regulators of herpesvirus replication, or whether there merely represent more transcriptional "noise" in infected cells is unknown.

1.4 Mechanistic Target of Rapamycin (mTOR)

1.4.1 mTOR Complex 1 (mTORC1)

mTOR is a large PI3K-family serine/threonine kinase. mTOR activity and target specificity is regulated by association with at least two large protein complexes, mechanistic target of rapamycin complex1 or complex 2 (mTORC1 or mTORC2), largely assembled through mTOR association with Raptor (mTORC1) or Rictor (mTORC2). Upstream regulatory signalling mTORC1 integrates growth signals, such as insulin and nutrient abundance. Apart from these inputs, cellular stress can limit mTORC1 activation (Sarbassov et al., 2005; Saxton and Sabatini, 2017). When active, mTORC1 kinase targets support translation, suppress autophagy, and promotes synthesis of lipids and nucleic acids. mTORC2 signalling supports cell cytoskeleton dynamics by PKC phosphorylation, but the major downstream effect of mTORC2 is phosphorylation of Akt Ser473, which promotes Akt activation (Sarbassov et al., 2005; Saxton and Sabatini, 2017).

AA abundance regulates mTORC1 recruitment to the lysosomal membrane. mTORC1 is recruited to the lysosome by Raptor interaction with two heterodimer Rag GTPase complexes, RagA/B and RagC/D. RagA/B bind to Raptor in the GTP-bound state, but not in the guanosine-diphosphate (GDP) bound state (Sancak et al., 2008). The Rag GTPases themselves are recruited to the lysosome by interaction with a pentameric Ragulator complex, which acts as a guanosine nucleotide exchange factor (GEF), promoting GTP loading for RagA/B, when AAs are abundant (Bar-Peled et al., 2012; Sancak et al., 2010). When AAs are limited, mTORC1 dissociates from the lysosome after hydrolysis of the RagA/B to GDP bound form. Hydrolysis is regulated by GATOR complex, which is made of the GAP-promoting GATOR1 complex, and the GATOR1 inhibitory complex GATOR2 (Bar-Peled et al., 2013; Fig 1.3).

Cytoplasmic AA concentration is monitored by specific sensing proteins that regulate the function of GATOR1 and GATOR2. CASTOR and Sestrins are sensors of leucine and arginine, respectively. When they are not bound to AAs, CASTOR and Sestrins inhibit GATOR2. When GATOR2 is inhibited, it cannot inhibit the GATOR1 RagA/B GAP, which stimulates GTP hydrolysis and subsequent release of mTORC1 from the lysosome. Similarly, SAMTOR is an AA sensor for methionine that when bound to AAs prevents recruitment of GATOR1 to the lysosome and preventing its RagA/B GAP activity (reviewed in J. Kim and Guan, 2018).

At the lysosomal membrane, mTORC1 kinase activity can be activated by interacting with Rheb GTPase. GTP-bound Rheb is required for mTORC1 activity, but how precisely Rheb promotes mTORC1 activity remains unclear (Saxton and Sabatini, 2017). The GTP state of Rheb is regulated by the trimeric TSC complex, comprising TSC1, TSC2, and TBC1D7 (Dibble et al., 2012), and sometimes called the Rhebulator. TSC2 is phosphorylated by a number of kinases in response to diverse cellular stimuli. TSC2 is phosphorylated and inhibited by Akt in response to insulin (Dibble et al., 2012; Inoki et al., 2002) (Fig 1.3). TSC2 is also inhibited by ERK and RSK in response to epidermal growth factor/Ras signalling (L. Ma et al., 2005). AMPK promotes TSC2 inhibition of Rheb when AMP levels are high due to glucose scarcity (Inoki et al., 2003). Several other stimuli, such as cytokine signalling and hypoxia, also affect TSC2 phosphorylation (reviewed in J. Huang and Manning, 2008). It is not fully understood

how different combinations of phosphorylation events of TSC proteins are integrated on TSC2, but the output may be limited to inhibition of Rheb at the lysosome.

TSC inhibition of mTORC1 during serum-starvation or AA scarcity requires TSC2 recruitment to the lysosome. TSC2 binds to the Rag GTPase complex in its inactive, AA-starved configuration where TSC2 acts as a GEF for Rheb. Only unphosphorylated TSC2 is recruited to the lysosome, suggesting that mTORC1 regulation integrates growth factor signalling and AA abundance at multiple levels (Demetriades et al., 2014; Menon et al., 2014). Other stresses that inhibit mTORC1 also re-localize TSC2 to lysosomes, including hypoxia, osmotic stress, or pH changes (Demetriades et al., 2015). It is unknown if this recruitment also requires an inactive Rag GTPase complex, or if TSC2 makes contact with another lysosomal protein.

mTORC1 kinase activity can be inhibited by small molecule inhibitors. The eponymous rapamycin binds to FKBP12 and forms an allosteric inhibitory complex that binds to mTORC1 (J. Kim and Guan, 2018). mTOR active site inhibitors were subsequently developed that directly inhibited kinase activity of both mTORC1 and mTORC2. Torin-1 was developed by modification of a lead compound in a small molecule screen for mTORC1 inhibitors. Torin is a highly specific and potent active site inhibitor of mTOR with an IC50 in the low nanomolar range (Thoreen et al., 2009). The degree of inhibition of mTORC1 affects the quality of its downstream signalling. The surrounding peptide sequence context of a mTORC1 phosphorylation site determines how efficiently it is phosphorylated by mTORC1. Poor sites, such as p70 S6K Thr389 are rapidly dephosphorylated by rapamycin treatment, whereas high quality substrates, such as Thr37/46 on 4E-BP are only dephosphorylated by starvation or active-site mTOR inhibitors (S. A. Kang et al., 2013).

1.4.2 Regulation of Translation Initiation by mTORC1

Active mTORC1 supports translation by phosphorylating p70 S6 Kinase (S6K) and phosphorylation and inactivation of the eIF4E binding protein, 4E-BP1. Phosphorylation of S6K liberates eIF3 to participate in initiation complexes. S6K promotes phosphorylation of eIF4B, small ribosomal protein S6, and a variety of other translation-promoting proteins (Holz et al., 2005). This has little effect on bulk protein

synthesis but may regulate translation of subsets of transcripts. eIF4F disruption by unphosphorylated 4E-BP1 is the primary means of translation regulation by mTORC1; in 4E-BP knockout cells, both Torin and Rapamycin fail to inhibit translation (Thoreen et al., 2012).

Hypophosphorylated 4E-BP1 binds to eIF4E1 by a YXXXXLϕ motif at the same site as eIF4G1 and prevents eIF4F formation (Merrick, 2015; Pause et al., 1994; Peter et al., 2015)(Fig 1.1B). 4E-BP has four mTORC1-dependent phosphorylation sites: Thr37/46, Ser65, Thr70. Thr37/46 phosphorylation is required for subsequent Ser65 and Thr70 phosphorylation (Gingras et al., 2001). Active site mTOR inhibitors like Torin cause complete dephosphorylation and inhibition of protein synthesis (Thoreen et al., 2009). Rapamycin does not inhibit mTORC1 sufficiently to observe complete loss of 4E-BP1 phosphorylation; Ser65 and Thr70 are both sensitive to rapamycin and serum starvation, but both Thr37 and Thr45 are high quality mTORC1 substrates and are insensitive to rapamycin (Gingras et al., 2001; S. A. Kang et al., 2013).

Unphosphorylated 4E-BP1 tightly binds to eIF4E, by a disordered-to-ordered transition of a YXXXXLϕ eIF4E1-binding motif (Bah et al., 2014); 4E-BP1 phosphorylation sites are outside of this motif (Sekiyama et al., 2015). In unphosphorylated 4E-BP2 (and likely 4E-BP1), the disordered YXXXXLϕ motif forms an ordered helical domain upon interaction with eIF4E1. Thr37/46 phosphorylation reduces the affinity of 4E-BP1 for eIF4E by 100-fold and buries the YXXXXLϕ motif in a beta-sheet, although this structure is unstable; further phosphorylation of Ser66 and Thr70 enhances stability of this structure. Thr37/46 can be phosphorylated when 4E-BP1 is bound to eIF4E (Gingras et al., 1999), suggesting a mechanism for disassembly of 4E-BP1 from eIF4E when mTORC1 activity is restored.

There are two homologues of 4E-BP1, 4E-BP2, and 4E-BP3. 4E-BP2 is the dominant isoform of 4E-BP in T and B lymphocytes. Phosphorylation of 4E-BP2 Thr37/46 is lost with rapamycin treatment while the homologous phosphorylation site in 4E-BP1, Thr36/45, remains phosphorylated. As a result, rapamycin has a potent inhibitory effect on protein synthesis in lymphocytes, similar to active-site mTOR-inhibitors. This effect is due to difference in the surrounding AAs (S. A. Kang et al., 2013; So et al., 2016). 4E-BP3 is transcriptionally upregulated during mTORC1

inhibition; 4E-BP3 protein also accumulates despite eIF4F disassembly. Like 4E-BP1 and 4E-BP2, 4E-BP3 binds to eIF4E1 and contributes to inhibition of protein synthesis during prolonged mTORC1 inhibition (Poulin et al., 1998; Tsukumo et al., 2016).

After scanning has initiated by the PIC, it appears that eIF4F is disassembled. This would expose eIF4E to regulation by the 4E-BP. Without eIF4F disassembly, 4E-BP1 would only prevent translation prior to the first round of eIF4F recruitment and would be unable to deplete mRNA from polysomes (Merrick, 2015). eIF4E may or not remain attached to the cap as it losses m^7GTP affinity when not associated with eIF4G (Haghighat and Sonenberg, 1997). Dissociation of eIF4F, might allow for association of alternative translation initiation complexes.

1.4.3 5' Tract of Oligopyrimidines (TOP) mRNA

While general protein synthesis is reduced when mTORC1 is inhibited, there is a greater decrease in a specific subset of proteins bearing a 5'-terminal oligopyrimidine (TOP) motif (Hsieh et al., 2012; Thoreen et al., 2012). Transcripts encoding ribosomal proteins and TIFs are especially enriched for TOP motifs (Yamashita et al., 2008). Translation suppression of TOP mRNAs are mediated by the cap-binding protein LARP1, which makes contacts with both the cap and adjacent nucleotides (Lahr et al., 2017; Philippe et al., 2017; Tcherkezian et al., 2014). LARP1 cap-binding likely prevents engagement of non-eIF4F translation initiation complexes, enforcing suppression of TOP mRNA during mTORC1 inhibition.

1.4.4 Regulation of Autophagy by mTORC1

Autophagy is a self-digestive mode of catabolic degradation and turnover. During autophagy cytoplasmic contents are enveloped within a double membrane vesicle, or autophagosome, which is then delivered to lysosome. Fusion of the autophagosome with the lysosome leads to degradation of autophagosome contents by hydrolytic enzymes. Autophagy is a regulated by highly conserved autophagy-related genes through several sequential events. Initiation of autophagy leads to recruitment of autophagy initiation proteins to the site of phagophore nucleation. This phagophore expands and isolates a portion of the cytoplasm that is enriched in cargo by specific autophagy adaptor proteins.

After sealing of the isolation membrane, the autophagosome fuses with a lysosome where its contents are degraded (Dikic and Elazar, 2018; Levine et al., 2011).

Stress, especially nutrient withdrawal or infection, initiates autophagy. mTORC1 normally inhibits autophagy by directly phosphorylating Atg13 and the Unc-51-like-kinase (ULK1), and restricts its kinase ability (Ganley et al., 2009; Hosokawa et al., 2009). ULK1, and its functionally redundant homologue ULK2, phosphorylate-= a broad array of autophagy related proteins, including Atg13 and FIP200, with which it forms a complex (Ganley et al., 2009; Hosokawa et al., 2009; Zachari and Ganley, 2017). ULK1 promotes autophagy initiation by phosphorylating a regulatory protein, Beclin1, of phagophore nucleation complex that includes Atg14 and the lipid kinase Vps34 (Russell et al., 2013). It remains unclear precisely which cellular membrane serves as the phagophore assembly site (PAS); it is possible that multiple membrane compartments can serve this purpose. Starvation stress, for example, uses a mitochondrial-ER contact site as the PAS (Hamasaki et al., 2013). The phagophore then expands around its cargo using membrane delivered from Atg9 containing vesicles. The growing isolation membrane is coated in by the ubiquitin-like protein LC3. The C-terminal two amino acids of LC3 (also called LC3-I) are first removed by the Atg4 protease; LC3 is then passed by the E1-like Atg7 to the E2-like Atg3 protein. Atg3 conjugates phosphoethanolamine (PE) to the newly-exposed LC3 carboxy-terminus. LC3-PE (also called LC3-II) is then inserted into the isolation membrane. Atg7 also functions as an E1 for Atg5, which is conjugated to Atg12; the Atg12-Atg5 conjugate is required to recruit Atg3 to the isolation membrane. Sealing of the autophagosome is still poorly understood.

mTORC1 inhibition indirectly supports autophagy by promoting transcription of autophagy-related genes, including lysosomal genes. This is directed by mTORC1 phosphorylation of the transcription factor TFEB, which prevents shuttling to the nucleus. Nuclear TFEB enhances transcription of many autophagy and lysosomal genes (Settembre et al., 2012). mTORC1 inactivation limits protein synthesis; it is not clear if these transcripts are preferentially translated during mTORC1inhibition. Past studies on the mTORC1-dependent translatome use short drug treatments to limit the effect on transcription (Hsieh et al., 2012; Thoreen et al., 2012). It is possible that extended

mTORC1 inhibition, or the translation of nascent transcripts might be differentially regulated.

During starvation, or mTORC1 inhibition, autophagic cargo is thought to be generally non-specific. However, autophagy can specifically be engaged to remove damaged organelles or infectious material from the cytoplasm. Ribosomes, damaged mitochondria, ER membrane, bacteria, and viruses are all cleared by autophagy (Dikic and Elazar, 2018; Wyant et al., 2018). LC3-II on the isolation membrane functions as a protein-receptor for the autophagosome. LC3-interacting proteins, such as p62, can bridge cargo, often decorated with ubiquitin, and LC3.

Viruses have a complicated relationship with autophagy. Single-stranded positive sense viruses tend to promote autophagy and benefit from its activation (Deretic and Levine, 2009). Some of these viruses repurpose autophagy-related proteins to promote extensive membrane remodelling in the cytoplasm, but without induction of typical macroautophagy (Abernathy et al., 2019). Autophagy is generally thought to be restrictive for herpesviruses. Some capsids have been detected in autophagosomes by transmission electron microscopy, and degradation of viral proteins by autophagy may create ligands for MHC-I presentation (Deretic, 2012; Deretic and Levine, 2009; Levine et al., 2011). Herpesviruses generally limit autophagy through the actions of viral proteins that bind to and inhibit essential autophagy proteins; Beclin-1 appears to be a target of convergent evolution of many herpesviruses (Orvedahl et al., 2007; Pattingre et al., 2005a). However, what is being degraded by autophagy and how this limits herpesvirus infection remains unclear.

1.4.5 Regulation of mTORC1 by Herpesviruses

Members of all three subfamilies of Herpesviridae regulate mTORC1 signaling, generally supporting or mimicking its activation during lytic replication. HCMV UL38 inhibits TSC2, activating mTORC1 and maintaining activation during serum starvation (Moorman et al., 2008). HCMV can also maintain mTORC1 activation during AA starvation, or following silencing of RagA and RagB (Clippinger et al., 2011). mTORC1 activation is required for eIF4F assembly during HCMV infection (Lenarcic et al., 2014; Moorman and Shenk, 2010). Like UL38, HSV-1 Ser/Thr kinase Us3 phosphorylates and

inactivates TSC2 to maintain mTORC1 activity and eIF4F formation (Chuluunbaatar et al., 2010). Us3 also maintains mTORC1 activation during starvation and high AMP:ATP ratios during AA starvation, in conjunction with UL46 (Vink et al., 2018; 2017). Us3 seems to act as a general Akt mimic and phosphorylates several Akt substrates, including TSC2 (Chuluunbaatar et al., 2010). Us3 and UL38 interaction and phosphorylation of TSC2 likely prevents its lysosomal association and may bolster mTORC1 activation during the stress of lytic replication.

Active-site mTOR inhibitors limit HCMV virus replication when present during early infection, but viral protein synthesis is more resistant to mTOR inhibition after infection is established (Lenarcic et al., 2014; Moorman and Shenk, 2010). Rapamycin has little effect on HSV1 or HCMV replication (Moorman and Shenk, 2010; Walsh, 2004). mTORC1 activation is required to maintain HSV1 latency in neurons (Kobayashi et al., 2012).

mTORC1 activation is a hallmark of KSHV infection (Arias et al., 2009); several KSHV gene products have been shown to stimulate or mimic mTORC1 activation and mTORC1 substrates are phosphorylated in KS lesions (Stallone et al., 2005). KSHV early lytic gene products K1 and vGPCR activate mTORC1 by stimulating Akt (Martin et al., 2013; Z. Zhang et al., 2016). Moreover, two other viral proteins partially mimic mTORC1 signaling. The viral Ser kinase ORF36 has limited homology to the mTORC1 substrate p70 S6K and phosphorylates a similar array of substrates, analogous the Akt mimicry by HSV1 Us3 (Bhatt et al., 2016). By contrast, ORF45 assembles an activated complex of ERK and RSK to stimulate phosphorylation of eIF4B and ribosomal protein S6, which are normally phosphorylated in an mTORC1/p70S6K1 dependent manner (Kuang et al., 2008). ORF45 is also required for mTORC1 activation in latently infected LECs, though it is unclear how this effect is mediated (H. H. Chang et al., 2013).

mTORC1 has a key role in KS progression. Treatment of KS from transplant patients with rapamycin is sufficient for rapid tumor regression (Stallone et al., 2005). Similarly, PEL cells require mTORC1-dependent paracrine signalling to maintain growth (Sin et al., 2007). Rapamycin treatment leads to a loss of phosphorylation on mTORC1 kinase targets in both vGPCR-expressing endothelial cells and latently-infected nude mouse xenografts (Martin et al., 2013; Roy et al., 2013). Interestingly, constitutive

mTORC1 activation in endothelial cells is sufficient to drive lymphangiosarcomas that are phenotypically similar to KS. These cells proliferate from mTORC1-dependent expression of VEGF-A (Sun et al., 2015). Similar to KS, tumours regress when mTORC1 is inhibited by rapamycin (Stallone et al., 2005; Sun et al., 2015). However, KS tumourigenesis in humans is likely more complex.

Activation of mTORC1 by herpesviruses should also decrease activation of autophagy, however inhibition of autophagy downstream of ULK1 and Atg13 could largely mask this effect. At least three KSHV proteins modulate autophagy. vFLIP prevents LC3 processing and conjugation by Atg3 (J.-S. Lee et al., 2009) during latency, thereby suppressing cell death and oncogene-induced senescence (Leidal et al., 2012). During lytic replication, K7 binds to Rubicon and prevents autophagosome maturation and the viral Bcl-2 homologue vBcl-2 inhibits autophagosome nucleation through its interaction with Beclin (Q. Liang et al., 2013; 2015).

Comparatively little is known on the role of mTORC2 in herpesvirus infection. mTORC2 could be involved in regulating type-I IFN responses to DNA viruses. Activated Akt phosphorylates cGAS, which limits its enzymatic activity; Akt inhibition during HSV-1 infection increases type I IFN production (Seo et al., 2015). mTORC2 itself is required for trafficking and signalling from TLR-3 after recognition of dsRNA generated during HSV-1 infection in neurons, which is required for a type I IFN response in these cells (Sato et al., 2018). In HSV-1 infections of Rictor knockout cells, Us3 might mask reduced Akt signalling. mTORC2 is also required for ISG production in response to type-I IFN (Kaur et al., 2012). There is also some evidence the mTORC2 can support herpesvirus replication. Rictor knockdown reduces HCMV virion production in multi-round replication in HFF (Kudchodkar et al., 2006). KSHV K1 is required for Akt phosphorylation at Ser473 during lytic replication, which is phosphorylated by mTORC2; K1 is also required for virion production, indirectly suggesting that mTORC2 might be important for KSHV replication (Tomlinson and Damania, 2004). vGPCR likely also signals through mTORC2 as it stimulates Akt Ser473 phosphorylation, (Sodhi et al., 2004); it is not clear if TSC2 is phosphorylated during KSHV replication independent of Akt. In general, it appears that any antiviral action of mTORC2 is dependent on Akt activation.

1.5 Non-eIF4F Mechanisms of Translation Initiation

eIF4F is the predominant means of translation initiation of rapidly dividing cells, grown in tissue culture, in atmospheric oxygen tension (~21%). It is responsible for approximately 60% of bulk protein synthesis under these conditions (Thoreen et al., 2012; Uniacke et al., 2013). However, various stresses can stimulate other translation initiation mechanisms either to persist, or become active, when eIF4F is not active. All of these initiation systems are regulated by distinct sets of TIFs and many promote specific translatomes (Fig 1.4).

1.5.1 Internal Ribosomal Entry Sites

Internal ribosomal entry sites (IRES) are highly structured RNA cis-elements that directly recruit and position the small ribosomal subunit at, or upstream, of the start codon without the involvement of the m^7GTP cap. These elements are common in single-stranded, positive sense viruses, including picornaviruses, dicistroviruses, and hepatitis C virus. The requirement of IRES RBPs or initiation factors varies. Some picornavirus IRESs require almost all cap-dependent initiation factors, while dicistrovirus can directly recruit, and assemble a 80S ribosomes from large and small ribosomal subunits (reviewed in (Jan et al., 2015).

KSHV contains one confirmed IRES in the bicistronic, latent transcript that encodes v-cyclin and FLIP. The IRES is present with the coding region of v-cyclin for translation of the co-cistronic vFLIP (Bieleski and Talbot, 2001; Grundhoff and Ganem, 2001; Low et al., 2001). The IRES makes direct contact with eIF4E, eIF4G1, eIF3 and the small ribosomal subunit; this is the first IRES described to require eIF4E (Othman et al., 2014). The presence of an IRES in an DNA virus is unusual and few examples are described. No other IRES elements have been detected in KSHV despite significant nesting of transcripts due to shared promoters and polyA sites (Arias et al., 2014).

While the structures and molecular mechanisms of viral IRES are well described, the existence of IRES in human mRNA is more controversial (Gilbert, 2010; Shatsky et al., 2018; Terenin et al., 2016). IRESs are often evaluated using a plasmid-based bicistronic reporter, where a strong promoter drives an mRNA containing, from 5’ to 3’,

Renilla with a stop codon, the putative IRES, and luciferase. Only the 5' Renilla cassette should be translated under normal conditions, unless the IRES element can recruit a ribosome downstream from the Renilla stop codon. While viral IRES are potent and provide a clear signal, putative cellular IRES are generally much weaker, providing more opportunity for artifacts to emerge. Putative IRES elements can contain cryptic splice sites, or promoter elements that can enhance expression of the downstream luciferase independent of IRES activity. The differences in sensitivity between detecting luciferase activity by luminometer compared to sensitivity of a northern blot to confirm that only a single RNA species is generated by the bicistronic promoter can contribute misidentification of IRESs (Gilbert, 2010; Terenin et al., 2016).

Human mRNA assumed to contain an IRES often have long, highly structured 5'UTRs, or uORFs that could impede scanning to the main ORF. However, cellular transcripts with putative-IRES are still capped, and mRNA secondary structure could be altered during stress, or be required for recruitment of proteins that promote cap-, and scanning-dependent translation initiation (Gilbert, 2010). Knowing this, cellular IRES might better be re-conceived as cap-independent translation-enhancers (CITE), or RNA elements that promote recruitment to ribosomes when eIF4F-dependent translation is limited (Shatsky et al., 2018). The activity of some putative IRESs are cell type-dependent, and some respond differently during cellular stress (Nevins et al., 2003). Engagement of non-eIF4F TIFs that become active during stress are likely responsible for sustained translation when eIF4F is depleted.

1.5.2 eIF4G2-dependent Translation

eIF4G2 (also known as p97, NAT1, or DAP-5) is a homologue of eIF4G that retains the central MIF4G domain and C-terminal domains of eIF4G1 but lacks the eIF4E- and PABP-binding N-terminal domain. This precludes the eIF4G2 forming an eIF4F-like construct, but allows for recruitment of eIF4A and eIF3 to the central domain, and Mnk1 to the C-terminal domain (Imataka et al., 1997; Levy-Strumpf et al., 1997; Pyronnet et al., 1999). eIF4G2 cannot be isolated with m^7GTP-conjugated Sepharose suggesting that it does not strongly associate with a non-eIF4E cap-binding protein (Liberman et al., 2015a).

eIF4G2 abundance has no effect on ectopically expressed cap-dependent luciferase reporters, but eIF4G2 depletion has a small effect on bulk protein synthesis (S. H. Lee and McCormick, 2006; Liberman et al., 2015b; Parra et al., 2018). eIF4G2 is instead required for some cap-independent translation, including that of putative IRES-containing mRNA for Bcl2 and Cdk1. (Marash et al., 2008) This activity of eIF4G2 requires eIF4A and eIF2β (Liberman et al., 2015a). However, eIF4G2 is present in polysomes during non-stressful conditions (S. H. Lee and McCormick, 2006). Translation of eIF4G2 itself is promoted by cellular stress, such as oxidative, endoplasmic reticulum (ER), or heat stress (Lewis et al., 2007; Nevins et al., 2003). Caspases activated during these stresses, such as the apoptotic caspase 3, can act on eIF4G2 to generate an N- and C-truncated middle fragment that retains some the ability to enhance translation of cellular transcripts with a putative IRES. Notably, caspase-cleaved eIF4G2 enhances the activity of the eIF4G2 IRES, or CITE (Henis-Korenblit et al., 2002; Nevins et al., 2003). Upregulation of eIF4G2 during endoplasmic reticulum stress is, however, caspase-independent (Lewis et al., 2007). Caspase activity caused by virus replication or cleavage of eIF4G1 or eIF4G3 by viral proteases can cause accumulation of truncated eIF4G species with similar domain architecture of the N-terminal truncated eIF4G2, and potentiate IRES activity (Haghighat et al., 1996; Nevins et al., 2003). eIF4G2 is also required for eIF3d-dependent translation as discussed below (Parra et al., 2018).

1.5.3 Translation during Hypoxia

1.5.3.1 eIF4E2-dependent Translation

During hypoxia, where low atmospheric oxygen reduces the oxygen tension in cell culture media, protein synthesis is reduced approximately 60% with a concomitant loss of mTORC1 activity and eIF4F formation (Uniacke et al., 2013). Hypoxia causes stabilization of hypoxia inducible factors (HIF) by inhibiting HIF hydroxylation by oxygen-dependent prolyl hydroxylase activity; hydroxylated HIF is recruited to, and ubiquitinated by, the E3 ligase VHL, which directs HIF degradation by the 26S proteasome (Gossage et al., 2015). Suppression of mTORC1 activity is caused by *de novo* expression of the HIF-1α responsive gene (HRE) REDD1, which limits mTORC1

activation by promoting activity of the inhibitory TSC2 (Brugarolas et al., 2004; DeYoung et al., 2008).

The remaining 40% of protein synthesis requires stabilization of HIF-2α, which promotes formation of an hypoxic eIF4F ($eIF4F_H$) comprising eIF4E2 (also known as 4E-homologous protein, 4E-HP), eIF4A1, and eIF4G3. Both HIF2α and eIF4E2 is required for protein synthesis during hypoxia where eIF4F is disrupted (Ho et al., 2016; Uniacke et al., 2013). Unlike eIF4E1, hypophosphorylated 4E-BP1 does not appear to bind to eIF4E2, which likely spares $eIF4F_H$ from mTORC1-dependent regulation (Uniacke et al., 2013). eIF4F and $eIF4F_H$ promote distinct but overlapping translatomes, whereby global changes in mRNA TE, and not only transcriptional differences, drive changes in protein output in response to hypoxia (Ho et al., 2016). eIF4E2 is required for establishment of the hypoxic core or *in vitro* spheroid culture, and solid tumours (Uniacke et al., 2014).

eIF4E2-dependent translation does not necessarily require the loss of eIF4F-dependent translation. During low oxygen tension (5-7%) that is insufficient to inactivate mTORC1 but is sufficient to inactivate prolyl hydroxylases, both eIF4E2 and eIF4E1 can be detected in polysomes. These oxygen tensions are more common in the body than ~21% atmospheric oxygen (Timpano and Uniacke, 2016). Lack of mTORC1 should lead to the accumulation of unphosphorylated 4E-BP1 in hypoxic cells; however, 4E-BP1 does not bind to eIF4E2 (Uniacke et al., 2013). It is unclear if other 4E-binding proteins regulate eIF4E2.

eIF4E2 can also associate with mRNA as a component of the CCR4-NOT complex where it is required for translational silencing of mRNA by miRNAs (Chapat et al., 2017). eIF4E2 also forms a cap-binding complex with the RBP GIGYF2 (Morita et al., 2012), that binds to, and is required for tristetraprolin (TTP)-dependent destabilization of ARE-containing mRNA (R. Fu et al., 2016). The affinity of eIF4E2 for the m^7GTP cap is 30-100 fold lower than eIF4E1 (Zuberek et al., 2007). eIF4E2 cap-affinity increases when the protein is modified by ISG15ylation, which slightly enhances its translation-inhibitory effects during normoxia (Okumura et al., 2007). A similar increase in affinity for the cap might be expected during hypoxia when HIF2α or GYGYF2 associates with eIF4E2, but this has not yet been demonstrated.

1.5.3.2 Hypoxia Response Elements in KSHV

KSHV contains several HREs, including in the promoter region of the IE gene RTA (Haque et al., 2003; Veeranna et al., 2011). Hypoxia enhances spontaneous or TPA-induced reactivation from latently-infected PEL cells (D. A. Davis, 2001), but the viral titers are very low, and a low percentage of the cells reactivate. The RTA promoter also contains XBP1-response elements that respond to spliced XBP1 that accumulates during ER stress caused by low oxygen (Dalton-Griffin et al., 2009; Haque et al., 2003). Furthermore, KSHV latency enhances stability of HIF1α, and KSHV lesions accumulate HIF1α and HIF2α (Carroll et al., 2006). Some KSHV gene products directly interact with HIF1α; vIRF3 and LANA both promote stabilization (Q. Cai et al., 2006; Y. C. Shin et al., 2008), whereas ORF34 promotes HIF1α ubiquitination and degradation in the proteasome (Haque and Kousoulas, 2013). Taken together, this suggests that KSHV lytic replication is competent for hypoxic translation, but whether $eIF4F_H$-dependent translation is required is unknown.

1.5.4 eIF4E3 Translation during MNK1 Activation

eIF4E3, like eIF4E2, is a homologue of eIF4E1. Less is known about its function than eIF4E1 or eIF4E2. Translation of eIF4E3 mRNA is under the control of Mnk1, a map-kinase activated kinase that is recruited to eIF4F by the C-terminal domain of eIF4G, whereby Mnk1 inhibition leads to an accumulation of eIF4E3 protein but not mRNA (Landon et al., 2014; Pyronnet et al., 1999). This is suggested to be due to alterations in the TE of eIF4E3 mRNA due to loss of eIF4E1 Ser209 phosphorylation (Landon et al., 2014). Over-expression of eIF4E1 or eIF4E3 produced slightly different populations of mRNA in the polysomes, but the majority of the changes seem to be due to differences at the transcription level (Landon et al., 2014). It also is not clear how overexpressing eIF4E1 alters the stoichiometry of eIF4E1 and Mnk1 and how this affects the saturation of eIF4E1 Ser209 phosphorylation. Further work will be needed to distinguish the loss of eIF4E1 phosphorylation from accumulation of eIF4E3 on the translatome.

1.5.5 Pioneer Translation

After export from the nucleus, mRNA bound either to eIF4E or the nuclear cap-binding complex (NCBP) are translated for the first time. This pioneer round of translation serves as a quality control step where exon-junction complexes are removed and transcripts containing premature termination codons are degraded. Both NCBP1- and eIF4E-bound transcripts are ligands for nonsense mediated decay (Durand and Lykke-Andersen, 2013; Ishigaki et al., 2001; Rufener and Mühlemann, 2013). In addition to a mechanism of protein quality control, NMD ligands are a significant source of peptide antigens for MHC-I presentation (Apcher et al., 2011).

NCBP-dependent translation requires a MIF4G-domain containing protein, CTIF, which recruits NCBP complex to the 43S PIC by bridging NCBP1 and eIF3g (Choe et al., 2012; K. M. Kim et al., 2009). CTIF is required for NCBP1 sedimentation with polysomes, but has little effect on bulk protein synthesis (K. M. Kim et al., 2009). CTIF recruits the eIF4AIII helicase, which is required for NCBP1 recruitment to polysomes, but CTIF does not bind to eIF4AI (Choe et al., 2014). NCBP1 has also been demonstrated to associate with eIF4G1 and eIF4G3 both *in vitro* or isolated from African Green Monkey fibroblasts (Cos cells), but whether this is required for recruitment of NCBP1 to polysomes has not been demonstrated (Lejeune et al., 2004). NCBP-dependent translation might also represent a stress-resistant mode of translation initiation as it should be exempt from 4E-BP1 regulation. NCBP-dependent translation was assumed to function during serum starvation and hypoxia on the basis that NMD occurs under these conditions (Oh et al., 2007a; 2007b); however, given that NMD can occur in a non-NCBP dependent manner it remains unclear how NCBP-dependent translation responds to stress.

NCBP-dependent translation has been suggested to be involved in the translation of the Gag protein from HIV. NCBP1 co-transfection enhances translation from a Gag luciferase reporter and NCBP1 co-localizes with Gag mRNA in the cytoplasm (Toro-Ascuy et al., 2018). HIV Gag mRNA can be detected on immunoprecipitated NCBP1, as well as eIF4E, and both cap-binding proteins can be detected in HIV virions. As both NCBP1 and eIF4E are present in the polysomes during HIV infection it is unclear if NCBP1 is directly involved in translating Gag (A. Sharma et al., 2012). In other reports,

neither NCBP1 nor eIF4E can be found in association with Gag mRNA and instead the helicase DDX3 co-localizes with the mRNA, along with eIF4G1 and PABPC (Soto-Rifo et al., 2013). A role for pioneer or NCBP-dependent translation in herpesviruses has not been described.

1.5.6 eIF3d-dependent Translation

eIF3d is a component of the thirteen subunit eIF3 complex. The eIF3 complex is the largest TIF; however, not all thirteen of these subunits are required for recruiting the small ribosomal subunit to mRNA. A minimal *in vitro* system with a functional core of six eIF3 proteins, eIF3a, eIF3b, eIF3c, eIF3e, eIF3f, and eIF3h is sufficient (Cate, 2017; Masutani et al., 2007) with eIF3a and eIF3b forming an essential core for the nucleation of a functional eIF3 complex (Wagner et al., 2016). eIF3d is a more peripheral factor that, while not required for eIF3 assembly, can limit protein synthesis and proliferation in its absence (Wagner et al., 2016). The role of the six core and other non-core eIF3 proteins seem to have various roles in promoting translation under specific situations or in cancer cell lines (reviewed in Hershey, 2015).

eIF3d is one of the four subunits (in addition to eIF3a, eIF3b, and eIF3g) that have been demonstrated in RNA-protein cross-linking experiments to make direct contact with mRNA (A. S. Y. Lee et al., 2015). However, they do not interact with all translating mRNA and only several hundred examples have been identified. These contact sites are largely limited to the 5'UTR of the mRNA, and crosslinking mRNA have only limited overlap between the eIF3 subunits. These contacts either promote or inhibit translation in a transcript-specific manner (A. S. Y. Lee et al., 2015). Unique among these four subunits, eIF3d also binds directly to the m^7GTP cap of mRNA by a conserved cap-binding domain. Access to the cap-binding pocket appears to be limited to mRNA possessing appropriate secondary structures in the 5'UTR. For example, c-Jun has a stem-loop that limits eIF4E cap-binding, but promotes eIF3d cap-binding (A. S. Y. Lee et al., 2016). A specific motif has not been identified for eIF3d-dependent translation and it is not clear if eIF3d binding always requires limited eIF4E binding; this phenomenon could be highly transcript-dependent. Interestingly, the eIF4G2-dependent translatome includes several eIF3d-dependent transcripts (Parra et al., 2018). eIF3d and eIF4G2 can

be directly chemically-crosslinked in cells, suggesting a functional dependence (Parra et al., 2018).

It is difficult to determine whether the small loss of protein synthesis cause by eIF4G2 depletion is due to loss of a small subset of specific, stress-mitigating proteins or if it is due to the loss of eIF3d-dependent translation. As eIF4G2 does not pulldown with m^7GTP-Sepharose, despite strong direct association as demonstrated by chemical-crosslinking (Parra et al., 2018), it is likely that m^7GTP Sepharose cannot access the cap-binding pocket of eIF3d.

1.5.7 N6-Methyladenosine (m^6A)

1.5.7.1 N6-Methyladenosine-dependent Translation

mRNA can be modified by RNA modifying enzymes. Many have been detected, and the functional consequences of these modifications is largely unclear, but their presence suggest an "epitranscriptome" modifying gene expression analogous to the DNA epigenome (Gilbert et al., 2016). N6-methyladenosine (m^6A) is a prominent mRNA modification, especially enriched near the transcription-start site and the stop-codon. m^6A is enriched in the RRACH motif where "R" represents a purine and "H" represent a non-guanine nucleoside; a methyl group is added to the central adenine (Dominissini et al., 2012; Meyer et al., 2012). m^6A is "written" on mRNA a nuclear complex containing the heterodimer of METTL3 and METTL14; METTL3 is catalytic unit, METTL14 enhances stability of the complex (J. Liu et al., 2013).

m^6A marks were first localized by deep-sequencing mRNA immunoprecipitation of mRNA with an m^6A-specific monoclonal antibody and measuring enrichment over a non-specific control antibody (Dominissini et al., 2012; Meyer et al., 2012). While this approach can identify enrichment on transcripts, it lacks a per-transcript quantitation; it is not possible to determine what percentage of a given mRNA species is modified (Gilbert et al., 2016). Marks are not permanent and can be removed by m^6A demethylases or "erasers", FTO and ALKBH5 *in vitro*. FTO and ALKBH5 depletion also increases m^6A abundance in cell culture (Jia et al., 2011; Zheng et al., 2013). Changes in the epitranscriptome may occur during stress, in what is likely a context and transcript-specific manner. While AA starvation leads to a global increase in 5'UTR m^6A and a

reciprocal decrease in 3'UTR m^6A, reduced methylation of m^6A in the 5' UTR uORF ATF4 by ALKBH5 promotes translation of the main ATF4 CDS (J. Zhou et al., 2018). Changes to m^6A abundance on a given mRNA is commonly described as dynamic as changes can be observed in a population of mRNA in over time, and both FTO and ALKBH5 can directly act on m^6A in a mRNA polymer. However, as both FTO and ALKBH5 appear to have exclusively nuclear localization (Jia et al., 2011; Zheng et al., 2013), it is not clear if a cytoplasmic mRNA can have an m^6A mark "erased" after nuclear export. Similarly, METTL3 binds directly to specific TSS sites on chromatin, which seems to co-translationally write m^6A modifications on resulting transcripts (Barbieri et al., 2017). It is not clear if m^6A can be added to mRNA after nuclear export.

m^6A modification has been shown to reduce mRNA stability or to enhance TE. These effects are mediated by RBPs that act as m^6A "readers". Members of the YTH domain family proteins, including YTHDF1, YTHDF2, YTHDF3, and YTHDC1 are prominent m^6A readers (Dominissini et al., 2012; X. Wang et al., 2015). m^6A modification can reduce transcript stability by promoting recruitment of CCR4-NOT deadenylation complex through YTHDF2 (Du et al., 2016; X. Wang et al., 2013). YTHDF1 binding to m^6A modifications can enhance translational efficiency of mRNA (X. Wang et al., 2015). Other nucleoside modifications, N4-acetylcytidine and N1-methyladenosine, can also alter translational efficiency of mRNA (Arango et al., 2018; Dominissini et al., 2016). This suggests that the relationship between mRNA modification and the fate of a given mRNA is complex, likely to be transcript specific, and include inputs from RBPs and TIFs.

Presence of a modified m^6A in the 5'UTR of mRNA can promote cap-independent, but scanning-dependent, translation initiation. eIF4F components are not required; interaction with eIF3 within a 43S PIC is sufficient in a minimal *in vitro* system (Meyer et al., 2015). As 5' to 3' scanning is required, m^6A does not function as an IRES. However, m^6A has been reported to be required for translation of back-spliced circular mRNA in a eIF4G2-dependent manner (Y. Yang et al., 2017). m^6A outside the 5'UTR can also modify translational efficiency of mRNA by the actions of m^6A-readers. The m^6A reader YTHDF1 can interact in an RNA-independent way with eIF3 and promote enhanced translational efficiency of target m^6A-modified mRNA (X. Wang et al., 2015).

The catalytic subunit of the m^6A writer, METTL3, can also bind to m^6A modifications on mRNA independent of its own catalytic ability to promote translation initiation without other m^6A reader proteins (S. Lin et al., 2016). This METTL3-dependent initiation requires ABCF1, which potentially is required to recruit eIF2 (Coots et al., 2017). METTL3 recruits eIF3 to m^6A-modified mRNA by bridging m^6A and eIF3h (Choe et al., 2018). METTL3 does not bind the m^7GTP cap (Coots et al., 2017), and METTL3-initiated mRNA can retain either eIF4E1 or NCBP1 on the cap (Choe et al., 2018). Recruitment of eIF3 by m^6A readers may still require the activities of other TIFs; translation of transcription repressor FOXO3 requires the actions of m^6A reader YTHDF3 and both eIF4G2 and PABPC (Y. Zhang et al., 2018).

In normoxia, when mTORC1 is inhibited, and eIF4F is disrupted, both METTL3 and ABCF1 are required for the residual protein synthesis (Coots et al., 2017). However, it is not clear if mRNAs that are being initiated in an eIF4F-independent manner are being initiated at an m^6A modification; it remains possible that these transcripts are initiated by factors that themselves are METTL3 or m^6A dependent. Outside of stress, METTL3 promotes translation of a subset of eIF4F-independent transcripts (Choe et al., 2018).

1.5.7.2 N6-Methyladenosine Modification of Viral Genomes and mRNA

Like cellular mRNA, the genomes of RNA viruses can also be modified METTL3. m^6A observed on positive-sense, single-stranded RNA genomes, including retroviruses, enteroviruses, and flaviviruses (Gokhale et al., 2016; Hao et al., 2018; Kennedy et al., 2016). The genome of the negative sense RNA virus influenza A also contains internal m^6A modifications (Courtney et al., 2017; Krug et al., 1976). The effects of m^6A modifications are virus-specific and some experimental results are somewhat contradictory. Mutating m^6A sites on enterovirus 71 reduces virus titer, but knockdown of known m^6A readers enhances titer (Hao et al., 2018). m^6A readers promotes HIV replication, while they suppress flavivirus replication (Gokhale et al., 2016; Kennedy et al., 2016). Viral proteins might be required to recruit METTL3 to sites of viral mRNA synthesis; the 3D polymerase of EV71 recruits METTL3 to sites of replication where m^6A modification is likely co-transcriptional (Hao et al., 2018). It is

unclear how METTL3 is recruited to sites of flavivirus replication, which occurs in specialized, membranous cytoplasmic compartments (Welsch et al., 2009). Confounding these studies was the unrecognized role of m^6A in regulating the type-I IFN response. m^6A is required for destabilizing IFN-β (Rubio et al., 2018; Winkler et al., 2018). Similarly, loss of the m^6A reader YTHDF3 has a similar effect on IFN-β (Y. Zhang et al., 2018). Increased IFN-β enhances expression of a broad array of ISGs; it remains unknown if m^6A also effects mRNA encoding these ISGs.

Some mRNA transcribed from DNA viruses, including SV40 and KSHV, contain m^6A modifications (Hesser et al., 2018; Tan et al., 2017; Tsai et al., 2018; Winkler et al., 2018; F. Ye et al., 2017). The role of m^6A on translation or stability of KSHV mRNA is unknown. Reports on the roles of m^6A readers are conflicting despite using similar model systems. Tan et al., (2017) reported that YTFDH2 depletion enhances replication while Hesser et al., (2018) reported the opposite effect. Cell-type specific differences in KSHV-infected epithelial and PEL cells have also been reported, but differences in the methods used to reactivate the virus in these model systems cloud interpretation (Hesser et al., 2018).

Specific nucleoside modifications could provide a means for herpesviruses to distinguish viral mRNA from cellular mRNA. Interestingly, the characteristic sites of Mta binding, which are GC-rich sequences near the first exon-intron boundary, are also enriched for N1-methyladenosine and N5-methylcytosine modifications (Dominissini et al., 2016; X. Yang et al., 2017). Binding to nucleoside modifications could explain the failure to identify a more specific sequence motif for Mta binding. More generally, roles for viral proteins in directly writing, reading, or erasing m^6A modifications have not been described.

1.5.8 Herpesvirus Control of Translation

Both alpha- and gammaherpesviruses stimulate shutoff of host protein synthesis during lytic replication. This effect is mediated by the viral endoribonucleases, HSV-1 Vhs or KSHV SOX (Glaunsinger and Ganem, 2004a; Kwong and Frenkel, 1987). Vhs and SOX cleave both viral and cellular mRNA (Abernathy et al., 2014; Oroskar and Read, 1989), which is then degraded by the host 5'-to-3' exonuclease Xrn1 (Covarrubias

et al., 2011). Vhs directly binds to eIF4B (Doepker et al., 2004), which could target Vhs to initiated transcripts. It is unclear how SOX is recruited to mRNA, but SOX is recruited to the 40S small ribosomal subunit and mRNA-cleavage occurs in the cytoplasm (Covarrubias et al., 2009; 2011). Some mRNAs can escape host shutoff. Although precise host shutoff escape mechanisms remain largely unknown, there have been reports of protective sequence elements that serve as binding sites for RBPs implicated in escape (Chandriani and Ganem, 2007; Muller et al., 2015).

Host shutoff might be a way to enhance translation of viral mRNA by limiting competition with host mRNA for TIFs and ribosomes. Host shutoff is required for efficient translation of some late viral mRNAs, but this effect seems to be cell-type specific and not due to structural features of late mRNA (Dauber et al., 2011; 2014). It is likely that host shutoff has more global effects on TE, but this has not been examined. Host translation is not shutoff during HCMV lytic replication, but the TE of ~2,000 host transcripts is altered; the mTORC1-activating HCMV UL38 protein accounts for about half of this amount, including many TOP-containing transcripts (McKinney et al., 2012). It is not clear if changes in non-TOP transcripts is due to the actions of other viral proteins, or the response of host translation machinery to the stress of infection.

Herpesvirus infection can change the abundance of TIFs. HCMV lytic replication features accumulation of eIF4F components and PABPC (Perez et al., 2010; Walsh et al., 2005); m^6A reading and writing machinery is also increased but a role for m^6A in translation of HCMV mRNA has not been demonstrated (Rubio et al., 2018; Winkler et al., 2018). In both HSV1 and KSHV infection the amount of eIF4F components appears constant, however eIF4E Ser209 phosphorylation is increased. Mnk1 inhibition limits HSV-1, HCMV, and KSHV replication with concomitant loss of eIF4E phosphorylation, but a direct role in eIF4E phosphorylation in supporting virus replication has not been demonstrated (Arias et al., 2009; Walsh, 2004; Walsh et al., 2005). During KSHV lytic replication, ORF45 recruits p90 RSK to phosphorylated eIF4B (Kuang et al., 2011), which may help enhance translation of some viral mRNAs with complex 5'UTRs (Avey et al., 2015).

Conserved herpesvirus Mta proteins can alter the TE of some mRNA; HSV-1 ICP27, HCMV UL69, EBV EB2, and KSHV ORF57 all co-sediment with polysomes

(Aoyagi et al., 2010; Boyne et al., 2010; Larralde et al., 2006; Mure et al., 2018; Ricci et al., 2009). This association seems be driven by binding to TIFs, but the different homologues have evolved different strategies for recruitment. All Mta proteins associate with PABP; ICP27 associates directly with PABP *in vitro*, while ORF57 requires PYM to bind to PABP (Boyne et al., 2010; Smith et al., 2017). ICP27 also makes direct contact with eIF3b and eIF3f (Fontaine-Rodriguez et al., 2004). These binding activities are confined to the C-terminal domain of Mta (Sandri-Goldin, 2011). No Mta protein has been shown to directly bind to m^7GTP; recombinant EB2 has been specifically shown not to bind m^7GTP Sepharose (Mure et al., 2018). Mta proteins promote the translation of specific subsets of, generally intron-less, transcripts (Boyne et al., 2010; Ricci et al., 2009). Tethering ICP27 to a transcript using M2 phage coat RNA-binding domains enhances translation of the transcript, suggesting that Mta binding is sufficient for translational enhancement (Smith et al., 2017). In this way, Mta could be considered to work by CITE elements. However, it is not clear how Mta supports translation of mRNA, and whether this applies to all bound mRNAs, or only a subset.

During infection, beyond its role in promoting nuclear export of viral mRNAs, Mta is required for support translation of a number of viral transcripts (Aoyagi et al., 2010; Ellison et al., 2005). It is unclear whether Mta nuclear-export clients are the same transcripts that benefit from Mta translation-enhancement. A role of mRNA nucleoside modification in Mta binding, or supporting translation in lytic replication, has not been described. Similarly, while TIFs have been shown to bind to Mta, it is not clear which TIFs are required for translation of Mta-bound transcripts. While herpesviruses support eIF4F formation, it is not clear if it is required for translation of viral mRNA or host mRNA. It is similarly not clear if non-eIF4F TIFs are activated during latency or lytic replication and whether these are required to support virus replication.

1.6 Rationale and Overview

Herpesviruses replication could exert significant stress on the host protein synthesis machinery. Herpesvirus mRNAs are structurally similar to host mRNA, but can be bound by a distinct complement of RBPs that direct their fate. mTORC1 has an important role in herpesvirus biology; viruses from all three families of herpesviruses

potently activate mTORC1 during replication. Furthermore, mTORC1 inhibition causes regression of KS lesions.

Here, I examine mTORC1 signalling in KSHV replication, the role of specific translation initiation complexes in the synthesis of viral proteins, and how lytic replication alters the composition of active translation complexes. KSHV enforces mTORC1 activation and mTORC1 target proteins are phosphorylated during lytic replication. mTORC1 activation is important for reactivation from latency in both PEL cells and epithelial cells. However, in epithelial cells, this requirement is not tied to ectopic RTA expression. Instead, mTORC1 activation seems required to provide a substitutable second-signal for reactivation.

Once lytic replication begins, the requirement for mTORC1 is reduced, if not dispensable. mTORC1 is not required to limit autophagy during latent or lytic infection, likely due to efficient control of autophagy by viral proteins. However, some autophagy related proteins have a significant effect on virus yield. Atg14 in particular is important in limiting viral reactivation from latency.

mTORC1 activation is required for phosphorylation of 4E-BP1 and formation of eIF4F during both latency and lytic replication. However, mTOR activation, while promoting virus replication, is not strictly required for virus replication. Fifty-percent of virion production is resistant to loss of eIF4F, and viral proteins appear to accumulate normally. Importantly, the translational efficiency of viral transcripts is unaltered during mTORC1 inhibition, and viral transcripts remain associated with the polysomes. This seems to be a specific property of viral transcripts rather than a change in regulation of translation, because TOP-mRNAs remain exquisitely sensitive to mTORC1 inhibition in these circumstances. This suggested that viral transcripts might be translated using non-eIF4F modes of translation initiation. However, a series of RNA silencing experiments targeting essential activators of non-eIF4F translation yielded little change in yield of infectious virions. In an attempt to determine what TIFs are active during latent and lytic replication, I pursued quantitative proteomics of proteins associated with translating mRNA. No clear translation machinery was enriched in polysomes during lytic replication, but several viral proteins were identified as new candidate RBPs.

KSHV requires host translation machinery to replicate its genome and make progeny virions. The results presented here suggest that KSHV has evolved mechanisms to ensure that viral protein synthesis can proceed when global translation is otherwise inhibited. What remains to be determined is what cap-dependent translation machinery KSHV can activate and what role, if any, viral RBPs have in this process.

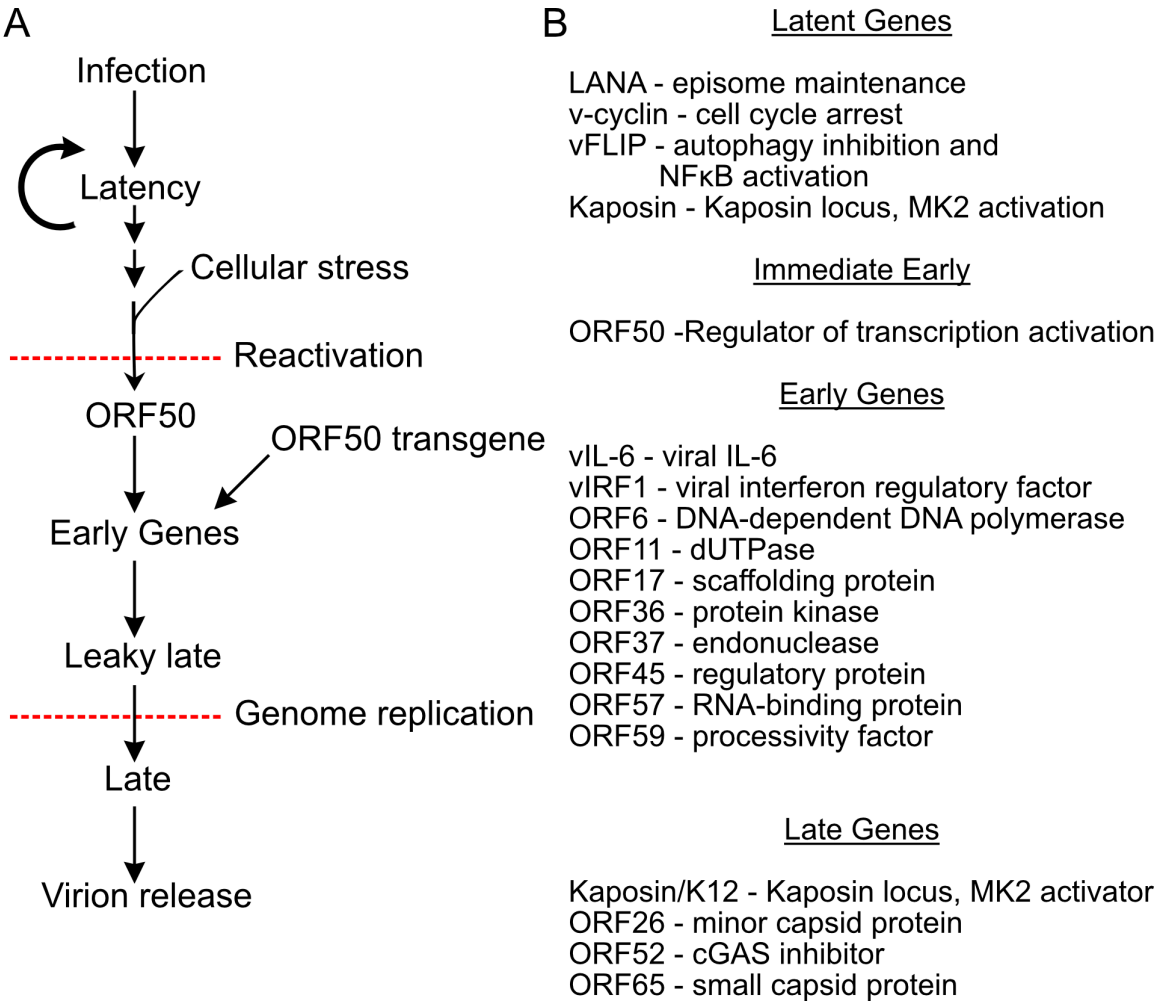

Fig 1.1 KSHV replication cycle and temporal classes. (A) KSHV establishes latency on infection. The viral episome is replicated with the host genome during cell division. Cellular stress stimulates expression of the immediate early protein ORF50 (RTA), which activates transcription of early proteins. Early proteins are required for replication of the viral genome and licensing expression of late genes. Late gene products encapsulate the newly synthesized viral genome in virions for egress. Ectopic expression of ORF50 (RTA) is sufficient to stimulate early gene expression. (B) A partial list of KSHV genes examined in the following chapters and their temporal classes.

Fig 1.2 eIF4F-dependent translation initiation. (A) Model of translation initiation: i) Cartoon diagram of messenger ribonucleic acid (mRNA). ii) mRNA is highly structured in the cell and associated with RNA-binding proteins (RBP). iii) The m^7GTP cap is bound by eIF4E in association with eIF4GI and eIF4A. eIF4A unwinds secondary structure in the 5' UTR. iv) eIF4G recruits eIF3, the small ribosomal subunit, and ternary complex, comprising eIF2, initiation methionine tRNA (Met-$tRNA_i$), and GTP. v) eIF4G may dissociate from eIF4E when scanning begins. vi) multiple rounds of initiation occur on the same mRNA molecule, new eiF4G can bind to eIF4E and begin a new round of initiation. (B) Unphosphorylated 4E-BP1 bind to eIF4E and prevents association with eIF4G, preventing initiation events on the mRNA. When active, mTORC1phosphorylates 4E-BP1 and prevents eIF4E binding.

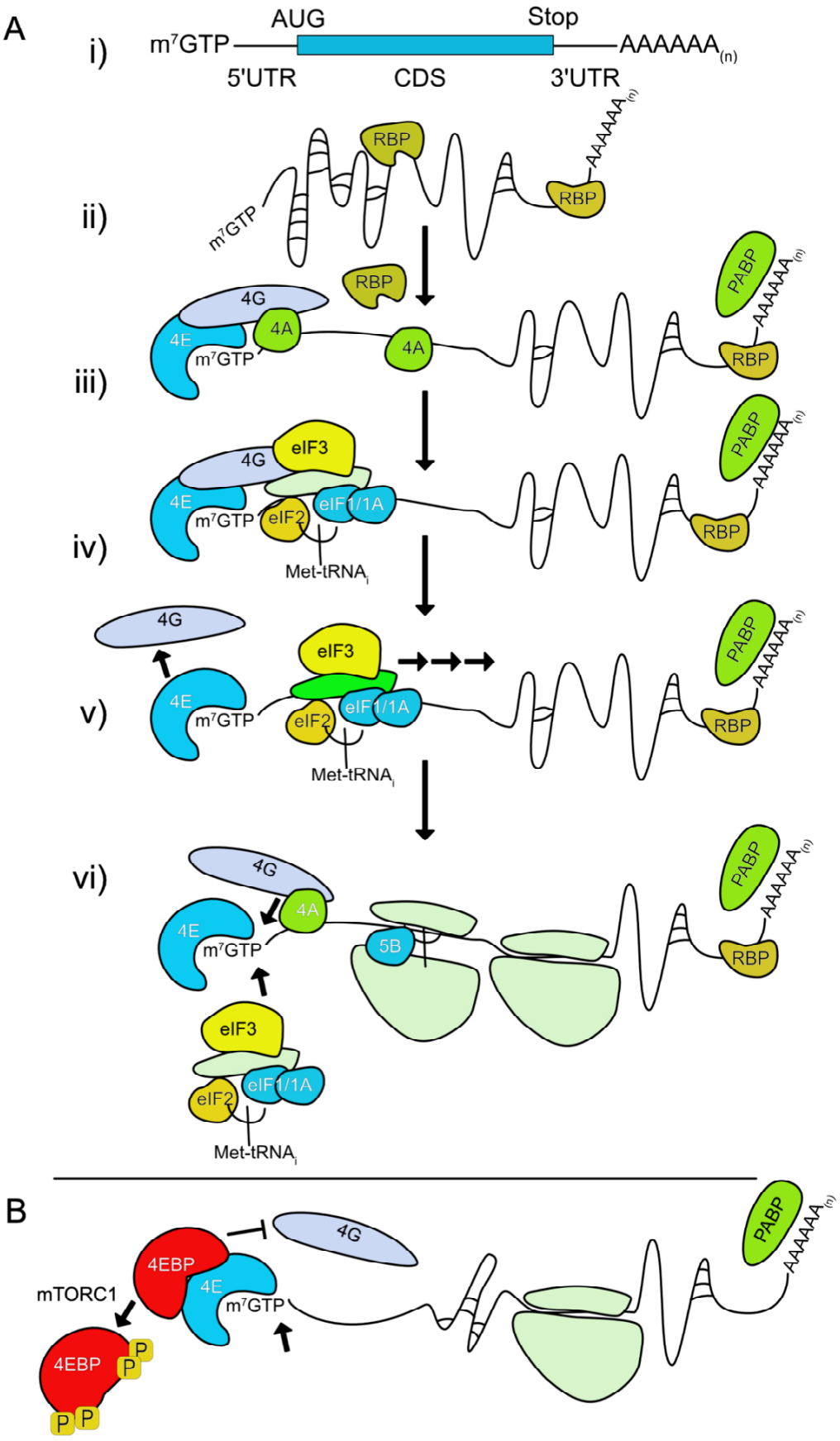
A
i)
AUG
Stop
m7GTP
AAAAAA(n)
5'UTR
CDS
3'UTR
ii)
RBP
m7GTP
AAAAAA(n)
iii)
4G
4A
4E
m7GTP
PABP
iv)
eIF3
eIF2
eIF1/1A
Met-tRNAi
v)
vi)
5B
B
mTORC1
4EBP
P

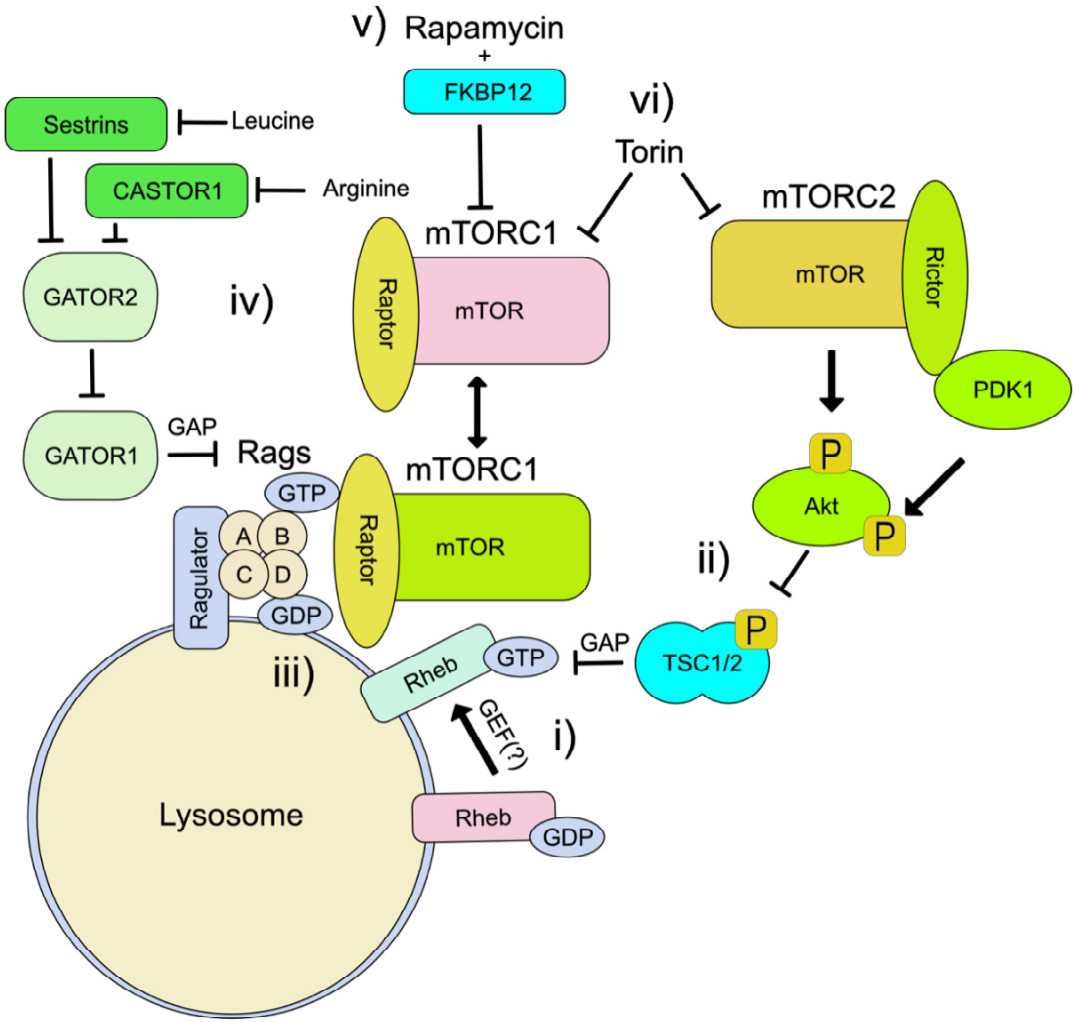

Fig 1.3 mTORC1 regulation. i) mTORC1 is activated on the lysosomal surface by interacting wtih Rheb. ii) Rheb is inactivated by the guanosine activating protein (GAP) complex TSC1/2. TSC2 is inactivated by phosphorylation by Akt, which itself is activated by phosphorylation by mTORC2. Only active, GTP-bound Rheb can activate mTORC1 iii) mTORC1 is recruited to the lysosome where it can interact with Rheb by the Rag GTPases. iv) amino acid insufficiency activates the GATOR complex, which acts as a GAP for the Rag GTPases. This leads to dissociation of mTORC1 from the lysosome. v) Rapamycin forms a complex with FKBP12. This complex is an allosteric inhibitor of mTORC1. vi) Torin is an active site inhibitor of mTOR and inhibits both mTORC1 and mTORC2.

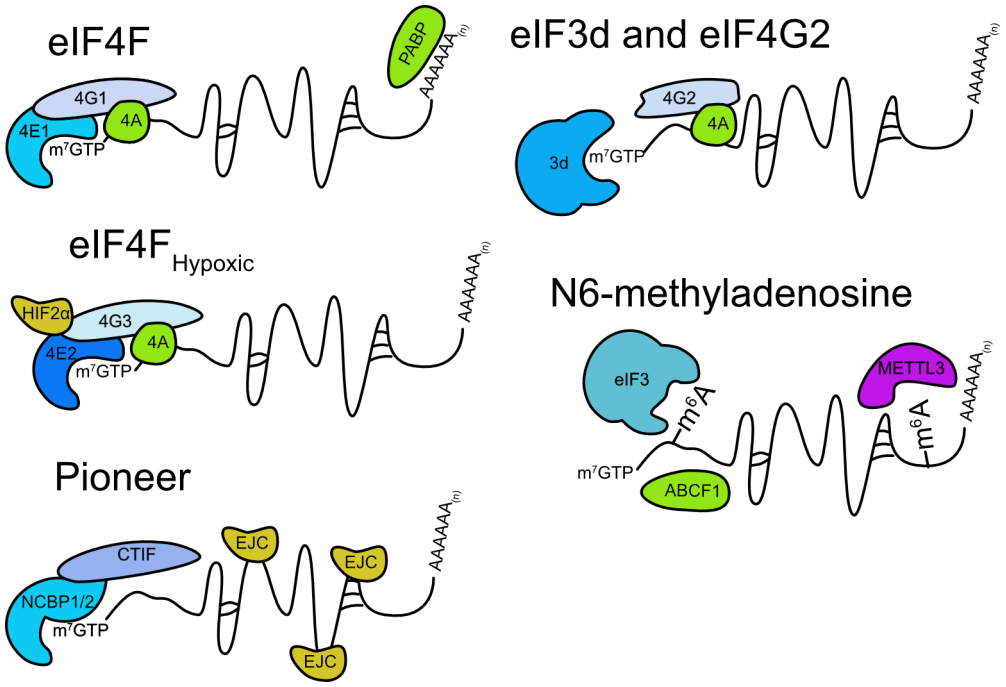

Fig 1.4 Non-eIF4F translation initiation complexes. eIF4F comprises the eIF4E1 cap-binding protein, the eIF4G1 scaffolding protein, and the RNA helicase eIF4A. During hypoxia, translation initiation requires the $eIF4F_{Hypoxic}$, which is similar to eIF4F with the exception of using the eIF4E2 cap-binding protein and the eIF4G3 scaffolding protein. Formation of $eIF4F_{Hypoxic}$ requires stabilization by HIF2α. The first round of translation of an mRNA is the pioneer round. Some mRNA undergoes a pioneer round using eIF4F, but the nuclear cap-binding proteins NCBP1 and 2 can also direction translation initiation through association with the CTIF, which contains a domain similar to the eIF3-recruiting middle domain of eIF4G1 and 3. mRNA can also recruited directly to eIF3 without a eIF4F-like complex by association of the m^7GTP cap with eIF3 subunit eIF3d. On many eIF3d-bound mRNA, this also seems to require eIF4G2 activity. mRNA can also be initiated in a scanning-dependent, but m^7GTP-independent manner by binding of N6-methyladenosine (m^6A) to eIF3. This requires the eIF2-interacting protein ABCF1. METTL3, part of the m^6A methyltransferase complex of METTL3, METTL14, and WTAP. Can also bind to m^6A on mRNA and promote it translation by bridging m^6A-modified mRNA and eIF3h.

Chapter Two – Materials and Methods

2.1 Cell Lines

293A cells were obtained from the ThermoFisher Scientific (R70507). iSLK and iSLK.219 cells (Myoung and Ganem, 2011) were a kind gift from Don Ganem. iSLK cells are a subclone of Caki-1 kidney epithelial cells that have been modified to carry the KSHV immediate early protein RTA under a tetracycline-regulated promoter (Myoung and Ganem, 2011; Stürzl et al., 2012). iSLK.219 cells are a subclone of iSLK cells latently infected with recombinant rKSHV.219 virus (Myoung and Ganem, 2011; Vieira and O'Hearn, 2004). These cells were cultured in DMEM with 10% v/v heat-inactivated FBS with 100 IU of each penicillin and streptomycin. TREx-BCBL1-RTA cells (Nakamura et al., 2003), a kind gift from Jae Jung, were cultured in RPMI-1640 supplemented with 10% v/v heat-inactivated FBS, 500 μM β-mercaptoethanol, with 100 IU of each penicillin and streptomycin. Like the iSLK cells, TREx-BCBL1-RTA cells express RTA on a tetracycline-regulated promoter. All cells were maintained at 37^{o}C with 5% carbon dioxide atmosphere. iSLK.219 cells were cultured in the presence of 10 μg/mL of puromycin (ThermoFisher) to maintain copy number of the episomal rKSHV.219 genomes (Myoung and Ganem, 2011; Vieira and O'Hearn, 2004). Puromycin was not included in the medium of cells seeded for experiments. iSLK.219 cells were diluted to a density of 10^5 cells/mL for seeding in all experiments. To induce *RTA*-transgene expression in iSLK.219 cells, on the day following seeding medium was refreshed and supplemented with 1 μg/mL doxycycline (Sigma). TREx-BCBL1-RTA cells were resuspended at a density of 2.5 x 10^5 cells/mL supplemented with 1 μg/mL doxycycline to induce *RTA*-transgene expression. For hypoxia experiments, cells were placed in a Hypoxia Incubation Chamber (StemCell); the chamber was purged with nitrogen at 2 psi for 5 min prior to sealing. 15 mM HEPES was added to the media in all hypoxia experiments to maintain media pH.

2.2 Fluorescent Imaging and Cell Counting

iSLK.219 cells were seeded in a 6-well plate and fixed with 4% paraformaldehyde (PFA) and the nuclei were stained with Hoechst 33342 (ThermoFisher) using standard procedures. Fluorescent images were captured using an

EVOS FL Cell Imaging System (ThermoFisher) and RFP+ cells and Hoechst+ cells were counted using a custom CellProfiler (Carpenter et al., 2006) script.

2.3 Chemical Inhibitors

Torin 1, referred to as "Torin" here, (Toronto Research Chemicals) (Thoreen et al., 2009) and rapamycin (Sigma) were resuspended in DMSO, which was used as a vehicle control in all experiments. Unless otherwise stated, both rapamycin and Torin were used at a concentration of 250 nM. Phosphonoacetic acid (PAA, Sigma) was used at 500 μM, chloroquine diphosphate (CQ; Sigma) was used at 50 μM, sodium butyrate (NaB; Sigma) used at 1 mM, and sodium arsenite (Sigma) was used at 500 μM. 4EGi (Moerke et al., 2007) and 4E1RCat (Cencic et al., 2011b) were purchased from Sigma and resuspended in DMSO.

2.4 Immunoblotting (IB)

The TREx-BCBL1-RTA cells are non-adherent. To harvest these cells, media was collected, and cells were pelleted by centrifugation at 1,500 x for 5 minutes. Cells were washed with ice-cold PBS and pelleted again. Supernatant was then removed and the pellet was lysed with 2x Laemmli buffer (4% w/v sodium dodecyl sulfate (SDS), 20% v/v glycerol, 120 mM Tris-HCl pH 6.8). Adherent cells were first washed 1x with ice-cold PBS then lysed in 2x Laemmli buffer. When harvesting lysate from lytic cell populations, non-adherent cells were collected as suspension cells, remaining cells were removed from the dish with a rubber scrapper in ice-cold PBS, then collected by centrifugation as described above. Non-adherent and scrapped cells pellets were pooled and the cell pellet was lysed with 2x Laemmli buffer. DNA was sheared by repeated pipetting with a fine gauge needle and a sample of lysate was reserved for quantification. 100 mM of dithiothreitol (DTT) was then added to each sample prior to boiling at 95^{o}C for 5 min. Samples were stored at -20^{o}C prior to analysis.

The protein concentration of whole cell lysates was quantified by DC protein assay (Bio-Rad) and equal quantities of protein were loaded for SDS-polyacrylamide gel electrophoreses (PAGE) and transferred to PVDF membranes (Bio-Rad) using a semi-dry rapid transfer apparatus (Bio-Rad). For proteins isolated from pulldowns or precipitated

form polysome fractions, equal volumes of lysate were loaded. Membranes were blocked with 5% w/v skim milk Tris-buffered-saline, 0.1% v/v Tween (TBS-T), or 5% w/v bovine serum albumin (BSA) TBS-T, and probed at 4^{o}C overnight primary antibodies as listed in Table 2.1. Primary antibody binding was detected with horseradish-peroxidase conjugated anti-mouse (Cell Signaling; #7076) and anti-rabbit (Cell Signaling; #7074) secondary antibodies. Blots were developed with Clarity-ECL chemiluminescence reagent (Bio-Rad) and imaged on a Bio-Rad Chemidoc-Touch.

2.5 Immunofluorescence (IFA)

Coverslips (#1.5, Zeiss) were coated with 1 mM poly-D-lysine (Sigma) in PBS for 30 minutes at room temperature (RT) then washed with PBS and allowed to dry completely before seeding 2.5 x 10^5 TREx-BCBL1-RTA cells. Cells were left to adhere overnight. After treatment, cells were washed once with PBS and fixed with either 4% PFA or glyoxal solution (Richter et al., 2017) at pH 5 for 15 minutes. Fixative was removed, cells were washed and stored with PBS at 4^{o}C before staining. Cells were permeablized and blocked in blocking buffer (1% v/v heat-inactivated human serum (Sigma), 0.1% v/v Triton X-100 PBS) for 1 h, at RT with gentle agitation. Coverslips were stained with 1:500 mouse anti-ORF57 or 1:500 mouse anti-ORF59 monoclonal antibodies in blocking buffer overnight at 4^{o}C. Coverslips were washed with 3x with PBS for 5 min with gentle agitation before staining with 1:1,000 donkey anti-rabbit Alexa-555 secondary antibody (ThermoFisher) for 1 h at RT. Coverslips were briefly washed with PBS before, incubated with 300 nM DAPI (ThermoFisher) in PBS for 5 min, briefly washed several times with PBS then mounted with ProLong Gold Anti-fade reagent (ThermoFisher). Slides were imaged on an LSM710 confocal microscope (Zeiss) using Zen software. Z-stacks obtained and a subset of these images was used to generate maximum intensity projections. Fluorescent images containing transmitted light were captured at a single focal plane. Contrast and pseudo-colour were adjusted using Fiji (Schindelin et al., 2012) and images were assembled into figures using Affinity Designer for masOS (Serif).

2.6 Viral Genome Amplification and qRT-PCR

DNA was harvested from the cells using QIAamp DNA Mini Kit (Qiagen) as per the manufacturers' directions. qPCR was performed with primers to ORF26 and β-actin GoTaq (Promega). KSHV genome copy number is represented as fold excess of ORF26 over ß-actin. For RT-qPCR, total RNA was extracted using RNeasy extraction (Qiagen), reverse transcribed using MaximaH (ThermoFisher) using random hexamers for priming as per the manufactures' directions. qPCR was performed using GoTaq. Both adherent and non-adherent cells were harvested in each sample. Transcripts are normalized to abundance of 18S rRNA using the ΔΔCt method. Primer sequences are in listed in Table 2.2. All primers used a 60^{o}C annealing temperature.

2.7 KSHV Titering and Infection

2.7.1 DNAse-protected Virion qPCR

At the time of harvest, the cells and debris were pelleted for 5 min at 5,000 x *g*. 180 µL of the supernatant was treated with 20 µL of 3 mg/mL DNase I (Sigma) for 30 min at 37^{o}C. DNA was then extracted from the treated supernatant using RNeasy Blood and Tissue Minikit (Qiagen) as per the manufacturers' instructions with the following modifications: lysis buffer AL was spiked with 5 µg/sample of salmon sperm DNA (Invitrogen) and 1 ng of the luciferase (*luc*) containing plasmid, pGL4.26 (Clontech). qPCR was performed with primers to ORF26 to detect viral genomes and the *luc* carrier plasmid using Go-Taq (Promega). ORF26 quantity was normalized to *luc* using the ΔΔCT method.

2.7.2 KSHV Infection and Titering Flow Cytometry

rKSHV.219 contains an EGFP cassette under a constitutive EF1α promoter, allowing for quantification by fluorescence (Vieira et al., 2004). Supernatant was harvested from iSLK.219 cells as indicated and stored at -80^{o}C until titering. One day prior to titering, 2.5x10^{5} 293A cells were plated in each well of a 12-well plate. The thawed inoculum was mixed by inversion then centrifuged at 5,000 x *g* for 5 min to pellet debris. The cells were then infected with diluted inoculum and centrifuged at 800 x *g* for 90 or 120 min (Yoo et al., 2008). Immediately after spinoculation, the inoculum was

removed, the cells were washed once with PBS, and fresh media was added, and the cells were returned to an incubator. The day following infection, 293A cells were lifted with trypsin, washed once in cold PBS then resuspended in 1% v/v PFA PBS. GFP+ cells were recorded from 10,000 events in an arbitrary live forward and side scatter gate with a FACScalibur (BD Bioscience). Data was analysed using Flowing Software ver 2.5 (Perttu Terho, Turku Centre for Biotechnology, Finland. www.flowingsoftware.com).

2.8 Puromycin Translation Assay

TREx-BCBL1-RTA were reactivated with 20 ng/mL of TPA and 1 µg/mL doxycycline. Cells were treated with 10 µg/mL puromycin for 10 min prior to harvest in 2x Laemmli buffer. C-terminal puromycin was probed by immunoblot using an anti-puromycin antibody clone (Schmidt et al., 2009). Immunoblots were performed on 4-15% Mini-PROTEAN TGX Stain-Free gradient gels (Bio-Rad) as per the manufacturers' instructions. The Stain-Free protein loading control was used to quantitate the anti-puromycin signal.

2.9 m^7GTP Pulldown

$2x10^6$ iSLK, iSLK.219 cells, or $5x10^6$ TRex-BCBL1-RTA cells were used for each pull-down. After treatment, cells were washed twice with ice-cold PBS and scrapped to harvest. The cells were centrifuged for 5 min at 1,000 x *g* and the pellet was lysed, on ice for 10 min, in 20 mM Tris-HCl, 150 mM NaCl, 0.5% v/v NP-40 with protease and phosphatase inhibitors. The lysate was centrifuged for 5 min at 10 000 *g* and the supernatant was pre-cleared with 30 µL settled volume of unconjugated agarose beads (Jena Biosciences) by incubating, with end-over-end rotation, for 10 min at 4°C. The beads were pelleted by centrifugation for 30 s at 500 x *g* and the 50 µL of supernatant was removed as 5% input control. The remaining supernatant incubated with m^7GTP agarose beads (Jena Biosciences) for 4-6 h at 4°C, with agitation. The beads were washed four times with lysis buffer. To harvest bound protein, the beads were then resuspended in 50 µL of 1x Laemmli buffer with 100 mM DTT and boiled at 55°C for 10 min. Lysates were analysed by immunoblot as described above. Equal loading of 10-20 µL was used on each gel.

2.10 Polysome Analysis

2.10.1 Polysome Isolation

Polysomes were isolated by ultracentrifugation of cytosolic lysate through a 7-47% w/v linear sucrose gradient in high salt (20 mM Tris HCl, 300 mM NaCl, 25 mM $MgCl_2$ in DEPC-treated or nuclease-free water) or low salt (15 mM Tris HCl, 50 mM KCl, 10 mM $MgCl_2$) lysis buffer with RNAse and protease inhibitors. High salt conditions were used to isolate RNA from gradients and low salt conditions were used for isolating proteins. Gradients were prepared using manufactures' settings on a Gradient Master 108 (Biocomp). For each gradient, ~8 x 10^6 iSLK.219 or 1.3 x 10^7 TRex-BCBL-RTA cells were seed. Cells treated with 100 µg/mL cycloheximide (CHX, Acros Organics or Sigma) for three min prior to harvest. Cells were washed with ice-cold PBS and scraped in a tube containing the spent media and PBS wash. The cells were pelleted by centrifugation for 5 min at 500 x *g* and washed again with ice-cold PBS. Cell pellets were resuspended in lysis buffer (high or low salt buffer, with 1% v/v Triton X-100, 400 units/ml RNAseOUT (Invitrogen), 100 µg/mL CHX, and protease and phosphatase inhibitors) for 10 min on ice. Lysate was centrifuged for 10 min at 2,300 x *g* the supernatant was transferred to a new tube and centrifuged for 10 min at 15,000 x *g*. The supernatant was overlaid on the sucrose gradients. Gradients were centrifuged at 39,000 rpm for 90 min on a SW-41 rotor. The bottom of the centrifuge tube was punctured and 60% w/v sucrose was underlain by syringe pump in order to collect 500 µL fractions from the top of the gradient with simultaneous A_{260} measurement using a UA-6 detector (Brandel, MD). Polysome sedimentation graphs were generated with Prism8 (GraphPad).

2.10.2 RNA-Seq Analysis of Polysome Fractions

Total RNA or pooled fractions from heavy polysomes were isolated using Ribozol (Amresco) or Trizol (ThermoFisher) using standard procedures, except the precipitant in the aqueous fraction was isolated using an RNeasy column (QIAGEN). mRNA was isolated from these total fractions using polyA enrichment (Dynabeads mRNA DIRECT Micro Purification Kit, ThermoFisher) according to the manufacturers' protocol, then library preparation was performed with Ion Total RNA-Seq Kit v2.0

(ThermoFisher). Library size, concentration, and quality was assessed using a 2200 TapeStation (Agilent). Libraries were sequenced on Proton sequencer (ThermoFisher Scientific) with a PI chip and the Ion PI Hi-Q Sequencing 200 Kit for 520 flows. Ion Torrent reads were processed using combined Human Hg19 and KSHV (Accession GQ994935) reference transcriptomes. The KSHV genome was manually re-annotated with the transcript definitions from KSHV2.0 (Arias et al., 2014) reference transcriptome and the Quasi-Mapping software Salmon (Patro et al., 2017). Normalized counts per million (cpm) were estimated for individual transcripts using the R package limma (Ritchie et al., 2015). Two biological replicates were combined as a geometric mean (Quackenbush, 2002). The transcripts were ordered by abundance and the mean, standard deviation (SD), and Z-score were calculated using a sliding window of 200 transcripts of similar abundance (Andreev et al., 2015; Quackenbush, 2002). The most abundant 100 and the least abundant 100 transcripts used the mean and SD of the adjacent bin. Translational efficiency (TE) of a transcript treatment was determined by the formula TE = $\log_2$(polysome/total). The change in translational efficiency (ΔTE) = TE_{Torin}-TE_{DMSO}.

2.10.3 Polysome RT-qPCR

TREx-BCBL1-RTA were reactivated with 1 μg/mL doxycycline for 24h. Torin or DMSO was added two hours prior to harvest in high salt lysis buffer as described above. Fractions were mixed 1:1 with Trizol and isolated as per manufacturer's directions except that 30-60 μg of GlycoBlue Co-Precipitant (Ambion) and 100 ng of *in vitro* transcribed luciferase DNA (NEB T7 HiScribe) was added to the aqueous fractions during isopropanol precipitation. The resulting pellet was resuspended in water and reverse transcribed with random primers (Maxima H, Thermo). mRNA was normalized to luciferase spike to control for recovery. The quantity of mRNA detected in a given fraction was then calculated as a percentage of the total detected in all fractions. The RNA recovery was controlled by subtracting the Ct of the luciferase spike, which was assumed to be constant, from the target Ct: $\Delta Ct=Ct_{target}-Ct_{luc}$. This ΔCt value for each fraction was then subtracted from the lightest fraction: $\Delta\Delta Ct_n=\Delta Ct_1-\Delta Ct_n$ where n=fraction number. ΔΔCt was then normalized into a transcript quantity, $Q_n=2^{\Delta\Delta Ctn}$ for each transcript. The total quantity transcript (Q_{total}) was summed from all fractions:

$Q_{total}=Q_1+Q_2+Q_3+\ldots+Q_n$ and the proportion (P) of a transcript found in a fraction was determined by $P=Q_n/Q_{total}$ (Panda et al., 2017).

2.10.4 Polysome Immunoblot

500 µL fractions of sucrose gradient mixed with 45 µg of GlycoBlue and 1.5 mL of 100% ethanol and incubated overnight at -80°C. Fractions were centrifuged at 15,000 x *g* for 15 min at 4°C. Supernatant was decanted and the pellet was washed 70% v/v ethanol made with RNAase-free water. Residual ethanol was dried at 95°C and the pellet was resuspended in 1x Laemmli buffer with 100 mM DTT then boiled at 95°C for 5 min prior to SDS-PAGE.

2.11 Enzyme-linked Immunosorbent Assay (ELISA)

The media concentration of VEGF-A was measured using an ELISA kit, Human VEGF DuoSet ELISA as per the manufacturers' instructions (R&D Systems). Before seeding, cells were first washed in PBS to remove any residual cytokine. Absorbance was measure on a plate reader at 450 nm with 570 nm correction subtracted. VEGF quantity was calculated using a standard curve in Prism8. Values were then normalized to vehicle control in Excel (Microsoft).

2.12 shRNA Gene-silencing

shRNA was transduced using a either pLKO or pGIPZ lentiviral transduction. Lentiviruses were generated in 293T cells by using polyethylenimine MAX, (Polysciences, #24765) to co-transfect the pLKO or pGIPZ cassette, with the packaging plasmids pMD2.G (a gift from Didier Trono, Addgene plasmid #12259) and psPAX2 (a gift from Didier Trono, Addgene plasmid #12260). 48h post-transfection the supernatant was harvested, filtered at 0.45 µm, and frozen in aliquots at -80°C. TREx-BCBL1-RTA cells were transduced with lentivirus overnight in the presence of 4 µg/mL polybrene (Hexadimethrine bromide, Sigma). The following day, 1 µg/mL puromycin or 20 µg/mL blasticidin (ThermoFisher) was added to the cultures and cells were incubated for a further two days for selection before passage or seeding for experiments. Experiments were seeded without selection antibiotics. Transduced cells were freshly generated for

every experiment and not maintained in culture for long periods. shRNAs for eIF3d, eIF4E2, and eIF4G2 were selected from the GIPZ Lentiviral shRNA library (ThermoFisher, sh-eIF3d #1: V3LHS_302415; sh-eIF3d #2: V3LHS_302417; sh-eIF4E2: V2LHS_68041; sh-eIF4G2 #1: V3LHS_323383, sh-eIF4G2 #2: V3LHS_323384; sh-NCBP1 #1: V3LHS_639361, sh-NCBP1 #2: V3LHS_645476). shRNA sequences for METTL3, Beclin1, ATG12, and ATG14 were selected from the RNAi Consortium (shMETTL3 - #1: TRCN0000034715; shMETTL3 - #2: TRCN0000034714; shBeclin1: TRCN0000033549; shATG12: TRCN0000007393; shATG14: TRCN0000142647). Complementary DNA oligonucleotides were annealed and ligated between the AgeI and EcoRI sites of pLKO-blast (for Beclin1, ATG12, and ATG14; a gift from Keith Mostov, Addgene plasmid #26655), or pLKO.1-TRC (for METTL3; a gift from David Root, Addgene plasmid #10878 Moffat et al., 2006) as described by the RNA consortium. A non-targeting shRNA sequence was used as a control in all experiments either pGIPZ-NS (ThermoFisher, RHS_4346), pLKO-NS-BSD (a gift from Keith Mostov(Bryant et al., 2010) Addgene plasmid #26701). We replaced the BamHI/KpnI fragment of containing the blasticidin selection cassette of pLKO-NS-BSD with the BamHI/KpnI-flanked puromycin selection cassette from pLKO-TRC to generate pLKO-NS-Puro.

2.13 Nuclear-Cytoplasmic Fractionation

This assay was performed essentially as described in (Suzuki et al., 2010). $2.5x10^6$ TREx-BCBL1-RTA cells were seeded for each fractionation. At time of harvest, cells were collected by centrifugation at 500 x *g*, 5 min at 4^oC and washed in ice-cold PBS. The cell pellet was then resuspended in 900 µL of 0.1% v/v NP-40 PBS to lyse the cells. 300 µL was removed as whole cell lysate and combined with 100 µL 4x Laemmli buffer. The remaining 600 µL was centrifuged 800 x *g*, 5 min at 4^oC to pellet the nuclei. 300 µL of supernatant was removed and combined with 100 µL of 4x Laemmli buffer as the cytoplasmic fraction. The remaining supernatant was discarded and the pellet was washed in 1 mL of ice-cold 0.1% v/v NP-40 PBS and nuclei were pelleted as described above. The wash was discarded and the nuclear pellet was resuspended in 400 µL of 1x Laemmli buffer. DTT was added to the lysates to 100 mM and all lysates were boiled at 95^oC for 5 min. Equal proportions of whole cell lysate, cytoplasmic and nuclear fractions

were used for SDS-PAGE and immunoblot analysis; protein concentrations were not determined.

2.14 Proteomics

2.14.1 Sample Preparation for LC-MS3

For whole cell lysate (WCL), 20 mL of 2.5 x 10^5 cell/mL TREx-BCBL1-RTA suspension culture was treated with 1 μg/mL dox for 24 or 48 h. At the time of harvest, the cells were pelleted by centrifugation at 1,500 x *g* for 5 min, washed once in ice-cold PBS, then snap frozen in liquid nitrogen. Cell pellets were stored at -80^{o}C until processing. Polysome fractions were obtained as described above from 2.5x10^7 TREx-BCBL1-RTA cells with a low-salt buffer.

Cell pellets were lysed in 2% v/v SDS, 150 mM NaCl, 50 mM Tris (pH 8.8), 5 mM DTT with protease and phosphatase inhibitors, then disrupted with a probe sonicator. After disruption, lysate was incubated at 60^{o}C for 45 min to denature and reduce proteins. Lysates were then cooled to room temperature and iodoacetamide was added to a final concentration of 14 mM, before incubation in the dark, at room temperature, for 45 min to acetylate the thiol group of reduced cysteine residues. Proteins were purified by methanol-chloroform extraction. Briefly, 3 volumes of ice-cold methanol, 1 volume of chloroform, and 2.5 volumes of water were added to the lysate, which was then vortexed to mix. The solution was centrifuged at 4,000 x *g* for 10 min to separate phases and concentrate proteins at the interface. The supernatant was removed and 3 volumes of ice-cold methanol was added. Solution was centrifuged again at 4,000 x *g* for 5 min to pellet the protein. The pellet was washed with 3 volumes of ice-cold acetone, vortexed, and pelleted at 4,000 x *g* for 5 minutes. The pellet was then carefully moved to a micro-centrifuge tube and washed with acetone again. The precipitated protein was then dried in a SpeedVac and stored at -20^{o}C until digestion.

Before digestion, the pellet was resuspended in 100 μL 8M urea, 50 mM Tris (pH 8.8) and disrupted with a probe sonicator. Protein concentration was determined by DC protein assay (Bio-Rad). Approximately 100 μg of protein for each sample was diluted to 1 M urea before addition of ~2 μg of typsin protease (ThermoFisher). Each sample was digested overnight, with agitation, at 37^{o}C. Trypsin was added twice, first 1 μg was

added, then the second 1 µg was added ~6 h into the incubation. Samples were individually acidified to pH<3 with formic acid (FA) and trifluoroacetic acid, then desalted on a using a reverse-phase column (Waters), as per standard procedures and dried under vacuum. For tandem-mass tag (TMT) labelling, samples were resuspended in 100 µL of 200 mM HEPES. Approximately 400 µg of TMT reagent, resuspend in acetonitrile (ACN), and added to the samples, which were then incubated for 1 h at room temperature. Each TMT tag has the same mass, but fragments differently when collided in the mass spectrometer. In this study nine different TMT tags were used to label WCL (126, 127N, 127C, 128N, 129N, 129C, 130N, 130C, and 131) and six TMT tags were used for polysome proteins (126, 127N, 128C, 129N, 130C, and 131). TMT tags covalently bind free amino groups, including the N-terminus of peptides and lysine residues. The reaction was quench with 5% hydroxylamine for 15 min at room temp. A small amount of each labelled sample was removed, mixed together in equal proportions, desalted and analysed by LC-MS3 (as discussed below) to confirm labelling efficiency. All 9 samples were mixed in approximately equal parts, taking into account any differences in labelling efficiency, then diluted, acidified for desalting, and dried under vacuum.

Samples were then separated by high-pH reverse-phase liquid chromatography (F. Yang et al., 2012). Briefly, labelled peptides were resuspended in 5% ACN 10 mM ammonium formate, pH 9 then applied to a monolithic reverse phase column. Peptides were eluted over 1 h with increasing ACN concentrations and collected in 60 fractions. Every third fraction was then combined, and dried under vacuum. All twenty fractions were resuspended in 3% ACN 0.1% FA and analyzed by nano-liquid chromatography and mass spectrometry (LC-MS3) using a Orbitrap Velos Pro (ThermoFisher). Briefly, the first scan isolated intense peaks between 200 to 1400 m/z. The top ten most-intense peaks were analyzed sequentially by collision-induced fractionation (CID) for peptide fragmentation, then higher-energy collisional dissociation (HCD) to measure the relative amounts of the TMT reporter ions (Ting et al., 2011).

2.14.2 Data Analysis

Mass spectra were processed and analysis using Proteome Discoverer v2.2 (ThermoFisher). Spectra were identified using Sequest and searched using a peptide library comprising the human genome (Hg19), a custom database of AUG-initiated KSHV proteins based on KSHV2.0 with the addition of CUG-initiated Kaposin B (Arias et al., 2014), and the CRAPome repository of common protein contaminants (Mellacheruvu et al., 2013). Two missed cleavages were tolerated in the tryptic peptides; only peptides between 6 and 50 residues were analyzed. The precursor mass in the first scan was quantified by centroid, and a mass tolerance of 20 part per million (ppm) was used for peptide identification. Expected static peptide modifications included N-terminal TMT, lysine TMT, and cysteine carbamidomethyl. Methionine oxidation was set as a dynamic modification. Peptides were quantified using both unique and razor peptides. A razor peptide is one that can be matched to more than one protein; it is contributed to the protein that has the most evidence in the form of number of unique peptide and abundance. Protein abundance was normalized based on the total amount of protein detected. For analysis of the polysome proteome, a mass tolerance of 5 ppm was used and phosphorylation of serine, threonine, and tyrosine residues were searched as a dynamic modification. Ratios were calculated in Proteome Discoverer.

2.15 Statistical Analysis

All values were imported into Excel (Microsoft) for tabulation and normalization. All qPCR calculations were conducted in Excel. Values were then imported into Prism8 (GraphPad) for statistical analysis and graphing. T-tests were used to compare two conditions; one-way or two-way ANOVAs were used otherwise. P-values were represented as follows: $p<0.05$ = *, $p<0.01$ = **, $p < 0.001$ = ***, and ns = non-significant.

2.16 Gene Ontology Analysis

Gene lists were search for statistical over-representation for molecular functions, using the PANTHER Classification System (www.pantherdb.org, (Mi et al., 2013)). Lists were compared against the complete database using a Fisher's exact test, with a 1% FDR.

To determine enrichment of non-coding transcripts in the polysomes, transcripts were manually sorted into coding and non-coding (NMD, lincRNA, retained-intron, processed pseudogenes, or antisense transcripts) groups and compared using a Fisher's exact test, compared to all quantified transcripts with a 1% FDR.

Table 2.1 Antibodies used in this study

Target	Source	Identifier
4E-BP1	Cell Signaling (CST)	#9644
β-actin	CST	#5125
ATG14	CST	#5504
ATG12	CST	#4180
Beclin	Santa Cruz	sc-10087
DR1 (Kaposin)	Don Ganem	McCormick and Ganem, 2005
eIF2α	CST	#9722
peIF2α Ser51	CST	#3597
eIF3d	ProteinTech	10219
eIF4E	CST	#2067
eIF4G1	CST	#2858
eIF4G3	GeneTex	GTX118109
eIF4E2	GeneTex	GTX103977
K8.1	ABI	13-212-100
Lamin A/C	Santa Cruz	sc-20681
LANA	Don Ganem	Lukac et al., 1998
LC3	Novus	NBP2-19337
METTL3	CST	#96391
Myc	CST	#2276
NCBP1	Abcam	ab42389
ORF17	Charles Craik	n/a
ORF45	ThermoFisher	MA5-14769
ORF57	Santa Cruz	sc135746
ORF59 (IB)	Britt Glaunsinger	Hesser et al., 2018
ORF59 (IF)	ABI	13-211-100
ORF65	Jae Jung	n/a
Puromycin	EMD Millipore	MABE343

Table 2.1 (continued)

RTA	David Lukac	n/a
S6	Cell Signaling	#2217
pS6 Ser235/6	CST	#4858
STAT1	CST	#9172
pSTAT1 Tyr701	CST	#9167
Tubulin	Santa Cruz	sc-9035
ULK	CST	#8054
pULK Ser757	CST	#14202
vIRF1	Yuan Chang	n/a

Table 2.2 Sequences of oligonucleotides

qPCR	Forward 5'-3'	Reverse 5'-3'
18S	TTCGAACGTCTGCCCTATCAA	GATGTGGTAGCCGTTTCTCAGG
luciferase	ACACCCGAGGGGGATGATAA	CCAGATCCACAACCTTCGCT
luc2	TTCGGCAACCAGATCATCCC	TGCGCAAGAATAGCTCCTCC
B-actin	CTTCCAGCAGATGTGGATCA	AAAGCCATGCCAATCTCATC
ORF8/9/10/11	ACATTTGACAACACGCACCG	AAAATCAGCACGCTCGAGGA
ORF25/26	CAGTTGAGCGTCCCAGATGA	GGAATACCAACAGGAGGCCG
ORF47/46/45	TGATGAAATCGAGTGGGCGG	CTTAAGCCGCAAAGCAGTGG
ORF57	TCCAGTTTTGCTCCCCACTG	TTCTGCCGTATTGTAGGCGG
ORF59	CACCAGGCTTCTCCTCTGTG	TCGCTGACAGACACAGTCAC
ORF67/66/65	TGGCTCGCATGAATACCCTG	CTGCAGATGATCCCGCCTTT
ORFK8/K8.1	AGATACGTCTGCCTCTGGGT	AAAGTCACGTGGGAGGTCAC
LANA	TCCCACAGTGTTCACATCCG	GAGGTAAAGGTGTTGCGGGA
K12	CACGTATCGAGGAGCGGTG	CAGGGTTCGCAGGGTTCG
vIL-6	TCTCTTGCTGGTCGGTTCAC	CGGTACGGTAACAGAGGTCG
Rps20	TTGACTTGCACAGTCCTTCTGA	ATGGTGACTTCCACCTCAAC
RACK1	GTGCTTCTGGAGGCAAGGAT	TCCCCACCATCTAGCGTGTA
IL-6	TGCAATAACCACCCCTGACC	GTGCCCATGCTACATTTGCC
VEGF-A	CAGGACATTGCTGTGCTTTG	CTCAGAAGCAGGTGAGAGTAAG

Chapter Three – Requirement of mTORC1 for KSHV lytic replication

3.1 Introduction

At least three KSHV proteins support mTORC1 activation during lytic replication, ORF45, vGPCR, and K1 (reviewed in Bhatt and Damania, 2012). However, it is unclear if this convergent regulation of mTORC1 activity supports progression through lytic replication and virion production. mTORC1 supports both translation through 4E-BP1 and limits autophagy by phosphorylation of ULK1 (J. Kim et al., 2011; Thoreen et al., 2012). KSHV expresses at least three proteins that restrict autophagy after autophagosome initiation, vFLIP, vBcl2, and K7 (J.-S. Lee et al., 2009; Q. Liang et al., 2015; 2013). This strongly implies that efficient virion production requires control of autophagy. Activation of mTORC1 by viral proteins should similarly limit autophagy upstream of autophagosome initiation, but it is unclear if this activity is required to fully limit autophagy during KSHV replication.

Here I examine the role of mTOR in KSHV replication. mTORC1 is active during lytic replication and this activity is sustained even when AA are depleted. mTOR is required for reactivation from latency, but after reactivation is dispensable for genome replication and late gene expression. Sufficient viral structural proteins accumulate with mTORC1 inhibition to generate infectious virions, suggesting that mTORC1-dependent regulation of translation is compromised.

mTORC1 regulation of autophagy is similarly dysregulated. mTORC1 activation is required for ULK1 phosphorylation during lytic replication, but this is not required to suppress autophagy during lytic replication. This suggests that viral inhibitors of autophagy are sufficient to limit autophagy without persistent mTORC1 activation. However, autophagy proteins still influence virion production as silencing expression of several essential autophagy proteins enhanced virus titer. Curiously, silencing of ATG14, which forms part of the autophagosome initiation complex with Beclin1 and Vps34, prevents mTORC1 inhibition from limiting reactivation from latency or virion production. Reactivation in the presence of an HDAC inhibitor similarly relieved the requirement of mTORC1 for reactivation. This suggests mTOR kinase activity provides a second-signal for reactivation, but regulation of downstream mTORC1 effector functions are uncoupled from mTORC1.

3.2 Results

3.2.1 mTORC1 Is Dispensable for Genome Replication and Late Protein Synthesis

KSHV lytic replication features mTORC1 activation (Bhatt and Damania, 2012; H. H. Chang et al., 2013) but it is not yet known whether mTORC1 activity is required to support viral replication. I tested the requirement for mTORC1 activity in the iSLK.219 cell line (Myoung and Ganem, 2011), which displays stable latent KSHV infection and provides the IE *RTA* gene *in trans* under the control of a doxycycline (dox)-regulated promoter; dox addition causes accumulation of the RTA lytic switch protein and reactivation from latency. Early viral protein ORF45 was readily detected by 24h post-induction (hpi; Fig 3.1A), and genome replication and expression of late genes K8.1 and ORF65 were detected at 48 hpi (Fig 3.2A-D). Treatment of cells with the herpesvirus DNA polymerase inhibitor phosphonoacetic acid (PAA) at 24 hpi prevented genome replication (Fig 3.2A-B) and late protein accumulation (Fig 3.1A) indicating that only IE and E gene expression occurred prior to 24 hpi.

I used rapamycin and Torin to pharmacologically inhibit mTORC1 in this study. Rapamycin is a relatively inefficient allosteric mTORC1 inhibitor that does not target mTORC2 (Guertin and Sabatini, 2007; Thoreen et al., 2009). In iSLK.219 cells, rapamycin treatment delivered concurrently with dox inhibited phosphorylation of mTOR target S6 but had little effect on 4E-BP1 (Fig 1A). By contrast, the mTOR active site inhibitor Torin, which inhibits both mTORC1 and mTORC2 complexes (Thoreen et al., 2009), completely inhibited S6 and 4E-BP1 phosphorylation. Importantly, this demonstrates that no viral proteins are mimicking mTORC1 function by phosphorylating downstream proteins. Treatment with rapamycin at the time of dox-induced lytic reactivation (0 hpi) limited viral protein accumulation, whereas Torin potently inhibited accumulation viral proteins across all temporal classes, including IE (RTA), Early (ORF45) and Late (K8.1, ORF65) (Fig 1E). If early viral gene expression was allowed to proceed for 24 h prior to treatment with rapamycin or Torin, I could detect similar S6 and 4E-BP1 dephosphorylation as treatment at 0 hpi, suggesting that mTORC1 is similarly required for phosphorylation of these canonical target proteins throughout lytic replication. However, delaying treatment with Torin to 24 hpi allowed viral genomes to

replicate, and late mRNAs (K8.1 and ORF26) and viral proteins to accumulate to levels comparable to vehicle-treated controls over the subsequent 24-48 h (Fig 3.1A, 3.2A-D). These findings suggest that even though mTORC1 is active during KSHV lytic replication, it may be dispensable for synthesis of viral proteins in middle and late stages of the lytic replication cycle.

KSHV proteins K1, ORF45, and vGPCR promote mTORC1 activity by inhibiting TSC2, ensuring Rheb activation. vGPCR inhibits TSC2 function by Akt phosphorylation (Sodhi et al., 2004), and ORF45 and K1 are likely to similarly inhibit TSC2 (Bhatt and Damania, 2012). TSC2 inhibits the mTORC1 activator Rheb, but mTORC1 must be recruited to the lysosome in an AA-dependent manner to interact with Rheb (Fig 1.3 (Laplante and Sabatini, 2009). Both HSV-1 and HCMV are capable of maintaining mTORC1 activity in the absence of AAs (Clippinger et al., 2011; Vink et al., 2018), but it is unknown if KSHV can similarly evade normal mTORC1 regulation. To test this, TREx-BCBL1-RTA cells, a PEL cell line with dox-regulated RTA transgene, were grown as an adherent monolayer on poly-D-lysine coated plates. Latent or 24 hpi cells were washed with dPBS and incubated for an hour in full, serum-free, or AA-free with 10% dialyzed FBS, medium before harvest. There was no clear change in S6 Ser235/6 phosphorylation during serum-starvation in either the latent or lytic populations (Fig 3.1B). AA starvation of latent cells inhibited mTORC1 signalling, as indicated by loss of S6 Ser235/6 phosphorylation, but mTORC1 was resistant to starvation during lytic replication. This suggests that lytic proteins disrupt normal regulation of mTORC1 to maintain activity when nutrients are limited, while responses are normal during latency. TREx-BCBL1-RTA cells grow in a suspension culture and most experiments are conducted on cells grown in suspension. Here, I noticed that AA starvation, but not serum starvation, or Torin treatment caused rapid adherence of the suspension cells to the culture dish (within 30 minutes). Why this occurs is unclear, but to better control the experiment, all cells were grown adherently in all conditions in Fig 3.1B.

3.2.2 Infectious Virion Can be Produced with mTOR Inhibition

To determine whether mTOR inhibition affected virion production, I used a FACS-based titering assay to detect release of recombinant virions that bear a *GFP* gene

driven by a constitutive EF-1α promoter. Supernatants from iSLK.219 cultures were used to infect a monolayer of recipient 293A cells, and measure the number of GFP+ cells 24 h later. The first virions are produced by dox-treated iSLK.219 cells by 48 hpi and virion production is near-maximal by 96 hpi (Fig. 3.3A). Cells treated with Torin during lytic reactivation produced very few infectious virions but delaying Torin treatment to 12 hpi allowed ~ 50% of maximal virion production over the intervening 48 h, compared to vehicle control (Fig. 3.3B). Delaying Torin treatment to 24, 48, and 72 hpi steadily increased the release of infectious virions from these cells, such that treatment with Torin for the final 24 h nearly produced as many virions as vehicle control. I corroborated this finding in TREx-BCBL1-RTA cells (Nakamura et al., 2003), a modified PEL cell line which also bears a dox-inducible *RTA*-transgene. Like the iSLK.219 cells, dox addition to TREx-BCBL1-RTA cells is sufficient to induce lytic reactivation, but reactivation is more synchronous. Using an assay to detect DNAse-protected KSHV genomes in the cell supernatant by qPCR, I detected very few viral particles in the cell supernatant at 24 hpi, which greatly increased by 48 hpi (Fig. 3.3C). Torin treatment at 0 hpi completely inhibited release of DNase-protected genomes from TREx-BCBL1-RTA cells, but delay of Torin treatment to 24 hpi allowed the assembly and release of approximately 50% as many viral particles as vehicle control-treated cells (Fig 3.4D). These results indicate that, similar to iSLK.219 cells, virion release from TREx-BCBL1-RTA cells was resistant to Torin treatment once virus replication had begun.

After treatment with dox, a portion of the iSLK.219 cells continue to proliferate, and could be diluting out the drug treatment. Dose-response studies of Torin treatments at 0 or 24 hpi show an increased resistance of virion production to mTOR inhibition at even the highest concentrations tested (Fig 3.3E). The calculated IC_{50} for virus titer from 66 nM to 121 nM, suggesting that cell proliferation somewhat dilutes the effects of Torin. However, resistance to Torin treatment by 12h (Fig 3.3B), and the continued loss of phosphorylation of mTORC1 targets for 48h to 72h following treatment (Fig 3.1A) suggest that the amount of Torin in the culture is sufficient to completely inhibit mTORC1 for the duration of the experiments. This finding provides support for the existence of a viral protein synthesis mechanism that can overcome sustained mTORC1 inhibition.

3.2.3 mTORC1 Inhibition Limits RTA Expression

Lytic reactivation depends on expression of the essential IE gene RTA. While RTA expression is generally sufficient for lytic reactivation, as in no other viral proteins are required, but reactivation by RTA is not highly efficient in all systems. Other, largely unknown, criteria must also be fulfilled. Both the iSLK.219 and the TREx-BCBL1-RTA systems depend on expression of a RTA by transactivation of a tetracycline-response element and expression of this transgene could be limited by Torin. The *RTA*-transgene in TREx-BCBL1-RTA cells has a C-terminal myc-epitope tag and can be detected independently of the native-RTA. Treatment with Torin at the time of reactivation greatly diminished expression of RTA-transgene (Fig 3.4A). Interestingly, this reduction seems to be at the mRNA level and not only due to translational suppression as expected from loss of 4E-BP1 phosphorylation. It is unclear how mTORC1 is mediating an effect on the RTA transgene mRNA, whether it is limiting transcription or enhancing mRNA degradation. Nuclear accumulation of PABPC1 due to host shutoff is sufficient for inhibiting RNA polymerase II activity (Gilbertson et al., 2018), and perhaps prolonged mTORC1 inactivation mediates a similar effect due to translation inhibition, but this hypothesis is untested. The native-RTA can be distinguished from the *RTA*-transgene by using primers directed to their different 3'UTR sequences (Fig 3.4C). Low *RTA*-transgene expression is accompanied by low expression of native-*RTA* and the early gene ORF57. In the iSLK.219 cells, the transgene is untagged and indistinguishable from the native gene on an immunoblot. However, RTA can be detected in dox-treated, uninfected iSLK cells, which similarly to TREx-BCBL1-RTA cells is restricted at both the protein and mRNA level by Torin, though not as potently.

As this defective transgene expression limits interpretation on the role mTOR for reactivation or early lytic events, I next developed a *de novo* infection model. I previously observed that *de novo* infection of iSLK cells can bypass latency and progress to lytic replication (and generate lytic foci) if the cells are first treated with dox to induce *RTA* expression, similar to a previous report of lytic foci formed by infection of cells with KSHV-lyt, a BAC36-based recombinant virus that constitutively expresses RTA (Budt et al., 2011). This system should be able to circumvent limitations in transgene expression

by having RTA present at the time of virus infection. I treated monolayers of uninfected iSLK cells with dox for 24 hours to stimulate *RTA* expression and infected the cells with rKSHV.219. The inoculum was removed and replaced with fresh media containing dox. Torin or vehicle control was then spiked into the well either immediately after recovery or at 24 hours after *de novo* infection. At 96 hours post-infection, cell supernatants were harvested and virions were titered by flow cytometry as above. Torin treatment at either 0 or 24 h following *de novo* infection potently inhibited virion release (Fig 3.4E). This suggests that for virion production to resist mTORC1 inhibition, the virus must first establish latency. However, this does not help to determine if Torin only limits reactivation by suppressing the *RTA*-transgene.

During lytic replication, iSLK.219 cells express an *RFP* reporter transgene driven by a lytic promoter in the viral genome (Vieira and O'Hearn, 2004). This serves a marker for entry into lytic replication. Without the addition of additional chemical reagents such as TPA or NaB (Myoung and Ganem, 2011), lytic reactivation in iSLK.219 is relatively inefficient with only ~20% of cells expressing RFP (Fig 3.3F-G). In this way, the iSLK.219 cells is best viewed as a low multiplicity of infection model. Torin treatment also inhibited accumulation of the RTA-dependent RFP reporter, but it is unclear how much of this inhibition is due to lack of entry into lytic replication, or poor RFP expression. Torin limits reactivation from latency and also limits expression of the *RTA*-transgene. This suggests that reactivation from latency might not be mTORC1-dependent so much as reactivation in these Tet-inducible systems are limited by Torin.

3.2.4 mTORC1 Is Not Required to Inhibit Autophagy during Lytic Replication

mTORC1 inhibition by rapamycin, Torin, or starvation activates autophagy through loss of ULK1 phosphorylation. Autophagy is thought to be anti-viral for herpesviruses, which in defence encode proteins to restrict autophagy through direct interaction with essential autophagy proteins (Orvedahl et al., 2007; Pattingre et al., 2005b). KSHV encodes at least three autophagy restricting proteins, and at least three proteins that activate mTORC1. However, it is unknown if these anti-autophagy proteins are sufficient to limit autophagy during replication if mTORC1 is inhibited. I tested induction of autophagy in a dox-treated iSLK.219 population by applying Torin for both

a short and long duration (4 or 24 hours). I found that Torin treatment led to dephosphorylation of ULK1 Ser757. However, I observe no increase in the accumulation of lipidated LC3-II over vehicle treatment, suggesting that mTORC1 is required to limit autophagy during KSHV replication (Fig 3.5A). Chloroquine (CQ) inhibits acidification of lysosomes, which prevents degradation of intravesicular autophagic cargo. CQ treatment leads to accumulation of LC3-II suggesting that there is some degree of autophagy that is not effectively inhibited in this population, but Torin-1 treatment has little effect on this accumulation. This suggests that inhibition of autophagy by KSHV is sufficient to overcome autophagy initiation by mTORC1 inhibition. Similar results were observed with 2h Torin treatment of TREx-BCBL1-RTA cells (Fig 3.5B). CQ treatment did lead to accumulation of LC3-II in latent TREx-BCBL1-RTA cells and 24hpi iSLK.219. As the proportion of lytic cells at 24h in iSLK.219 is likely low (Fig 3.4F) the majority of this LC3-II signal is likely from the latent cells. This suggests that even in the presence of vFLIP, the latent protein that limits ATG3 activity, there is significant LC3 lipidation during latency, but mTORC1 inhibition did not increase this flux. Long-term treatment with Torin reduces both lipidated and non-lipidated LC3 compared to vehicle, but this is not altered by CQ treatment, suggesting that this decrease could be due to mTORC1-dependent transcription or translation of LC3. In 24hpi TREx-BCBL1-RTA autophagic flux is strongly inhibited without increase from Torin inhibition or CQ, but there is abundant, lipidated LC3-II (Fig 3.5B).

To confirm that Torin treatment was not limiting virus replication by induction of autophagy, I used shRNA to knock-down the essential autophagy proteins, ATG12, ATG14, or Beclin (Fig 3.6A). I noted that Beclin knock-down also lead to a decrease in ATG14 expression; complex formation with Beclin might be required for ATG14 stability. This has been reported previously, but the mechanism is unclear (Russell et al., 2013). Beclin silencing increased virus titer by two-fold, whereas ATG12 and ATG14 caused modest increases in virus titer that did not reach statistical significance (Fig 3.6B). However, Beclin and ATG12 silencing had little effect on mTOR-dependent virion production when Torin-1 treatment was delayed to 24h post-reactivation. By contrast, ATG14 silencing prevented the inhibitory effects of Torin treatment on both lytic reactivation and mTOR-dependent virion production during lytic replication (Fig 3.6B-

C). I tested whether ATG14 was impacting the ability of Torin-1 to inhibit mTORC1 in both latent and lytic cells yet observed no differences (Fig 3.7) in phosphorylation with Torin treatment. This suggests that ATG14 is not preventing uptake of the drug, normal mTORC1 targeting, or the activity of relevant phosphatases. It is not clear what effect ATG14 might be having on reactivation, but this suggests that physiological mTORC1 signalling and not only mTORC1-dependent expression of the *RTA*-transgene expression could be required for lytic reactivation. I did not observe any spontaneous lytic reactivation of ATG14 silenced cells.

3.2.5 Butyrate Removes the Requirement for mTOR during Lytic Reactivation

Reactivation of iSLK.219 cells is more efficient when doxycycline treatment is supplemented with the HDAC inhibitors butyrate or valproic acid (Myoung and Ganem, 2011). HDAC inhibitors promote an more open chromatin on the viral episome, including at the RTA promoter (Hopcraft et al., 2018; H. J. Shin et al., 2013). Both of these compounds are sufficient to reactivate KSHV from latency in several cell lines, including BCBL1 cells, but neither of these are sufficient to stimulate reactivation in SLK cells (Bechtel et al., 2003; Myoung and Ganem, 2011). Reactivating iSLK.219 cells with dox and sodium butyrate (NaB) prevented inhibition of viral gene expression by Torin, including RTA expression (Fig 3.8A). NaB treatment did not disrupt Torin activity as demonstrated by loss of S6 Ser236 phosphorylation. Surprisingly, Torin treatment under these conditions enhanced virus titer compared to DMSO controls (Fig 3.8B). Active-site mTOR-inhibitors have previously been shown to limit transcription of Type-I IFN, but the mechanics of this response are undefined (Zakaria et al., 2018). To test for IFN production, I probed for STAT1 Tyr701 phosphorylation, which is required for STAT1 dimerization and nuclear translocation. Torin limited phosphorylation of STAT1 Tyr701, but this could only be observed during reactivation with only dox, and not in the presence of NaB (Fig 3.8A). This suggests that Torin can limit Type-I IFN production during KSHV reactivation.

3.3 Discussion

The seminal discovery that rapamycin treatment causes regression of iatrogenic Kaposi's sarcoma (KS) lesions suggests a central role for mTORC1 in KSHV biology (Stallone et al., 2005). mTORC1 activity has since been shown to be required for pro-inflammatory signalling in KS models (Martin et al., 2013; Roy et al., 2013; Sodhi et al., 2006). However, it remained unclear what role mTORC1 activation had in viral replication. mTORC1 is active during lytic replication, and this activation is dysregulated from normal inhibitory signals. K1, vGPCR, and ORF45 should all support mTORC1 by Rheb activation by promoting TSC2 phosphorylation.

Prolonged mTORC1 activation during AA starvation in KSHV infected cells suggests that KSHV can maintain mTORC1 proximity to Rheb. The mechanism of this is unclear, but interaction of a viral ORF with components of the GATOR complex seem a likely mechanism (Fig 1.3). During AA starvation, mTORC1 activity is eventually reactivated by AA efflux from the lysosome. This process was dependent on autophagic degradation of cytosolic proteins (L. Yu et al., 2011). mTORC1 inhibition did not promote autophagic flux during in KSHV infection, but CQ treatment did lead to an accumulation of lipidated LC3, suggesting that there is some degree of autophagic flux during KSHV replication. This could possibly provide sufficient AA efflux to support mTORC1 localization with the lysosome. However, it is also possible that the accumulation of lipidated LC3 is from a population of cells that have failed to productively enter lytic replication (as high as 80%, Fig 3.5). A single cell analysis of these cells is likely necessary resolve this.

mTOR is required for lytic reactivation, but not for genome replication, or accumulation of late gene mRNAs or proteins (Fig 3.1A, 3.2). This requirement, however, can be relieved by knockdown of the autophagy protein ATG14 or reactivation in the presence of NaB. This suggests that, at least for the iSLK.219 cells, that the amount of RTA-transgene produced is sufficient to stimulate viral replication. It is not clear if episomal RTA expression is truly necessary for virus reactivation, or if sufficient RTA accumulates from the transgene to drive the lytic cycle.

As neither NaB or ATG14 knockdown inhibited mTORC1 kinase activity, it is likely that mTOR activation, of either mTORC1 or mTORC2, represents a second-signal

for RTA-dependent reactivation that could be fulfilled by other appropriate stimuli. More anecdotally, I consistently observed that cells treated with dox and Torin at reactivation would have much more cytopathic effect over the course of the experiment than latent cells only treated with Torin. This suggested to me that the cells are not only failing to enter lytic replication due to low RTA expression, but there is a frustrated, and toxic effort to reactivate from latency.

These experiments do not separate the effects of mTORC1 or mTORC2 inhibition on lytic replication and only mTORC1 targets were analysed. The limited effects of rapamycin treatment on viral gene production might be due to the relatively poor inhibition on mTORC1 (Fig 3.1A) (S. A. Kang et al., 2013). Additional studies with knockdown of the essential mTORC2 component Rictor could help separate these functions, but specifically inhibiting mTORC2 function after reactivation is not yet pharmacologically possible.

ULK1 Ser757 is desphosphorylated by mTORC1 inhibition during both latency and lytic replication, but there was no change in LC3 lipidiation (Fig 3.5). These experiments suggest that mTORC1 activation during lytic replication is not required to regulate autophagy. However, it is not clear if the normal ULK1-phosphorylation of Beclin Ser14 is uncoupled, or if KSHV anti-autophagy proteins, such as vBcl2, are sufficient to limit autophagy initiation (Pattingre et al., 2005a; Russell et al., 2013). The presence of numerous KSHV anti-autophagy proteins strongly suggests that autophagy restricts KSHV replication. In a limited survey of essential autophagy genes, Beclin was found to restrict KSHV virion production (Fig 3.6). Knockdown of either ATG12 or Beclin, however, did not enhance virion production when mTOR was inhibited, confirming that there is no autophagy promotion by mTORC1 inhibition limiting virion production. It is unclear why Beclin silencing, which also depletes ATG14, does not similarly relieve the requirement of mTORC1 for reactivation (Fig 3.6). Beclin1 exists in at least two complexes, Beclin1-Vps34-ATG14, and Beclin1-Vps34-UVRAG (Itakura et al., 2008). The ATG14-containing complex has a role in initiation of autophagy whereas the UVRAG-containing complex promotes autophagosome maturation (Funderburk et al., 2010). It is possible that ATG14 knockdown promotes formation of the UVRAG complex, but how this would promote viral reactivation is unclear.

It is similarly unclear how ATG14 knockdown alleviates the requirement for mTOR during reactivation.

mTORC1inhibition and loss of 4E-BP phosphorylation should limit the formation of eIF4F in both latency and lytic replication; however, there is a clear accumulation of viral proteins and infectious virions. While eIF4F is the dominant mode of translation in cells grown in culture, there are several other non-eIF4F systems for translation initiation. In the next chapter, I examine the regulation of eIF4F during lytic replication and its requirement for efficient translation of viral proteins.

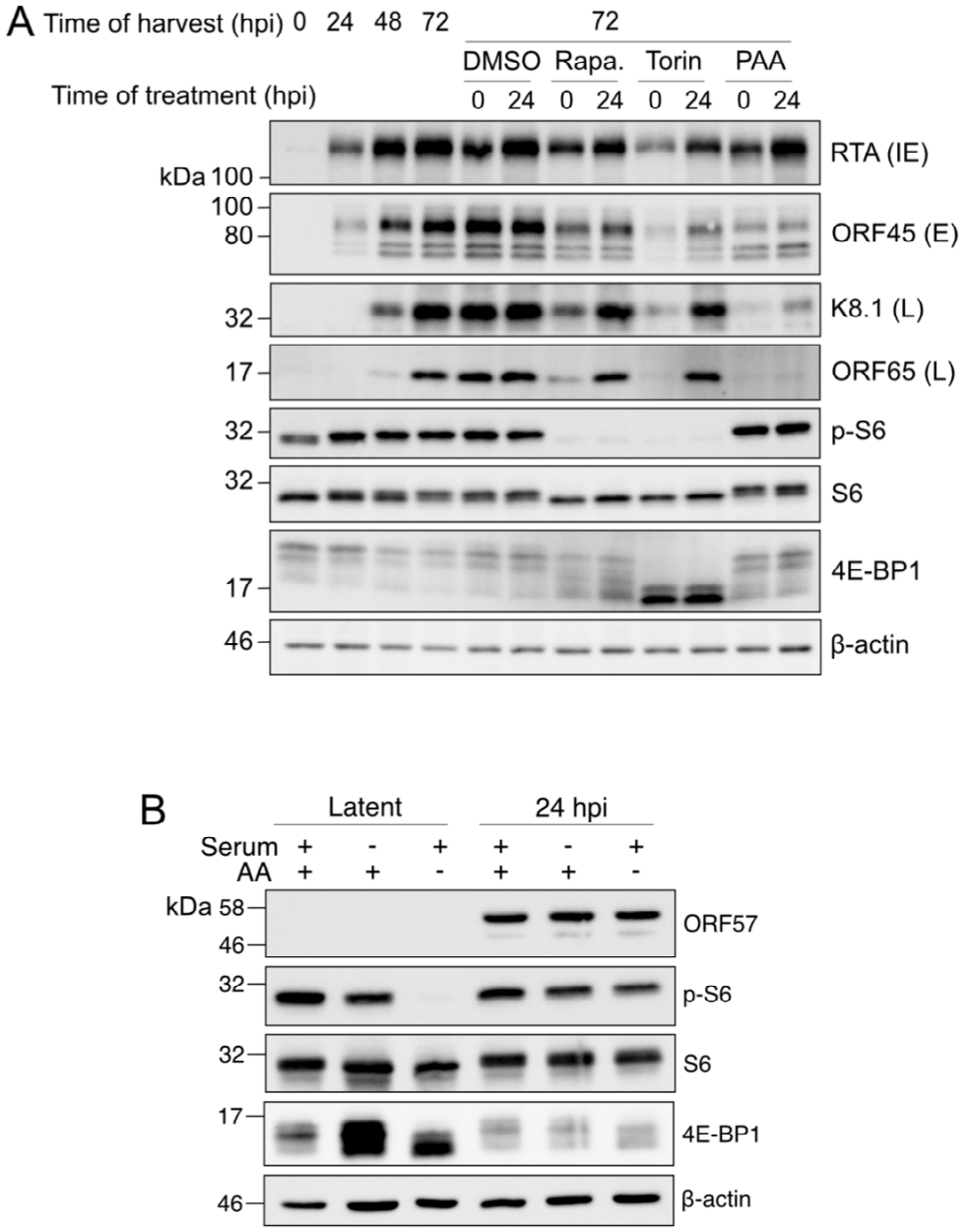

Fig 3.1. mTOR is active during lytic replication, but is not required for progression from early to late replication. (A) iSLK.219 cells treated with 1 μg/mL dox to induce lytic reactivation. DMSO vehicle control, Torin, Rapamycin or 500 μM phosphonoacetic acid (PAA) was added either at 0 or 24 hpi. Lysates were probed for immediate early protein (IE) RTA, early (E) protein ORF45, late (L) proteins K8.1 and ORF65. mTORC1 activity was determined probing for phospho-S6 Ser235/6 and 4E-BP1. (B) TREx-BCBL1-RTA cells were seeded onto poly-D-lysine coated cluster-dishes and left overnight. The following day, cells were washed with PBS and media was replaced with full media: + serum and + amino acids (AA), serum-free media, or amino acid-free media for one hour prior to harvest. Lysates were probed for E protein ORF57 and mTORC1 kinase targets.

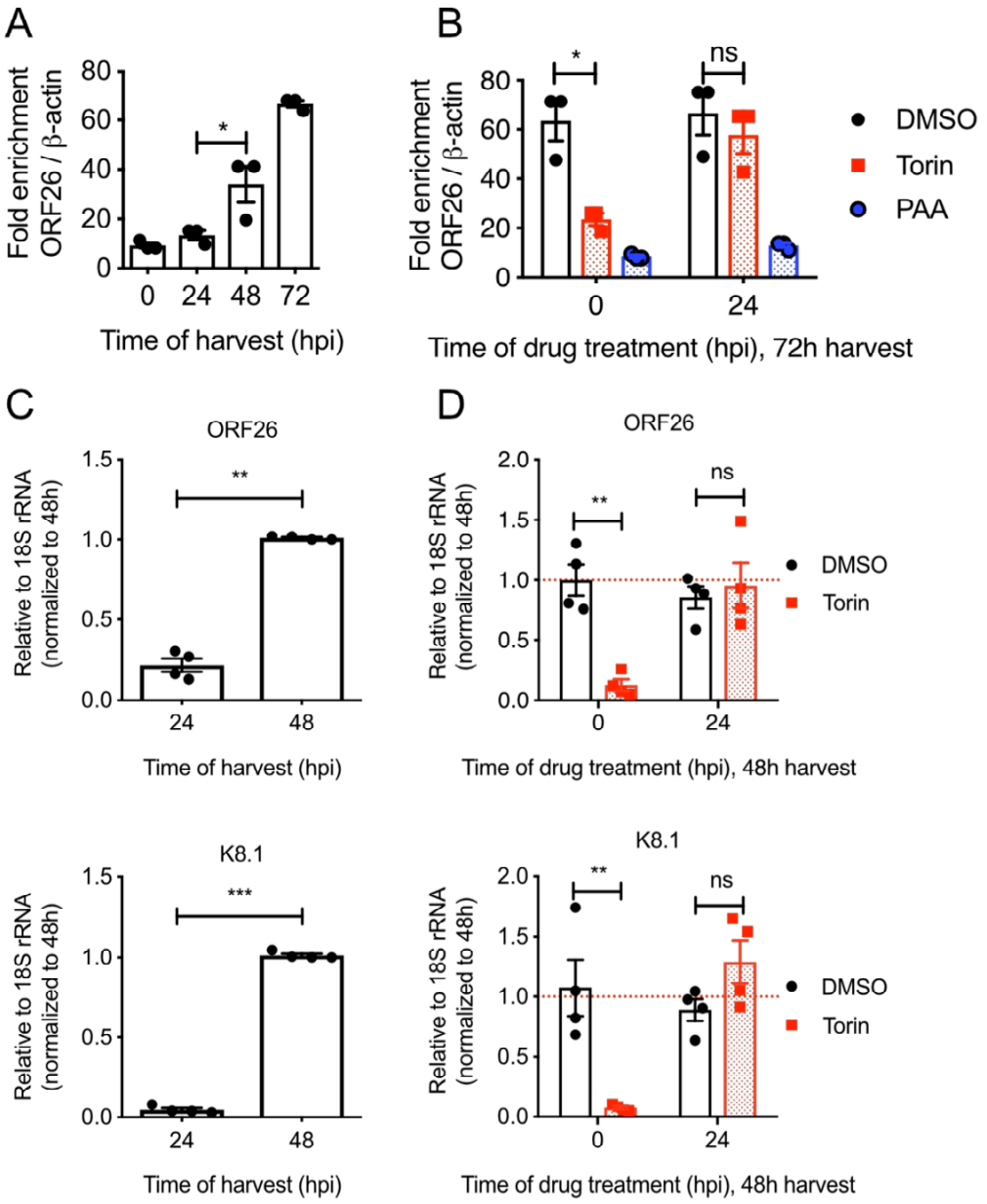

Fig 3.2 mTOR is required for reactivation from latency, but not progression from early to late replication (A) Viral genome replication. iSLK.219 cells were reactivated with 1 µg/mL doxycycline and treated with DMSO, Torin or PAA at 0 or 24 hpi. DNA was extracted from iSLK.219 cells at indicated times and the relative proportion of KSHV genome to human genome was quantified by qPCR for the viral gene ORF26 and the human gene β-actin (B) DNA was harvested from iSLK.219 cells at 72 hpi. Cells were treated as indicated with DMSO, Torin or phosphonoacetic acid (PAA) at either 0 or 24 hpi. n=3 ± SEM. (C-D) Viral late gene expression. As in (A and B) except RNA extracted and qRT-PCR performed for the late genes ORF26 (top) and K8.1 (bottom). n=4 ± SEM.

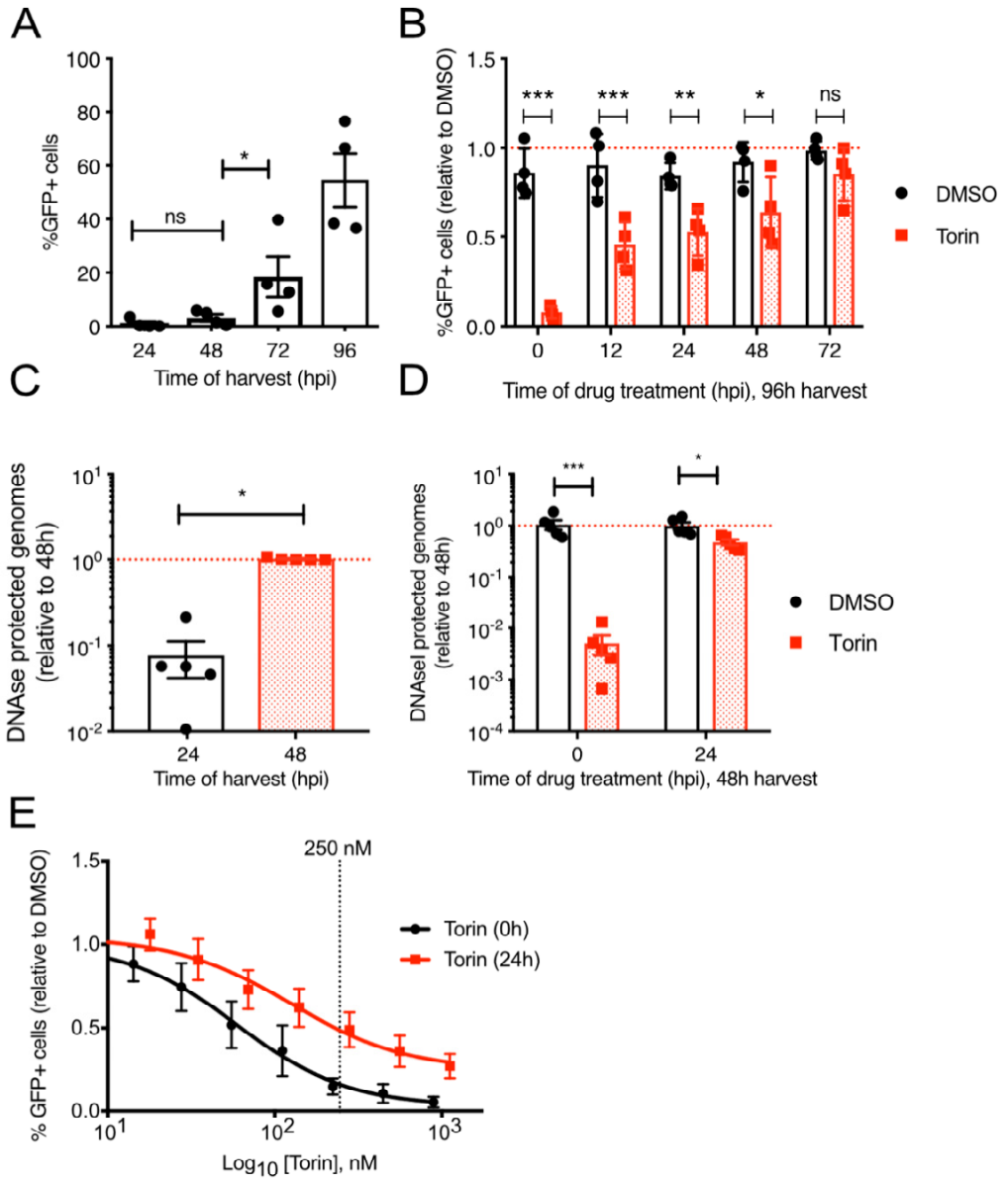

Fig 3.3 mTOR is not required for production of infectious virions after KSHV reactivation (A) iSLK.219 cells treated with 1 µg/mL dox one day after seeding. Supernatant harvested at times indicated and frozen at -80°C until titering on 293A cells. GFP+ cells from an arbitrary live-dead gate were recorded by flow cytometry. n=4, ±SEM. (B) As in A except Torin or DMSO were diluted in media and spiked into the cells at the time of doxycycline treatment (0 hpi) or the times indicated. Supernatant was harvested at 96 hpi for titering as described in (A). n=4, ±SEM. (C) TRex-BCBL1-RTA cells were reactivated from latency with 1 µg/mL dox. Cells and debris were removed by centrifugation, then supernatant was treated with DNase I before harvesting virion DNA. DNAse-protected viral genomes were quantified with qPCR using luciferase plasmid spike as a recovery control.(D) As in (C) but DMSO or Torin was added a 0 or 24 hpi. n=5, ±SEM. (E) As in (B) but iSLK.219 cells treated with a range of Torin concentrations at 0 or 24 hpi.

Fig 3.4 Effects of mTOR inhibition on RTA-transgene expression from iSLK and TREx-BCBL1-RTA cells (A) TREx-BCBL1-RTA cells or (B) Uninfected iSLK cells were treated with 1 μg/mL dox and, Torin or DMSO. (C-D) as in (A-B) but RNA was harvested for RT-qPCR using from (C) iSLK or (D) TREx-BCBL1-RTA cells. (C) iSLK, Primers targeting the CDS of the RTA-transgene, (D)TREx-BCBL1-RTA, primers targeting the 3'UTR of the viral RTA (Native), the *RTA*-transgene, or early gene ORF57. (E) De novo lytic replication in uninfected iSLK cells. iSLK cells were seeded and treated with 1 μg/mL dox for 24 hours to stimulate RTA expression. These cells were then infected with rKSHV.219, the inoculum was removed, the cells were washed, and media with 1 μg/mL dox was replaced. Torin or DMSO were spiked into the well at the time of media replacement or 24 hours-post-infection. 96 hours-post-infection, supernatant was removed and titered by infecting 293A cells as described in Fig 3.2. (F-G) RFP expression from rKSHV.219 PAN-RFP lytic reporter. iSLK.219 cells were treated with 1 μg/mL dox 24 hours after seeding. Torin or DMSO was diluted in media and spiked in with dox treatment (0 hours-post-induction, 0 hpi) or 24 later (24 hpi). Cells were fixed with 4% paraformaldehyde and nuclei were stained with Hoescht. RFP+ cells and nuclei were imaged on an inverted fluorescent microscope and enumerated with CellProfiler. n=3 ± SD

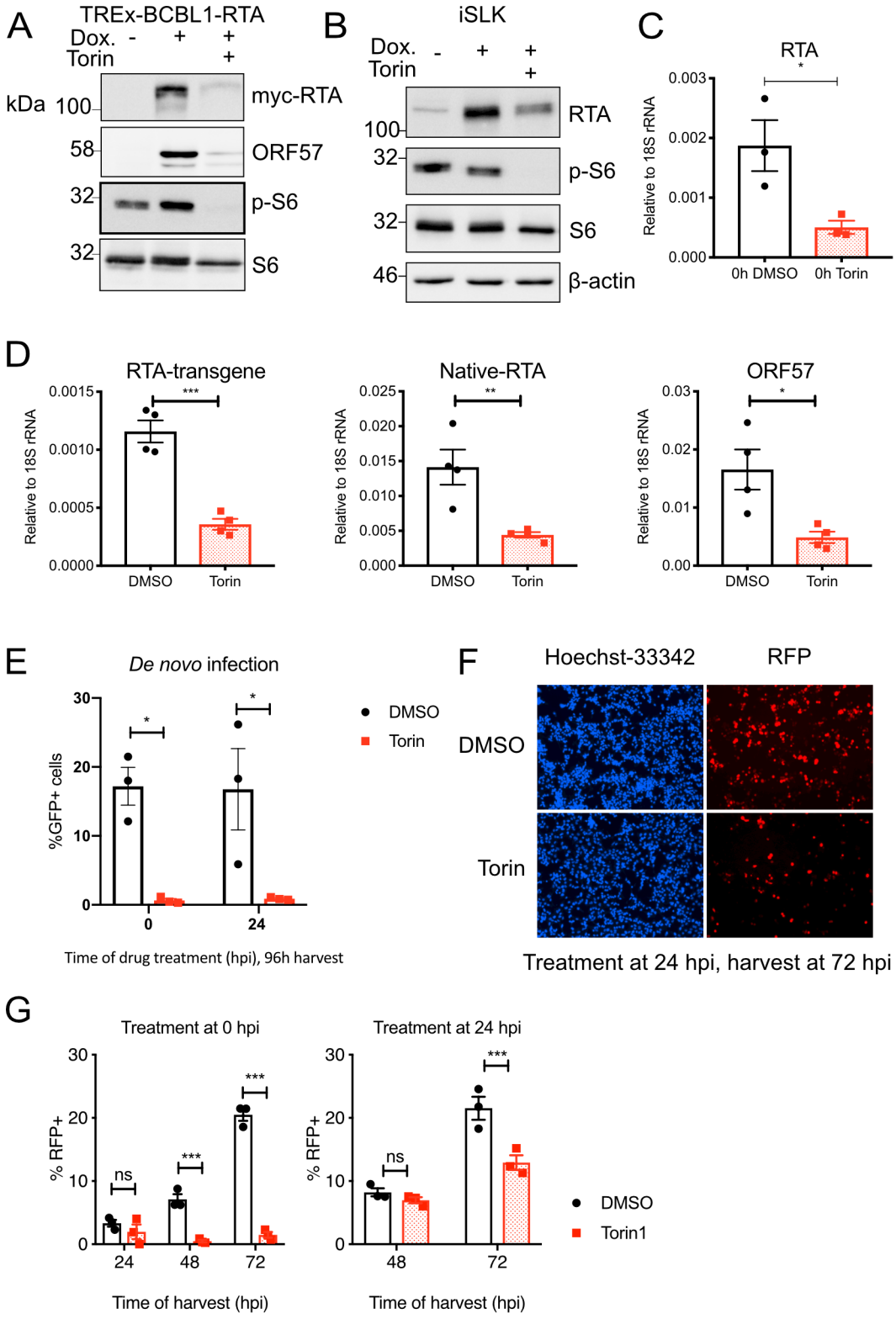
A
TREx-BCBL1-RTA
Dox. - + +
Torin +
kDa
100
58
32
32
myc-RTA
ORF57
p-S6
S6
B
iSLK
Dox. - + +
Torin +
100
32
32
46
RTA
p-S6
S6
β-actin
C
RTA
Relative to 18S rRNA
0.003
0.002
0.001
0.000
0h DMSO
0h Torin
D
RTA-transgene
Native-RTA
ORF57
Relative to 18S rRNA
DMSO
Torin
E
De novo infection
%GFP+ cells
30
20
10
0
0
24
DMSO
Torin
Time of drug treatment (hpi), 96h harvest
F
Hoechst-33342
RFP
DMSO
Torin
Treatment at 24 hpi, harvest at 72 hpi
G
Treatment at 0 hpi
Treatment at 24 hpi
% RFP+
ns
24
48
72
Time of harvest (hpi)
DMSO
Torin1

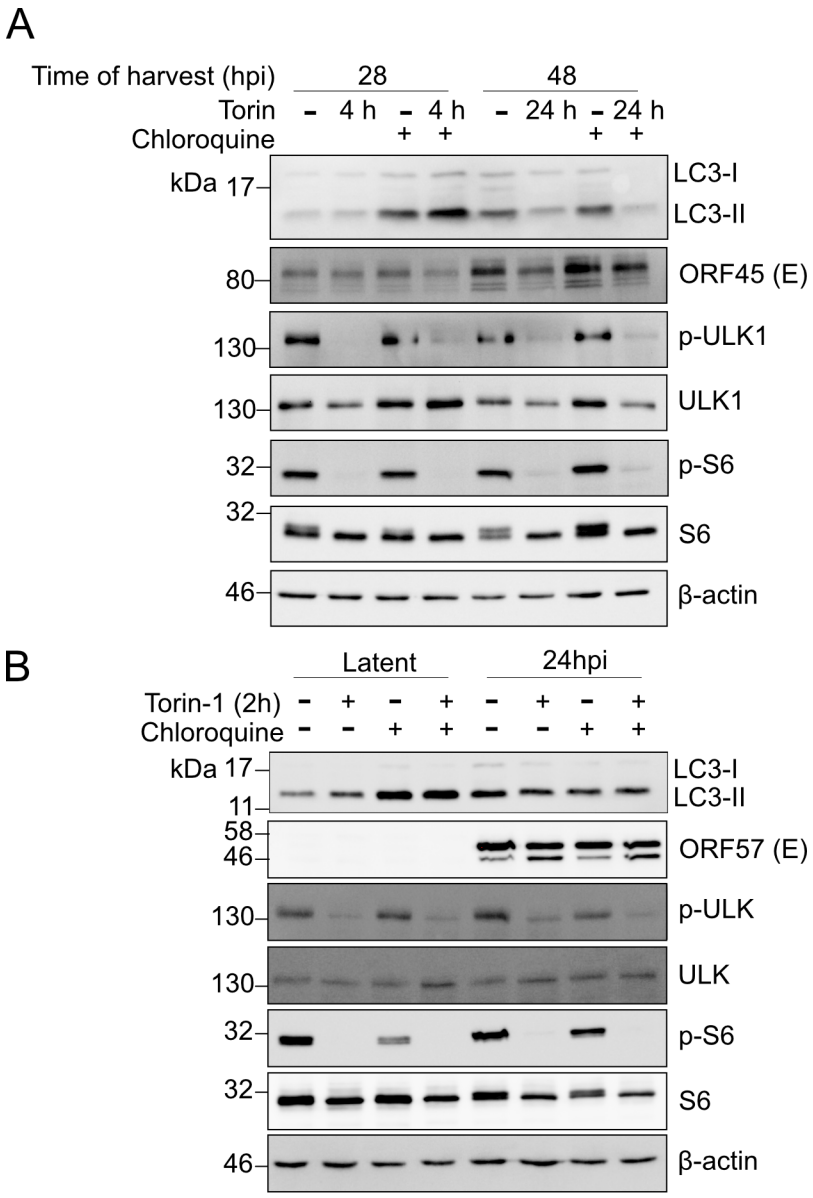

Fig 3.5 mTOR inhibition does not enhance autophagic flux during lytic replication
(A) iSLK.219 cells reactivated with 1 μg/mL dox were treated with DMSO vehicle control, Torin-1, or 50 μM (CQ) at 24 hpi as indicated. Lysate was harvested 4h or 24h later at 28 hpi or 48 hpi. Lysates were probed for early (E) protein ORF57, mTORC1 targets phospho-ULK1 Ser757 and phosphor-S6 Ser235/6. Autophagic flux was determined by detection of LC3-I and II. (B) As in A with TREx-BCBL-RTA latent or 24 hpi cells treated for two hours prior to harvest.

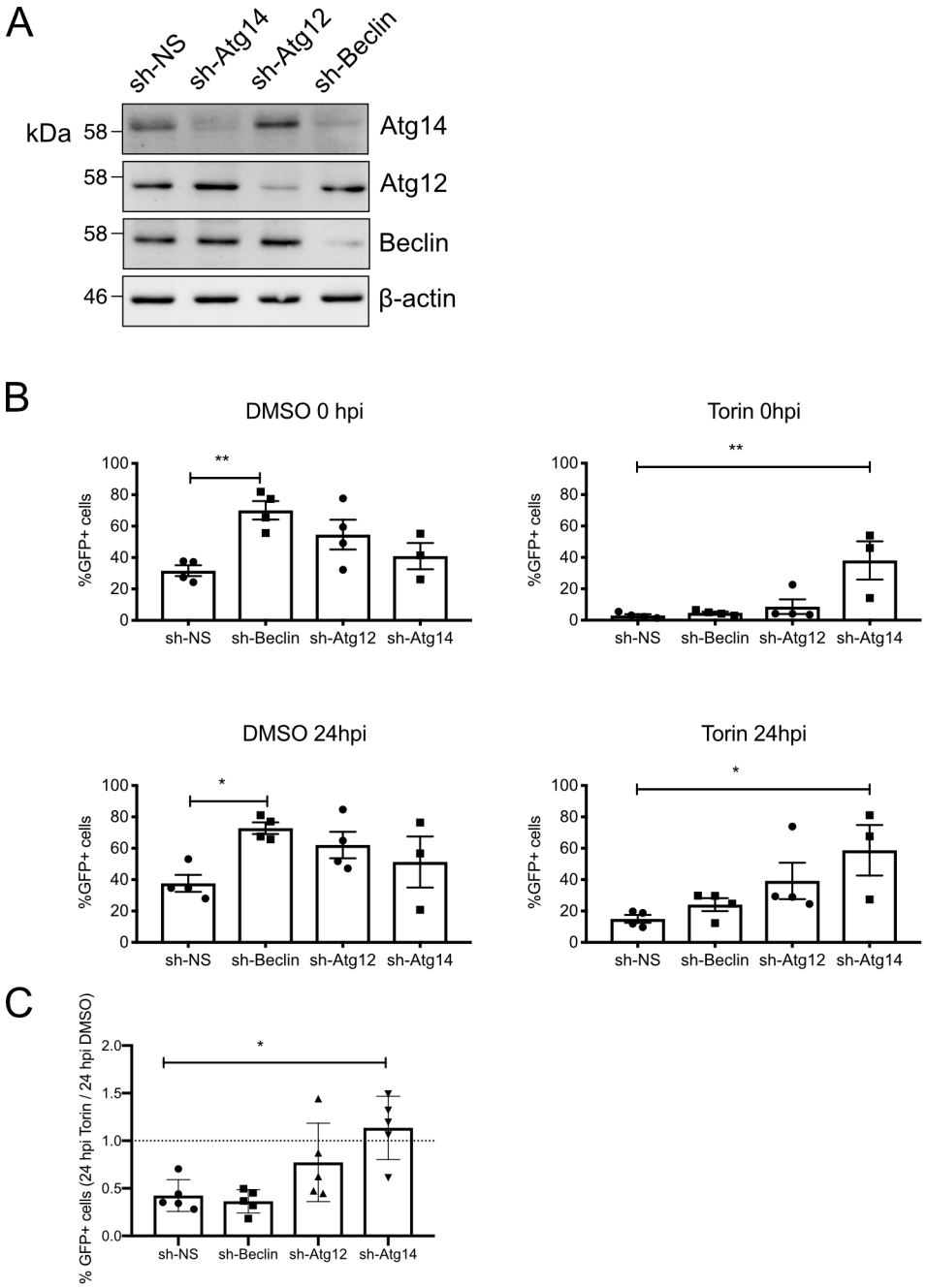

Fig 3.6 ATG14 is required for inhibitory effects of Torin on reactivation and virion production (A) iSLK.219 cells were transduced with lentiviruses targeting ATG14, ATG12, Beclin, of a non-targeting control (sh-NS). After selection with blasticidin, latent cells were seeded for immunoblot confirmation of knockdown. (B) Production of virions from shRNA-transduced iSLK.219 reactivated with 1 µg/mL dox. Supernatant harvested at times indicated used to infect a monolayer of 293A cells. Infected cells were enumerated as GFP+ events by flow cytometry. (C) From (B), the proportion of GFP+ cells of Torin or DMSO treated cells at 24 hpi. n=3-4, ±SEM. Carolyn Robinson (Department Microbiology and Immunology, Dalhousie) provided assistance by generating supernatant from shRNA-transduced iSLK.219.

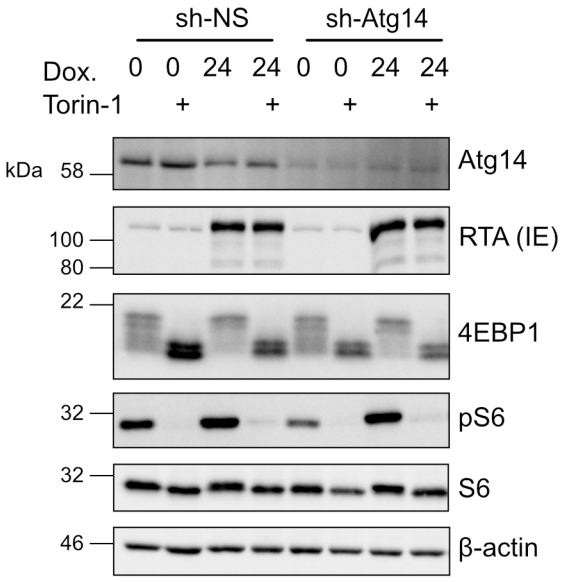

Fig 3.7 ATG14 is not required for mTORC1 kinase activity, or dephosphorylation of target proteins iSLK.219 cells transduced with shRNA and selected with blasticidin. Cells were reactivated with 1 μg/mL dox. Two hours prior to harvest, cells were treated with Torin or DMSO. At 24 hpi, cells were harvested and probed as indicated for immediate early protein RTA, and mTORC1 targets 4E-BP1 and phospho-S6 Ser235/6.

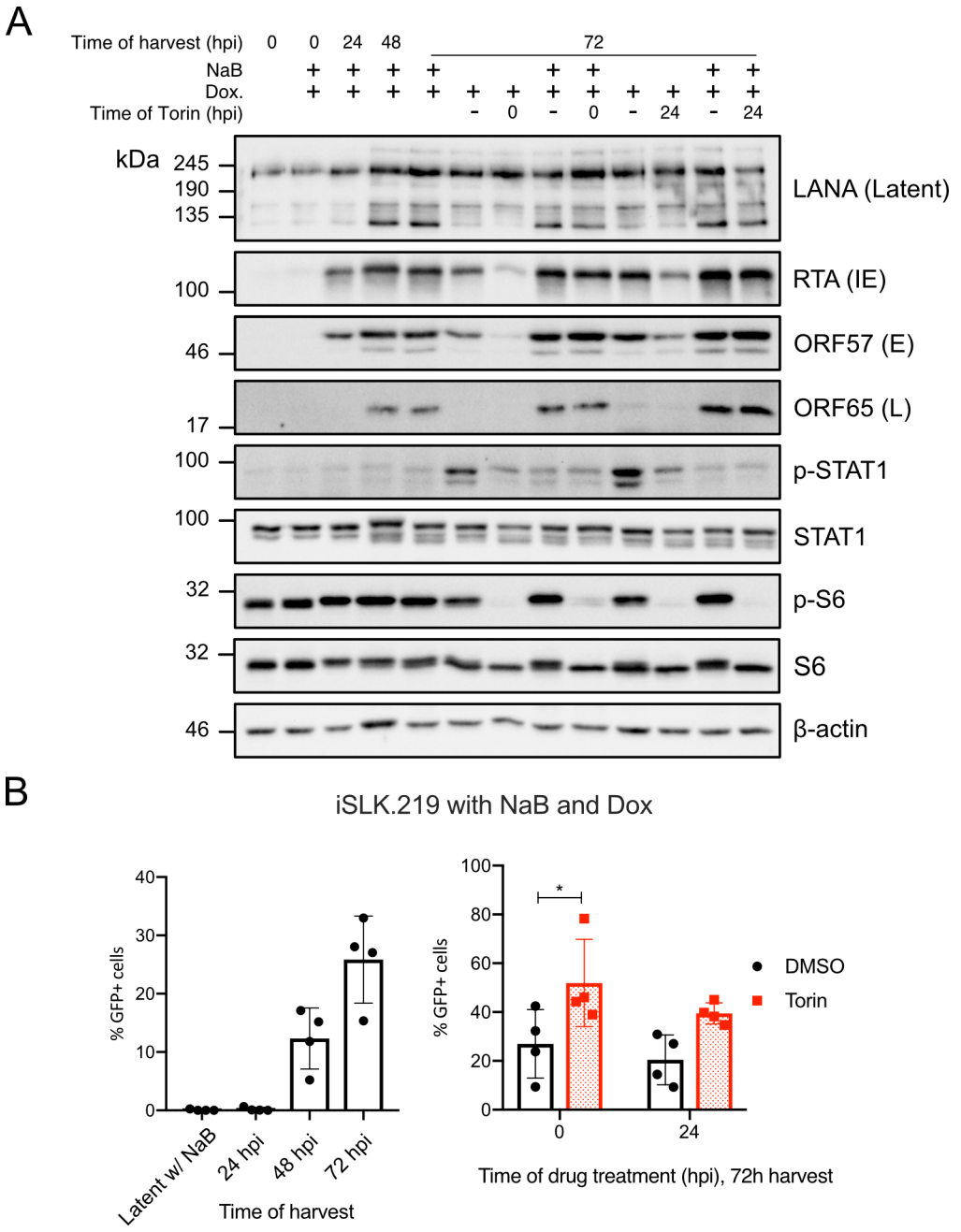

Fig 3.8 Butyrate overcomes the mTORC1 requirement for lytic reactivation (A) iSLK.219 cells treated with reactivated with 1 µg/mL dox with or without sodium butyrate treatment (NaB). Cells were treated with Torin or DMSO at either 0 or 24 hpi and harvested at the times indicated. Lysates were probed for immediate early (IE) protein RTA, early (E) protein ORF57, and late (L) protein ORF65. mTORC1 activity was determined by phosphor-S6 Ser235/6 and type I interferon signalling was assessed by presence of phosphor-STAT1 Tyr701. (B) Supernatants from cells reactivated with NaB and dox in (A) were used to infect a monolayer of 293A cells. GFP+ cells were counted by FACs. n=4 ± SEM.

Chapter Four – Translational Efficiency of Viral mRNA

4.1 Introduction

While mTORC1 activation can support lytic reactivation of KSHV, mTORC1 is largely dispensable for progression through lytic replication and production of progeny virions. mTORC1 is a critical regulatory of eIF4F-dependent translation through its control of 4E-BP; however, viral proteins accumulated normally when mTORC1 was inhibited (Fig 3.1). Torin treatment during both latency and lytic replication, inhibited mTORC1 kinase activity and downstream targets, including 4E-BP1, were completely unphosphorylated. This suggests that either KSHV is able to disrupt normal regulation of the mTORC1-4EBP1-eIF4F axis, or that the virus can translate proteins using a non-eIF4F initiation mechanism. Herpesvirus from all subfamilies have been demonstrated to activate mTORC1 during lytic replication (Clippinger et al., 2011; Walsh et al., 2005). Yet, like KSHV, there is evidence that both HSV and HCMV virion production is resistant to mTORC1 inhibition (Lenarcic et al., 2014; McMahon et al., 2010).

mTORC1 activation is a hallmark of KSHV infection; several KSHV gene products have been shown to stimulate or mimic mTORC1 activation (reviewed in Bhatt and Damania, 2012) and mTORC1 substrates are phosphorylated in KS lesions (Stallone et al., 2005). KSHV early lytic gene products K1 and vGPCR activate mTORC1 by stimulating the upstream mTORC1 kinase Akt (Martin et al., 2013; Z. Zhang et al., 2016). Moreover, ORF36 and ORF45 partially mimic mTORC1 signalling. eIF4F assembly has been detected in lytic TREx-BCBL1-RTA cells suggesting that eIF4F is available for translation of viral protein (Arias et al., 2009). Given that mTORC1 appears to be a central node of KSHV host subversion, I was surprised that viral protein synthesis appeared mTORC1-independent.

Therefore, in this chapter, I examined global protein synthesis during KSHV replication and the translational efficiencies of viral mRNA under the stress of reactivation or mTORC1 inhibition. To test the role of mTORC1 inhibition on viral mRNA translation, I used RNA sequencing of polysomes during lytic replication to measure the translational efficiencies (TE). This approach provides a global assessment of all viral and cellular transcripts and allows for comparison of differential regulation of both populations of mRNA. I also analysed the requirement for continued mTOR activity

for maintaining eIF4F composition, both unbound and polysome associated, and examined several translation initiation factors are essential for non-eIF4F translation.

In this chapter, I demonstrate that global protein synthesis remaining after host shut off is sensitive to mTOR inhibition. However, the efficient translation of viral mRNAs is resistant to mTORC1 inhibition. eIF4F assembly is readily detectable during latency and lytic replication and is lost when mTORC1 is inhibited, suggesting that the mTORC1-4EBP1-eIF4F axis is intact. Like eIF4F, several other initiation factors required for non-eIF4F translation initiation were also dispensable for virion production, including the m^7GTP-binding protein eIF4E2 and eIF3d. However, silencing of the essential m^6A methyltransferase METTL3, which would result in defects of m^6A-dependent translation, caused a ten-fold loss in virion production, with defective late gene accumulation. Taken together, this data suggests that eIF4F is dispensable for virion production, and that KSHV transcripts are initiated using an alternative mechanism.

4.2 Results

4.2.1 mTOR Activity Promotes Bulk Protein Synthesis

Host shutoff is a feature of KSHV lytic replication whereby bulk synthesis of host proteins is inhibited, which limits the ability of the host cell to restrict virus infection and may improve access of viral mRNA to the host protein synthesis machinery. Host shutoff is largely coordinated by the viral endonuclease SOX, which cleaves both viral and cellular messages (Glaunsinger and Ganem, 2004a; 2004b). mTOR-mediated eIF4F assembly is required for bulk cellular protein synthesis but its role during KSHV lytic replication is unknown. To address this directly, I employed the efficient TRex-BCBL1-RTA cell model, and treated cells with doxycycline and TPA to ensure efficient lytic reactivation. At 10 min prior to harvest, 10 μg/mL puromycin was added to these cells to measure new protein synthesis; puromycin resembles charged tyrosyl-tRNA and is incorporated at the carboxy-terminus of nascent polypeptide chains, thereby preventing elongation. As the amount of puromycin incorporation is directly proportional to the quantity of lengthening transcripts, detection of puromycin by immunoblotting can be used as a proxy for global protein synthesis(Schmidt et al., 2009).

Puromycin incorporation into newly synthesized peptides was greatest in latently infected cells (Fig 4.1 lane 1), this was reduced to less than 50% incorporation by 12 hpi (lane 4) and ~10% incorporation by 24 hpi (lane 7), consistent with host shutoff during the KSHV lytic cycle (Glaunsinger and Ganem, 2004a). In this assay, sodium arsenite served as a potent positive control; treatment of cells with sodium arsenite for 10 min prior to addition of puromycin (20 min prior to harvest) caused eIF2α phosphorylation and largely ablated puromycin incorporation indicating a comparable loss of global protein synthesis in latent (lane 3), early lytic (lane 6) and late lytic (lane 9) cells. Treatment with Torin caused a significant loss of 60% of bulk protein synthesis during latency (lane 2). Torin further decreased bulk protein synthesis during lytic replication at 12 hpi (lane 5) or 24 hpi (lane 8) beyond the already diminished rate. Importantly, Torin completely inhibited mTOR-mediated phosphorylation of 4E-BP1 in both latent and lytic cells (lanes 2, 5, 8), indicating that the residual bulk protein synthesis in cells experiencing host shutoff is resistant to 4E-BP, which would normally be expected to efficiently suppress cap-dependent translation. Together, these data suggest that there is continued dependence on mTORC1 for protein synthesis in lytic cells.

4.2.2 mTOR Inhibition Does Not Affect Translational Efficiency of Viral mRNA

In response to nutrient stress or pharmacologic inhibition, mTORC1 inactivation prevents eIF4F assembly, which would be expected to broadly inhibit cap-dependent protein synthesis; however, studies of mTORC1 inhibitors in cancer cells have shown that the regulation of mRNA translational efficiency (TE) is complex. For example, select mRNAs bearing terminal oligopyrimidine (TOP) sequences (Thoreen et al., 2012) or pyrimidine-rich translational element sequences (Hsieh et al., 2012) at their 5′ ends are strongly sensitive to mTORC1 inhibition, whereas other mRNAs can be more efficiently translated for unknown reasons. I used polysome analysis followed by RNA-Seq, also known as Pol-Seq, to determine whether mTORC1 inhibition affects the TE of viral mRNA. In these experiments, I reactivated iSLK.219 with dox only in an attempt to limit other stresses on the cell. As mentioned above, under these conditions many of the iSLK.219 cells either fail to reactivate, or undergo an abortive replication; thus, dox treatment renders a mixed population of lytic and non-lytic cells.

Torin treatment of latent iSLK.219 or uninfected SLK cells for 2 h prior to harvest resulted in a substantial shift of mRNA from the well-translated heavy polysomes to the poorly-translated sub-polysomal fractions (Fig 4.2A), consistent with previous observations of diminished rates of global protein synthesis in the TREx-BCBL-RTA model (Fig 4.1, lane 2). Similarly, by 48 hpi, there was a substantial decrease in the mRNA associated with the polysome fractions in lytic cells compared to latently infected cells (Fig 4.2A), consistent with the actions of SOX (Covarrubias et al., 2011). Addition of Torin to the 48 hpi cell population for 2 h prior to harvest resulted in further shift of mRNA to sub-polysomal fractions. I isolated mRNA from the polysomes of 48 hpi cells treated with Torin or vehicle control for 2 h, and total RNA from these populations from two independent biological replicates. All eight samples were then subjected to library preparation and sequencing by Ion Torrent. Reads were mapped on a per-transcript basis using the Hg19 build of the human genome concatenated to the KSHV genome from JSC-1 cells; this is the parental virus strain of the rKSHV.219 cell line (Myoung and Ganem, 2011; Vieira and O'Hearn, 2004) that I manually re-annotated with the transcript information from the KSHV2.0 annotation (Arias et al., 2014). I assessed TE by simple division of the number of reads isolated from the polysomes compared to the reads found in the total RNA fraction (#reads polysome / #reads total). The abundance of KSHV transcripts differed by as much as 100,000 fold with ten-fold more of the non-coding PAN RNA than the next most abundant RNA. After PAN, the most abundant protein-coding viral mRNA encode the ORF59 processivity factor, Kaposin (K12), vIL-6, and the viral dUTPase-mimic ORF11 (Fig 4.2B).

Consistent with the literature, Torin caused broad alterations in the TE of cellular mRNA, with populations of mRNA displaying increased or decreased TE (Fig 4.2C). Differences in translational efficiencies were scored by using a sliding-window to calculate a Z-score of each detected transcript compared to the surrounding 200 transcripts of similar abundance as measured by count per million (CPM). The ΔTE of ~90% viral mRNA was sustained in the presence of Torin, and changed less than 1 SD from the mean (Fig 4.2C, Z-score within 1 SD of the mean in blue, Z-score > 1 SD of the mean in red). I analysed transcripts with a greater than 1.5-fold increase or reduction in translational efficiency using the Panther GO-Slim Molecular Function analysis (Fig

4.2D). Both ribosomal structural proteins and TIF were over-represented in transcripts with reduced TE during Torin treatment. This is consistent with previously published datasets that documented mTORC1 inhibition of translation (Hsieh et al., 2012; Thoreen et al., 2012), and suggests that TOP-containing transcripts are normally regulated during KSHV lytic replication. Using the GO-Slim terms, I did not detect enrichment of any molecular function in transcripts with up-regulated TE. Because this annotation was linked to individual transcripts rather than genes, I was able to detect a slight yet significant ($p<0.0001$) enrichment of normally-labile pseudogene mRNA in high TE groups, and their corresponding diminishment in low TE groups (Fig.4.2E). This result is not likely due to enhanced translation initiation of pseudogene mRNA, but instead due to accumulation of ribosomes on these transcripts due to halted elongation while the mRNA is processed by nonsense-mediated decay (NMD) and other ribosomal quality control processes (reviewed in Joazeiro, 2017). Thus, during KSHV lytic replication, host cell transcripts are regulated by the mTORC1-4EBP1-eIF4F signalling axis as expected, whereas viral transcripts are not.

I confirmed these findings in the TRex-BCBL1-RTA cell model by assessing the distribution of host and viral mRNA in polysomal and sub-polysomal fractions. Consistent with observations in the iSLK.219 model, Torin treatment of lytic TRex-BCBL1-RTA cells for 2 h prior to harvest resulted in a moderate shift of bulk mRNA from polysomes to the sub-polysomal fractions (Fig 4.3A). I harvested mRNA from polysome, monosome, and sub-monosome fractions, and performed RT-qPCR on select mRNAs as an additional measure of TE. Torin treatment caused a large shift of β-actin mRNA from heavy polysomes to the monosome and sub-monosome fractions (Fig 4.3A). However, a significant proportion of translating β-actin mRNA remained in the polysome fractions despite Torin treatment. By contrast, Torin treatment caused the TOP-mRNAs encoding Rps20 and RACK1 to completely shift from polysome fractions to monosome and sub-monosome fractions. Viral mRNA from all three transcriptional classes were evaluated for polysomal distribution: Latent (LANA, Kaposin), early (ORF 8/9/10/11, ORF 47/46/45, vIL-6), and late (K8/K8.1, ORF 25/26, ORF67/66/65). As the viral genome is heavily nested with shared promoters and polyA sites, the originating mRNA of RT-qPCR products cannot be readily distinguished (Arias et al., 2014). The TE of all

viral mRNA tested generally seemed to resist Torin inhibition, but a slight shift towards the sub-polysomal fractions can be detected (Fig 4.3B).

4.2.3 Translation of Cytokines

VEGF-A and IL-6, two cytokines with significant contributions to KS pathogenesis (Martin et al., 2013; Roy et al., 2013; Sodhi et al., 2006) were abundant in the monosome fraction in both vehicle control and Torin-treated cells. To determine if mTORC1 inhibition could limit VEGF-A production, latent or reactivated cells were treated with Torin or rapamycin and supernatant was harvested for ELISA. Cells were pelleted and washed with PBS before treatment to ensure that only cytokines secreted post-treatment were measured. Accumulation of VEGF-A in latent TREx-BCBL1-RTA cells was inhibited by either rapamycin or Torin treatment, consistent with previously published reports (Sin et al., 2007) (Fig 4.4A). mTORC1 inhibition will limit proliferation of cells over the course of the experiment, which will contribute to less cytokine secretion. It is interesting that Torin had less effect on cells that were also reactivated with doxycycline, even though there is little evidence of lytic reactivation under these conditions (Fig 3.3). This suggests that accumulation of cytokine during lytic replication might better be considered an accompaniment to, rather than a part of, the lytic program. Delaying Torin or rapamycin treatment until 24 hpi had no effect on VEGF-A accumulation. These findings suggest that key pathogenic host cytokines are normally translated in monosomes or light polysomes and Torin treatment does not displace these mRNAs from the monosomes.

4.2.4 mTOR Inhibition in Lytic Replication Disrupts eIF4F Assembly

mTORC1 primarily regulates translation initiation by preventing assembly of the eIF4F initiation complex. When unphosphorylated, 4E-BP1 can bind to the eIF4E cap-binding protein, which prevents recruitment the eIF4G scaffolding protein. mTORC1-mediated phosphorylation of 4E-BP1 enables eIF4F assembly and subsequent recruitment of the eIF3 complex and the small ribosomal subunit (Glaunsinger, 2015; Jan et al., 2015). mTORC1 activity during KSHV replication was previously shown to enable the assembly of eIF4F (Arias et al., 2009). To further examine the role of mTORC1

activity eIF4F regulation during lytic replication. I performed m^7GTP Sepharose bead pull-downs in native lysates from both iSLK.219 cell and TRex-BCBL1-RTA cell models, and probed for assembly of canonical and alternative eIF4F constituent proteins in the presence or absence of Torin. eIF4G1 and eIF4G3 were co-captured on m^7GTP Sepharose beads with eIF4E1 and eIF4E2 cap-binding proteins from latent and lytic iSLK.219 lysates (Fig 4.5A, lanes 3, 5, 7), suggesting the potential for formation of canonical and non-canonical eIF4F complexes at all stages of viral replication. eIF4G1 and eIF4G3 were depleted from these complexes when cells were treated with Torin for 2 h prior to harvest, while there was a reciprocal increase in unphosphorylated 4E-BP1 detected in the pulldowns (Fig 4.5A, lanes 4, 6, 8). Interestingly, I detected a marked increase in binding of eIF4E2 to the m^7GTP Sepharose beads as the lytic cycle progressed, but this did not aid recruitment of eIF4G3 in the presence of Torin (Fig 4.5A, lanes 4-8). Together, these data confirm that eIF4F can indeed be disrupted by mTORC1 inhibition during the lytic cycle.

To investigate the effects of long-term mTORC1 inhibition in this model, I treated iSLK.219 cells with Torin at 24 hpi and harvested lysates for m^7GTP Sepharose bead pulldown at 48 hpi. Similar to the 2 h Torin treatments in Fig 4.5A, 24 h of sustained mTORC1 inhibition during lytic replication also impaired eIF4F assembly (Fig 4.5B), while selectively inhibiting the accumulation of total eIF4G1 and eIF4E2 proteins. I corroborated these findings in the TRex-BCBL1-RTA cell model; treatment of latent or lytic cells with Torin for 2 h prior to lysate harvest completely inhibited eIF4F assembly by allowing unphosphorylated 4E-BP1 to block recruitment of eIF4G1 or eIF4G3 to eIF4E1/eIF4E2 proteins (Fig 4.5C). It is important to note that there is a limitation to the experiments described in Fig 4.5; as the bait is an analogue of the mRNA cap, the m^7GTP Sepharose bead pulldown assay should only detect free eIF4F complexes that are not already bound to mRNA in the lysate. Thus, it is possible that viral mRNPs retain intact eIF4F in these lysates, making them exempt from regulation by 4E-BP1. However, long-term Torin treatments in Fig 3.1-3.3 which began during early replication and proceeded to late replication permitted efficient synthesis of viral late proteins and release of infectious virions, respectively. Taken together, these data suggest that in Torin-treated cells late viral mRNA are being efficiently initiated under conditions where eIF4F is

depleted. This suggests that either viral mRNA can efficiently scavenge the remaining residual pool of eIF4F in the cell, or that initiation of these transcripts can be accomplished independently of intact eIF4F.

4.2.5 Non-eIF4F-dependent Accumulation of Viral Proteins

To determine if viral mRNPs can retain intact eIF4F, I assessed the protein composition of mRNPs in polysomes in latent or lytic TREx-BCBL-RTA cells by immunoblotting proteins harvested from gradient fractions. I elected to use a low-salt lysis buffer in these experiments to aid retention of eIF4F components and other RBPs, consistent with previous ribosome isolation protocols (Belin et al., 2010; Mehta et al., 2012). Fractions were isolated from the 40S, 60S, and 80S sub-polysomal peaks, as well as light and heavy polysomes; RNA and associated proteins were precipitated using ethanol and a glycogen co-precipitant.

The m^7GTP cap-binding proteins eIF4E1, eIF4E2, and NCBP1 were associated with polysomes in all conditions tested (Fig 4.6). Torin leads to a progressive loss eIF4F components eIF4G1 and eIF4G3 from polysomal fractions, consistent with the displacement of eIF4G from the eIF4F complex by hypophosphorylated 4E-BP1. However, eIF4G2, which was found primarily in the 80S monosome peak and sub-monosomal fractions, was unaffected by mTORC1 inhibition. I noted a clear accumulation of a faster migrating species of eIF4G1 that matches a previously reported caspase-3 cleavage fragment (Bushell et al., 2000) consistent with induction of apoptosis in this population of cells (Tabtieng et al., 2018). Hyper-phosphorylated 4E-BP1 was associated with polysomes in vehicle-treated samples, consistent with other reports of 4E-binding proteins co-sedimenting with polysome fractions (Castelli et al., 2015). Hypophosphorylated 4E-BP1 was found in sub-polysomal fractions of Torin-treated cells in both the latent and lytic cell populations. This is likely due to dynamic disassembly of eIF4F on mRNA in polysomes allowing opportunistic binding of 4E-BP1 to eIF4E (Merrick, 2015). Finally, consistent with previous reports (Boyne et al., 2010), ORF57 was associated with mRNPs in polysomes, which remained when mTORC1 was inhibited (Fig 4.6). Taken together, these findings indicate that mTORC1 is active during lytic replication and eIF4F is assembled, but also that synthesis of viral proteins has a limited

requirement for eIF4F, and there is remodeling of polysome- and monosome-associated mRNP complexes during mTORC1 inhibition during both latency and lytic replication.

During lytic replication and during Torin treatment, NCBP1, and eIF4E2 remained associated with the polysomes. Both these factors have roles in alternative translation initiation and could potentially support translation of viral mRNA, either constitutively or when eIF4F is limiting. To test this, I used a lentiviral shRNA to silence these factors and measured effects on virus replication. NCBP1 and eIF4E2 could serve directly as cap-binding proteins for viral mRNA. eIF4G2 may function as a eIF4G-like factor for eIF3d-dependent translation, or may be recruited to viral mRNA by other factors. However, knockdown of NCBP1 or eIF4G2 had no effect on virus replication, with or without mTORC1 inhibition (Fig 4.7). Similarly, knockdown of eIF3d, while not very efficient, did not affect the accumulation of viral antigens in the presence or absence of Torin (Fig 4.8).

KSHV replicates to normal titres in the absence of eIF4E2. When challenged to replicate in a hypoxia environment, virus titers were unaffected, with or without the mTORC1 inhibition. This suggests that KSHV is competent to complete its replication cycle in during hypoxia using an eIF4E2- or an $eIF4F_H$-independent mechanism. During hypoxia, REDD1 promotes the inhibitory activity the TSC complex on mTORC1. While the actions of viral simulators of mTORC1 activity might limit the actions of REDD1 on TSC2 (Brugarolas et al., 2004), eIF4F is similarly not required for virion production during hypoxia (Fig 4.7). eIF4E1 remains associated with polysomes during Torin treatment. eIF4E1 association with eIF4G1 can be directly inhibited independent of mTORC1 and 4E-BP1 by the small molecules 4EGi or 4E1RCat. Treatment with either compound had similar effects whether applied at reactivation or at 24hpi (Fig. 4.9). 4EGi enhances virus titer at lower concentrations, similar to the effects of Torin on IFN expression (Fig 3.8), but it is unclear if this is similar phenomena. As these molecules make direct contact with eIF4E1 (Cencic et al., 2011a; Moerke et al., 2007), they might additionally interfere with other eIF4E1 protein-protein interactions, complicating interpretation of this experiment.

4.2.6 N6-methyladenosine Modification during Lytic Replication

N6-methyladenosine (m^6A) modification of RNA can stimulate translation in response to eIF4F loss (Coots et al., 2017). m^6A promotes translation by either recruiting eIF3 directly, or by the actions of m^6A reader proteins (Choe et al., 2018; Meyer et al., 2015). Several viral transcripts are modified with m^6A methylation, including ORF11 and ORF57 but the mark is not present on all transcripts. METTL3 and the m^6A reader YTHDC2 have been shown to modulate virus titer, but with conflicting results (Hesser et al., 2018; Tan et al., 2017). Both of these studies used NaB on their iSLK cells to enhance replication; Hesser et al., (2018) also used TPA in their TREx-BCBL1-RTA studies. This in part might explain the different responses of the cells to METTL3 knockdown. In these experiments, I used only doxycycline to reactivate the TREx-BCBL1-RTA in an attempt to minimize variables. In the TREx-BCBL1-RTA, METTL3 is rapidly depleted during lytic replication (FIG 4.10), in contrast to its accumulation in HCMV infection (Rubio et al., 2018; Winkler et al., 2018). Despite being generally absent during lytic replication, METTL3 knockdown diminished virion output by nearly 10-fold. This is consistent with Hesser et al., (2018) METTL3 knockdown experiments in iSLK.219 or iSLK.BAC16, but contrasts with their TREx-BCBL1-RTA findings. Early gene replication and genome accumulation appeared to be unaffected by knockdown, but there was a clear loss in the expression of late protein ORF65. Importantly, ORF57 accumulates normally when METTL3 is absent, suggesting that m^6A is not required for eIF4F-dependent, or independent translation of ORF57. Similarly, ORF59, which requires ORF57 binding for mRNA export (Verma et al., 2015), accumulates normally in METTL3 knockdown, suggesting that m^6A is not required for ORF57 association with mRNA (Fig 4.6).

4.3 Discussion

During lytic replication, there is a loss of global protein synthesis consistent with host-shutoff. In this low translation environment, mTORC1 still contributes to protein synthesis (Fig 4.1). The loss of ~60% of global protein synthesis with Torin treatment of latently infected cells is consistent with other studies in uninfected cells (Hsieh et al., 2012; Thoreen et al., 2012). mTORC1 inhibition leads a severe downregulation in the translational efficiency of TOP-containing transcripts. The identified transcription start-

sites for KSHV mRNAs as annotated in KSHV2.0 generally lacked TOP sequences, which suggested that their translation might not be especially susceptible to mTORC1 inhibition (Arias et al., 2014). In these experiments, Torin treatments caused a global change in translational efficiencies (Fig 4.1), but the TE of viral transcripts remained similar to vehicle control, demonstrating that mTORC1 is not required for efficient synthesis of viral proteins. TOP-transcripts were strongly down-regulated, suggesting that eIF4F and LARP1 are regulated normally during lytic replication.

These observations are consistent with reports from Lenarcic, et. al. (2014), who demonstrated that mTORC1 is dispensable for HCMV late protein synthesis and that TE of viral mRNAs were minimally affected by Torin. Together, these reports suggest that resistance to eIF4F loss might be a general feature of herpesvirus translation, even for viruses like HCMV that do not shut off host gene expression.

This Pol-Seq analysis was restricted to heavy translating polysomes, but light polysomes and monosomes also make important contributions to bulk protein synthesis (Heyer and M. J. Moore, 2016). Pol-Seq data as validated by measuring the distribution of select viral and host transcripts in sub-polysomal and polysomal fractions. Many viral transcripts had a consistent distribution in the heaviest fractions, but these is a shift towards the sub-polysome fractions (Fig 4.3). Kaposin in particular appears to be very poorly initiated, yet this mRNA is one of the most abundant viral transcripts detected in the cell. The translated Kaposin repeats contain numerous poly-proline sequences, which are slowly decoded by elongating ribosomes (Gutierrez et al., 2013). One such tract occurs shortly after the start codon; slow decoding of this tract might partially obscure the start codon and slow new 80S assembly.

Interestingly, there was abundant hIL-6 and VEGF-A mRNA in the monosome fraction with little material present in heavier polysome fractions. The monosome fraction was long thought to make insignificant contributions to bulk protein synthesis, but recent ribosomal foot-printing studies have revealed that monosomes contain translationally active mRNA (Heyer and M. J. Moore, 2016). Monosomes are enriched for short transcripts (ORF length < 590 nt) and hIL-6 approaches this limit (639 nt CDS, Accession NM_000600.4). hIL-6 contains several upstream start codons, but does not appear to encode any uORFs. VEGF-A is twice the length of average ORFs found in

monosomes (1239 nt CDS, Accession NM_001025366.2), but its translation is regulated by a convoluted arrangement of two putative IRES sites, near-cognate start codons, and uORFs, likely accounting for its inefficient initiation (reviewed in Arcondeguy et al., 2013).

Inhibition of mTORC1 during lytic replication leads to disassembly of eIF4G from the cap-binding eIF4E. I could observe this disassembly both in a cap-analogue pulldown experiments (Fig 4.5) and through displacement of eIF4G1 and eIF4G3 from lytic polysomes without loss of cap-binding proteins (eIF4E1, eIF4E2, NCBP1) and no change in eIF4G2, a homologue of eIF4G that lacks the N-terminal eIF4E binding domain (Fig 4.6). This data is consistent with destabilization of eIF4G association with eIF4E on cap binding and dynamic disassembly of eIF4F after initiation, as hypothesized by Merrick (2015). eIF4E appears to remain associated with the cap of the polysomal mRNA, allowing a surface for interaction with either eIF4G, or a 4E-BP1 protein that would prevent additional eIF4G association and subsequent rounds of eIF4F-dependent initiation. I hypothesize that the presence of hyper-phosphorylated 4E-BP1 in vehicle-treated polysomes is due to low affinity binding of 4E-BP1 to eIF4E; high affinity binding of hypo-phosphorylated 4E-BP causes rapid loss of initiation on these mRNAs and their subsequent shift to sub-polysomal fractions. Importantly, when eIF4G1 and eIF4G3 are depleted from polysomes, ORF57, and many viral transcripts are not depleted.

KSHV lytic proteins have been shown to activate mTORC1 that should promote assembly of eIF4F by displacing 4E-BP1. However, the rapid disassembly of free eIF4F and displacement of eIF4G from polysomes upon Torin treatment during all stages of KSHV infection suggests that KSHV gene products only enforce eIF4F-dependent translation upstream of mTORC1 and have no downstream mechanism to sustain eIF4F assembly. Importantly, late viral mRNA accumulates normally and can be initiated for translation when Torin is applied during early replication (Fig 3.1-2); these transcripts are efficiently translated despite being first transcribed under conditions where eIF4F is disassembled and unavailable. This suggests that while mTORC1 is active during lytic replication, it is largely dispensable for translation of viral mRNA.

During times of stress, non-eIF4F translation mechanisms can be activated. I used a series of knockdown experiments to determine if any known alternative translation initiation complexes are active during KSHV replication, or if they can substitute for eIF4F during mTORC1-inhibition. RTA expression can be activated by hypoxia (Haque et al., 2003), which suggested that KSHV might be competent for hypoxic translation. HCMV has previously been shown to replicate and spread in hypoxia (Kudchodkar et al., 2004). Hypoxia stabilizes HIF2α, which activates eIF4E2 to support translation during hypoxia (Uniacke et al., 2013). Hypoxia also restricts mTORC1 function by REDD1 activation of the TSC complex. However, viral proteins may support mTORC1 activation during hypoxia. The same cell population can support both eIF4F- and $eIF4F_H$-dependent translation during physiological oxygen concentrations (Timpano and Uniacke, 2016). It was surprising to detect eIF4E2 in polysomes, as it had only been reported previously in the context of hypoxia. The latent gene product LANA can stabilize HIF1α, so it might also be capable of stabilizing HIF2α (Q. Cai et al., 2006). However, it is also possible that in these cells that eIF4E2 is instead associated with a CCR4-NOT complex and not the mRNA cap, but it is clear that eIF4E2 does not contribute to virion production in normoxia or hypoxia (Fig 4.7).

mRNA can retain the nuclear cap-binding complex in the cytoplasm, which can direct a pioneer round of translation (Maquat et al., 2010). NCBP1 was abundant in polysomes during lytic replication, but knockdown had no effect on virus titers. Non-eIF4E-dependent, nuclear mRNA export requires NCBP2. NCBP1 is not required for this function as it NCBP3 can substitute for its loss (Gebhardt et al., 2015). However, it is not clear if NCBP3 can similarly associate with translating mRNA. It is unknown if ORF57-dependent export of mRNA specifically requires any of the NCBP1 proteins.

eIF3d likely does not function as the cap-binding protein for KSHV mRNA as knockdown of either eIF3d or its putative co-factor eIF4G2 did not limit virus replication (Fig 4.7-8). eIF4E3 is an eIF4E1 homologue that I did not evaluate in these studies. I detected very few transcripts for eIF4E3 in the Pol-Seq dataset. eIF4E3 translation is enhanced during loss of eIF4E1 phosphorylation, which is phosphorylated in KSHV lytic replication, and required for virion production (Arias et al., 2009). The requirement for eIF4E1-phosphorylation could involve a role for eIF4E1 binding directly to viral mRNA,

or it could be due to translation of cellular transcripts. The strong inhibitory effect of high concentration 4EGi and 4E1Cat suggest that eIF4E1 could have a more direct role in viral mRNA translation, however, this would likely require a protein to functionally substitute for eIF4G.

Several studies have reported m^6A modification of KSHV mRNA, and m^6A modification of RTA is required for proper splicing (Hesser et al., 2018; Tan et al., 2017; F. Ye et al., 2017). However, for the most part precise roles for m^6A modifications and m^6A 'reader' proteins in the biogenesis and fate of KSHV mRNA remain to be discovered, and may be dependent on cell type and different chemical stimuli of lytic reactivation (Hesser et al., 2018). N^6-methyladenosine (m^6A) dependent translation initiation has been shown to contribute to residual translation following eIF4F disassembly in normoxia (Coots et al., 2017). Unlike HCMV, METTL3 is rapidly depleted during KSHV lytic replication (Fig 4.10A) (Rubio et al., 2018; Winkler et al., 2018). This likely precludes a significant role for m^6A modification as a global mechanism of translation of viral mRNA, especially late transcripts. This could explain why m^6A has only been detected on the IE gene RTA and early genes such as ORF6, K3, ORF57, ORF4, and ORF11 (Tan et al., 2017; F. Ye et al., 2017). The effects of m^6A on virus titer might largely be explained by a Type-I IFN response. Loss of m^6A marks on IFN-β mRNA promotes stabilization of the transcript and leads to the accumulation of ISGs (Rubio et al., 2018; Winkler et al., 2018).

During Torin treatment, both the TOP-containing transcript Rps20 and the non-TOP β-actin transcript were depleted from polysome fractions that retained viral mRNA (Fig 5B). In these same fractions eIF4G1 and eIFG3 are also lost, but ORF57 is retained. ORF57 and related herpesvirus homologues (EBV EB2, HSV1/2 ICP27) have previously been shown to interact with initiation factors, and could be found in polysomes (Larralde et al., 2006; Ricci et al., 2009). In our experiments, loss of eIF4G from polysomes with Torin treatment suggested that ORF57-dependent recruitment of eIF4G to viral mRNA was not required for their translation, yet ORF57 is clearly present in the same fractions as viral mRNA and is not displaced with eIF4F loss.

This data suggests that while mTORC1 is active during KSHV lytic, it is not required for the translation of viral mRNA. While eIF4F is assembled during lytic

replication, it is not required for the association of viral mRNA with the polysomes. Alternative translation initiation factors, including eIF4E2, eIF4G2, NCBP1, and eIF3d are also not required for virion production. Similarly, m^6A is not required for the translation of ORF57 mRNA. However, ORF57 remains associated with the polysomes in the absence of eIF4F. It is possible that ORF57, or other viral factors are required for KSHV translation initiation, but the complement of host and viral proteins associating with translating mRNA during lytic replication is unknown.

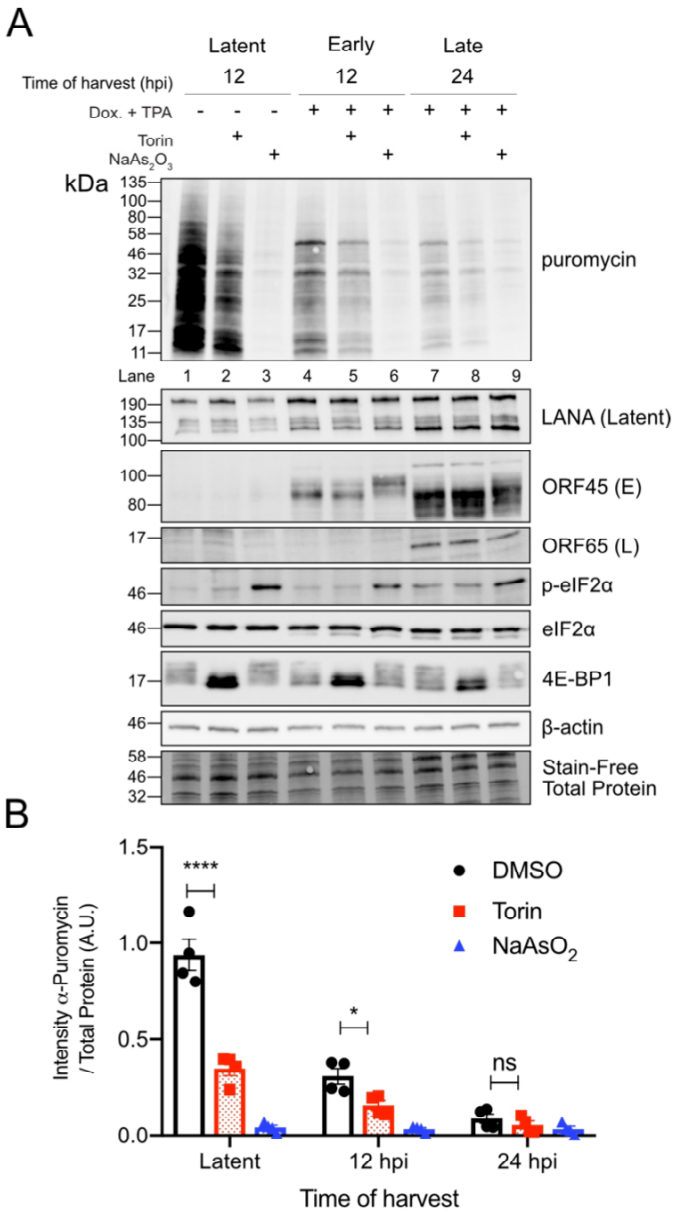

Fig 4.1 mTORC1 promotes bulk protein synthesis during lytic replication (A) TREx-BCBL1-RTA cells were reactivated from latency with 1 µg/mL dox and 20 ng/mL TPA. Cells were treated with Torin or DMSO for 2 h prior to harvest or with sodium arsenite for 20 min prior to harvest. All cells were pulsed with 10 µg/mL puromycin 10 min prior to harvest in 2x Laemmli buffer. Lysates were probed by immunoblot for incorporation of puromycin in nascent polypeptide chains indicates the rate or protein synthesis as detected by probing with an anti-puromycin antibody. Viral latent protein LANA, early (E) protein ORF45, and late (L) protein ORF654 and phospho-eIF2α Ser51 were probed as indicated. 4E-BP1 was probed to assess mTORC1 activity. (B) The puromycin intensity in A was quantified and compared to the total protein load as described in Methods. Intensities were normalized to the latent, DMSO-treated cells (Lane 1). Lane numbers correspond to lanes reading left to right in A. n=4, ± SD. * indicates p value < 0.05 by one-way ANOVA.

Fig 4.2 Effect of Torin treatment on translational efficiencies of viral mRNA (A) Polysome profiles of uninfected, latent, or 48 hpi iSLK.219 treated with either Torin or DMSO for 2 h prior to harvest. Cells were treated with 100 μg/mL cycloheximide (CHX) for 5 minutes prior to harvest to prevent elongation. Cells were lysed in the presence of CHX and loaded on a 7-47% linear sucrose gradient. After separation by ultracentrifugation, the abundance of RNA (A_{260} nm) in the gradient was continually measured as fractions were collected. RNA from the 48 hpi polysome fractions was isolated for sequencing. (B) mRNA from translating ribosomes (of DMSO treated cells) was sequenced and aligned to both the human and KSHV genomes. Viral transcripts are depicted in blue on top of the grey background of cellular genes. The dashed line represents the mean TE of all transcripts. (C) The Δ TE of viral transcripts is depicted in blue or red on a grey background of cellular genes. Viral transcripts beyond one SD of the mean are red, viral transcripts within on SD are depicted in blue. Vertical lines represent a 1.5-fold change in transcript TE. (D) Panther Gene Ontology-Slim molecular functions with a decreased TE during Torin treatment. (E) Depletion or enrichment of transcripts not predicted to encode functional proteins from TE < -1.5 Z or TE > 1.5 Z, respectively. Sequencing library was prepared by Nicholas Crapoulet with input from Stephan Lewis (Atlantic Cancer Research Institute). Initial read mapping and data normalization into cpm was performed by Daniel Gaston (Department of Pathology, Dalhousie University).

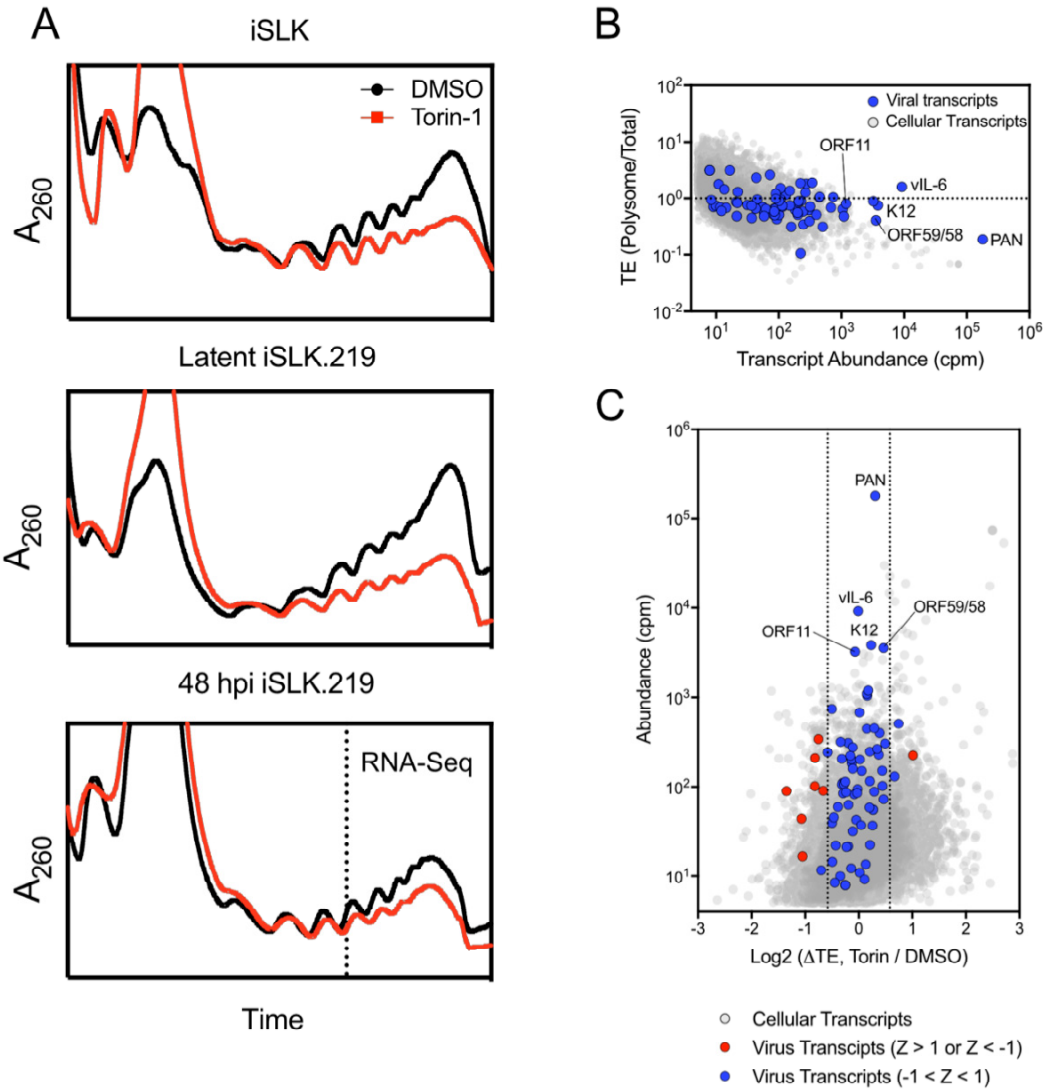
A
iSLK
DMSO
Torin-1
A260
Latent iSLK.219
48 hpi iSLK.219
RNA-Seq
Time
B
Viral transcripts
Cellular Transcripts
ORF11
vIL-6
K12
ORF59/58
PAN
TE (Polysome/Total)
Transcript Abundance (cpm)
C
PAN
vIL-6
ORF59/58
ORF11
K12
Abundance (cpm)
Log2 (ΔTE, Torin / DMSO)
Cellular Transcripts
Virus Transcipts (Z > 1 or Z < -1)
Virus Transcripts (-1 < Z < 1)
D
Panther GO-Slim Molecular Function (TE < -1.5 Z)
-log10 (p-value)
structural constituent of ribosome (GO:0003735)
26.7
translation initiation factor activity (GO:0003743)
3.06
translation regulator activity (GO:0045182)
3.57
structural molecule activity (GO:0005198)
14.7
RNA binding (GO:0003723)
2.87
Fold Enrichment (Log2)
E
Non-coding RNAs, pseudogenes, or nonsense mRNAs
-log10 (p-value)
TE < -1.5 Z
1.32
TE > 1.5 Z
4.00
Fold Enrichment (Log2)

Fig 4.3 Distribution of viral and cellular mRNA in polysome fractions (A) Polysome profile of TRex-BCBL1-RTA cells induced with 1 μg/mL dox for 24 h. Torin or DMSO control were added 2 h prior to harvest and polysome analysis. (B) qRT-PCR analysis of cellular and viral transcripts in polysome fractions. Total RNA was isolated from polysome fractions. RNA was co-precipitated with GlycoBlue and T7-transcribed luciferase RNA to improve and normalize for recovery. RNA was analysed by qRT-PCR for cellular, and latent, early (E), and late (L) viral transcripts. Vertical lines depict the boundaries between the monosomes, light polysome, and heavy polysome fractions. n=3 ± SEM. Andrea Monjo and Katrina Bouzanis (Department of Microbiology and Immunology, Dalhousie University) assisted in performing RT-qPCR.

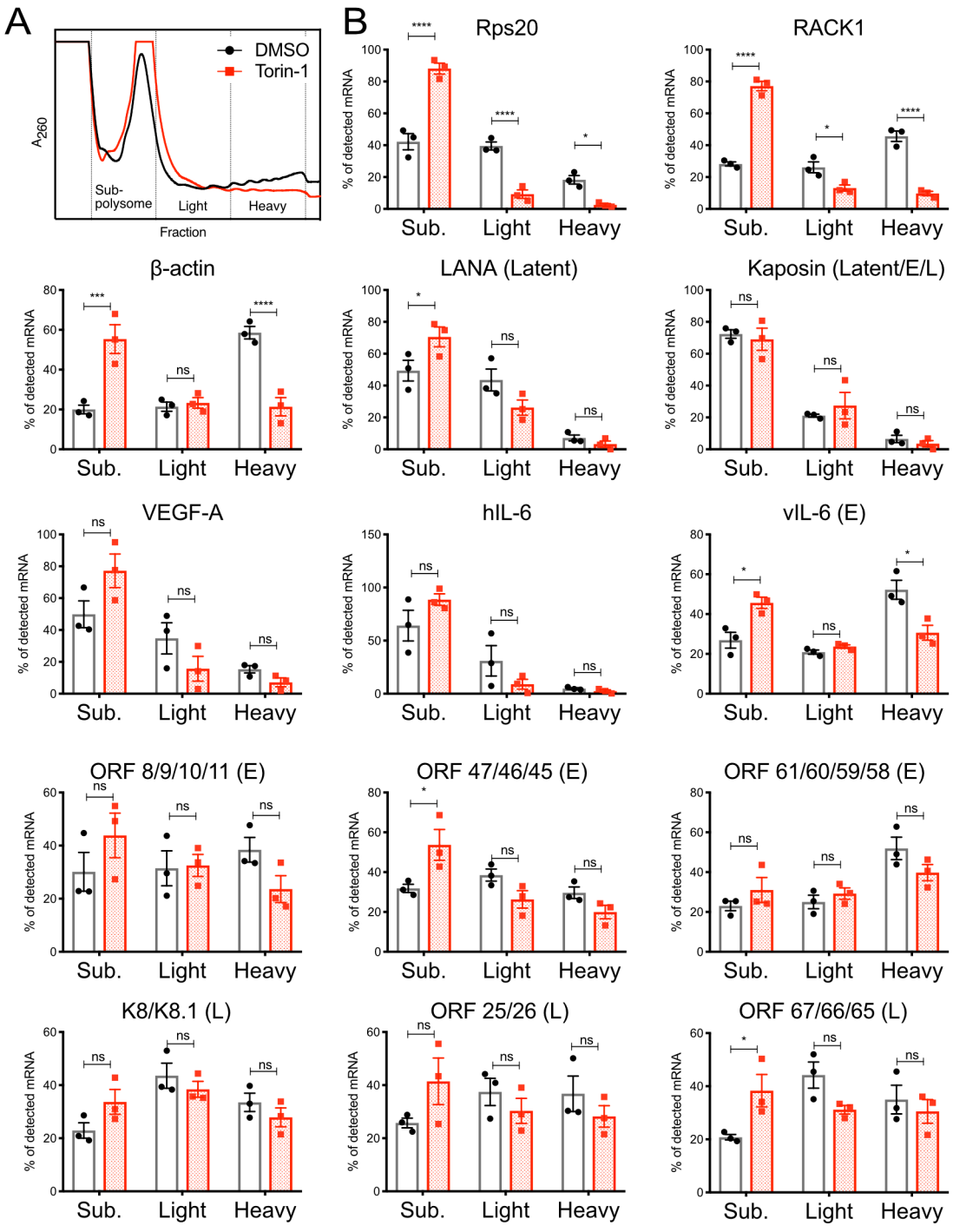
A
DMSO
Torin-1
A260
Sub-polysome
Light
Heavy
Fraction
B
Rps20
RACK1
β-actin
LANA (Latent)
Kaposin (Latent/E/L)
VEGF-A
hIL-6
vIL-6 (E)
ORF 8/9/10/11 (E)
ORF 47/46/45 (E)
ORF 61/60/59/58 (E)
K8/K8.1 (L)
ORF 25/26 (L)
ORF 67/66/65 (L)
% of detected mRNA
Sub.
Light
Heavy
ns

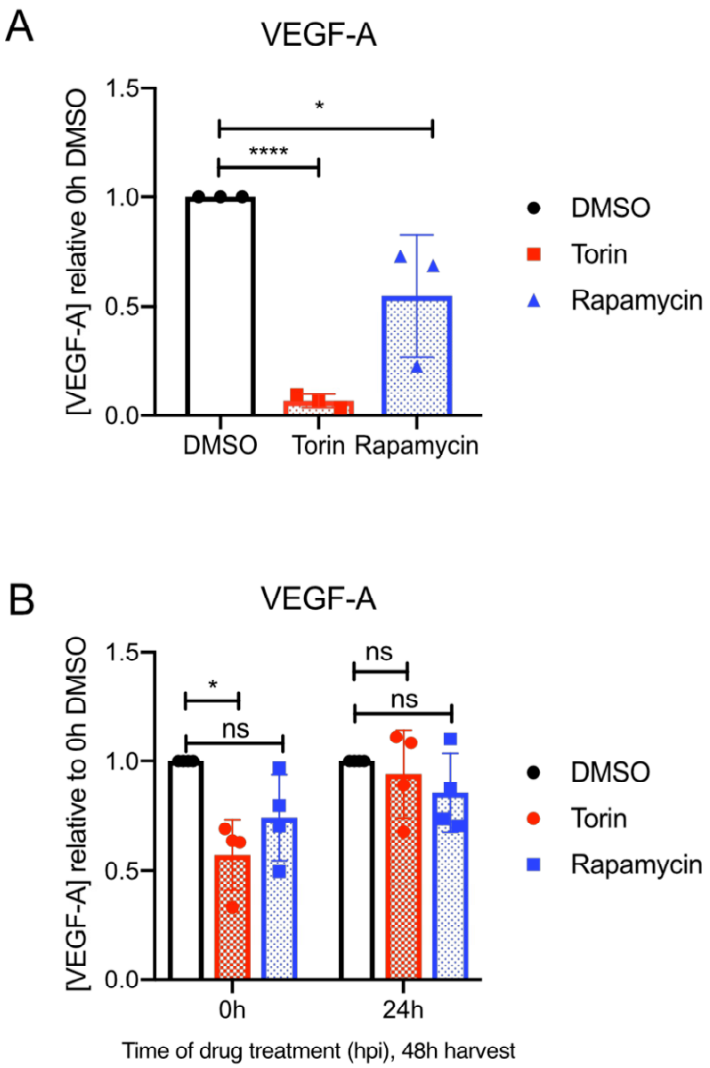

Fig 4.4 VEGF-A release is restricted by mTORC1 inhibition during latency (A) Latent TREx-BCBL1-RTA cells were treated with 250 nM Torin, 250 nM Rapamycin, or DMSO. Supernatant was harvested 48h after drug treatment and the quantity of VEGF-A was measured by ELISA. (B) As in A, but cells were reactivated with 1 µg/mL doxycycline. Torin, Rapamycin or DMSO was added at either 0 hpi or 24 hpi. n=3-4 ± SEM.

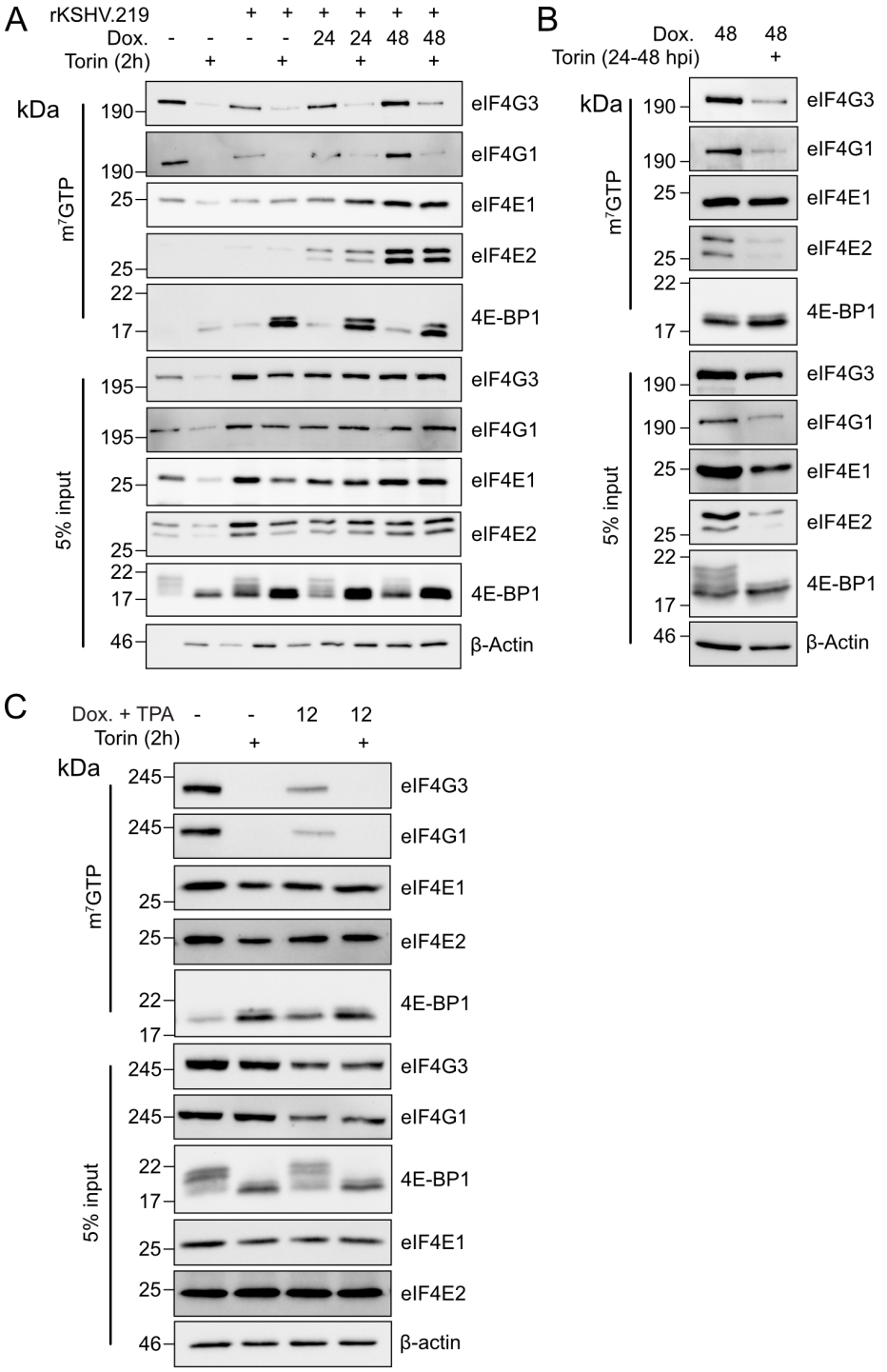

Fig 4.5 mTOR inhibition disrupts eIF4F formation during latency and lytic replication (A) m^7GTP pulldown. iSLK.219 or uninfected iSLK cells were reactivated with 1 μg/mL dox and harvested at the time indicated. Torin or DMSO was added 2 h prior to harvest. Cell lysate was incubated with m^7GTP Sepharose, washed and eluted by boiling in 1x Laemmli buffer and analysis by immunoblot. (B) As in A. except iSLK.219 cells were treated with Torin or vehicle for 24 hours prior to harvest. (C) m^7GTP pulldown with TRex-BCBL1-RTA cells reactivated with doxycycline and TPA for the time indicated. Torin or vehicle was added two hours prior to harvest.

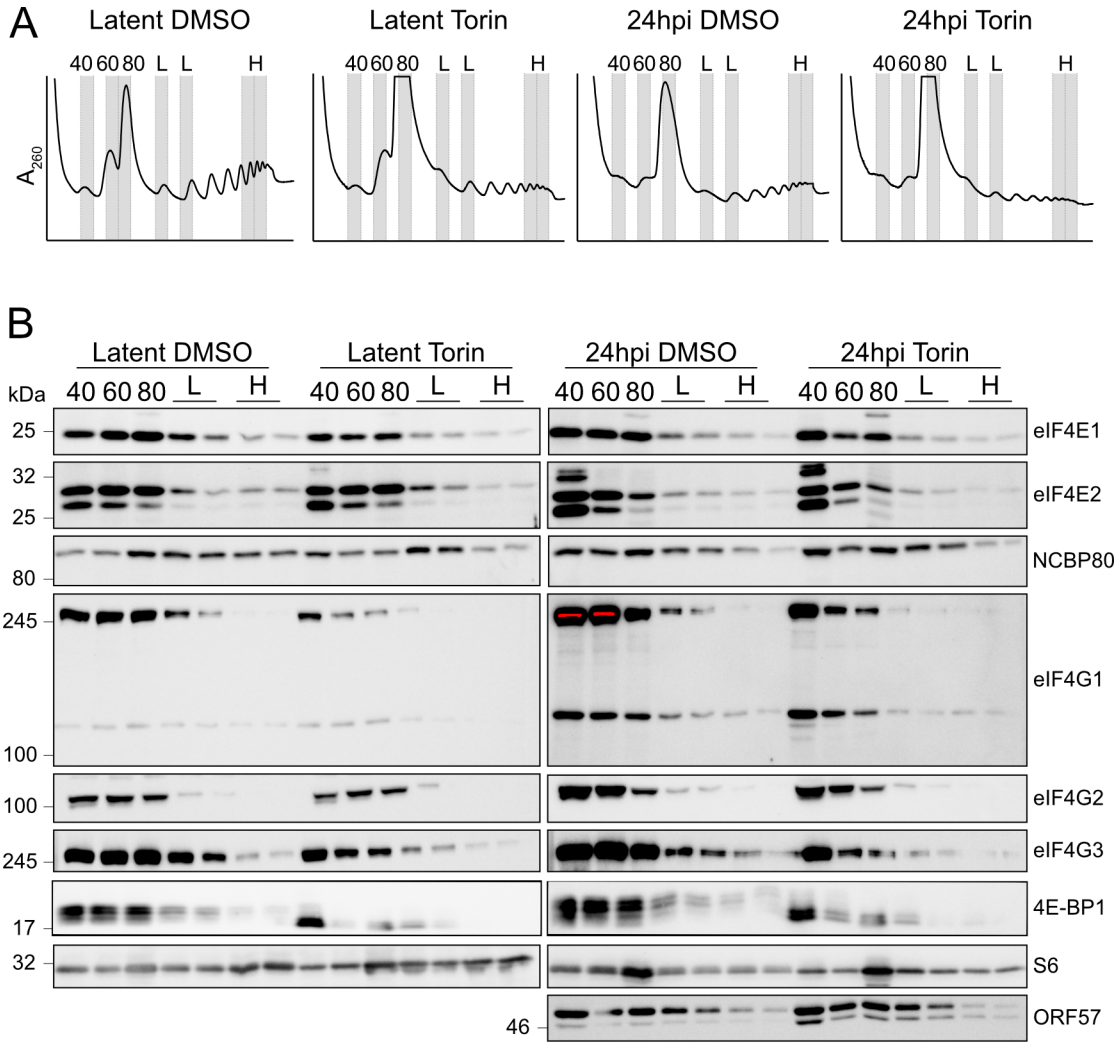

Fig 4.6 Association of translation initiation factors during viral latency and lytic replication (A) Polysome profiles of TREx-BCBL1-RTA cells at 0 or 24 hpi, treated with Torin or DMSO control. Indicated 40S, 60S, 80S, light, and heavy polysome fractions were isolated for analysis. (B) Fractions were precipitated with glycogen and ethanol. The precipitate was resuspended in 1x Laemmli buffer and used for immunoblot analysis of translation initiation factors and the early protein ORF57 as indicated. Equal volume was loaded in all lanes. Andrea Monjo (Department of Microbiology and Immunology, Dalhousie) helped perform western blot analysis of additional replicates.

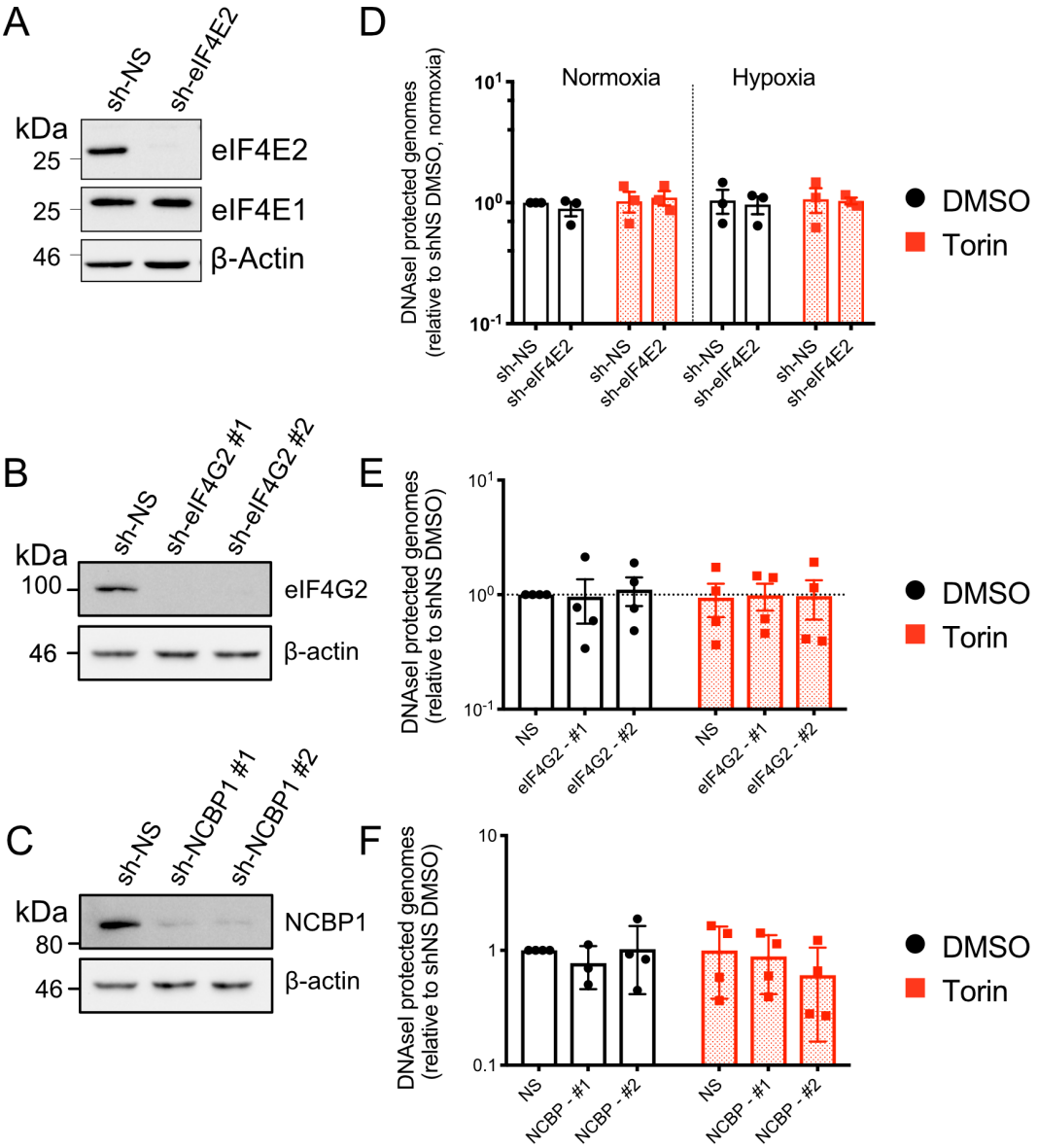

Fig 4.7 Silencing of translation initiation factors that are not displaced from the polysomes by Torin does not restrict virion production (A-C) TREx-BCBL1-RTA cells were transduced with lentiviral shRNA constructs and selected with puromycin. Knockdown of eIF4E2, NCBP1, or eIF4G2 in latent TREx-BCBL1-RTA cells was confirmed by immunoblot. (D) eIF4E2 knockdown cells were reactivated with 1 µg/mL dox. At 24 hpi, cells were treated with DMSO or Torin, then either maintained in normal culture conditions, or were moved to a hypoxia chamber. Supernatant was harvested at 48 hpi and processed for detection of DNase-protected genomes. (E-F) Reactivated TREx-BCBL-RTA cells were treated with DMSO or Torin at 24hpi. Supernatant was harvested at 48 hpi and processed for detection of DNase-protected genomes. n=3-4 ± SEM.

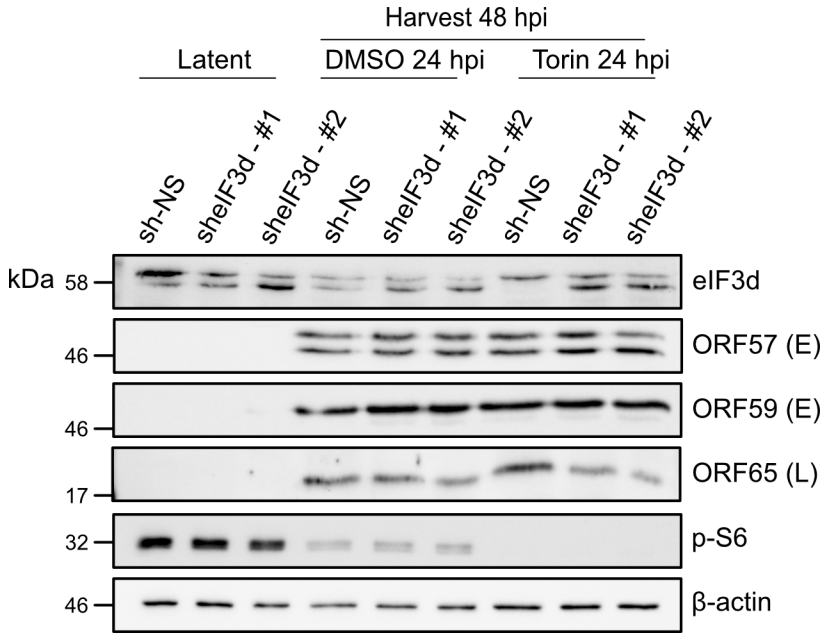

Fig 4.8 eIF3d silencing does not affect viral protein accumulation TREx-BCBL1-RTA cells were transduced with lentiviral shRNA constructs and selected with puromycin. Cells were reactivated with 1 μg/mL dox and treated at 24 hpi with Torin or DMSO. Lysates were harvested for immunoblot analysis at 48 hpi and probed for eIF3d, early (E) proteins ORF57 and ORF59, or late (L) protein ORF65. mTORC1 activity was determined by phospho-S6 Ser235/6.

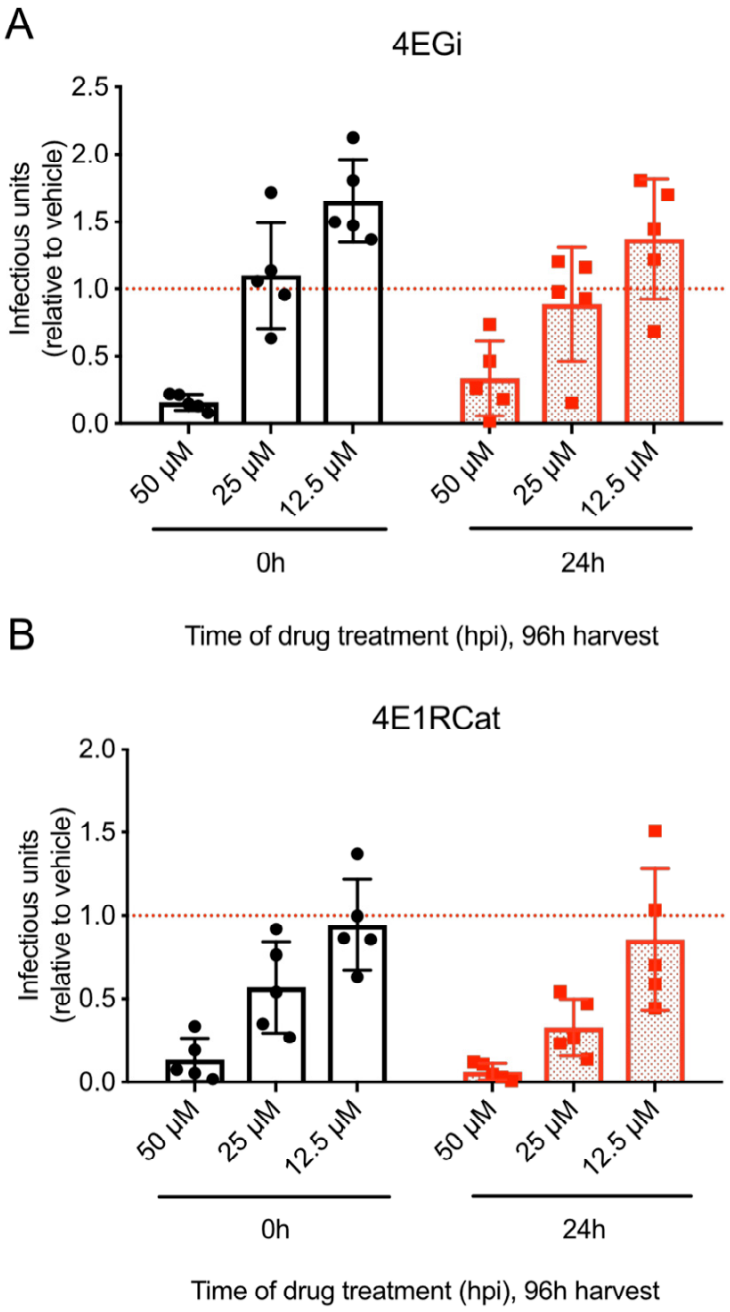

Fig 4.9 eIF4F inhibitors 4EGi and 4E1RCat inhibit virus replication iSLK.219 cells were reactivated with 1 µg/mL doxycycline. (A) 4EGi, or (B) 4E1RCat was added to the culture at 0 or 24 hpi. At 96 h, supernatants were harvested and used to infect a monolayer of 293A cells. After 24 h, GFP+ cells were recorded by flow cytometry. n=5 ± SEM.

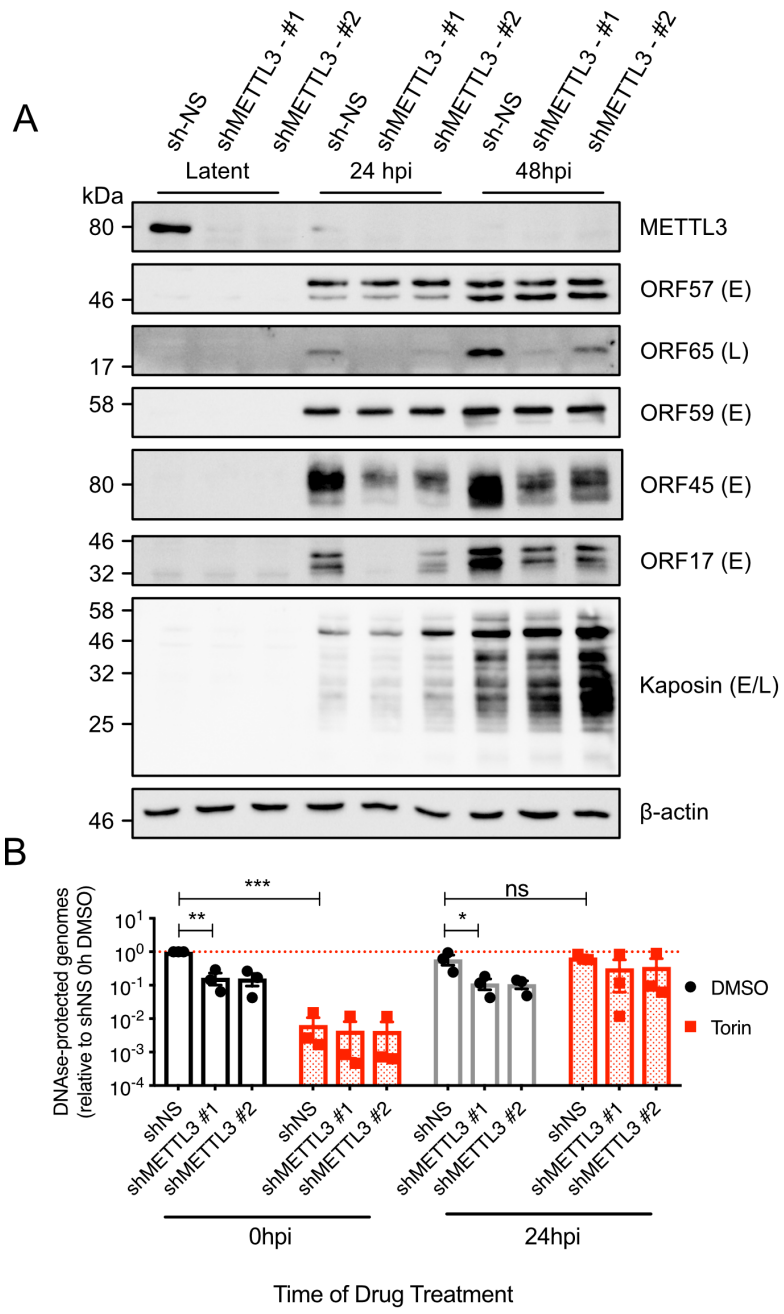

Fig 4.10 METTL3 is required for virion production (A) TREx-BCBL1-RTA cells were transduced with lentiviral shRNA constructs and selected with puromycin. Cells were reactivated with 1 µg/mL doxycycline and harvested as indicated. Lysates were probed for METTL3, early (E) proteins ORF57, ORF59 and ORF17 or late (L) proteins ORF65 or Kaposin. (B) Cells transduced and reactivated as in (A) were treated with DMSO or Torin at 0 or 24 hpi. Supernatant was harvested at 48hpi and processed for detection of DNase-protected genomes. n=3 ± SEM.

Chapter Five – Lytic Messenger Ribonucleoproteins

5.1 Introduction

The accumulated data presented in Chapters 3 and 4 indicate that mTORC1 is dispensable for the accumulation of viral proteins during the lytic cycle. Likewise, careful measurement of translational efficiencies during the lytic cycle revealed that viral mRNAs were resistant to mTORC1-inhibition and eIF4F dissolution whereas cellular mRNA remains sensitive to perturbations in mTORC1 activity (Fig 4.2-3). Several factors with important roles in eIF4F-independent translation initiation were similarly dispensable for virion production (Fig 4.8-9). In the polysomes, Torin treatment displaced eIF4F components eIF4G1 and eIF4G2. However, the viral Mta ORF57 remained associated with lytic polysomes in the absence of eIF4F (Fig 4.6). ORF57 has previously been shown to associate with polysomes, as have its homologues in HSV-1, HCMV, and EBV (Aoyagi et al., 2010; Boyne et al., 2010; Smith et al., 2017). HSV-1 ICP27 and EBV EB-2 can both promote translation of reporter transcripts when tethered directly to mRNA, but if Mta more generally enhances or supports translation of bound mRNA is unclear (Mure et al., 2018; Smith et al., 2017). Mta broadly affects splicing, and nuclear export of viral mRNA (Sandri-Goldin, 2011). As nuclear export is required for translation, it is difficult to separate translational enhancement of Mta proteins from nuclear export during lytic reactivation.

With the exception of the HSV-1 host shutoff nuclease Vhs, and Mta, few other herpesvirus proteins have been reported to associate with translating mRNP or TIFs. HSV-1 ICP6 has been reported to bind to eIF4G1 and promote association with eIF4E (Walsh and Mohr, 2006). Other groups have made progress in this area by isolating proteins associated with polyA-RNA during HCMV infections and identified several viral RBPs (Lenarcic et al., 2015). However, this approach did not enrich for translating mRNA and few ribosomal proteins or TIFs were isolated, which makes it unclear what contribution these viral RBPs have in regulating translation. I used a proteomic approach in an attempt to discover the TIFs and viral RBPs associated with translating mRNP in KSHV lytic infection. I examined the abundance of known translation initiation factors in both WCL or polysome fractions derived from KSHV infected cells. I observed that the bulk host cell proteome remains largely unchanged over the course of the lytic replication

cycle, compared to latently-infected controls, suggesting that KSHV host shutoff is largely restricted to accumulation of new proteins and does not accelerate bulk degradation of existing proteins. Similarly, the abundance of host translation initiation factors did not change significantly following reactivation from latency.

Viral proteins accumulated over infection and five viral proteins were specifically enriched in the polysome fraction. In agreement with immunoblot analysis and previous literature, ORF57 was highly enriched in the polysomes (Fig 4.6; Boyne et al., 2010). Also enriched were three viral proteins with known or putative roles in the regulation of the innate immune response, vIRF1, ORF11, and ORF52, but there was a decrease in two innate immune sensors, PKR and cGAS. Unexpectedly, the viral processivity factor ORF59 was the most abundant viral protein detected in infected cells and was highly enriched on the polysome. This analysis suggests that the ribosome itself is likely a site of coordinated viral regulation.

5.2 Results

5.2.1 Proteome of Translating mRNP in Lytic Replication

I used the TREx-BCBL1-RTA cells in these experiments because they reactivate more synchronously than iSLK.219 cells, and as suspension cells are easily scaled up for increased yield of cell lysates. I harvested WCL from latent, 24 hpi, or 48 hpi cells, and polysome fractions from latent and 24 hpi cells, all reactivated with doxycycline. The WCL from three independent replicates was digested into tryptic peptides and labelled with nine different tandem-mass tags (TMT) isobaric labels (Fig 5.1A). Similarly, latent and 24 hpi polysome fractions from three independent replicates were labelled with six different TMT tags. Preliminary experiments using a lysis buffer with a higher salt concentration for the polysome fractions failed to isolate known TIFs, whereas they were readily identified using a low salt buffer (data not shown). For this reason, I used a low salt buffer in these polysome fractionation experiments to capture weakly-interacting proteins likely to play important functional roles in translation, like the aforementioned host initiation complex proteins, despite the potential isolation of non-specific interacting proteins.

I quantified 53 viral and 2,876 cellular proteins identified with at least two unique peptide spectra matches in WCLs (Fig 5.1B). At both 24 hpi and 48hpi, there were very few changes in the viral proteome of the cells compared to latent (Fig 5.1). This is similar to what was observed in the total proteome of EBV-infected cells in early stages of replication (Ersing et al., 2017), but it is still a surprising result given the clear inhibition of bulk protein synthesis during lytic replication (Fig. 4.1). This suggests that while the translatome of the cell was heavily remodelled by host shutoff, these changes failed to translate to changes in total protein abundance during viral replication. I identified 29 viral proteins and 2,399 cellar proteins in the polysome proteome. It is very unlikely that these are all genuine RNA-binding proteins and or ribosomal interacting proteins. This unexpectedly higher yield of proteins is likely due to the sensitivity of the instrument and difference in the complexity of the analyte; the polysome fractions are less complex and provide a more complete proteome than the WCL. Like the WCL, there was limited change in the proteome of the polysomes during reactivation from latency and later stages of lytic replication. I compared the change in WCL between latency and 24 hpi to changes in polysome abundance to look for proteins that are specifically recruited or excluded from the polysomes using a 1.5-fold enrichment as a cut-off (Fig 5.2). There was clear presence of non-ribosomal complexes in the polysome proteome, including the proteasome, spliceosome factors and mitochondrial proteins. In light of these findings, I believe that polysome fractionation might be better viewed as an enrichment of translating mRNP and ribosomes rather than an isolation of pure complexes. However, there was a clear enrichment of TIFs, ribosomal proteins, RNA-binding proteins, and folding-chaperones (Fig 5.2C).

5.2.2 Association of Viral Proteins with Translating mRNA

It is difficult to ascribe a viral protein as an RBP or a ribosome-associated protein as there is some co-isolation of non polysome complexes in this dataset. If viral proteins are interacting non-specifically, one could predict that their co-isolation with ribosomes would be proportional to their abundance in the cell. This requires a specious assumption that every viral proteins is equally “sticky”, but is a useful, early data filter. Comparing abundance of viral proteins in polysomes and WCL, five viral proteins were

enriched in the polysome fraction: vIRF1, ORF11, ORF52, ORF57, and ORF59 (Fig 5.3). SOX was not readily detectable on the polysomes, suggesting its targeting to mRNA is distinct from HSV-1 Vhs (Doepker et al., 2004). Of these five proteins, only ORF57 has previously been reported to have RNA-binding activity or to associate with polysomes (Boyne et al., 2010). As phosphorylation events of TIFs, such as eIF4E1 Ser209 and eIF4B Ser422, have been reported during KSHV lytic replication (Arias et al., 2009; Kuang et al., 2008), peptide library search of the polysome-associated proteins included the potential for phosphorylated Ser, Thr, and Tyr residues. I was not able to detect these two specific phosphorylations, but I was able to detect several phosphorylations on viral proteins (Table 5.1). However, absence of evidence for eIF4E1 Ser209 and eIF4B Ser422 phosphorylation is not evidence of absence. Only two of these phosphorylations, ORF57 Ser95 and Ser97, have been previously reported; phosphorylation at these sites limit Caspase7 cleavage of ORF57 (Majerciak et al., 2015). The significance of other phosphorylations is unclear, but could be important in association of these proteins with the polysomes. These phosphorylations could also provide a means of differentiating between different functions of the same protein, particularly ORF59, as discussed below.

The abundance of ORF59 in both the polysome and in WCL was surprising. ORF59 is a herpesvirus processivity factor that binds to the viral DNA polymerase ORF9 and aids viral genome replication (Chan and Chandran, 2000). Processivity factors act as a sliding clamps to promote DNA polymerase association with the template; the ORF59 dimer interacts with a single ORF9 polymerase in 2:1 stiochiometry (Baltz et al., 2009). Many viral proteins have multiple roles, but to date no auxiliary function of ORF59 or homologous proteins in other herpesviruses have been reported. This limited role for ORF59 suggests that its abundance should be comparable to other genome replication machinery, such as ORF9; however, ORF59 was consistently the most abundant viral protein detected, and one of the most abundant of all quantified proteins. ORF58/59 mRNA was also one of the most abundant viral mRNAs detected in lytic iSLK.219 (Fig. 4.2). ORF59 co-immunoprecipitates with several other proteins in during lytic replication, including ORF9, the viral protein kinase ORF36, vIRF1, and ORF57. ORF59 cellular binding partners include some translation initiation factors and ribosomal proteins (Strahan et al., 2017), but they are not strongly enriched. The surprisingly high

levels of ORF59 expression and its presence in polysome fractions suggest that it may have an auxiliary role in regulating viral protein synthesis.

To date, immunofluorescence experiments have firmly placed ORF59 in the nucleus of the cell (Chan et al., 1998; X. Zhou et al., 2010). However, new fixation techniques have been developed that are more rapid and penetrate more deeply than standard PFA fixation, which could change the apparent distribution of antigens (Richter et al., 2017). I used glyoxal fixation to compare the subcellular distribution of ORF59 and the RNA-export and translation-enhancing ORF57 protein. With 4% PFA, ORF57 and ORF59 displayed diffuse and nuclear staining patterns in 24 hpi TREx-BCBL1-RTA cells; by contrast, fixation with glyoxal yielded a clear cytoplasmic signal for both ORF57 and ORF59 (Fig 5.4A). In subcellular fractionation experiments, both ORF57 and ORF59 are similarly predominantly nuclear with some cytoplasmic signal (Fig 5.4B). While this does not confirm a role for ORF59 in translation, it suggests that it at least has a similar subcellular distribution as a known polysome-interacting viral protein.

5.3 Discussion

5.3.1 Quality of the Polysome Proteome

Few studies have globally explored the ribosome proteome. A similar methodology of sucrose-density ultracentrifugation was performed on a variety of cancer cell lines with metabolic isotopic labelling and off-line SDS-PAGE fractionation (Reschke et al., 2013). An alternative approach of immunoprecipitation of epitope-tagged ribosomes (Simsek et al., 2017). Both of these studies used higher-salt concentrations in their buffers than I used in this study. High salt concentrations increase the stringency of ribosome isolation, but many important TIFs can be lost (data not shown; Belin et al., 2010). Comparing these two studies with this dataset suggests that I was more successful in isolating translation initiation complexes. For example, both studies only isolated five or fewer eIF3 subunits in a given experiment while I could quantify all thirteen with a high degree of coverage. While it is a useful benchmark for a riboproteome, the Simsek et al., (2017) dataset is difficult to compare with this dataset as they used no enrichment for translating ribosomes and free large and small ribosome subunits will contribute to detected proteins. Lenarcic et al., (2015) used an oligo-dT purification strategy to isolate

viral RNA-binding proteins from CMV-infected cells. They also used high-salt lysis conditions, and while they isolated some viral proteins, they failed to isolate any translation initiation factors or known RBPs, such as the CMV Mta protein UL69.

There are some important caveats to consider about the method of polysome isolation described in this thesis. As seen in Fig 4.3, the distribution of mRNA in polysome profiles varies by both species and treatment. Some viral transcripts, such as Kaposin, are poorly initiated. TIFs specific to the translation of this mRNA would not be enriched in the heavy polysome fractions that were isolated in our study. This analysis also could not determine whether a given RBP or an mRNA directed accumulation of an mRNP in the polysomes. For example, Zc3h12d is an RNAse that degrades IL-6 mRNA via specific interaction with its 3'UTR (S. Huang et al., 2015). This protein is enriched from the polysomes, but the majority of IL-6 mRNA is in the monosome fraction (Fig 4.3, 5.2). It is unclear if Zc3h12d is recruited to IL-6 mRNA and thereby depleted from heavy polysomes, or if a viral process is restricting Zc3h12d mRNA-binding to stabilize IL-6 mRNA, such as stimulation of MK2 activation by Kaposin B or vGPCR (Corcoran et al., 2012; McCormick and Ganem, 2005). Similarly, reduction of the ribosome quality control (RQC) protein ZNF598 (Juszkiewicz et al., 2018) could reflect fewer ribosomal collisions due to reduced initiation during lytic replication, or viral subversion of RQC to support translation of difficult sequences, or recruitment to poorly initiated transcripts that reduced in heavy polysome, such as Kaposin. Defective RQC might also explain the accumulation of non-coding transcripts in polysomes during mTORC1 inhibition in lytic cells (Fig 4.2). Detection of both RQC components and co-translational chaperone complexes suggest that this assay might be useful to investigate the quality of the nascent proteome during virus infection. Despite the limitations mentioned above, differences in the polysome association of a protein still may provide useful information and warrant further analysis.

Some additional confidence in this dataset is found in the similar distribution of proteins known to form complexes, including FarsA-FarsB, Zc3h15-Drg1, and Denr-Mcts1 (Banerjee and Chakraborty, 2016; Ishikawa et al., 2009; Schleich et al., 2014). This suggests that the assay can accurately report difference in polysome composition. These complexes might also have significant roles in regulating translation during lytic

replication. The increase in both Denr and Mcts1 in polysomes suggest that there is more re-initiation in a lytic population, possibly due to stress-dependent reactivation of uORFs (Schleich et al., 2014). Alternatively their association might be driven by increases in non-AUG initiation on viral transcripts, such as Kaposin B or capsid protein ORF62 (Arias et al., 2014; Sadler et al., 1999). Zc3h15 is a regulatory subunit of the GTPase Drg1. Complex formation between Zc3h15 and Drg1 promotes their association with polysomes, but the functional significance of this is unclear (Ishikawa et al., 2009). FarsA and FarsB are both subunits of phenylalanine-tRNA synthetase, and are both greatly reduced from the polysome profiles, while all other tRNA synthetases that were identified were at a similar level in both the latent and 24 hpi samples. It is unclear why these proteins are associated with polysomes and why this association would change with lytic replication. KSHV has a similar Phe usage as the human genome (4.2% vs. 4%) and the distribution of Phe in the viral genome is unremarkable. A brief survey of several human ISGs did not appear to contain a greater or lesser Phe inclusion (OAS1 - 5.5%; IFI27 - 2.5%; IFI6 - 3.8%; IFR1 - 2%; IRF9 - 4.6%; PKR - 4.2%; ISG15 - 3.0%; Schoggins and Rice, 2011). One of the Phe codons, UUU is involved in a decoding wobble contributes to a frameshift during translation in an influenza A polymerase subunit (Jagger et al., 2012). One programmed frameshift that has been identified in KSHV in a repetitive region generates truncated LANA proteins, but this does not include UUU codons (Kwun et al., 2014). tRNA synthetases have progressively gained additional domains over evolution that can contribute new functions to aminoacyl-tRNA synthetases (Guo et al., 2010). IFN-γ dependent translational silencing of specific mRNAs requires the binding of Glu- and Pro-tRNA synthetases, for example. Few of these non-canonical roles have been described for aminoacyl-tRNA synthetase, and no additional functions have yet been described for Phe-tRNA synthetase. The strong displacement of both subunits of Phe-tRNA synthetase suggests a possible role in promoting or limiting viral infection.

The limited change of TIFs in the polysome fractions suggest that translation initiation is not globally dysregulated during lytic replication. It is hard to predict what proportion of the polysomes comprise viral mRNP and their degree of contribution to the proteins detected. I could not detect eIF4E3 or CTIF in either dataset. NCBP3, which can

functionally substitute for NCBP1 in nuclear export of most mRNA, is present in polysomes but at a much lower abundance than NCBP1 or NCBP2. I could not detect METTL3 in latent or 24 hpi polysomes, but many of the m6A readers identified by Dominisini et al., (2012) were present. Of these only YTHDF2 was decreased in both total abundance and in polysome association. This protein has been variously demonstrated to restrict or be required for KSHV replication (Hesser et al., 2018; Tan et al., 2017). Similarly, YTHDF2 has been reported to both enhance, and restrict IFN-β, while the m^6A writer complex of METTL3 and METTL14 inhibit IFN-β stability (Rubio et al., 2018; Winkler et al., 2018). As METTL3 is depleted by lytic reactivation in these cells (Fig 4.10) it suggests that METTL3 readers are recruited to the polysomes by pre-existing m^6A marks. It is unclear how YTHDF2 depletion from polysomes contributes to virus replication.

. There was limited change in the composition of the ribosome. Rpl22l1 was slightly less associated with the ribosome, but there was no change in its paralog Rlp22. Both paralogs are functional, but with non-overlapping RNA-interactions, and one cannot *trans*-complement the loss of the other (Y. Zhang et al., 2013). Rpl22 is notable for binding to the EBV small, non-coding RNA EBER1. EBER1 seems to prevent Rpl22 association with the ribosome, but the functional consequences of this association is still unclear (Toczyski et al., 1994).

5.3.2 Viral Proteins Associated with Polysomes

I compared the five viral proteins isolated in the polysome proteome to a comprehensive affinity-purified proteome obtained from ectopic expression of streptavidin-tagged viral ORFs (Z. H. Davis et al., 2014). There were no "high-confidence" interactions between vIRF1, ORF11, ORF52, ORF57, or ORF59 and ribosomal proteins or TIFs as determined by inclusion criteria and scoring system of Davis et al. (2014). TIFs could be located in the "low-confidence" dataset, but these were also detected in association with a broad array of viral proteins and likely represent experimental background. However, ORF57 clearly associates with polysomes during lytic replication (Boyne et al., 2010; Fig 4.6). Similarly, the "high-confidence" interactome for the well-studied vIRF1 lacks any component of innate signalling

pathways. This suggests that the protein-interactions are highly-dependent on the lytic environment and stresses the importance of isolating viral protein complexes within the context of infection.

ORF57, ORF52, and vIRF1 are directly transcribed by RTA without the need for other viral protein synthesis (Guito and Lukac, 2012), and seem well-positioned to subvert translation initiation during infection. ORF59 and ORF11 are both early genes. ORF59 expression is dependent on ORF57-mediated export of ORF59 mRNA, while ORF11 is independent. No antibody is available ORF11 and it is unclear how ORF57 affects its protein accumulation. Like ORF59, ORF11 mRNA is one of the most abundant in lytic iSLK.219 cells (Fig 4.2). The abundance of ORF59 mRNA and protein seems incongruent with a limited role as a processivity factor, especially as ORF59 mRNA is more efficiently translated than Kaposin mRNA, which is similarly abundant (Fig 4.2-3). Interestingly, homologous processivity factors, EBV BMRF1 and HCMV UL44, were among the most abundant viral proteins detected in proteomic surveys of infected cells (Ersing et al., 2017; Weekes et al., 2014), suggesting that the expression of herpesvirus processivity factors is also conserved. We do not yet know whether ORF59 is detectable on polysomes because of its high abundance, or conversely, whether the protein is abundant as a large amount of it is needed to associate with abundant ribosomes or mRNA. UL44 was not detected by Lenarcic et al., (2015) on oligo-dT cellulose beads, suggesting that processivity factors are not non-specifically binding RNA and are more likely ribosome-binding proteins rather than RBPs.

ORF59 forms a homodimer *in vitro* and in cells and can only bind to DNA when dimerized (X. Chen et al., 2004). ORF59 dimerizes in the cytoplasm and is imported into the nucleus as a dimer (X. Zhou et al., 2010). ORF36 binds and phosphorylates ORF59 on Ser376 and 379, neither of which were detected in this study; Ser376 and 379 phosphorylation promote the ORF59 binding to RTA and promote initiation of genome replication at the lytic origin of replication (McDowell et al., 2013). It is possible that ORF59 may interact differently as a monomer, or its functions could be regulated by post-translational modifications or associations with other viral proteins. The new potential phosphorylation sites identified on ORF59 (Table 5.1) in particular might play a role in regulating whether ORF59 functions in a DNA-replication, or in a translation-

regulation role. ORF59 has a similar sub-cellular distribution as ORF57 (Fig 5.4) and has been co-isolated with ORF57 (Strahan et al., 2017). However, further investigation is required before a role for ORF59 in translation can be defined or discounted.

Two cytoplasmic sensors of pathogen-associated molecular patterns, PKR and cGAS were reduced in the polysomes. PKR is one the four eIF2α kinases that phosphorylates Ser51in response to cytoplasmic dsRNA, which is abundant during herpesvirus replication (Burgess and Mohr, 2018; Pakos Zebrucka et al., 2016). cGAS binds to cytoplasmic DNA and produces cyclic guanosine-adenosine monophosphate, which stimulates STING dimerization and recruitment and activation of TBK1 (X. Cai et al., 2014). PKR has previously been shown to bind to the ribosome by its dsRNA-binding domain, but, unlike dsRNA, ribosome binding limits PKR activity (Raine et al., 1998; S. Zhu et al., 1997). It is possible that PKR and cGAS association with the polysomes is due to less stringent requirements for nucleic acid binding, which could benefit their roles in innate immune surveillance. Loss of these proteins from the polysomes might be due to decreased nucleic acid affinity due to interaction with viral proteins, such as PKR with ORF57 and cGAS with ORF52, or possibly vIRF1 as discussed below (Z. Ma et al., 2015; N. R. Sharma et al., 2017; Wu et al., 2015). Decreased PKR and cGAS could also represent increased recruitment away from the ribosomes by ligand binding. However, accumulation of three proteins implicated in regulation of the immune response in polysomes is unexpected.

ORF52 is a late tegument protein also known as KicGAS; ORF52 binds to both DNA and cGAS and limits cyclic guanosine monophosphate-adenosine monophosphate production (W. Li et al., 2016; Wu et al., 2015). Isolation of ORF52 is not likely due to co-sedimentation of virions in polysome fractions because capsid proteins and other tegument proteins are not enriched in the polysome fractions. Similarly, it is unclear what role ORF11 and vIRF1 have when associated with polysomes, although some modulation of the Type-I IFN response is a good possibility. Little is known about ORF11 function in KSHV. ORF11 is one of three viral dUTPases in KSHV, the other being ORF10 and ORF54 (Davison and Stow, 2005). Of the three, only ORF11 was enriched in the polysomes. Only ORF54 retains dUTPase activity, hydrolyzing deoxy-UTP to deoxy-UMP (Davison and Stow, 2005; Kremmer et al., 1999). dUTPase exaptation is

widespread across Herpesviridae, but few homologs retain dUTPase activity and their functions are largely undefined. The ORF11 homologue in γHV68 binds to the kinase domain TBK1, preventing its binding and phosphorylation of IRF3, which is important for limiting Type-I IFN production during lytic replication (H. R. Kang et al., 2014). It is possible that KSHV ORF11 has a similar function as γHV68, but the proteins have only 22% identify (H. R. Kang et al., 2014). Despite losing conserved residues required for enzymatic function (Davison and Stow, 2005), it is possible that ORF11 has retained some nucleotide-binding activity.

vIRF1 is one of four viral interferon regulatory factors (IRF) encoded by KSHV. All four have limited homology to each other and to human IRFs (Baresova et al., 2013), and contain a DNA-binding domain. The other three vIRF proteins were not isolated on the polysome, suggesting that vIRF1 polysome association may be specific. vIRF1 strongly limits both Type-I IFN production in response to cytoplasmic DNA by disrupting the cGAS-STING pathway and downstream ISG transcription (Gao et al., 1997; Z. Ma et al., 2015). A proportion of vIRF1 is directed to mitochondria by MAVS during infection, where it inhibits MAVS signalling (Hwang and Choi, 2016); it is possible that vIRF1 detected in the polysome fractions could be due to contamination with mitochondria.

These proteomic experiments are still preliminary and require validation, but they provide important insight into translation regulation during KSHV replication. There do not appear to be large global changes in the proteome or in polysome-associated proteins during lytic replication. No known eIF4F functional equivalents were enriched. There was a slight increase in Denr-Mcts1 complex usage, suggesting more re-initiation events, and a decline in ZNF598, suggesting suppression of normal RQC processes. Future experiments should also examine the role of eIF4F-depletion on the polysome proteome, as it is possible that displacement of eIF4G might allow recruitment of proteins that are otherwise excluded from the polysomes. Some of these factors might be important to non-eIF4F translation initiation during KSHV replication as well.

The most significant difference in the polysomes during lytic replication is association of viral proteins, of which ORF57 and ORF59 are strong-candidates for stimulating translation independently of eIF4F. The association of three viral immunity-

regulating proteins might implicate the ribosome as another hub of innate immunity, but there is no clear explanation of how this might be regulated. The association of viral proteins with translational machinery is a largely unexplored area and could prove to be an important area of host-pathogen interaction.

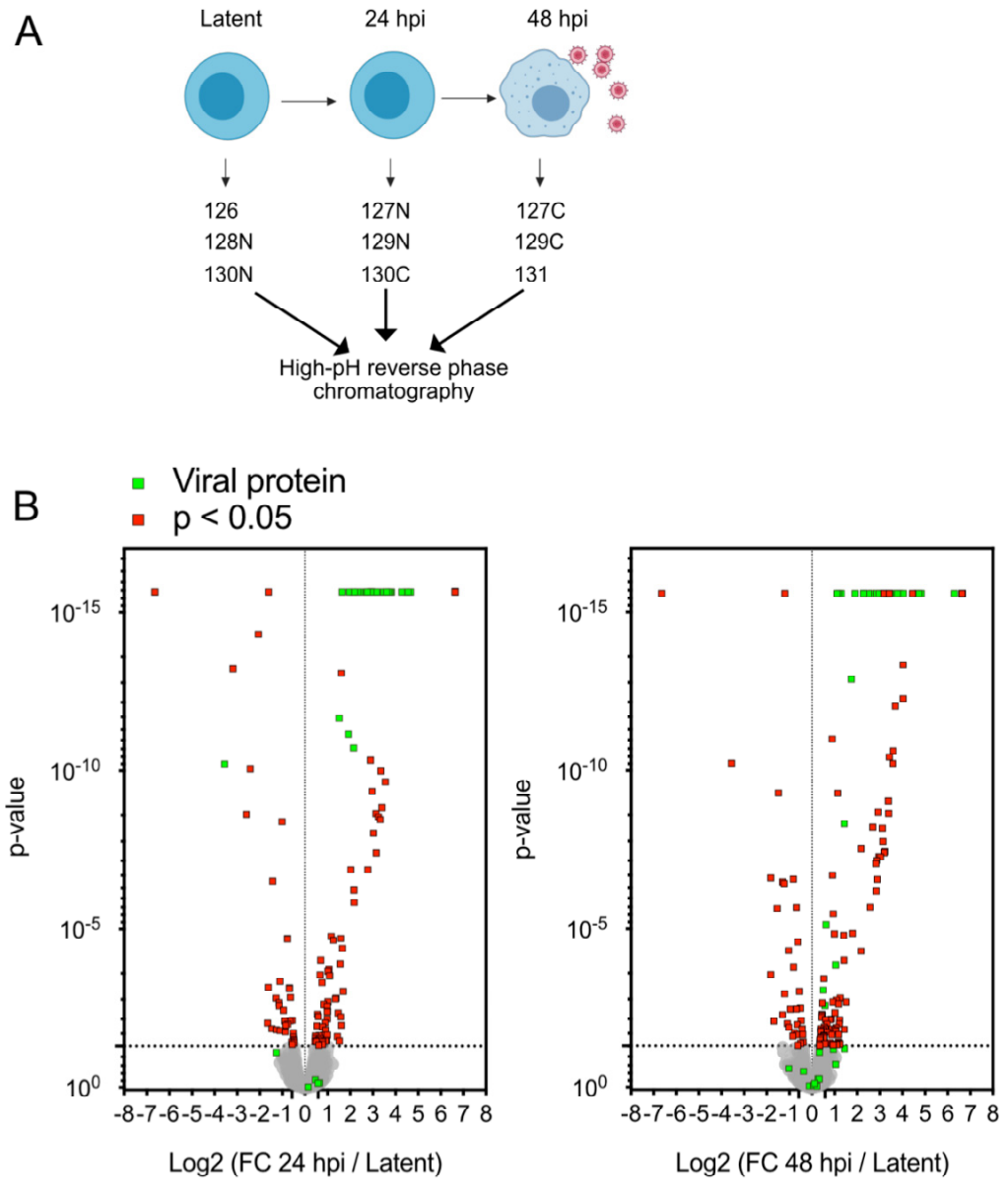

Fig 5.1 Changes in whole cell proteome over lytic replication (A) Experimental setup. TREx-BCBL1-RTA cells were reactivated with 1 µg/mL dox. Three biological replicates of latent, 24 hpi, or 48 hpi cells were harvested, processed into tryptic peptides, and labelled with TMT isobaric labels as indicated. All nine samples were pooled and pre-fractionated by High-pH reverse phase chromatography before LC-MS3 analysis. (B) Volcano plots of proteome changes compared to latent cells at 24 hpi, and 48 hpi.

Fig 5.2 Quantitative proteomics of polysomes during latency and 24 hpi (A) Polysome profiles of TREx-BCBL1-RTA cells during latency or reactivated with 1 μg/mL dox for 24h. Proteins were isolated from heavy polysomes, indicated by shaded regions, from three biological replicates, processed into tryptic peptides, and labelled with TMT isobaric labels. All six samples were pooled and pre-fractionated by High-pH reverse phase chromatography before LC-MS3 analysis. (B) High confidence cellular proteins identified in polysomes compared to their abundance in whole cell lysate (WCL, from Fig 5.1). Gene ontology annotations for ribosomal proteins, or translation initiation are labelled in green or blue, respectively. (C) Protein list from polysome were analysed GO protein class analysis.

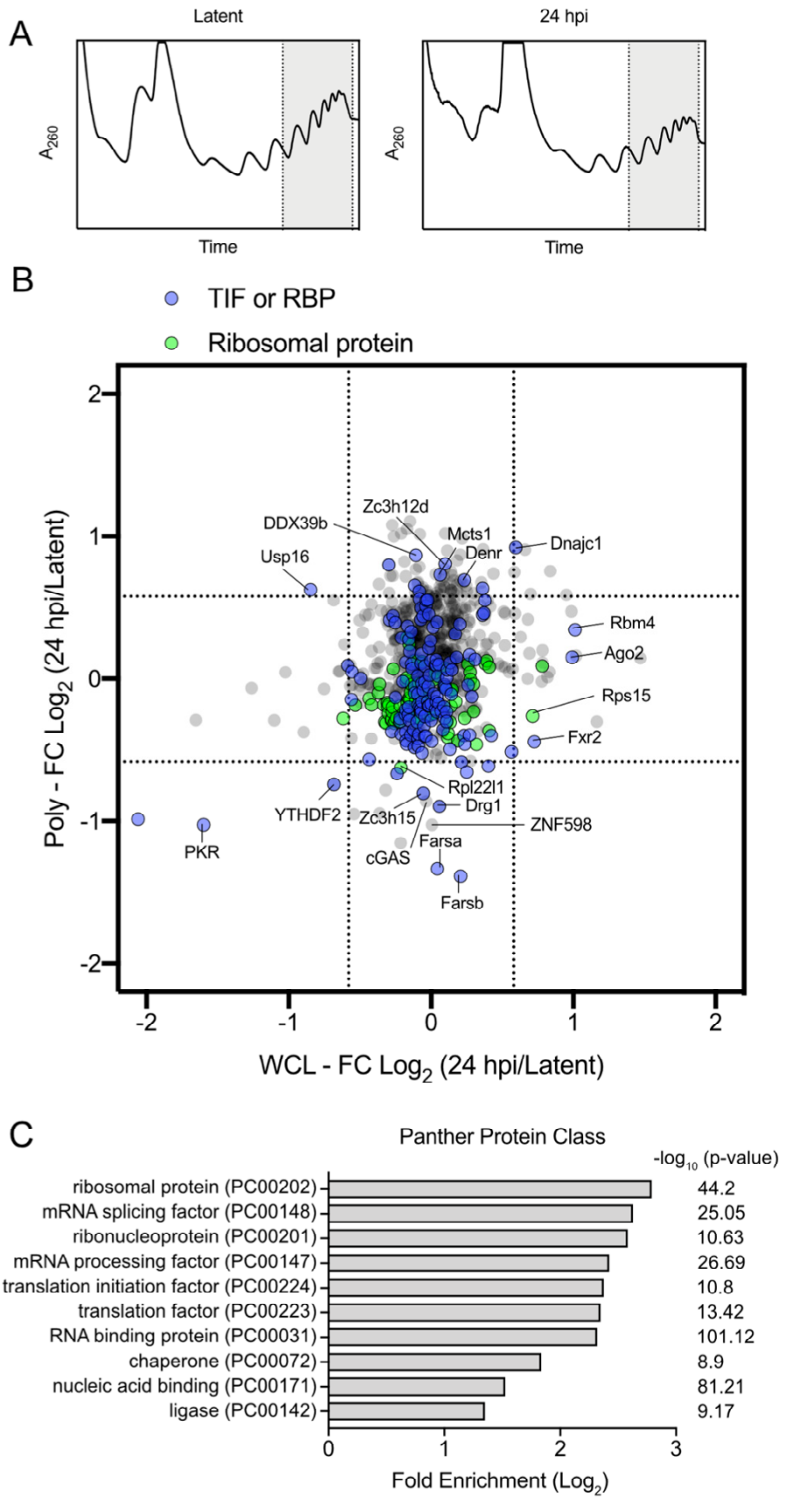
A
Latent
24 hpi
A260
Time
B
TIF or RBP
Ribosomal protein
Poly - FC Log2 (24 hpi/Latent)
WCL - FC Log2 (24 hpi/Latent)
Zc3h12d
DDX39b
Mcts1
Denr
Dnajc1
Usp16
Rbm4
Ago2
Rps15
Fxr2
Rpl22l1
Drg1
YTHDF2
Zc3h15
ZNF598
Farsa
cGAS
PKR
Farsb
C
Panther Protein Class
-log10 (p-value)
ribosomal protein (PC00202) 44.2
mRNA splicing factor (PC00148) 25.05
ribonucleoprotein (PC00201) 10.63
mRNA processing factor (PC00147) 26.69
translation initiation factor (PC00224) 10.8
translation factor (PC00223) 13.42
RNA binding protein (PC00031) 101.12
chaperone (PC00072) 8.9
nucleic acid binding (PC00171) 81.21
ligase (PC00142) 9.17
Fold Enrichment (Log2)

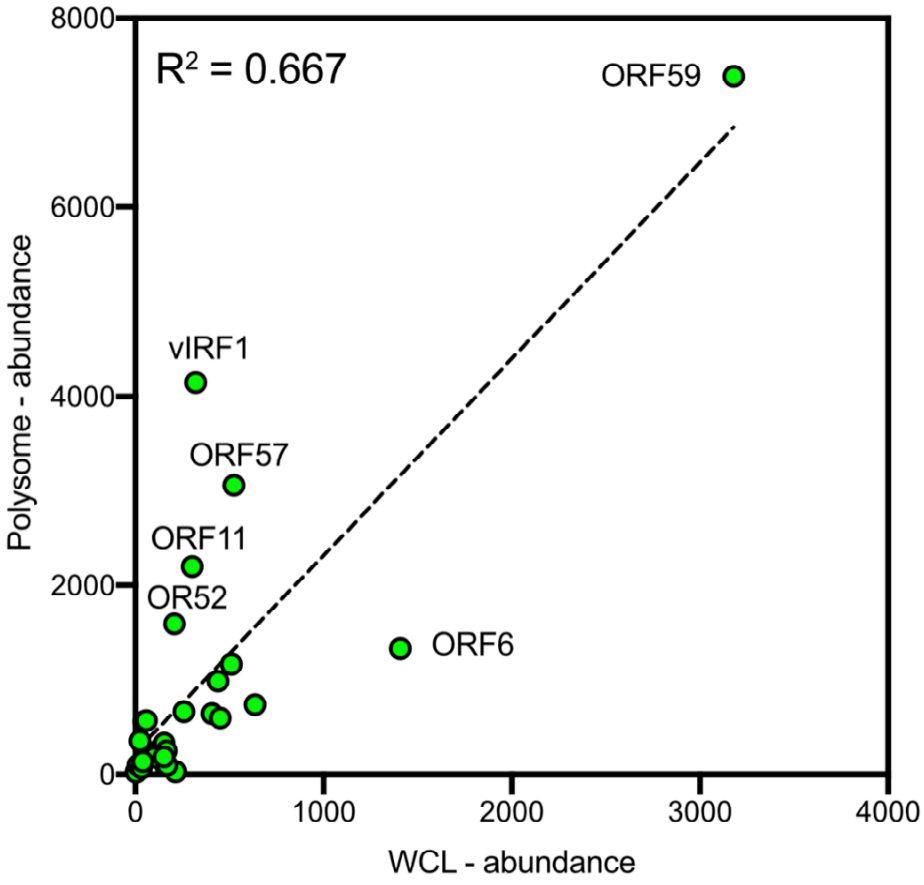

Fig 5.3 Unscaled Abundance of quantified viral proteins detected in lytic polysomes
The abundance of viral proteins identified in polysomes compared to abundance in whole cell lysate (from Fig 5.2).

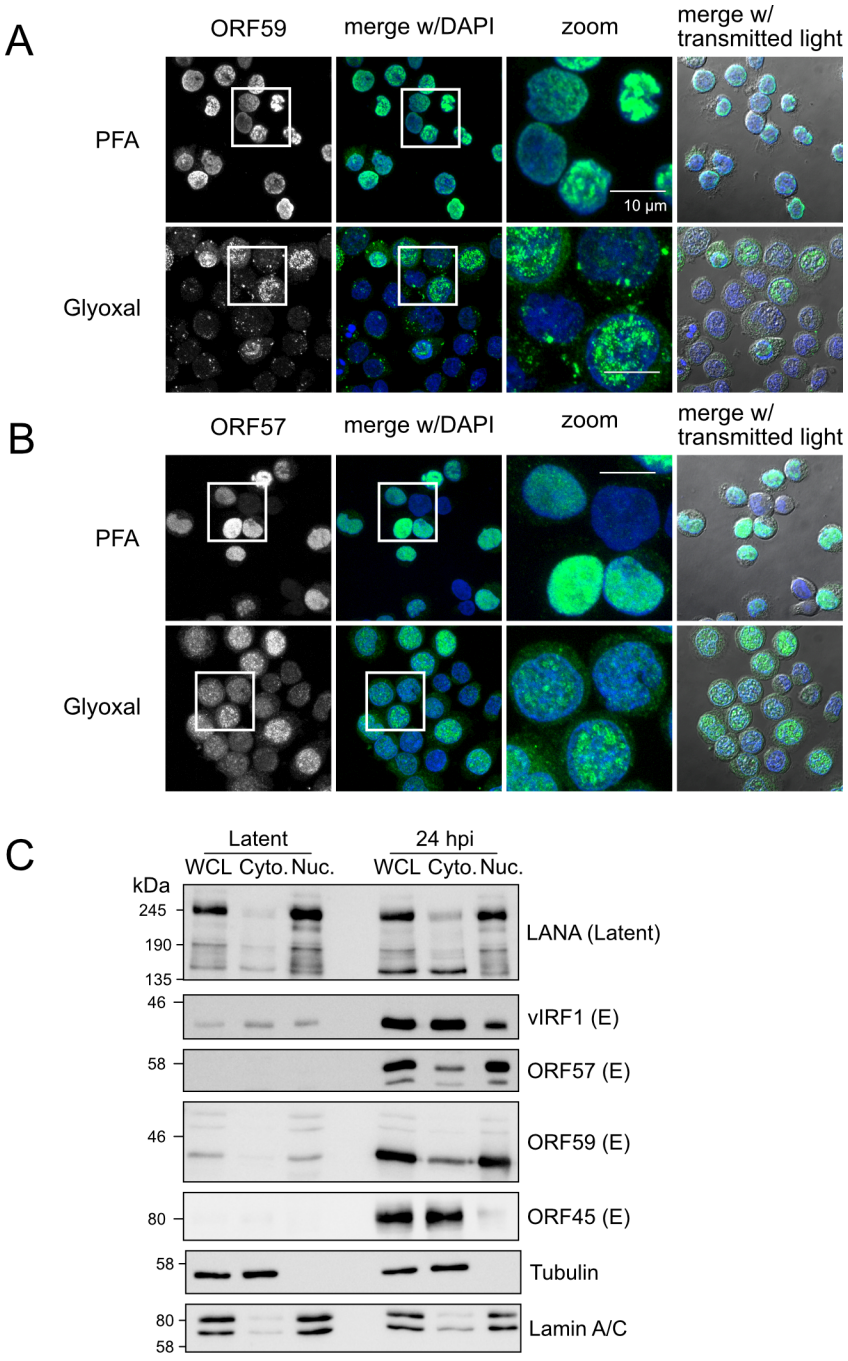

Fig 5.4 Cytoplasmic localization of ORF59 and ORF57 TREx-BCBL1-RTA cells seeded on poly-D-lysine coated coverglass and reactivated with 1 µg/mL dox the following day. Fixed with 4% PFA or glyoxal for 15 minutes. Cells were stained with (A) mouse anti-ORF59 or (B) mouse anti-ORF57 and anti-mouse Alexa 488 secondary antibodies. Z-stacks with maximum-intensity projection shown. (C) Nuclear-cytoplasmic fraction immunoblot of latent and 24 hpi TREx-BCBL1-RTA cells were probed for latent protein LANA, and early (E) proteins vIRF1, ORF57, ORF59, and ORF45 as indicated.

Table 5.1 Viral proteins detected in polysomes

Protein	Total Abundance	Polysome Abundance	Polysome Enrichment	Detected Phosphorylations
vIRF1	320	4147	13.0	Ser30, 32, 227, 393 Thr29, 396
ORF11	303	2201	7.3	Ser220
ORF52	207	1590	7.7	n/a
ORF57	523	3057	5.8	Ser91, 95, 97
ORF59	3180	7381	2.3	Ser330, 333, 349, 354 Thr337

Chapter Six – Conclusions

6.1 Summary

KSHV is the most recently discovered gammaherpesvirus. Like EBV, KSHV is a lymphocryptovirus that establishes life-long latency in B lymphocytes. KHSV is an oncovirus and the etiologic agent of Kaposi's sarcoma and two lymphoproliferative diseases, primary effusion lymphoma and multicentric Castleman's disease (Ganem, 2010; Speck and Ganem, 2010). KS tumour progression and maintenance in both human diseases, and in animal models, requires mTORC1 activation; treatment with mTORC1 inhibitors, such as rapamycin, leads to tumor regression (Roy et al., 2013; Stallone et al., 2005). At least three lytic viral proteins promote mTORC1 activation (Bhatt and Damania, 2012). This places mTORC1, the master regulator of cell growth, near the centre of KSHV biology, but very little is known about the role of the kinase in virus replication. The work presented here aimed to determine the importance of mTORC1 signalling in supporting virion production.

During KSHV lytic replication, mTORC1 is active and resistant to normal inhibitory signals for unknown reasons. In this context, mTORC1 can phosphorylate well-described target proteins as expected, including ULK1 and 4E-BP1, which mediate two of the main effector functions of mTORC1. ULK1 Ser757 phosphorylation is dependent on mTORC1 activation, and its loss normally stimulates induction of autophagy. This phosphorylation site is still regulated by mTORC1 during lytic replication, but mTORC1 inhibition at this time does not contribute to any change in autophagic flux (Chapter Three). mTORC1 promotes translation through phosphorylation of 4E-BP1, the dominant regulator of eIF4F. mTORC1 inhibition causes 4E-BP1 dephosphorylation and disruption of eIF4F, but this has little effect on translation of viral mRNA or virion release. Silencing components of several non-eIF4F initiation factors similarly did not limit virion production, even when combined with mTORC1-inhibition (Chapter Four).

A proteomic survey of lytic replication, and of proteins associated with translating ribosomes, revealed few changes in the composition of the proteome or the activity of TIFs (Chapter Five). The most prominent change in the polysomes was the accumulation of viral proteins, two of which, ORF57 and ORF59, are promising candidates for viral

TIFs. It remains unclear precisely why the virus promotes mTORC1 activity that is dispensable for viral protein synthesis. Perhaps mTORC1 activation plays a more prominent role *in vivo*. In general, the KSHV field lacks appropriate *in vivo* models to test these ideas. Nevertheless, this work has advanced our understanding of KSHV translation and I have made the unexpected discovery that the virus can efficiently produce virions in the absence of mTORC1 activity and eIF4F-dependent translation.

6.2 mTORC1 Activation during KSHV Infection

Throughout this study, it remained unclear why mTORC1 was active during lytic replication if not for inhibition of autophagy or promotion of translation. A simple explanation might be that KSHV needs to maintain mTORC1-dependent translation of some cellular factor to promote its replication. However, this simple answer seems incorrect in light of a few observations: i) KSHV has many proteins, including viral homologues, that dysregulate signalling pathways (Russo et al., 1996); ii) herpesvirus seem to encode viral kinase mimics to maintain signalling as needed (Bhatt et al., 2016; Chuluunbaatar et al., 2010; Moorman et al., 2008) and; iii) There is little change in the actual proteome during lytic replication (Fig 5.1). It's possible that the more efficient virion production is beneficial enough to select for mTORC1-stimulation by KSHV. But, given the role of mTORC1 in supporting Type-I IFN responses (Zakaria et al., 2018), this seems unlikely.

I think it is more likely that mTORC1 activity is not important for virion production so much as it is required to promote specific intercellular interactions in the host. In humans, very few tissues are exposed to normal atmospheric oxygen. Most tissue is closer to 5% oxygen tension or lower; arterial blood is only 12% (Timpano and Uniacke, 2016). Deep within lymphoid tissues, where KSHV might establish a latent reservoir, oxygen tension is closer to 1% (Caldwell et al., 2001). mTORC1 is likely inactive in this hypoxic tissue and non-eIF4F protein synthesis would have to dominate until stimulation of a germinal centre reaction (Ersching et al., 2017; L. Ye et al., 2017).

In the germinal centre dark zone, where activated B lymphocytes undergo proliferation, mTORC1 actively promotes cell growth. mTORC1 activity must then decline for expanded clones to interact with follicular dendritic cells and cognate T

lymphocytes in the light zone (Ersching et al., 2017). If like EBV, KSHV replication emulates B lymphocyte and differentiation (Speck and Ganem, 2010), maintaining mTORC1 activation might be a way to manipulate progression through the germinal centre reaction to benefit establishment of latency, or to expand the latent reservoir through new infection. This would be difficult to test experimentally in KSHV; however, a similar process is likely to occur in mouse infection with γHV68. KSHV replication in the lymph nodes might also be where KSHV first infects a lymphoid progenitor cell that subsequently seeds a KS lesion.

Maintaining mTORC1 activation is important for growth and maintenance of KS lesions (Stallone et al., 2005); mTORC1-dependent expression of VEGF-A appears largely sufficient to drive the tumour (Martin et al., 2013; Sin et al., 2007). A KS-like lesion also arises from dysregulated expression of VEGF-A (Sun et al., 2015). A small proportion of lytic cells is frequently detected in KS lesion and are often proposed to be the source of pro-inflammatory cytokines driving the lesion (Ganem, 2010; Mutlu et al., 2007). The paracrine secretions from ectopic expression of the lytic protein vGPCR are sufficient as a source of VEGF-A and tumour growth (Bais et al., 1998). While the PEL cell line TREx-BCBL1-RTA is different from endothelial lineage cells that give rise to KS, I did confirm that VEGF-A secretion was mTORC1-dependent. mTORC1 was more required for VEGF-A expression in latent cells than lytic cells, but I did not investigate expression of a broad array of cytokines in this study. The secretory environment that maintains the KS lesions might be a by-product of the cytokine-rich milieu required by KSHV to thrive in lymphoid tissues. Similarly, the requirement for mTORC1 activation as a "second-signal" for reactivation from latency could be a locational cue for the virus to initiate replication in the appropriate tissue niche, such as the germinal centre dark zone.

6.3 A Second-Signal for KSHV Reactivation

Like other herpesviruses, the *in vivo* stimuli for lytic reactivation is poorly understood. Here, I demonstrate that maintaining mTORC1 activity is an important requirement for reactivation (Chapter Three). However, mTORC1 kinase activity itself does not seem required to reactivate the virus, suggesting that instead mTORC1

activation is only one of a possible set of second-signals for reactivation that needs to be met in addition to RTA accumulation. Both ATG14 knockdown or NaB can also fulfill this second-signal, even when mTORC1 is inhibited and downstream kinase targets are unphosphorylated. Second-signals are common modes of signal integration in cell biology. A relevant example to this work is found in mTORC1 recruitment to the lysosome by AA sufficiency, to encounter GTP-bound Rheb, which is only active when the TSC complex GAP is sequestered by abundance growth-promoting signals (Fig 1.3). This second-signal for reactivation is a check to balance between stressors that might stimulate RTA expression and the suitability of the environment for virion production. An important advantage of herpesvirus latency might be discretion. Viruses, especially small RNA viruses, that cannot establish latency must replicate immediately upon infection and essentially outrun the immune response regardless of local circumstance. After KSHV latency is established, there is little pressure on the virus to produce progeny until its cellular reservoir is threatened, or there is a favourable environment for virion release and spread. This suggests that the mTORC1, ATG14, and NaB might not all coordinate on the same signalling pathway.

The role of ATG14 in Torin-mediated restriction of reactivation was an unexpected result of the experiment. ATG12 and Beclin silencing did not give a similar result, despite ATG14 loss on Beclin silencing, suggesting that ATG14 might be acting outside of its established role in autophagy. From my data, it is hard to establish how ATG14 might be acting in this capacity, but its localization to the mitochondrial-associated membranes (MAMs) could be important (Hamasaki et al., 2013). ATG14 is recruited to MAMs during AA-starvation and functions in the complex that nucleates an autophagosome at this site. MAMs are also important signalling platforms for MAVS-dependent signalling from dsRNA sensors RIG-I or MDA-5 (Horner et al., 2011). Even though KSHV is a DNA virus, herpesviruses produce dsRNA, and MAVS-dependent immune responses restrict KSHV replication (Burgess and Mohr, 2018; Y. Zhao et al., 2018). It is possible that the absence ATG14 could be interfering with the normal function of this compartment. Alternatively, ATG14 silencing might drive increased Beclin association with UVRAG (Itakura et al., 2008), but it is not clear how this might promote reactivation.

Sodium butyrate, as an HDAC inhibitor, may not activate a second-signal so much as it might bypass that signal. Treatment with NaB and a variety of other HDAC inhibitors promotes more open chromatin at the RTA promoter, but also widely across the viral genome (Hopcraft et al., 2018; H. J. Shin et al., 2013). In many cells, this is sufficient to stimulate lytic replication. However, in the iSLK.219 cell line, HDAC inhibitors are not sufficient to stimulate virus replication (Bechtel et al., 2003; Myoung and Ganem, 2011; Fig 3.8). It is unclear why these cells do not respond to this treatment, as they are permissive for lytic replication, but loss of target HDACs is likely.

6.4 Translation Initiation Without eIF4F

It remains unclear exactly how KSHV transcripts are initiated when mTORC1 is inhibited. The persistence of eIF4E1 in polysomes, and the inhibitory effects of 4EGi and 4E1Rcat on virion production suggest that the caps or viral mRNA are bound to eIF4E1, if they are bound at all. From the polysome proteome analysis, it does not appear that any known initiation factors are being activated during lytic replication (Chapter Five) and silencing of essential TIFs from non-eIF4F initiation complexes had no effect on virus titer, save METTL3 (Chapter Four). It is possible that one of the viral proteins identified in the proteome may function as an eIF4G functional equivalent and recruit viral mRNA to eIF3 and the small ribosomal subunit.

The concept of cap-independent translational elements (CITE), might be applicable to herpesvirus mRNA. CITEs are mRNA secondary structures that recruit RNA-binding proteins to promote translation initiation independent of the m^7GTP cap (Shatsky et al., 2018). While KSHV 5' and 3' UTRs are generally too short for large RNA secondary structures, and are diverse in sequence, a viral protein bound co-transcriptionally to the viral mRNA, like ORF57, could work similarly. Considering that HSV-1, HCMV, and KSHV protein synthesis is resistant to mTORC1-inhibition ((Lenarcic et al., 2014; McMahon et al., 2010), if a viral protein functions like a CITE, then it is likely to be conserved between subfamilies. Of the five candidate proteins identified in this study, only the Mta ORF57 and the processivity factor ORF59 have homologues in both other viruses. The essential role of ORF57 in expression of ORF59, and the essential role of ORF59 for genome replication complicate functional

mutagenesis studies. Also, the disparity in protein interactions of these viral proteinsand cellular proteins during infection or ectopic expression limit the interpretations of over-expression studies. These two considerations might explain why a role for ORF59 in translation has not previously been described. If viral proteins contribute to translation, their recruitment to RNA is likely regulated. Co-transcriptional binding, or imprinting, of a viral mRNA with a viral protein seems a likely strategy.

It is unclear how ORF57 is recruited to mRNA; a clear binding motif has likewise not been determined for other herpesvirus Mta proteins. Numerous RNA modifications have been defined, but the functional significance is only recently emerging. It is possible that failure to identify a conserved sequence motif for ORF57 binding could be due to cryptic epitranscriptome marks that are not detected in PCR-based RNA-sequencing platforms. Direct RNA sequencing by Nanopore (Garalde et al., 2018) is capable of detecting these modifications, but the technology is still in its infancy. An alternative approach could involve immunoprecipitation of viral RBPs, followed by RNA extraction and hydrolysis with RNase. Component nucleotides can could then be analyzed by mass spectrometry to discover nucleoside composition and modifications over-represented in bound mRNA. Further defining the role of the viral proteins identified in this study could provide important insight into regulation of translation during herpesvirus replication.

6.5 Future Investigations

The findings of this work immediately suggest some directions for future investigations. The role of ATG14 in restricting virus replication could be further defined, and the contributions of ORF57 and ORF59 to viral translation warrant more study. However, there are some hypothesis-generating results from the proteomic studies that could be broadly applied outside of KSHV replication. It was unexpected to isolate three KSHV proteins with roles in innate immune subversion in the polysome fractions; more unusual was the presence of cGAS in polysomal fractions (Fig 5.2). It will first be important to confirm that there are directly associated with RNA, possibly by dissociating polysomes with RNAse or puromycin treatments and analyzing heavy sucrose fractions for these proteins. PKR was previously identified as a ribosome-interacting protein (Raine et al., 1998; S. Zhu et al., 1997), but binding of cGAS to ribosomes has not been

previously reported. Association of innate immune sensors to ribosomes of polysomes could implicate these structures as sites of immune signalling.

The depletion of phenylalanine tRNA-synthase subunits similarly stood out in the analysis. Almost all the other tRNA synthases could be identified in this study, and of them all, only FarsA and FarsB were depleted from polysomes. This strongly suggests a non-aminoacyl tRNA synthetase role for these proteins. While these proteins are essential to the cell, the unique domains accrued through evolution and are associated with new functions in other tRNA synthetases, are likely dispensable and may be amenable to experimental manipulation (Guo et al., 2010). Alternatively, defining the stressor that displaces FarsA and FarsB from the polysomes could help delineate their function. Type-I IFN, eIF2α Ser51 phosphorylation, or ectopic expression of the viral proteins identified in this study would all be interesting stimuli to test. Given that non-aminoacyl tRNA synthetase roles are emerging for other tRNA synthetases, it is notable that no other tRNA synthetase was dysregulated during lytic replication.

The methods developed in Chapter Five to evaluate polysome-associated proteins could be broadly applied to other experimental systems. It would be interesting to complete a similar analysis on uninfected cells treated with Torin to evaluate what proteins are displaced from the polysomes by eIF4F-dependent translation. A similar experiment could also be used in hypoxic conditions to fully elucidate the $eIF4F_H$-translation initiation machinery. Cells could also be treated with different stimuli, such as Type-I interferons to search for ISGs that interact with the translation machinery or infected with other viruses.

Collectively, the work presented here helps define the role of mTORC1 in KSHV replication. More importantly, I think it demonstrates that the obvious answer is not necessarily the correct one. With several viral proteins enhancing mTORC1 activity, and the critical role of mTORC1 signalling in maintenance of KS lesions, it was surprising that two of the main effector functions of mTORC1, autophagy and eIF4F-dependent translation had little effect on virus replication. The differential effects of knocking down different autophagy-related proteins on virus replication also demonstrate that molecular functions of a pathway, or process, in a cell can differ from the individual components of that process. This reinforces the importance of orthogonal approaches in the study of

cellular phenotypes. KSHV retains the ability to produce virions in a variety of translational environments, and likely in the presence of myriad stressors. The ability of KSHV to modulate host-signalling pathways, yet find them dispensable, may be the quintessential definition of a herpesvirus, and further demonstrates the inimitable adaptation of these viruses to their host.

References

Abernathy, E., Clyde, K., Yeasmin, R., Krug, L.T., Burlingame, A., Coscoy, L., Glaunsinger, B., 2014. Gammaherpesviral gene expression and virion composition are broadly controlled by accelerated mRNA degradation. PLoS Pathogens 10, e1003882. doi:10.1371/journal.ppat.1003882.s006

Abernathy, E., Gilbertson, S., Alla, R., Glaunsinger, B., 2015. Viral nucleases induce an mRNA degradation-transcription feedback loop in mammalian cells. Cell Host Microbe 18, 243–253. doi:10.1016/j.chom.2015.06.019

Abernathy, E., Mateo, R., Majzoub, K., van Buuren, N., Bird, S.W., Carette, J.E., Kirkegaard, K., 2019. Differential and convergent utilization of autophagy components by positive-strand RNA viruses. PloS Biology 17, e2006926. doi:10.1371/journal.pbio.2006926.s013

Andreev, D.E., O'Connor, P.B.F., Fahey, C., Kenny, E.M., Terenin, I.M., Dmitriev, S.E., Cormican, P., Morris, D.W., Shatsky, I.N., Baranov, P.V., 2015. Translation of 5' leaders is pervasive in genes resistant to eIF2 repression. eLife 4, e03971. doi:10.7554/eLife.03971

Aoyagi, M., Gaspar, M., Shenk, T.E., 2010. Human cytomegalovirus UL69 protein facilitates translation by associating with the mRNA cap-binding complex and excluding 4EBP1. Proceedings of the National Academy of Sciences 107, 2640–2645. doi:10.1073/pnas.0914856107

Apcher, S., Daskalogianni, C., Lejeune, F., Manoury, B., Imhoos, G., Heslop, L., Fåhraeus, R., 2011. Major source of antigenic peptides for the MHC class I pathway is produced during the pioneer round of mRNA translation. Proceedings of the National Academy of Sciences 108, 11572–11577. doi:10.1073/pnas.1104104108

Arango, D., Sturgill, D., Alhusaini, N., Dillman, A.A., Sweet, T.J., Hanson, G., Hosogane, M., Sinclair, W.R., Nanan, K.K., Mandler, M.D., Fox, S.D., Zengeya, T.T., Andresson, T., Meier, J.L., Coller, J., Oberdoerffer, S., 2018. Acetylation of cytidine in mRNA promotes translation efficiency. Cell 1–40. doi:10.1016/j.cell.2018.10.030

Arcondeguy, T., Lacazette, E., Millevoi, S., Prats, H., Touriol, C., 2013. VEGF-A mRNA processing, stability and translation: a paradigm for intricate regulation of gene expression at the post-transcriptional level. Nucleic Acids Research 41, 7997–8010. doi:10.1016/j.cell.2011.10.002

Arias, C., Walsh, D., Harbell, J., Wilson, A.C., Mohr, I., 2009. Activation of host translational control pathways by a viral developmental switch. PLoS Pathogens 5, e1000334. doi:10.1371/journal.ppat.1000334.s001

Arias, C., Weisburd, B., Stern-Ginossar, N., Mercier, A., Madrid, A.S., Bellare, P., Holdorf, M., Weissman, J.S., Ganem, D., 2014. KSHV 2.0: a comprehensive annotation of the Kaposi's Sarcoma-associated herpesvirus genome using next-generation sequencing reveals novel genomic and functional features. PLoS Pathogens 10, e1003847. doi:10.1371/journal.ppat.1003847

Avey, D., Tepper, S., Li, W., Turpin, Z., Zhu, F., 2015. Phosphoproteomic analysis of KSHV-infected cells reveals roles of ORF45-activated RSK during lytic replication. PLoS Pathogens 11, e1004993. doi:10.1371/journal.ppat.1004993.s008

Avey, D., Tepper, S., Pifer, B., Bahga, A., Williams, H., Gillen, J., Li, W., Ogden, S., Zhu, F., 2016. Discovery of a coregulatory interaction between Kaposi's Sarcoma-associated Herpesvirus ORF45 and the viral protein kinase ORF36. Journal of Virology 90, 5953–5964. doi:10.1128/JVI.00516-16

Bah, A., Vernon, R.M., Siddiqui, Z., Krzeminski, M., Muhandiram, R., Zhao, C., Sonenberg, N., Kay, L.E., Forman-Kay, J.D., 2014. Folding of an intrinsically disordered protein by phosphorylation as a regulatory switch. Nature 1–15. doi:10.1038/nature13999

Bais, C., Santomasso, B., Coso, O., Arvanitakis, L., Raaka, E.G., Gutkind, J.S., Asch, A.S., Cesarman, E., Gershengorn, M.C., Mesri, E.A., Gerhengorn, M.C., 1998. G-protein-coupled receptor of Kaposi's Sarcoma-associated herpesvirus is a viral oncogene and angiogenesis activator. Nature 391, 86–89. doi:10.1038/34193

Baltz, J.L., Filman, D.J., Ciustea, M., Silverman, J.E.Y., Lautenschlager, C.L., Coen, D.M., Ricciardi, R.P., Hogle, J.M., 2009. The crystal structure of PF-8, the DNA polymerase accessory subunit from Kaposi's Sarcoma-associated Herpesvirus. Journal of Virology 83, 12215–12228. doi:10.1128/JVI.01158-09

Banerjee, R., Chakraborty, S., 2016. Phenylalanyl-tRNA synthetase. Research and Reports in Biochemistry 25. doi:10.2147/RRBC.S83482

Bar-Peled, L., Chantranupong, L., Cherniack, A.D., Chen, W.W., Ottina, K.A., Grabiner, B.C., Spear, E.D., Carter, S.L., Meyerson, M., Sabatini, D.M., 2013. A tumor suppressor complex with GAP activity for the Rag GTPases that signal amino acid sufficiency to mTORC1. Science 340, 1100–1106. doi:10.1126/science.1232044

Bar-Peled, L., Schweitzer, L.D., Zoncu, R., Sabatini, D.M., 2012. Ragulator is a GEF for the Rag GTPases that signal amino acid levels to mTORC1. Cell 150, 1196–1208. doi:10.1016/j.cell.2012.07.032

Barbieri, I., Tzelepis, K., Pandolfini, L., Shi, J., Millán-Zambrano, G., Robson, S.C., Aspris, D., Migliori, V., Bannister, A.J., Han, N., De Braekeleer, E., Ponstingl, H., Hendrick, A., Vakoc, C.R., Vassiliou, G.S., Kouzarides, T., 2017. Promoter-bound METTL3 maintains myeloid leukaemia by m^6A-dependent translation control. Nature 552, 126–131. doi:10.1038/nature24678

Baresova, P., Pitha, P.M., Lubyova, B., 2013. Distinct roles of Kaposi's Sarcoma-associated Herpesvirus-encoded viral interferon regulatory factors in inflammatory response and cancer. Journal of Virology 87, 9398–9410. doi:10.1128/JVI.01851-12

Bechtel, J.T., Liang, Y., Hvidding, J., Ganem, D., 2003. Host range of Kaposi's Sarcoma-associated Herpesvirus in cultured cells. Journal of Virology 77, 6474–6481. doi:10.1128/JVI.77.11.6474-6481.2003

Belin, S., Hacot, S., Daudignon, L., Therizols, G., Pourpe, S., Mertani, H.C., Rosa-Calatrava, M., Diaz, J.-J., 2010. Purification of ribosomes from human cell lines. Current Protocols in Cell Biology Chapter 3, Unit 3.40. doi:10.1002/0471143030.cb0340s49

Bhatt, A.P., Damania, B., 2012. AKTivation of PI3K/AKT/mTOR signaling pathway by KSHV. Frontiers in Immunology 3, 401. doi:10.3389/fimmu.2012.00401

Bhatt, A.P., Wong, J.P., Weinberg, M.S., Host, K.M., Giffin, L.C., Buijnink, J., van Dijk, E., Izumiya, Y., Kung, H.-J., Temple, B.R.S., Damania, B., 2016. A viral kinase mimics S6 kinase to enhance cell proliferation. Proceedings of the National Academy of Sciences 201600587. doi:10.1073/pnas.1600587113

Bieleski, L., Talbot, S.J., 2001. Kaposi's Sarcoma-associated Herpesvirus vcyclin open reading frame contains an internal ribosome entry site. Journal of Virology 75, 1864–1869. doi:10.1128/JVI.75.4.1864-1869.2001

Bigi, R., Landis, J.T., An, H., Caro-Vegas, C., Raab-Traub, N., Dittmer, D.P., 2018. Epstein–Barr virus enhances genome maintenance of Kaposi Sarcoma-associated herpesvirus. Proceedings of the National Academy of Sciences 115, E11379–E11387. doi:10.1128/JVI.00506-13

Boutell, C., Everett, R.D., 2013. Regulation of alphaherpesvirus infections by the ICP0 family of proteins. Journal of General Virology 94, 465–481. doi:10.1128/JVI.05098-11

Boyne, J.R., Jackson, B.R., Taylor, A., Macnab, S.A., Whitehouse, A., 2010. Kaposi's Sarcoma-associated herpesvirus ORF57 protein interacts with PYM to enhance translation of viral intronless mRNAs. The EMBO Journal 29, 1851–1864. doi:10.1038/emboj.2010.77

Brugarolas, J., Lei, K., Hurley, R.L., Manning, B.D., Reiling, J.H., Hafen, E., Witters, L.A., Ellisen, L.W., Kaelin, W.G., 2004. Regulation of mTOR function in response to hypoxia by REDD1 and the TSC1/TSC2 tumor suppressor complex. Genes & Development 18, 2893–2904. doi:10.1101/gad.1256804

Brulois, K., Wong, L.-Y., Lee, H.-R., Sivadas, P., Ensser, A., Feng, P., Gao, S.-J., Toth, Z., Jung, J.U., 2015. Association of Kaposi's Sarcoma-associated Herpesvirus ORF31 with ORF34 and ORF24 is critical for late gene expression. Journal of Virology 89, 6148–6154. doi:10.1128/JVI.00272-15

Bryant, D.M., Datta, A., Rodríguez-Fraticelli, A.E., Peränen, J., Martín-Belmonte, F., Mostov, K.E., 2010. A molecular network for de novo generation of the apical surface and lumen. Nature Cell Biology 12, 1035–1045. doi:10.1038/ncb2106

Bu, W., Palmeri, D., Krishnan, R., Marin, R., Aris, V.M., Soteropoulos, P., Lukac, D.M., 2008. Identification of direct transcriptional targets of the Kaposi's Sarcoma-associated Herpesvirus Rta lytic switch protein by conditional nuclear localization. Journal of Virology 82, 10709–10723. doi:10.1128/JVI.01012-08

Budt, M., Hristozova, T., Hille, G., Berger, K., Brune, W., 2011. Construction of a lytically replicating Kaposi's Sarcoma-associated Herpesvirus. Journal of Virology 85, 10415–10420. doi:10.1128/JVI.05071-11

Burgess, H.M., Mohr, I., 2018. Defining the role of stress granules in innate immune suppression by the Herpes Simplex Virus 1 endoribonuclease VHS. Journal of Virology 92. doi:10.1128/JVI.00829-18

Bushell, M., Poncet, D., Marissen, W.E., Flotow, H., Lloyd, R.E., Clemens, M.J., Morley, S.J., 2000. Cleavage of polypeptide chain initiation factor eIF4GI during apoptosis in lymphoma cells: characterisation of an internal fragment generated by caspase-3-mediated cleavage. Cell Death and Differentiation 7, 628–636. doi:10.1038/sj.cdd.4400699

Cai, Q., Lan, K., Verma, S.C., Si, H., Lin, D., Robertson, E.S., 2006. Kaposi's Sarcoma-associated Herpesvirus latent protein LANA interacts with HIF-1 to upregulate RTA expression during hypoxia: latency control under low oxygen conditions. Journal of Virology 80, 7965–7975. doi:10.1128/JVI.00689-06

Cai, X., Chiu, Y.-H., Chen, Z.J., 2014. The cGAS-cGAMP-STING pathway of cytosolic DNA sensing and signaling. Molecular Cell 54, 289–296. doi:10.1016/j.molcel.2014.03.040

Caldwell, C.C., Kojima, H., Lukashev, D., Armstrong, J., Farber, M., Apasov, S.G., Sitkovsky, M.V., 2001. Differential effects of physiologically relevant hypoxic conditions on T lymphocyte development and effector functions. The Journal of Immunology 167, 6140–6149. doi:10.4049/jimmunol.167.11.6140

Carpenter, A.E., Jones, T.R., Lamprecht, M.R., Clarke, C., Kang, I.H., Friman, O., Guertin, D.A., Chang, J.H., Lindquist, R.A., Moffat, J., Golland, P., Sabatini, D.M., 2006. CellProfiler: image analysis software for identifying and quantifying cell phenotypes. Genome Biology 7, R100. doi:10.1186/gb-2006-7-10-r100

Carroll, P.A., Kenerson, H.L., Yeung, R.S., Lagunoff, M., 2006. Latent Kaposi's Sarcoma-associated Herpesvirus infection of endothelial cells activates hypoxia-induced factors. Journal of Virology 80, 10802–10812. doi:10.1128/JVI.00673-06

Castelli, L.M., Talavera, D., Kershaw, C.J., Mohammad-Qureshi, S.S., Costello, J.L., Rowe, W., Sims, P.F.G., Grant, C.M., Hubbard, S.J., Ashe, M.P., Pavitt, G.D., 2015. The 4E-BP Caf20p mediates both eIF4E-dependent and independent repression of translation. PLoS Genetics 11, e1005233. doi:10.1371/journal.pgen.1005233.s008

Cate, J.H.D., 2017. Human eIF3: from “blobology” to biological insight. Phil. Trans. R. Soc. B 372, 20160176. doi:10.1016/j.cell.2015.10.012

Cencic, R., Desforges, M., Hall, D.R., Kozakov, D., Du, Y., Min, J., Dingledine, R., Fu, H., Vajda, S., Talbot, P.J., Pelletier, J., 2011a. Blocking eIF4E-eIF4G Interaction as a strategy to impair coronavirus replication. Journal of Virology 85, 6381–6389. doi:10.1128/JVI.00078-11

Cencic, R., Hall, D.R., Robert, F., Du, Y., Min, J., Li, L., Qui, M., Lewis, I., Kurtkaya, S., Dingledine, R., Fu, H., Kozakov, D., Vajda, S., Pelletier, J., 2011b. Reversing chemoresistance by small molecule inhibition of the translation initiation complex eIF4F. Proceedings of the National Academy of Sciences 108, 1046–1051. doi:10.1073/pnas.1011477108

Cesarman, E., Chang, Y., Moore, P.S., Said, J.W., Knowles, D.M., 1995. Kaposi's Sarcoma-associated herpesvirus-like DNA sequences in AIDS-related body-cavity-based lymphomas. New England Journal of Medicine 332, 1186–1191. doi:10.1056/NEJM199505043321802

Chan, S.R., Bloomer, C., Chandran, B., 1998. Identification and characterization of human herpesvirus-8 lytic cycle-associated ORF 59 protein and the encoding cDNA by monoclonal antibody. Virology 240, 118–126. doi:10.1006/viro.1997.8911

Chan, S.R., Chandran, B., 2000. Characterization of human herpesvirus 8 ORF59 protein (PF-8) and mapping of the processivity and viral DNA polymerase-interacting domains. Journal of Virology 74, 10920–10929.

Chandriani, S., Ganem, D., 2007. Host transcript accumulation during lytic KSHV infection reveals several classes of host responses. PLoS ONE 2, e811. doi:10.1371/journal.pone.0000811.s004

Chang, H.H., Chang, H.H., Ganem, D., Ganem, D., 2013. A Unique Herpesviral Transcriptional program in KSHV-Infected lymphatic endothelial cells leads to mTORC1 activation and rapamycin sensitivity. Cell Host Microbe 13, 429–440. doi:10.1016/j.chom.2013.03.009

Chang, Y., Cesarman, E., Pessin, M.S., Lee, F., Culpepper, J., Knowles, D.M., Moore, P.S., 1994. Identification of herpesvirus-like DNA sequences in AIDS-associated Kaposi's sarcoma. Science 266, 1865–1869.

Chapat, C.M., Jafarnejad, S.M., Matta-Camacho, E., Hesketh, G.G., Gelbart, I.A., Attig, J., Gkogkas, C.G., Alain, T., Stern-Ginossar, N., Fabian, M.R., Gingras, A.-C., Duchaine, T.F., Sonenberg, N., 2017. Cap-binding protein 4EHP effects translation silencing by microRNAs. Proceedings of the National Academy of Sciences 114, 5425–5430. doi:10.1093/nar/gkv720

Chen, D., Sandford, G., Nicholas, J., 2008. Intracellular signaling mechanisms and activities of Human Herpesvirus 8 Interleukin-6. Journal of Virology 83, 722–733. doi:10.1128/JVI.01517-08

Chen, X., Lin, K., Ricciardi, R.P., 2004. Human Kaposi's Sarcoma Herpesvirus Processivity Factor-8 functions as a dimer in DNA Synthesis. Journal of Biological Chemistry 279, 28375–28386. doi:10.1074/jbc.M400032200

Cho, J., Kang, M.-S., Kim, K.-M., 2016. Epstein-Barr Virus-Associated gastric carcinoma and specific features of the accompanying immune response. Journal of Gastric Cancer 16, 1. doi:10.5230/jgc.2016.16.1.1

Choe, J., Lin, S., Zhang, W., Liu, Q., Wang, L., Ramirez-Moya, J., Du, P., Kim, W., Tang, S., Sliz, P., Santisteban, P., George, R.E., Richards, W.G., Wong, K.-K., Locker, N., Slack, F.J., Gregory, R.I., 2018. mRNA circularization by METTL3–eIF3h enhances translation and promotes oncogenesis. Nature 1–25. doi:10.1038/s41586-018-0538-8

Choe, J., Oh, N., Park, S., Lee, Y.K., Song, O.-K., Locker, N., Chi, S.-G., Kim, Y.K., 2012. Translation initiation on mRNAs bound by nuclear cap-binding protein complex CBP80/20 requires interaction between CBP80/20-dependent translation initiation factor and eukaryotic translation initiation factor 3g. Journal of Biological Chemistry 287, 18500–18509. doi:10.1074/jbc.M111.327528

Choe, J., Ryu, I., Park, O.H., Park, J., Cho, H., Yoo, J.S., Chi, S.W., Kim, M.K., Song, H.K., Kim, Y.K., 2014. eIF4AIII enhances translation of nuclear cap-binding complex-bound mRNAs by promoting disruption of secondary structures in 5'UTR. Proceedings of the National Academy of Sciences 111, E4577–E4586. doi:10.1038/nature08170

Chuluunbaatar, U., Roller, R., Feldman, M.E., Brown, S., Shokat, K.M., Mohr, I., 2010. Constitutive mTORC1 activation by a herpesvirus Akt surrogate stimulates mRNA translation and viral replication. Genes & Development 24, 2627–2639. doi:10.1101/gad.1978310

Clippinger, A.J., Maguire, T.G., Alwine, J.C., 2011. Human Cytomegalovirus infection maintains mTOR activity and its perinuclear localization during amino acid deprivation. Journal of Virology 85, 9369–9376. doi:10.1128/JVI.05102-11

Coots, R.A., Liu, X.-M., Mao, Y., Dong, L., Zhou, J., Wan, J., Zhang, X., Qian, S.-B., 2017. A Facilitates eIF4F-independent mRNA translation. Molecular Cell 68, 504–514.e7. doi:10.1016/j.molcel.2017.10.002

Corbin-Lickfett, K.A., Chen, I.-H.B., Cocco, M.J., Sandri-Goldin, R.M., 2009. The HSV-1 ICP27 RGG box specifically binds flexible, GC-rich sequences but not G-quartet structures. Nucleic Acids Research 37, 7290–7301. doi:10.1038/emboj.2008.221

Corcoran, J.A., Johnston, B.P., McCormick, C., 2015. Viral Activation of MK2-hsp27-p115RhoGEF-RhoA signaling axis causes cytoskeletal rearrangements, P-body disruption and ARE-mRNA stabilization. PLoS Pathogens 11, e1004597. doi:10.1371/journal.ppat.1004597.s006

Corcoran, J.A., Khaperskyy, D.A., Johnston, B.P., King, C.A., Cyr, D.P., Olsthoorn, A.V., McCormick, C., 2012. Kaposi's Sarcoma-associated Herpesvirus G-Protein-Coupled Receptor prevents AU-rich-element-mediated mRNA decay. Journal of Virology 86, 8859–8871. doi:10.1128/JVI.00597-12

Courtney, D.G., Kennedy, E.M., Dumm, R.E., Bogerd, H.P., Tsai, K., Heaton, N.S., Cullen, B.R., 2017. Epitranscriptomic Enhancement of Influenza A Virus gene expression and replication. Cell Host Microbe 22, 377–386.e5. doi:10.1016/j.chom.2017.08.004

Covarrubias, S., Gaglia, M.M., Kumar, G.R., Wong, W., Jackson, A.O., Glaunsinger, B.A., 2011. Coordinated destruction of cellular messages in translation complexes by the gammaherpesvirus host shutoff factor and the mammalian exonuclease Xrn1. PLoS Pathogens 7, e1002339. doi:10.1371/journal.ppat.1002339.s007

Covarrubias, S., Richner, J.M., Clyde, K., Lee, Y.J., Glaunsinger, B.A., 2009. Host shutoff is a conserved phenotype of gammaherpesvirus infection and is orchestrated exclusively from the cytoplasm. Journal of Virology 83, 9554–9566. doi:10.1128/JVI.01051-09

Dalton-Griffin, L., Wilson, S.J., Kellam, P., 2009. X-Box Binding Protein 1 contributes to induction of the Kaposi's Sarcoma-associated Herpesvirus lytic cycle under hypoxic conditions. Journal of Virology 83, 7202–7209. doi:10.1128/JVI.00076-09

Dauber, B., Pelletier, J., Smiley, J.R., 2011. The Herpes Simplex Virus 1 vhs protein enhances translation of viral true late mRNAs and virus production in a cell type-Dependent Manner. Journal of Virology 85, 5363–5373. doi:10.1128/JVI.00115-11

Dauber, B., Saffran, H.A., Smiley, J.R., 2014. The herpes simplex virus 1 virion host shutoff protein enhances translation of viral late mRNAs by preventing mRNA overload. Journal of Virology 88, 9624–9632. doi:10.1128/JVI.01350-14

Davis, D.A., 2001. Hypoxia induces lytic replication of Kaposi Sarcoma-associated herpesvirus. Blood 97, 3244–3250. doi:10.1182/blood.V97.10.3244

Davis, Z.H., Verschueren, E., Jang, G.M., Kleffman, K., Johnson, J.R., Park, J., Dollen, Von, J., Maher, M.C., Johnson, T., Newton, W., Jäger, S., Shales, M., Horner, J., Hernandez, R.D., Krogan, N.J., Glaunsinger, B.A., 2014. Global mapping of herpesvirus-host protein complexes reveals a transcription strategy for late genes. Molecular Cell 1–12. doi:10.1016/j.molcel.2014.11.026

Davison, A.J., Stow, N.D., 2005. New genes from old: Redeployment of dUTPase by herpesviruses. Journal of Virology 79, 12880–12892. doi:10.1128/JVI.79.20.12880-12892.2005

Demetriades, C., Doumpas, N., Teleman, A.A., 2014. Regulation of TORC1 in response to amino acid starvation via lysosomal recruitment of TSC2. Cell 156, 786–799. doi:10.1016/j.cell.2014.01.024

Demetriades, C., Plescher, M., Teleman, A.A., 2015. Lysosomal recruitment of TSC2 is a universal response to cellular stress. Nature Communications 7, 10662. doi:10.1038/ncomms10662

Deretic, V., 2012. Autophagy: An emerging immunological paradigm. The Journal of Immunology 189, 15–20. doi:10.4049/jimmunol.1102108

Deretic, V., Levine, B., 2009. Autophagy, immunity, and microbial adaptations. Cell Host Microbe 5, 527–549. doi:10.1016/j.chom.2009.05.016

Desai, P.J., Pryce, E.N., Henson, B.W., Luitweiler, E.M., Cothran, J., 2011. Reconstitution of the Kaposi's Sarcoma-associated Herpesvirus nuclear egress complex and formation of nuclear membrane vesicles by coexpression of ORF67 and ORF69 Gene Products. Journal of Virology 86, 594–598. doi:10.1128/JVI.76.12.6185-6196.2002

DeYoung, M.P., Horak, P., Sofer, A., Sgroi, D., Ellisen, L.W., 2008. Hypoxia regulates TSC1/2 mTOR signaling and tumor suppression through REDD1-mediated 14-3-3 shuttling. Genes & Development 22, 239–251. doi:10.1101/gad.1617608

Dibble, C.C., Elis, W., Menon, S., Qin, W., Klekota, J., Asara, J.M., Finan, P.M., Kwiatkowski, D.J., Murphy, L.O., Manning, B.D., 2012. TBC1D7 is a third subunit of the TSC1-TSC2 complex ppstream of mTORC1. Molecular Cell 47, 535–546. doi:10.1016/j.molcel.2012.06.009

Dikic, I., Elazar, Z., 2018. Mechanism and medical implications of mammalian autophagy. Nature Reviews Molecular and Cellular Biology 1–16. doi:10.1038/s41580-018-0003-4

Doepker, R.C., Hsu, W.L., Saffran, H.A., Smiley, J.R., 2004. Herpes Simplex Virus Virion Host Shutoff protein is stimulated by translation initiation factors eIF4B and eIF4H. Journal of Virology 78, 4684–4699. doi:10.1128/JVI.78.9.4684-4699.2004

Dominissini, D., Moshitch-Moshkovitz, S., Schwartz, S., Salmon-Divon, M., Ungar, L., Osenberg, S., Cesarkas, K., Jacob-Hirsch, J., Amariglio, N., Kupiec, M., Sorek, R., Rechavi, G., 2012. Topology of the human and mouse m^6A RNA methylomes revealed by m^6A-seq. Nature 485, 201–206. doi:10.1038/nature11112

Dominissini, D., Nachtergaele, S., Moshitch-Moshkovitz, S., Peer, E., Kol, N., Ben-Haim, M.S., Dai, Q., Di Segni, A., Salmon-Divon, M., Clark, W.C., Zheng, G., Pan, T., Solomon, O., Eyal, E., Hershkovitz, V., Han, D., Doré, L.C., Amariglio, N., Rechavi, G., He, C., 2016. The dynamic N^1-methyladenosine methylome in eukaryotic messenger RNA. Nature 530, 441–446. doi:10.1038/nature16998

Doolittle, W.F., Brunet, T.D.P., Linquist, S., Gregory, T.R., 2014. Distinguishing between "function" and “effect” in genome biology. Genome Biology and Evolution 6, 1234–1237. doi:10.1186/1471-2148-12-159

Du, H., Zhao, Y., He, J., Zhang, Y., Xi, H., Liu, M., Ma, J., Wu, L., 2016. YTHDF2 destabilizes m^6A-containing RNA through direct recruitment of the CCR4-NOT deadenylase complex. Nature Communications 7, 1–11. doi:10.1038/ncomms12626

Durand, S., Lykke-Andersen, J., 2013. Nonsense-mediated mRNA decay occurs during eIF4F-dependent translation in human cells. Nature Structural & Molecular Biology 20, 702–709. doi:10.1016/S0092-8674(00)00214-2

Ellison, K.S., Maranchuk, R.A., Mottet, K.L., Smiley, J.R., 2005. Control of VP16 translation by the Herpes Simplex Virus Type 1 immediate-early Protein ICP27. Journal of Virology 79, 4120–4131. doi:10.1128/JVI.79.7.4120-4131.2005

Ersching, J., Efeyan, A., Mesin, L., Jacobsen, J.T., Pasqual, G., Grabiner, B.C., Dominguez-Sola, D., Sabatini, D.M., Victora, G.D., 2017. Germinal center selection and affinity maturation require dynamic regulation of mTORC1 kinase. Immunity 46, 1045–1064.e0. doi:10.1016/j.immuni.2017.06.005

Ersing, I., Nobre, L., Wang, L.W., Soday, L., Ma, Y., Paulo, J.A., Narita, Y., Ashbaugh, C.W., Jiang, C., Grayson, N.E., Kieff, E., Gygi, S.P., Weekes, M.P., Gewurz, B.E., 2017. A temporal proteomic map of Epstein-Barr Virus lytic replication in B cells. Cell Reports 19, 1479–1493. doi:10.1016/j.celrep.2017.04.062

Fontaine-Rodriguez, E.C., Taylor, T.J., Olesky, M., Knipe, D.M., 2004. Proteomics of herpes simplex virus infected cell protein 27: association with translation initiation factors. Virology 330, 487–492. doi:10.1016/j.virol.2004.10.002

Friborg, J., Kong, W., Hottiger, M.O., Nabel, G.J., 1999. p53 inhibition by the LANA protein of KSHV protects against cell death. Nature 402, 889–894. doi:10.1038/47266

Fu, B., Kuang, E., Li, W., Avey, D., Li, X., Turpin, Z., Valdes, A., Brulois, K., Myoung, J., Zhu, F., 2015. Activation of p90 ribosomal S6 kinases by ORF45 of Kaposi's Sarcoma-associated herpesvirus is critical for optimal production of infectious viruses. Journal of Virology 89, 195–207. doi:10.1128/JVI.01937-14

Fu, R., Olsen, M.T., Webb, K., Bennett, E.J., Lykke-Andersen, J., 2016. Recruitment of the 4EHP-GYF2 cap-binding complex to tetraproline motifs of tristetraprolin promotes repression and degradation of mRNAs with AU-rich elements. RNA 22, 373–382. doi:10.1261/rna.054833.115

Funderburk, S.F., Wang, Q.J., Yue, Z., 2010. The Beclin 1-VPS34 complex - at the crossroads of autophagy and beyond. Trends in Cell Biology 20, 355–362. doi:10.1016/j.tcb.2010.03.002

Ganem, D., 2010. KSHV and the pathogenesis of Kaposi sarcoma: listening to human biology and medicine. Journal of Clinical Investigation 120, 939–949. doi:10.1172/JCI40567

Ganem, D., 2006. KSHV infection and the pathogenesis of Kaposi's sarcoma. Annual Review of Pathology 1, 273–296. doi:10.1146/annurev.pathol.1.110304.100133

Ganley, I.G., Lam, D.H., Wang, J., Ding, X., Chen, S., Jiang, X., 2009. ULK1·ATG13·FIP200 complex mediates mTOR signaling and is essential for autophagy. Journal of Biological Chemistry 284, 12297–12305. doi:10.1016/j.cellsig.2007.10.021

Gao, S.J., Boshoff, C., Jayachandra, S., Weiss, R.A., Chang, Y., Moore, P.S., 1997. KSHV ORF K9 (vIRF) is an oncogene which inhibits the interferon signaling pathway. Oncogene 15, 1979–1985. doi:10.1038/sj.onc.1201571

Garalde, D.R., Snell, E.A., Jachimowicz, D., Sipos, B., Lloyd, J.H., Bruce, M., Pantic, N., Admassu, T., James, P., Warland, A., Jordan, M., Ciccone, J., Serra, S., Keenan, J., Martin, S., McNeill, L., Wallace, E.J., Jayasinghe, L., Wright, C., Blasco, J., Young, S., Brocklebank, D., Juul, S., Clarke, J., Heron, A.J., Turner, D.J., 2018. highly parallel direct RNA sequencing on an array of nanopores. Nature Methods 1–10. doi:10.1038/nmeth.4577

Gardella T., Medveczhy P., Sairenji T., Mulder C., 1984. Detection of circular and linear Herpesvirus DNA molecules in mammalian cells by gel electrophoresis. Journal of Virology 50, 248-254.

Gebhardt, A., Habjan, M., Benda, C., Meiler, A., Haas, D.A., Hein, M.Y., Mann, A., Mann, M., Habermann, B., Pichlmair, A., 2015. mRNA export through an additional cap-binding complex consisting of NCBP1 and NCBP3. Nature Communications 6, 1–13. doi:10.1038/ncomms9192

Gilbert, W.V., 2010. Alternative ways to think about cellular internal ribosome entry. Journal of Biological Chemistry 285, 29033–29038. doi:10.1016/j.molcel.2009.11.013

Gilbert, W.V., Bell, T.A., Schaening, C., 2016. Messenger RNA modifications: Form, distribution, and function. Science 352, 1408–1412. doi:10.1038/nchembio.2040

Gilbertson, S., Federspiel, J.D., Hartenian, E., Cristea, I.M., Glaunsinger, B., 2018. Changes in mRNA abundance drive shuttling of RNA binding proteins, linking cytoplasmic RNA degradation to transcription. eLife 7. doi:10.7554/eLife.37663

Gingras, A.C., Gygi, S.P., Raught, B., Polakiewicz, R.D., Abraham, R.T., Hoekstra, M.F., Aebersold, R., Sonenberg, N., 1999. Regulation of 4E-BP1 phosphorylation: a novel two-step mechanism. Genes & Development 13, 1422–1437.

Gingras, A.C., Raught, B., Gygi, S.P., Niedzwiecka, A., Miron, M., Burley, S.K., Polakiewicz, R.D., Wyslouch-Cieszynska, A., Aebersold, R., Sonenberg, N., 2001. Hierarchical phosphorylation of the translation inhibitor 4E-BP1. Genes & Development 15, 2852–2864. doi:10.1101/gad.912401

Glaunsinger, B., Ganem, D., 2004a. Lytic KSHV infection inhibits host gene expression by accelerating global mRNA turnover. Molecular Cell 13, 713–723.

Glaunsinger, B., Ganem, D., 2004b. Highly selective escape from KSHV-mediated host mRNA shutoff and its implications for viral pathogenesis. Journal of Experimental Medicine 200, 391–398. doi:10.1182/blood.V97.10.3244

Glaunsinger, B.A., 2015. Modulation of the translational landscape during herpesvirus infection. Annual Review of Virology 2, 311–333. doi:10.1146/annurev-virology-100114-054839

Gokhale, N.S., McIntyre, A.B.R., McFadden, M.J., Roder, A.E., Kennedy, E.M., Gandara, J.A., Hopcraft, S.E., Quicke, K.M., Vazquez, C., Willer, J., Ilkayeva, O.R., Law, B.A., Holley, C.L., Garcia-Blanco, M.A., Evans, M.J., Suthar, M.S., Bradrick, S.S., Mason, C.E., Horner, S.M., 2016. N6-Methyladenosine in flaviviridae viral RNA genomes regulates infection. Cell Host Microbe 20, 654–665. doi:10.1016/j.chom.2016.09.015

Gossage, L., Eisen, T., Maher, E.R., 2015. VHL, the story of a tumour suppressor gene. Nature Rev Cancer 15, 55–64. doi:10.1038/nrc3844

Gottwein, E., 2012. Kaposi's Sarcoma-associated herpesvirus microRNAs 1–13. doi:10.3389/fmicb.2012.00165/abstract

Grossmann, C., Podgrabinska, S., Skobe, M., Ganem, D., 2006. Activation of NF-κB by the Latent vFLIP gene of Kaposi's Sarcoma-associated Herpesvirus is required for the spindle shape of virus-infected endothelial cells and contributes to their proinflammatory phenotype. Journal of Virology 80, 7179–7185. doi:10.1128/JVI.01603-05

Grundhoff, A., Ganem, D., 2004. Inefficient establishment of KSHV latency suggests an additional role for continued lytic replication in Kaposi Sarcoma pathogenesis. Journal of Clinical Investigation 113, 124–136. doi:10.1172/JCI200417803

Grundhoff, A., Ganem, D., 2001. Mechanisms Governing Expression of the v-FLIP Gene of Kaposi's Sarcoma-associated Herpesvirus. Journal of Virology 75, 1857–1863. doi:10.1128/JVI.75.4.1857-1863.2001

Guasparri, I., Keller, S.A., Cesarman, E., 2004. KSHV vFLIP is essential for the survival of infected lymphoma cells. Journal of Experimental Medicine 199, 993–1003. doi:10.1038/sj.onc.1204895

Guertin, D.A., Sabatini, D.M., 2007. Defining the role of mTOR in cancer. Cancer Cell 12, 9–22. doi:10.1016/j.ccr.2007.05.008

Guito, J., Lukac, D.M., 2012. KSHV Rta promoter specification and viral reactivation. Frontiers in Microbiology. 3, 1–21. doi:10.3389/fmicb.2012.00030/abstract

Guo, M., Yang, X.-L., Schimmel, P., 2010. New functions of aminoacyl-tRNA synthetases beyond translation. Nature Reviews Molecular and Cellular Biology 11, 668–674. doi:10.1038/nrm2956

Gutierrez, E., Shin, B.-S., Woolstenhulme, C.J., Kim, J.-R., Saini, P., Buskirk, A.R., Dever, T.E., 2013. eIF5A promotes translation of polyproline motifs. Molecular Cell 51, 35–45. doi:10.1016/j.molcel.2013.04.021

Haghighat, A., Sonenberg, N., 1997. eIF4G dramatically enhances the binding of eIF4E to the mRNA 5'-cap structure. Journal of Biological Chemistry 272, 21677–21680.

Haghighat, A., Svitkin, Y., Novoa, I., Kuechler, E., Skern, T., Sonenberg, N., 1996. The eIF4G-eIF4E complex is the target for direct cleavage by the rhinovirus 2A proteinase. Journal of Virology 70, 8444–8450.

Hamasaki, M., Furuta, N., Matsuda, A., Nezu, A., Yamamoto, A., Fujita, N., Oomori, H., Noda, T., Haraguchi, T., Hiraoka, Y., Amano, A., Yoshimori, T., 2013. Autophagosomes form at ER–mitochondria contact sites. Nature 1–7. doi:10.1038/nature11910

Hamza, M.S., Reyes, R.A., Izumiya, Y., Wisdom, R., Kung, H.-J., Luciw, P.A., 2004. ORF36 protein minase of Kaposi's Sarcoma Herpesvirus activates the c-Jun N-terminal kinase signaling pathway. Journal of Biological Chemistry 279, 38325–38330. doi:10.1128/JVI.77.2.1441-1451.2003

Hao, H., Hao, S., Chen, H., Chen, Z., Zhang, Y., Wang, J., Wang, H., Zhang, B., Qiu, J., Deng, F., Guan, W., 2018. N6-methyladenosine modification and METTL3 modulate enterovirus 71 replication. Nucleic Acids Research 8, e1002732. doi:10.1093/nar/gky1007

Haque, M., Davis, D.A., Wang, V., Widmer, I., Yarchoan, R., 2003. Kaposi's Sarcoma-associated Herpesvirus (Human Herpesvirus 8) contains hypoxia response elements: Relevance to lytic induction by hypoxia. Journal of Virology 77, 6761–6768. doi:10.1128/JVI.77.12.6761-6768.2003

Haque, M., Kousoulas, K.G., 2013. The Kaposi's Sarcoma-associated Herpesvirus ORF34 protein binds to HIF-1 and causes its degradation via the proteasome pathway. Journal of Virology 87, 2164–2173. doi:10.1128/JVI.02460-12

Henis-Korenblit, S., Shani, G., Sines, T., Marash, L., Shohat, G., Kimchi, A., 2002. The caspase-cleaved DAP5 protein supports internal ribosome entry site-mediated translation of death proteins. Proceedings of the National Academy of Sciences USA 99, 5400–5405. doi:10.1073/pnas.082102499

Hershey, J.W.B., 2015. The role of eIF3 and its individual subunits in cancer.Biochimica et Biophysica Acta. 1849, 792–800. doi:10.1016/j.bbagrm.2014.10.005

Hesser, C.R., Karijolich, J., Dominissini, D., He, C., Glaunsinger, B.A., 2018. N6-methyladenosine modification and the YTHDF2 reader protein play cell type specific roles in lytic viral gene expression during Kaposi's Sarcoma-associated herpesvirus infection. PLoS Pathogens 14, e1006995. doi:10.1371/journal.ppat.1006995.s009

Heyer, E.E., Moore, M.J., 2016. Redefining the translational status of 80S monosomes. Cell 164, 757–769. doi:10.1016/j.cell.2016.01.003

Hinnebusch, A.G., 2014. The scanning mechanism of eukaryotic translation initiation. Annual Review of Biochemistry. 83, 779–812. doi:10.1146/annurev-biochem-060713-035802

Ho, J.J.D., Wang, M., Audas, T.E., Kwon, D., Carlsson, S.K., Timpano, S., Evagelou, S.L., Brothers, S., Gonzalgo, M.L., Krieger, J.R., Chen, S., Uniacke, J., Lee, S., 2016. Systemic reprogramming of translation efficiencies on oxygen stimulus. Cell Reports 14, 1293–1300. doi:10.1016/j.celrep.2016.01.036

Holz, M.K., Ballif, B.A., Gygi, S.P., Blenis, J., 2005. mTOR and S6K1 mediate assembly of the translation preinitiation complex through dynamic protein interchange and ordered phosphorylation events. Cell 123, 569–580. doi:10.1016/j.cell.2005.10.024

Hong, Y.-K., Foreman, K., Shin, J.W., Hirakawa, S., Curry, C.L., Sage, D.R., Libermann, T., Dezube, B.J., Fingeroth, J.D., Detmar, M., 2004. Lymphatic reprogramming of blood vascular endothelium by Kaposi sarcoma–associated herpesvirus. Nature Genet 36, 683–685. doi:10.1128/JVI.77.10.5975-5984.2003

Hopcraft, S.E., Pattenden, S.G., James, L.I., Frye, S., Dittmer, D.P., Damania, B., 2018. Chromatin remodeling controls Kaposi's Sarcoma-associated herpesvirus reactivation from latency. PLoS Pathogens 14, e1007267. doi:10.1371/journal.ppat.1007267.s002

Horner, S.M., Liu, H.M., Park, H.S., Briley, J., Gale, M., 2011. Mitochondrial-associated endoplasmic reticulum membranes (MAM) form innate immune synapses and are targeted by hepatitis C virus. Proceedings of the National Academy of Sciences 108, 14590–14595. doi:10.1073/pnas.1110133108

Hosokawa, N., Hara, T., Kaizuka, T., Kishi, C., Takamura, A., Miura, Y., Iemura, S.-I., Natsume, T., Takehana, K., Yamada, N., Guan, J.-L., Oshiro, N., Mizushima, N., 2009. Nutrient-dependent mTORC1 association with the ULK1-ATG13-FIP200 complex required for autophagy. Molecular Biology of the Cell 20, 1981–1991. doi:10.1091/mbc.e08-12-1248

Hsieh, A.C., Hsieh, A.C., Liu, Y., Liu, Y., Edlind, M.P., Edlind, M.P., Ingolia, N.T., Ingolia, N.T., Janes, M.R., Janes, M.R., Sher, A., Sher, A., Shi, E.Y., Shi, E.Y., Stumpf, C.R., Stumpf, C.R., Christensen, C., Christensen, C., Bonham, M.J., Bonham, M.J., Wang, S., Wang, S., Ren, P., Ren, P., Martin, M., Martin, M., Jessen, K., Jessen, K., Feldman, M.E., Feldman, M.E., Weissman, J.S., Weissman, J.S., Shokat, K.M., Shokat, K.M., Rommel, C., Rommel, C., Ruggero, D., Ruggero, D., 2012. The translational landscape of mTOR signalling steers cancer initiation and metastasis. Nature 485, 55–61. doi:10.1038/nature10912

Huang, J., Manning, B.D., 2008. The TSC1–TSC2 complex: a molecular switchboard controlling cell growth. Biochemistry Journal. 412, 179–190. doi:10.1042/BJ20080281

Huang, S., Liu, S., Fu, J.J., Tony Wang, T., Yao, X., Kumar, A., Liu, G., Fu, M., 2015. Monocyte Chemotactic Protein-induced Protein 1 and 4 form a complex but act independently in regulation of Interleukin-6 mRNA degradation. Journal of Biological Chemistry 290, 20782–20792. doi:10.1038/nsmb.1405

Hwang, K.Y., Choi, Y.B., 2016. Modulation of mitochondrial antiviral signaling by Human Herpesvirus 8 Interferon Regulatory Factor 1. Journal of Virology 90, 506–520. doi:10.1128/JVI.01903-15

Imataka, H., Olsen, H.S., Sonenberg, N., 1997. A new translational regulator with homology to eukaryotic translation initiation factor 4G. The EMBO Journal 16, 817–825. doi:10.1093/emboj/16.4.817

Inoki, K., Li, Y., Zhu, T., Wu, J., Guan, K.-L., 2002. TSC2 is phosphorylated and inhibited by Akt and suppresses mTOR signalling. Nature Cell Biology 4, 648–657. doi:10.1038/35078107

Inoki, K., Zhu, T., Guan, K.-L., 2003. TSC2 mediates cellular energy response to control cell growth and survival. Cell 115, 577–590.

Ishigaki, Y., Li, X., Serin, G., Maquat, L.E., 2001. Evidence for a pioneer round of mRNA translation: mRNAs subject to nonsense-mediated decay in mammalian cells are bound by CBP80 and CBP20. Cell 106, 607–617.

Ishikawa, K., Akiyama, T., Ito, K., Semba, K., Inoue, J.-I., 2009. Independent stabilizations of polysomal Drg1/Dfrp1 complex and non-polysomal Drg/Drfp2 complex in mammalian cells. Biochemical and Biophysical Research Communications 390, 552–556. doi:10.1016/j.bbrc.2009.10.003

Itakura, E., Kishi, C., Inoue, K., Mizushima, N., 2008. Beclin 1 forms two distinct phosphatidylinositol 3-kinase complexes with mammalian ATG14 and UVRAG. Molecular Biology of the Cell 19, 5360–5372. doi:10.1091/mbc.e08-01-0080

Izumiya, Y., Izumiya, C., Hsia, D., Ellison, T.J., Luciw, P.A., Kung, H.J., 2009. NF-κB serves as a cellular sensor of Kaposi's Sarcoma-associated Herpesvirus latency and negatively regulates K-Rta by antagonizing the RBP-J Coactivator. Journal of Virology 83, 4435–4446. doi:10.1128/JVI.01999-08

Izumiya, Y., Kobayashi, K., Kim, K.Y., Pochampalli, M., Izumiya, C., Shevchenko, B., Wang, D.-H., Huerta, S.B., Martinez, A., Campbell, M., Kung, H.-J., 2013. Kaposi's Sarcoma-associated Herpesvirus K-Rta exhibits SUMO-targeting ubiquitin ligase (STUbL) like activity and is essential for viral reactivation. PLoS Pathogens 9, e1003506. doi:10.1371/journal.ppat.1003506.s005

Jagger, B.W., Wise, H.M., Kash, J.C., Walters, K.A., Wills, N.M., Xiao, Y.L., Dunfee, R.L., Schwartzman, L.M., Ozinsky, A., Bell, G.L., Dalton, R.M., Lo, A., Efstathiou, S., Atkins, J.F., Firth, A.E., Taubenberger, J.K., Digard, P., 2012. An overlapping protein-coding region in Influenza A Virus segment 3 modulates the host response. Science 337, 199–204. doi:10.1099/vir.0.82809-0

Jan, E., Mohr, I., Walsh, D., 2016. A cap-to-tail guide to mRNA translation strategies in virus-infected cells. Annual Review of Virology 3, 283-307. doi:10.1146/annurev-virology-100114-055014

Jia, G., Fu, Y., Zhao, X., Dai, Q., Zheng, G., Yang, Y., Yi, C., Lindahl, T., Pan, T., Yang, Y.-G., He, C., 2011. N6-Methyladenosine in nuclear RNA is a major substrate of the obesity-associated FTO. Nature Chemical Biology 7, 885–887. doi:10.1038/nchembio.482

Joazeiro, C.A.P., 2017. Ribosomal stalling during translation: Providing substrates for ribosome-associated protein quality control. Annual Review of Cell and Developmental Biology. 33, 343–368. doi:10.1146/annurev-cellbio-111315-125249

Jones, T., Ye, F., Bedolla, R., Huang, Y., Meng, J., Qian, L., Pan, H., Zhou, F., Moody, R., Wagner, B., Arar, M., Gao, S.-J., 2012. Direct and efficient cellular transformation of primary rat mesenchymal precursor cells by KSHV. J Clin Invest 122, 1076–1081. doi:10.1172/JCI58530DS1

Juszkiewicz, S., Chandrasekaran, V., Lin, Z., Kraatz, S., Ramakrishnan, V., Hegde, R.S., 2018. ZNF598 is a quality control sensor of collided ribosomes. Molecular Cell 72, 469–481.e7. doi:10.1016/j.molcel.2018.08.037

Kang, H.R., Cheong, W.C., Park, J.E., Ryu, S., Cho, H.J., Youn, H., Ahn, J.H., Song, M.J., 2014. Murine Gammaherpesvirus 68 encoding Open Reading Frame 11 targets TANK Binding Kinase 1 to negatively regulate the host Type I Interferon response. Journal of Virology 88, 6832–6846. doi:10.1128/JVI.79.22.14149-14160.2005

Kang, S.A., Pacold, M.E., Cervantes, C.L., Lim, D., Lou, H.J., Ottina, K., Gray, N.S., Turk, B.E., Yaffe, M.B., Sabatini, D.M., 2013. mTORC1 phosphorylation sites encode their sensitivity to starvation and rapamycin. Science 341, 1236566–1236566. doi:10.1126/science.1236566

Kaur, S., Sassano, A., Majchrzak-Kita, B., Baker, D.P., Su, B., Fish, E.N., Platanias, L.C., 2012. Regulatory effects of mTORC2 complexes in type I IFN signaling and in the generation of IFN responses. Proceedings of the National Academy of Sciences 109, 7723–7728. doi:10.1073/pnas.1118122109

Kearse, M.G., Wilusz, J.E., 2017. Non-AUG translation: a new start for protein synthesis in eukaryotes. Genes & Development 31, 1717–1731. doi:10.1073/pnas.1315438110

Kennedy, E.M., Bogerd, H.P., Kornepati, A.V.R., Kang, D., Ghoshal, D., Marshall, J.B., Poling, B.C., Tsai, K., Gokhale, N.S., Horner, S.M., Cullen, B.R., 2016. Posttranscriptional m6A editing of HIV-1 mRNAs enhances viral gene expression. Cell Host Microbe 19, 675–685. doi:10.1016/j.chom.2016.04.002

Kim, J., Guan, K.-L., 2018. mTOR as a central hub of nutrient signalling and cell growth. Nature Cell Biology 1–9. doi:10.1038/s41556-018-0205-1

Kim, J., Kundu, M., Viollet, B., Guan, K.-L., 2011. AMPK and mTOR regulate autophagy through direct phosphorylation of Ulk1. Nature Cell Biology 13, 132–141. doi:10.1038/ncb2152

Kim, K.M., Cho, H., Choi, K., Kim, J., Kim, B.W., Ko, Y.G., Jang, S.K., Kim, Y.K., 2009. A new MIF4G domain-containing protein, CTIF, directs nuclear cap-binding protein CBP80/20-dependent translation. Genes & Development 23, 2033–2045. doi:10.1101/gad.1823409

Kobayashi, M., Wilson, A.C., Chao, M.V., Mohr, I., 2012. Control of viral latency in neurons by axonal mTOR signaling and the 4E-BP translation repressor. Genes & Development 26, 1527–1532. doi:10.1101/gad.190157.112

Koopal, S., Furuhjelm, J.H., Järviluoma, A., Jäämaa, S., Pyakurel, P., Pussinen, C., Wirzenius, M., Biberfeld, P., Alitalo, K., Laiho, M., Ojala, P.M., 2007. Viral oncogene–induced DNA damage response is activated in Kaposi Sarcoma tumorigenesis. PLoS Pathogens 3, e140. doi:10.1371/journal.ppat.0030140.sg005

Kremmer, E., Sommer, P., Holzer, D., Galetsky, S.A., Molochkov, V.A., Gurtsevitch, V., Winkelmann, C., Lisner, R., Niedobitek, G., Grässer, F.A., 1999. Kaposi's Sarcoma-associated herpesvirus (human herpesvirus-8) ORF54 encodes a functional dUTPase expressed in the lytic replication cycle. Journal General Virology. 80 (Pt 5), 1305–1310. doi:10.1099/0022-1317-80-5-1305

Krug, R.M., Morgan, M.A., Shatkin, A.J., 1976. Influenza viral mRNA contains internal N6-methyladenosine and 5'-terminal 7-methylguanosine in cap structures. Journal of Virology 20, 45–53

Kuang, E., Fu, B., Liang, Q., Myoung, J., Zhu, F., 2011. Phosphorylation of Eukaryotic Translation Initiation Factor 4B (EIF4B) by Open Reading Frame 45/p90 Ribosomal S6 Kinase (ORF45/RSK) signaling axis facilitates protein translation during Kaposi Sarcoma-associated Herpesvirus (KSHV) lytic replication. Journal of Biological Chemistry 286, 41171–41182. doi:10.1074/jbc.M111.280982

Kuang, E., Tang, Q., Maul, G.G., Zhu, F., 2008. Activation of p90 Ribosomal S6 Kinase by ORF45 of Kaposi's Sarcoma-associated Herpesvirus and its role in viral lytic replication. Journal of Virology 82, 1838–1850. doi:10.1128/JVI.02119-07

Kuang, E., Wu, F., Zhu, F., 2009. Mechanism of sustained activation of Ribosomal S6 Kinase (RSK) and ERK by Kaposi Sarcoma-associated Herpesvirus ORF45:Multiprotein complexes retain active phosphorylated ERK and RSK and protect them from dephosphorylation. Journal of Biological Chemistry 284, 13958–13968. doi:10.1074/jbc.M900025200

Kudchodkar, S.B., Yu, Y., Maguire, T.G., Alwine, J.C., 2006. Human Cytomegalovirus infection alters the substrate specificities and rapamycin sensitivities of raptor- and rictor-containing complexes. Proceedings of the Nationl Academy of Sciences USA 103, 14182–14187. doi:10.1073/pnas.0605825103

Kudchodkar, S.B., Yu, Y., Maguire, T.G., Alwine, J.C., 2004. Human Cytomegalovirus infection induces rapamycin-insensitive phosphorylation of downstream effectors of mTOR kinase. Journal of Virology 78, 11030–11039. doi:10.1128/JVI.78.20.11030-11039.2004

Kwong, A.D., Frenkel, N., 1987. Herpes simplex virus-infected cells contain a function(s) that destabilizes both host and viral mRNAs. Proceedings of the National Academy of Sciences 84, 1926–1930.

Kwun, H.J., Toptan, T., Ramos da Silva, S., Atkins, J.F., Moore, P.S., Chang, Y., 2014. Human DNA tumor viruses generate alternative reading frame proteins through repeat sequence recoding. Proceedings of the National Academy of Sciences 111, E4342–E4349. doi:10.1093/hmg/dds036

Lahr, R.M., Fonseca, B.D., Ciotti, G.E., Al-Ashtal, H.A., Jia, J.-J., Niklaus, M.R., Blagden, S.P., Alain, T., Berman, A.J., 2017. La-related protein 1 (LARP1) binds the mRNA cap, blocking eIF4F assembly on TOP mRNAs. eLife 6. doi:10.7554/eLife.24146

Landon, A.L., Muniandy, P.A., Shetty, A.C., Lehrmann, E., Volpon, L., Houng, S., Zhang, Y., Dai, B., Peroutka, R., Mazan-Mamczarz, K., Steinhardt, J., Mahurkar, A., Becker, K.G., Borden, K.L., Gartenhaus, R.B., 2014. MNKs act as a regulatory switch for eIF4E1 and eIF4E3 driven mRNA translation in DLBCL. Nature Communications 5, 1–15. doi:10.1038/ncomms6413

Laplante, M., Sabatini, D.M., 2009. mTOR signaling at a glance. Journal of Cell Science 122, 3589–3594. doi:10.1242/jcs.051011

Larralde, O., Smith, R.W.P., Wilkie, G.S., Malik, P., Gray, N.K., Clements, J.B., 2006. Direct Stimulation of Translation by the Multifunctional Herpesvirus ICP27 Protein. Journal of Virology 80, 1588–1591. doi:10.1128/JVI.80.3.1588-1591.2006

Lee, A.S.Y., Kranzusch, P.J., Cate, J.H.D., 2015. eIF3 targets cell-proliferation messenger RNAs for translational activation or repression. Nature 522, 111–114. doi:10.1038/nature14267

Lee, A.S.Y., Kranzusch, P.J., Doudna, J.A., Cate, J.H.D., 2016. eIF3d is an mRNA cap-binding protein that is required for specialized translation initiation. Nature 1–16. doi:10.1038/nature18954

Lee, B.S., Lee, S.H., Feng, P., Chang, H., Cho, N.H., Jung, J.U., 2005. Characterization of the Kaposi's Sarcoma-associated Herpesvirus K1 signalosome. Journal of Virology 79, 12173–12184. doi:10.1128/JVI.79.19.12173-12184.2005

Lee, J.-S., Li, Q., Lee, J.-Y., Lee, S.H., Jeong, J.H., Lee, H.-R., Chang, H., Zhou, F.-C., Gao, S.-J., Liang, C., Jung, J.U., 2009. FLIP-mediated autophagy regulation in cell death control. Nature Cell Biology 11, 1355–1362. doi:10.1038/ncb1980

Lee, S.H., McCormick, F., 2006. p97/DAP5 is a ribosome-associated factor that facilitates protein synthesis and cell proliferation by modulating the synthesis of cell cycle proteins. The EMBO Journal 25, 4008–4019. doi:10.1038/sj.emboj.7601268

Leidal, A.M., Cyr, D.P., Hill, R.J., Lee, P.W.K., McCormick, C., 2012. Subversion of autophagy by Kaposi's Sarcoma-associated Herpesvirus impairs oncogene-induced senescence. Cell Host Microbe 11, 167–180. doi:10.1016/j.chom.2012.01.005

Lejeune, F., Ranganathan, A.C., Maquat, L.E., 2004. eIF4G is required for the pioneer round of translation in mammalian cells. Nature Structural & Molecular Biology 11, 992–1000. doi:10.1038/sj.cdd.4400750

Lenarcic, E.M., Ziehr, B., De Leon, G., Mitchell, D., Moorman, N.J., 2014. Differential role for host translation factors in host and viral protein synthesis during Human Cytomegalovirus infection. Journal of Virology 88, 1473–1483. doi:10.1128/JVI.02321-13

Lenarcic, E.M., Ziehr, B.J., Moorman, N.J., 2015. An unbiased proteomics approach to identify human cytomegalovirus RNA-associated proteins. Virology 481, 13–23. doi:10.1016/j.virol.2015.02.008

Levine, B., Mizushima, N., Virgin, H.W., 2011. Autophagy in immunity and inflammation. Nature 469, 323–335. doi:10.1038/nature09782

Levy-Strumpf, N., Deiss, L.P., Berissi, H., Kimchi, A., 1997. DAP-5, a novel homolog of eukaryotic translation initiation factor 4G isolated as a putative modulator of gamma interferon-induced programmed cell death. Molecular and Cellular Biology 17, 1615–1625.

Lewis, S.M., Cerquozzi, S., Graber, T.E., Ungureanu, N.H., Andrews, M., Holcik, M., 2007. The eIF4G homolog DAP5/p97 supports the translation of select mRNAs during endoplasmic reticulum stress. Nucleic Acids Research 36, 168–178. doi:10.1093/nar/gkm1007

Li, R., Zhu, J., Xie, Z., Liao, G., Liu, J., Chen, M.-R., Hu, S., Woodard, C., Lin, J., Taverna, S.D., Desai, P., Ambinder, R.F., Hayward, G.S., Qian, J., Zhu, H., Hayward, S.D., 2011. Conserved Herpesvirus kinases target the DNA damage response pathway and TIP60 histone acetyltransferase to promote virus replication. Cell Host Microbe 10, 390–400. doi:10.1016/j.chom.2011.08.013

Li, W., Avey, D., Fu, B., Wu, J.-J., Ma, S., Liu, X., Zhu, F., 2016. Kaposi's Sarcoma-associated Herpesvirus Inhibitor of cGAS (KicGAS), encoded by ORF52, is an abundant tegument protein and is required for production of infectious progeny viruses. Journal of Virology 90, 5329–5342. doi:10.1128/JVI.02675-15

Li, X., Du, S., Avey, D., Li, Y., Zhu, F., Kuang, E., 2015. ORF45-mediated prolonged c-Fos accumulation accelerates viral transcription during the late stage of lytic replication of Kaposi's Sarcoma-associated Herpesvirus. Journal of Virology 89, 6895–6906. doi:10.1128/JVI.00274-15

Li, X., Yang, L., Chen, L.-L., 2018. The biogenesis, functions, and challenges of circular RNAs. Molecular Cell 71, 428–442. doi:10.1016/j.molcel.2018.06.034

Li, Y., Zhang, C., Chen, X., Yu, J., Wang, Y., Yang, Y., Du, M., Jin, H., Ma, Y., He, B., Cao, Y., 2011. ICP34.5 protein of Herpes Simplex Virus facilitates the initiation of protein translation by bridging eukaryotic initiation factor 2 (eIF2) and protein phosphatase 1. Journal of Biological Chemistry 286, 24785–24792. doi:10.1074/jbc.M111.232439

Liang, Q., Chang, B., Brulois, K.F., Castro, K., Min, C.K., Rodgers, M.A., Shi, M., Ge, J., Feng, P., Oh, B.H., Jung, J.U., 2013. Kaposi's Sarcoma-associated Herpesvirus K7 modulates rubicon-mediated inhibition of autophagosome maturation. Journal of Virology 87, 12499–12503. doi:10.1128/JVI.01898-13

Liang, Q., Chang, B., Lee, P., Brulois, K.F., Ge, J., Shi, M., Rodgers, M.A., Feng, P., Oh, B.-H., Liang, C., Jung, J.U., 2015. Identification of the essential role of vBcl2 for KSHV lytic replication. Journal of Virology JVI.00102–15. doi:10.1128/JVI.00102-15

Liang, Q., Fu, B., Wu, F., Li, X., Yuan, Y., Zhu, F., 2012. ORF45 of Kaposi's Sarcoma-associated Herpesvirus inhibits phosphorylation of interferon regulatory factor 7 by IKKε and TBK1 as an alternative substrate. Journal of Virology 86, 10162–10172. doi:10.1128/JVI.77.7.4221-4230.2003

Liang, Y., Chang, J., Lynch, S.J., Lukac, D.M., Ganem, D., 2002. The lytic switch protein of KSHV activates gene expression via functional interaction with RBP-Jkappa (CSL), the target of the Notch signaling pathway. Genes & Development 16, 1977–1989. doi:10.1101/gad.996502

Liberman, N., Gandin, V., Svitkin, Y.V., David, M., Virgili, G., Jaramillo, M., Holcik, M., Nagar, B., Kimchi, A., Sonenberg, N., 2015a. DAP5 associates with eIF2 and eIF4AI to promote Internal Ribosome Entry Site driven translation. Nucleic Acids Research 43, 3764–3775. doi:10.1093/nar/gkv205

Liberman, N., Gandin, V., Svitkin, Y.V., David, M., Virgili, G., Jaramillo, M., Holcik, M., Nagar, B., Kimchi, A., Sonenberg, N., 2015b. DAP5 associates with eIF2β and eIF4AI to promote Internal Ribosome Entry Site driven translation. Nucleic Acids Research 43, 3764–3775. doi:10.1038/nrm3083

Lin, S., Choe, J., Du, P., Triboulet, R., Gregory, R.I., 2016. A methyltransferase METTL3 promotes translation in human cancer cells. Molecular Cell 62, 335–345. doi:10.1016/j.molcel.2016.03.021

Lin, Y.-T., Sullivan, C.S., 2011. Expanding the role of Drosha to the regulation of viral gene expression. Proceedings of the National Academy of Sciences 108, 11229–11234. doi:10.1073/pnas.1105799108

Liu, J., Yue, Y., Han, D., Wang, X., Fu, Y., Zhang, L., Jia, G., Yu, M., Lu, Z., Deng, X., Dai, Q., Chen, W., He, C., 2013. A METTLE–METTL4 complex mediates mammalian nuclear RNA N^6-adenosine methylation. Nature Chemical Biology 10, 93–95. doi:10.1038/nchembio.1432

Liu, L., Eby, M.T., Rathore, N., Sinha, S.K., Kumar, A., Chaudhary, P.M., 2002. The Human Herpes Virus 8-encoded Viral FLICE Inhibitory Protein physically associates with and persistently activates the IκB Kinase complex. Journal of Biological Chemistry 277, 13745–13751. doi:10.1074/jbc.M008356200

Low, W., Harries, M., Ye, H., Du, M.Q., Boshoff, C., Collins, M., 2001. Internal Ribosome Entry Site regulates translation of Kaposi's Sarcoma-associated Herpesvirus FLICE Inhibitory Protein. Journal of Virology 75, 2938–2945. doi:10.1128/JVI.75.6.2938-2945.2001

Lukac, D.M., Renne, R., Kirshner, J.R., Ganem, D., 1998. Reactivation of Kaposi's Sarcoma-associated herpesvirus infection from latency by expression of the ORF 50 transactivator, a homolog of the EBV R protein. Virology 252, 304–312. doi:10.1006/viro.1998.9486

Ma, L., Chen, Z., Erdjument-Bromage, H., Tempst, P., Pandolfi, P.P., 2005. Phosphorylation and functional inactivation of TSC2 by Erk. Cell 121, 179–193. doi:10.1016/j.cell.2005.02.031

Ma, Z., Jacobs, S.R., West, J.A., Stopford, C., Zhang, Z., Davis, Z., Barber, G.N., Glaunsinger, B.A., Dittmer, D.P., Damania, B., 2015. Modulation of the cGAS-STING DNA sensing pathway by gammaherpesviruses. Proceedings of the National Academy of Sciences 112, E4306–E4315. doi:10.1038/ni.1932

Majerciak, V., Pripuzova, N., Chan, C., Temkin, N., Specht, S.I., Zheng, Z.-M., 2015. Stability of Structured Kaposi's Sarcoma-associated Herpesvirus ORF57 protein is regulated by protein phosphorylation and homodimerization. Journal of Virology 89, 3256–3274. doi:10.1128/mBio.00268-10

Malik, P., Clements, J.B., 2004. Protein kinase CK2 phosphorylation regulates the interaction of Kaposi's Sarcoma-associated herpesvirus regulatory protein ORF57 with its multifunctional partner hnRNP K. Nucleic Acids Research 32, 5553–5569. doi:10.1093/nar/gkh876

Maquat, L.E., Tarn, W.-Y., Isken, O., 2010. The pioneer round of translation: Features and functions. Cell 142, 368–374. doi:10.1016/j.cell.2010.07.022

Marash, L., Liberman, N., Henis-Korenblit, S., Sivan, G., Reem, E., Elroy-Stein, O., Kimchi, A., 2008. DAP5 promotes cap-independent translation of Bcl-2 and CDK1 to facilitate cell survival during mitosis. Molecular Cell 30, 447–459. doi:10.1016/j.molcel.2008.03.018

Martin, D., Nguyen, Q., Molinolo, A., Gutkind, J.S., 2013. Accumulation of dephosphorylated 4EBP after mTOR inhibition with rapamycin is sufficient to disrupt paracrine transformation by the KSHV vGPCR oncogene. Oncogene 1–8. doi:10.1038/onc.2013.193

Martin, D.F., Kuppermann, B.D., Wolitz, R.A., Palestine, A.G., Li, H., Robinson, C.A., 1999. Oral ganciclovir for patients with cytomegalovirus retinitis treated with a ganciclovir implant. Roche Ganciclovir Study Group. New England Journal of Medicine 340, 1063–1070. doi:10.1056/NEJM199904083401402

Masutani, M., Sonenberg, N., Yokoyama, S., Imataka, H., 2007. Reconstitution reveals the functional core of mammalian eIF3. The EMBO Journal 26, 3373–3383. doi:10.1038/sj.emboj.7601765

McCormick, C., Ganem, D., 2005. The kaposin B protein of KSHV activates the p38/MK2 pathway and stabilizes cytokine mRNAs. Science 307, 739–741. doi:10.1126/science.1105779

McCormick, C., Khaperskyy, D.A., 2017. Translation inhibition and stress granules in the antiviral immune response. Nature Reviews Immunology 1–14. doi:10.1038/nri.2017.63

McDowell, M.E., Purushothaman, P., Rossetto, C.C., Pari, G.S., Verma, S.C., 2013. Phosphorylation of Kaposi's Sarcoma-associated Herpesvirus Processivity Factor ORF59 by a viral kinase modulates its ability to associate with RTA and oriLyt. Journal of Virology 87, 8038–8052. doi:10.1128/JVI.03460-12

McKinney, C., Perez, C., Mohr, I., 2012. Poly(A) binding protein abundance regulates eukaryotic translation initiation factor 4F assembly in human cytomegalovirus-infected cells. Proceedings of the National Academy of Sciences 109, 5627–5632. doi:10.1073/pnas.1202829109

McMahon, R., Zaborowska, I., Walsh, D., 2010. Noncytotoxic inhibition of viral infection through eIF4F-independent suppression of translation by 4EGi-1. Journal of Virology 85, 853–864. doi:10.1128/JVI.01873-10

Mehta, P., Woo, P., Venkataraman, K., Karzai, A.W., 2012. Ribosome purification approaches for studying interactions of regulatory proteins and RNAs with the ribosome. Methods Mol. Biology. 905, 273–289. doi:10.1007/978-1-61779-949-5_18

Mellacheruvu, D., Wright, Z., Couzens, A.L., Lambert, J.-P., St-Denis, N.A., Li, T., Miteva, Y.V., Hauri, S., Sardiu, M.E., Low, T.Y., Halim, V.A., Bagshaw, R.D., Hubner, N.C., al-Hakim, A., Bouchard, A., Faubert, D., Fermin, D., Dunham, W.H., Goudreault, M., Lin, Z.-Y., Badillo, B.G., Pawson, T., Durocher, D., Coulombe, B., Aebersold, R., Superti-Furga, G., Colinge, J., Heck, A.J.R., Choi, H., Gstaiger, M., Mohammed, S., Cristea, I.M., Bennett, K.L., Washburn, M.P., Raught, B., Ewing, R.M., Gingras, A.-C., Nesvizhskii, A.I., 2013. The CRAPome: a contaminant repository for affinity purification–mass spectrometry data. Nature Methods 10, 730–736. doi:10.1038/nmeth.2557

Menon, S., Dibble, C.C., Talbott, G., Hoxhaj, G., Valvezan, A.J., Takahashi, H., Cantley, L.C., Manning, B.D., 2014. Spatial control of the TSC complex integrates insulin and nutrient regulation of mTORC1 at the lysosome. Cell 156, 771–785. doi:10.1016/j.cell.2013.11.049

Merrick, W.C., 2015. eIF4F: A retrospective. Journal of Biological Chemistry 290, 24091–24099. doi:10.1074/jbc.R115.675280

Mesri, E.A., Feitelson, M.A., Münger, K., 2014. Human viral oncogenesis: A cancer hallmarks analysis. Cell Host Microbe 15, 266–282. doi:10.1016/j.chom.2014.02.011

Mettenleiter, T.C., 2002. Herpesvirus assembly and egress. Journal of Virology 76, 1537–1547. doi:10.1128/JVI.76.4.1537-1547.2002

Meyer, K.D., Patil, D.P., Zhou, J., Zinoviev, A., Skabkin, M.A., Elemento, O., Pestova, T.V., Qian, S.-B., Jaffrey, S.R., 2015. m^6A promotes cap-independent translation. Cell 1–13. doi:10.1016/j.cell.2015.10.012

Meyer, K.D., Saletore, Y., Zumbo, P., Elemento, O., Mason, C.E., Jaffrey, S.R., 2012. Comprehensive analysis of mRNA methylation reveals enrichment in 3'UTR and near stop codons. Cell 149, 1635–1646. doi:10.1016/j.cell.2012.05.003

Mi, H., Muruganujan, A., Casagrande, J.T., Thomas, P.D., 2013. Large-scale gene function analysis with the PANTHER classification system. Nature Protocols 8, 1551–1566. doi:10.1186/1471-2105-8-426

Miller, G., Rigsby, M.O., Heston, L., Grogan, E., SUN, R., Metroka, C., Levy, J.A., Gao, S.J., Chang, Y., Moore, P., 1996. Antibodies to butyrate-inducible antigens of Kaposi's Sarcoma-associated herpesvirus in patients with HIV-1 infection. New England Journal of Medicine 334, 1292–1297. doi:10.1056/NEJM199605163342003

Moerke, N.J., Aktas, H., Chen, H., Cantel, S., Reibarkh, M.Y., Fahmy, A., Gross, J.D., Degterev, A., Yuan, J., Chorev, M., Halperin, J.A., Wagner, G., 2007. Small-molecule inhibition of the interaction between the translation initiation factors eIF4E and eIF4G. Cell 128, 257–267. doi:10.1016/j.cell.2006.11.046

Moffat, J., Grueneberg, D.A., Yang, X., Kim, S.Y., Kloepfer, A.M., Hinkle, G., Piqani, B., Eisenhaure, T.M., Luo, B., Grenier, J.K., Carpenter, A.E., Foo, S.Y., Stewart, S.A., Stockwell, B.R., Hacohen, N., Hahn, W.C., Lander, E.S., Sabatini, D.M., Root, D.E., 2006. A lentiviral RNAi library for human and mouse genes applied to an arrayed viral high-content screen. Cell 124, 1283–1298. doi:10.1016/j.cell.2006.01.040

Moore, P.S., Gao, S.J., Dominguez, G., Cesarman, E., Lungu, O., Knowles, D.M., Garber, R., Pellett, P.E., McGeoch, D.J., Chang, Y., 1996. Primary characterization of a herpesvirus agent associated with Kaposi's sarcoma. Journal of Virology 70, 549–558.

Moorman, N.J., Cristea, I.M., Terhune, S.S., Rout, M.P., Chait, B.T., Shenk, T., 2008. Human Cytomegalovirus protein UL38 inhibits host cell stress responses by antagonizing the Tuberous Sclerosis Protein Complex. Cell Host Microbe 3, 253–262. doi:10.1016/j.chom.2008.03.002

Moorman, N.J., Shenk, T., 2010. Rapamycin-resistant mTORC1 kinase activity is required for Herpesvirus Replication. Journal of Virology 84, 5260–5269. doi:10.1128/JVI.02733-09

Morita, M., Ler, L.W., Fabian, M.R., Siddiqui, N., Mullin, M., Henderson, V.C., Alain, T., Fonseca, B.D., Karashchuk, G., Bennett, C.F., Kabuta, T., Higashi, S., Larsson, O., Topisirovic, I., Smith, R.J., Gingras, A.C., Sonenberg, N., 2012. A novel 4EHP-GIGYF2 translational repressor complex is essential for mammalian development. Molecular and Cellular Biology 32, 3585–3593. doi:10.1261/rna.453107

Moustafa, A., Xie, C., Kirkness, E., Biggs, W., Wong, E., Turpaz, Y., Bloom, K., Delwart, E., Nelson, K.E., Venter, J.C., Telenti, A., 2017. The blood DNA virome in 8,000 humans. PLoS Pathogens 13, e1006292. doi:10.1371/journal.ppat.1006292.s008

Muller, M., Hutin, S., Marigold, O., Li, K.H., Burlingame, A., Glaunsinger, B.A., 2015. A ribonucleoprotein complex protects the Interleukin-6 mRNA from degradation by distinct herpesviral endonucleases. PLoS Pathogens 11, e1004899. doi:10.1371/journal.ppat.1004899.s015

Mure, F., Panthu, B., Zanella-Cléon, I., Delolme, F., Manet, E., Ohlmann, T., Gruffat, H., 2018. Epstein-Barr Virus protein EB2 stimulates translation initiation of mRNAs through direct interactions with both Poly(A)-Binding Protein and Eukaryotic Initiation Factor 4G. Journal of Virology 92. doi:10.1128/JVI.01917-17

Mutlu, A.D., Cavallin, L.E., Vincent, L., Chiozzini, C., Eroles, P., Duran, E.M., Asgari, Z., Hooper, A.T., La Perle, K.M.D., Hilsher, C., Gao, S.-J., Dittmer, D.P., Rafii, S., Mesri, E.A., 2007. In vivo-restricted and reversible malignancy induced by Human Herpesvirus-8 KSHV: A cell and animal model of virally induced Kaposi's Sarcoma. Cancer Cell 11, 245–258. doi:10.1016/j.ccr.2007.01.015

Myoung, J., Ganem, D., 2011. Generation of a doxycycline-inducible KSHV producer cell line of endothelial origin: maintenance of tight latency with efficient reactivation upon induction. Journal of Virological Methods 174, 12–21. doi:10.1016/j.jviromet.2011.03.012

Nakamura, H., Lu, M., Gwack, Y., Souvlis, J., Zeichner, S.L., Jung, J.U., 2003. Global changes in Kaposi's Sarcoma-associated Virus gene expression patterns following expression of a tetracycline-Inducible Rta transactivator. Journal of Virology 77, 4205–4220. doi:10.1128/JVI.77.7.4205-4220.2003

Nealon, K., Newcomb, W.W., Pray, T.R., Craik, C.S., Brown, J.C., Kedes, D.H., 2001. Lytic replication of Kaposi's Sarcoma-associated Herpesvirus results in the formation of multiple capsid species: Isolation and molecular characterization of A, B, and C capsids from a Gammaherpesvirus. Journal of Virology 75, 2866–2878. doi:10.1128/JVI.75.6.2866-2878.2001

Nevins, T.A., Harder, Z.M., Korneluk, R.G., Holčík, M., 2003. Distinct regulation of Internal Ribosome Entry Site-mediated translation following cellular stress is mediated by apoptotic fragments of eIF4G translation initiation factor family members eIF4GI and p97/DAP5/NAT1. Journal of Biological Chemistry 278, 3572–3579. doi:10.1073/pnas.082102499

Oh, N., Kim, K.M., Cho, H., Choe, J., Kim, Y.K., 2007a. Pioneer round of translation occurs during serum starvation. Biochemical and Biophysical Research Communications 362, 145–151. doi:10.1016/j.bbrc.2007.07.169

Oh, N., Kim, K.M., Choe, J., Kim, Y.K., 2007b. Pioneer round of translation mediated by nuclear cap-binding proteins CBP80/20 occurs during prolonged hypoxia. FEBS Letters 581, 5158–5164. doi:10.1038/sj.onc.1203196

Okumura, F., Zou, W., Zhang, D.E., 2007. ISG15 modification of the eIF4E cognate 4EHP enhances cap structure-binding activity of 4EHP. Genes & Development 21, 255–260. doi:10.1101/gad.1521607

Oroskar, A.A., Read, G.S., 1989. Control of mRNA stability by the virion host shutoff function of herpes simplex virus. Journal of Virology 63, 1897–1906.

Orvedahl, A., Alexander, D., Tallóczy, Z., Sun, Q., Wei, Y., Zhang, W., Burns, D., Leib, D.A., Levine, B., 2007. HSV-1 ICP34.5 confers neurovirulence by targeting the Beclin 1 autophagy protein. Cell Host Microbe 1, 23–35. doi:10.1016/j.chom.2006.12.001

Othman, Z., Sulaiman, M.K., Willcocks, M.M., Ulryck, N., Blackbourn, D.J., Sargueil, B., Roberts, L.O., Locker, N., 2014. Functional analysis of Kaposi's Sarcoma-associated herpesvirus vFLIP expression reveals a new mode of IRES-mediated translation. RNA. doi:10.1261/rna.045328.114

Pakos Zebrucka, K., Koryga, I., Mnich, K., Ljujic, M., Samali, A., Gorman, A.M., 2016. The integrated stress response. EMBO Reports 17, 1374–1395. doi:10.15252/embr.201642195

Panda, A., Martindale, J., Gorospe, M., 2017. Polysome fractionation to analyze mRNA distribution profiles. BIO-PROTOCOL 7. doi:10.21769/BioProtoc.2126

Pantry, S., Medveczky, P., 2017. Latency, integration, and reactivation of Human Herpesvirus-6. Viruses 9, 194. doi:10.1182/blood-2017-03-775759

Papadopoulos, E., Jenni, S., Kabha, E., Takrouri, K.J., Yi, T., Salvi, N., Luna, R.E., Gavathiotis, E., Mahalingam, P., Arthanari, H., Rodriguez-Mias, R., Yefidoff-Freedman, R., Aktas, B.H., Chorev, M., Halperin, J.A., Wagner, G., 2014. Structure of the eukaryotic translation initiation factor eIF4E in complex with 4EGI-1 reveals an allosteric mechanism for dissociating eIF4G. Proceedings of the National Academy of Sciences 111, E3187–E3195. doi:10.1016/S0022-2836(02)00328-5

Papp, B., Motlagh, N., Smindak, R.J., Jang, S.J., Sharma, A., Alonso, J.D., Toth, Z., 2018. Genome-wide identification of direct RTA targets reveals key host factors for KSHV lytic reactivation. Journal of Virology. doi:10.1128/JVI.01978-18

Parra, C., Ernlund, A., Alard, A., Ruggles, K., Ueberheide, B., Schneider, R.J., 2018. A widespread alternate form of cap-dependent mRNA translation initiation. Nature Communications 1–9. doi:10.1038/s41467-018-05539-0

Patro, R., Duggal, G., Love, M.I., Irizarry, R.A., Kingsford, C., 2017. Salmon provides fast and bias-aware quantification of transcript expression. Nature Methods 14, 417–419. doi:10.1038/nmeth.4197

Pattingre, S., Pattingre, S., Tassa, A., Tassa, A., Qu, X., Qu, X., Garuti, R., Garuti, R., Liang, X.H., Liang, X.H., Mizushima, N., Mizushima, N., Packer, M., Packer, M., Schneider, M.D., Schneider, M.D., Levine, B., Levine, B., 2005a. Bcl-2 antiapoptotic proteins inhibit Beclin 1-dependent autophagy. Cell 122, 927–939. doi:10.1016/j.cell.2005.07.002

Pause, A., Belsham, G.J., Gingras, A.C., Donzé, O., Lin, T.A., Lawrence, J.C., Sonenberg, N., 1994. Insulin-dependent stimulation of protein synthesis by phosphorylation of a regulator of 5'-cap function. Nature 371, 762–767. doi:10.1038/371762a0

Perez, C., McKinney, C., Chulunbaatar, U., Mohr, I., 2010. Translational control of the abundance of Cytoplasmic Poly(A) Binding Protein in Human Cytomegalovirus-infected cells. Journal of Virology 85, 156–164. doi:10.1128/JVI.01778-10

Peter, D., Igreja, C., Weber, R., Wohlbold, L., Weiler, C., Ebertsch, L., Weichenrieder, O., Izaurralde, E., 2015. Molecular architecture of 4E-BP translational inhibitors bound to eIF4E. Molecular Cell 57, 1074–1087. doi:10.1016/j.molcel.2015.01.017

Philippe, L., Vasseur, J.-J., Debart, F., Thoreen, C.C., 2017. La-related protein 1 (LARP1) repression of TOP mRNA translation is mediated through its cap-binding domain and controlled by an adjacent regulatory region. Nucleic Acids Research. doi:10.1093/nar/gkx1237

Pietrek, M., Brinkmann, M.M., Glowacka, I., Enlund, A., Havemeier, A., Dittrich-Breiholz, O., Kracht, M., Lewitzky, M., Saksela, K., Feller, S.M., Schulz, T.F., 2010. Role of the Kaposi's Sarcoma-associated Herpesvirus K15 SH3 binding site in inflammatory signaling and B-cell activation. Journal of Virology 84, 8231–8240. doi:10.1128/JVI.01696-09

Poulin, F., Gingras, A.C., Olsen, H., Chevalier, S., Sonenberg, N., 1998. 4E-BP3, a new member of the eukaryotic initiation factor 4E-binding protein family. Journal of Biological Chemistry 273, 14002–14007.

Purushothaman, P., Thakker, S., Verma, S.C., 2015. Transcriptome analysis of Kaposi's Sarcoma-associated Herpesvirus during de novo primary infection of human B and endothelial Cells. Journal of Virology 89, 3093–3111. doi:10.1128/JVI.02507-14

Pyronnet, S., Imataka, H., Gingras, A.C., Fukunaga, R., Hunter, T., Sonenberg, N., 1999. Human eukaryotic translation initiation factor 4G (eIF4G) recruits MNK1 to phosphorylate eIF4E. The EMBO Journal 18, 270–279. doi:10.1093/emboj/18.1.270

Qin, J., Li, W., Gao, S.-J., Lu, C., 2017. KSHV microRNAs: Tricks of the devil. Trends in Microbiology 1–14. doi:10.1016/j.tim.2017.02.002

Quackenbush, J., 2002. Microarray data normalization and transformation. Nature Genet 32, 496–501. doi:10.1038/ng1032

Radkov, S.A., Kellam, P., Boshoff, C., 2000. The latent nuclear antigen of Kaposi Sarcoma-associated herpesvirus targets the retinoblastoma-E2F pathway and with the oncogene Hras transforms primary rat cells. Nature Medicine 6, 1121–1127. doi:10.1038/80459

Raine, D.A., Jeffrey, I.W., Clemens, M.J., 1998. Inhibition of the double-stranded RNA-dependent protein kinase PKR by mammalian ribosomes. FEBS Letters 436, 343–348.

Renne, R., Lagunoff, M., Zhong, W., Ganem, D., 1996a. The size and conformation of Kaposi's Sarcoma-associated herpesvirus (Human Herpesvirus 8) DNA in infected cells and virions. Journal of Virology 70, 8151–8154.

Renne, R., Zhong, W., Herndier, B., McGrath, M., Abbey A., Kedes D., Ganem, D., 1996b. Lytic growth of Kaposi's Sarcoma-associated herpesvirus (Human Herpesvirus 8) in culture. Nature Medicine 2, 342–346.

Reschke, M., Clohessy, J.G., Seitzer, N., Goldstein, D.P., Breitkopf, S.B., Schmolze, D.B., Ala, U., Asara, J.M., Beck, A.H., Pandolfi, P.P., 2013. Characterization and analysis of the composition and dynamics of the mammalian riboproteome. Cell Reports 4, 1276–1287. doi:10.1016/j.celrep.2013.08.014

Ricci, E.P., Mure, F., Gruffat, H., Decimo, D., Medina-Palazon, C., Ohlmann, T., Manet, E., 2009. Translation of intronless RNAs is strongly stimulated by the Epstein–Barr virus mRNA export factor EB2. Nucleic Acids Research 37, 4932–4943. doi:10.1128/JVI.02665-06

Richter, K.N., Revelo, N.H., Seitz, K.J., Helm, M.S., Sarkar, D., Saleeb, R.S., D'Este, E., Eberle, J., Wagner, E., Vogl, C., Lazaro, D.F., Richter, F., Coy Vergara, J., Coceano, G., Boyden, E.S., Duncan, R.R., Hell, S.W., Lauterbach, M.A., Lehnart, S.E., Moser, T., Outeiro, T., Rehling, P., Schwappach, B., Testa, I., Zapiec, B., Rizzoli, S.O., 2017. Glyoxal as an alternative fixative to formaldehyde in immunostaining and super-resolution microscopy. The EMBO Journal e201695709. doi:10.15252/embj.201695709

Ritchie, M.E., Phipson, B., Wu, D., Hu, Y., Law, C.W., Shi, W., Smyth, G.K., 2015. limma powers differential expression analyses for RNA-sequencing and microarray studies. Nucleic Acids Research 43, e47–e47. doi:10.1186/s13059-014-0465-4

Rivas, C., Thlick, A.E., Parravicini, C., Moore, P.S., Chang, Y., 2001. Kaposi's Sarcoma-associated Herpesvirus LANA2 Is a B-cell-specific latent viral protein that inhibits p53. Journal of Virology 75, 429–438. doi:10.1128/JVI.75.1.429-438.2001

Roizman, B., Whitley, R.J., 2013. An inquiry into the molecular basis of HSV latency and reactivation. Annual Review of Microbiology. 67, 355–374. doi:10.1146/annurev-micro-092412-155654

Roy, D., Roy, D., Sin, S.H., Sin, S.H., Lucas, A., Lucas, A., Venkataramanan, R., Venkataramanan, R., Wang, L., Wang, L., Eason, A., Eason, A., Chavakula, V., Chavakula, V., Hilton, I.B., Hilton, I.B., Tamburro, K.M., Tamburro, K.M., Damania, B., Damania, B., Dittmer, D.P., Dittmer, D.P., 2013. mTOR inhibitors block Kaposi Sarcoma growth by inhibiting essential autocrine growth factors and tumor angiogenesis. Cancer Research 73, 2235–2246. doi:10.1158/0008-5472.CAN-12-1851

Rubio, R.M., Depledge, D.P., Bianco, C., Thompson, L., Mohr, I., 2018. RNA m 6A modification enzymes shape innate responses to DNA by regulating interferon β. Genes & Development 32, 1472–1484. doi:10.1073/pnas.94.25.13985

Rufener, S.C., Mühlemann, O., 2013. eIF4E-bound mRNPs are substrates for nonsense-mediated mRNA decay in mammalian cells. Nature Structural & Molecular Biology 20, 710–717. doi:10.1261/rna.030247.111

Russell, R.C., Tian, Y., Yuan, H., Park, H.W., Chang, Y.-Y., Kim, J., Kim, H., Neufeld, T.P., Dillin, A., Guan, K.-L., 2013. ULK1 induces autophagy by phosphorylating Beclin-1 and activating VPS34 lipid kinase. Nature Cell Biology 15, 741–750. doi:10.1111/j.1365-2443.2008.01188.x

Russo, J.J., Bohenzky, R.A., Chien, M.C., Chen, J., Yan, M., Maddalena, D., Parry, J.P., Peruzzi, D., Edelman, I.S., Chang, Y., Moore, P.S., 1996. Nucleotide sequence of the Kaposi Sarcoma-associated herpesvirus (HHV8). Proceedings of the National Academy of Sciences USA 93, 14862–14867.

Rutkowski, A.J., Erhard, F., L'Hernault, A., Bonfert, T., Schilhabel, M., Crump, C., Rosenstiel, P., Efstathiou, S., Zimmer, R., Friedel, C.C., Dölken, L., 2015. Widespread disruption of host transcription termination in HSV-1 infection. Nature Communications 6, 7126. doi:10.1038/ncomms8126

Sadler, R., Wu, L., Forghani, B., Renne, R., Zhong, W., Herndier, B., Ganem, D., 1999. A complex translational program generates multiple novel proteins from the latently expressed kaposin (K12) locus of Kaposi's Sarcoma-associated herpesvirus. Journal of Virology 73, 5722–5730.

Said, W., Chien, K., Takeuchi, S., Tasaka, T., Asou, H., Cho, S.K., de Vos, S., Cesarman, E., Knowles, D.M., Koeffler, H.P., 1996. Kaposi's Sarcoma-associated herpesvirus (KSHV or HHV8) in primary effusion lymphoma: ultrastructural demonstration of herpesvirus in lymphoma cells. Blood 87, 4937–4943.

Sancak, Y., Peterson, T.R., Shaul, Y.D., Lindquist, R.A., Thoreen, C.C., Bar-Peled, L., Sabatini, D.M., 2008. The Rag GTPases bind raptor and mediate amino acid signaling to mTORC1. Science 320, 1496–1501. doi:10.1126/science.1157535

Sancak, Y., Sancak, Y., Bar-Peled, L., Bar-Peled, L., Zoncu, R., Zoncu, R., Markhard, A.L., Markhard, A.L., Nada, S., Nada, S., Sabatini, D.M., Sabatini, D.M., 2010. Ragulator-Rag complex targets mTORC1 to the lysosomal surface and Is necessary for its activation by amino acids. Cell 141, 290–303. doi:10.1016/j.cell.2010.02.024

Sandri-Goldin, R.M., 2011. The many roles of the highly interactive HSV protein ICP27, a key regulator of infection. Future Microbiology 6, 1261–1277. doi:10.2217/fmb.11.119

Sarbassov, D.D., Guertin, D.A., Ali, S.M., Sabatini, D.M., 2005. Phosphorylation and regulation of Akt/PKB by the rictor-mTOR complex. Science 307, 1098–1101. doi:10.1126/science.1106148

Sato, R., Kato, A., Chimura, T., Saitoh, S.-I., Shibata, T., Murakami, Y., Fukui, R., Liu, K., Zhang, Y., Arii, J., Sun-Wada, G.-H., Wada, Y., Ikenoue, T., Barber, G.N., Manabe, T., Kawaguchi, Y., Miyake, K., 2018. Combating herpesvirus encephalitis by potentiating a TLR3–mTORC2 axis. Nature Immunology 1–17. doi:10.1038/s41590-018-0203-2

Saxton, R.A., Sabatini, D.M., 2017. mTOR Signaling in Growth, Metabolism, and Disease. Cell 168, 960–976. doi:10.1016/j.cell.2017.02.004

Schindelin, J., Arganda-Carreras, I., Frise, E., Kaynig, V., Longair, M., Pietzsch, T., Preibisch, S., Rueden, C., Saalfeld, S., Schmid, B., Tinevez, J.-Y., White, D.J., Hartenstein, V., Eliceiri, K., Tomancak, P., Cardona, A., 2012. Fiji: an open-source platform for biological-image analysis. Nature Methods 9, 676–682. doi:10.1093/bioinformatics/btr390

Schleich, S., Strassburger, K., Janiesch, P.C., Koledachkina, T., Miller, K.K., Haneke, K., Cheng, Y.-S., Küchler, K., Stoecklin, G., Duncan, K.E., Teleman, A.A., 2014. DENR–MCT-1 promotes translation re-initiation downstream of uORFs to control tissue growth. Nature 512, 208–212. doi:10.1016/j.cmet.2007.11.010

Schmidt, E.K., Clavarino, G., Ceppi, M., Pierre, P., 2009. SUnSET, a nonradioactive method to monitor protein synthesis. Nature Methods 6, 275–277. doi:10.1038/nmeth.1314

Schoggins, J.W., Rice, C.M., 2011. Interferon-stimulated genes and their antiviral effector functions. Current Opinion in Virology 1, 519–525. doi:10.1016/j.coviro.2011.10.008

Sei, E., Wang, T., Hunter, O.V., Xie, Y., Conrad, N.K., 2015. HITS-CLIP analysis uncovers a link between the Kaposi's Sarcoma-associated Herpesvirus ORF57 protein and host pre-mRNA metabolism. PLoS Pathogens 11, e1004652. doi:10.1371/journal.ppat.1004652.s012

Sekiyama, N., Arthanari, H., Papadopoulos, E., Rodriguez-Mias, R.A., Wagner, G., Léger-Abraham, M., 2015. Molecular mechanism of the dual activity of 4EGI-1: Dissociating eIF4G from eIF4E but stabilizing the binding of unphosphorylated 4E-BP1. Proceedings of the National Academy of Sciences 201512118. doi:10.1073/pnas.1512118112

Seo, G.J., Yang, A., Tan, B., Kim, S., Liang, Q., Choi, Y., Yuan, W., Feng, P., Park, H.-S., Jung, J.U., 2015. Akt kinase-mediated checkpoint of cGAS DNA sensing pathway. Cell Reports 13, 440–449. doi:10.1016/j.celrep.2015.09.007

Settembre, C., Zoncu, R., Medina, D.L., Vetrini, F., Erdin, S., Erdin, S., Huynh, T., Ferron, M., Karsenty, G., Vellard, M.C., Facchinetti, V., Sabatini, D.M., Ballabio, A., 2012. A lysosome-to-nucleus signalling mechanism senses and regulates the lysosome via mTOR and TFEB. The EMBO Journal 31, 1095–1108. doi:10.1038/emboj.2012.32

Sharma, A., Yilmaz, A., Marsh, K., Cochrane, A., Boris-Lawrie, K., 2012. Thriving under stress: Selective translation of HIV-1 structural protein mRNA during Vpr-mediated impairment of eIF4E translation activity. PLoS Pathogens 8, e1002612. doi:10.1371/journal.ppat.1002612.s003

Sharma, N.R., Majerciak, V., Kruhlak, M.J., Zheng, Z.-M., 2017. KSHV inhibits stress granule formation by viral ORF57 blocking PKR activation. PLoS Pathogens 13, e1006677. doi:10.1371/journal.ppat.1006677.s008

Shatsky, I.N., Terenin, I.M., Smirnova, V.V., Andreev, D.E., 2018. Cap-independent translation: What's in a name? Trends in Biochemical Sciences 1–14. doi:10.1016/j.tibs.2018.04.011

Shin, H.J., DeCotiis, J., Giron, M., Palmeri, D., Lukac, D.M., 2013. Histone deacetylase classes I and II regulate Kaposi's Sarcoma-associated Herpesvirus reactivation. Journal of Virology 88, 1281–1292. doi:10.1074/jbc.M110.198325

Shin, Y.C., Joo, C.H., Gack, M.U., Lee, H.R., Jung, J.U., 2008. Kaposi's Sarcoma-associated Herpesvirus Viral IFN Regulatory Factor 3 stabilizes Hypoxia-Inducible Factor-1 to induce Vascular Endothelial Growth Factor expression. Cancer Research 68, 1751–1759. doi:10.1158/0008-5472.CAN-07-2766

Si, H., Robertson, E.S., 2005. Kaposi's Sarcoma-associated Herpesvirus-encoded latency-associated nuclear antigen induces chromosomal instability through inhibition of p53 function. Journal of Virology 80, 697–709. doi:10.1128/JVI.80.2.697-709.2006

Simsek, D., Tiu, G.C., Flynn, R.A., Byeon, G.W., Leppek, K., Xu, A.F., Chang, H.Y., Barna, M., 2017. The mammalian ribo-interactome reveals ribosome functional diversity and heterogeneity. Cell 169, 1051–1057.e18. doi:10.1016/j.cell.2017.05.022

Sin, S.H., Roy, D., Wang, L., Staudt, M.R., Fakhari, F.D., Patel, D.D., Henry, D., Harrington, W.J., Damania, B.A., Dittmer, D.P., 2007. Rapamycin is efficacious against primary effusion lymphoma (PEL) cell lines in vivo by inhibiting autocrine signaling. Blood 109, 2165–2173. doi:10.1182/blood-2006-06-028092

Smith, R.W.P., Anderson, R.C., Larralde, O., Smith, J.W.S., Gorgoni, B., Richardson, W.A., Malik, P., Graham, S.V., Gray, N.K., 2017. Viral and cellular mRNA-specific activators harness PABP and eIF4G to promote translation initiation downstream of cap binding. Proceedings of the National Academy of Sciences 114, 6310–6315. doi:10.1016/S0022-2836(02)00655-1

So, L., Lee, J., Palafox, M., Mallya, S., Woxland, C.G., Arguello, M., Truitt, M.L., Sonenberg, N., Ruggero, D., Fruman, D.A., 2016. The 4E-BP-eIF4E axis promotes rapamycin-sensitive growth and proliferation in lymphocytes. Science Signaling 9, ra57. doi:10.1126/scisignal.aad8463

Sodhi, A., Chaisuparat, R., Hu, J., Ramsdell, A.K., Manning, B.D., Sausville, E.A., Sawai, E.T., Molinolo, A., Gutkind, J.S., Montaner, S., 2006. The TSC2/mTOR pathway drives endothelial cell transformation induced by the Kaposi's Sarcoma-associated herpesvirus G protein-coupled receptor. Cancer Cell 10, 133–143. doi:10.1016/j.ccr.2006.05.026

Sodhi, A., Montaner, S., Patel, V., Gómez-Román, J.J., Li, Y., Sausville, E.A., Sawai, E.T., Gutkind, J.S., 2004. Akt plays a central role in sarcomagenesis induced by Kaposi's sarcoma herpesvirus-encoded G protein-coupled receptor. Proceedings of the National Academy of Sciences 101, 4821–4826. doi:10.1073/pnas.0400835101

Sokolowski, M., Scott, J.E., Heaney, R.P., Patel, A.H., Clements, J.B., 2003. Identification of Herpes Simplex Virus RNAs that interact specifically with regulatory protein ICP27 in vivo. Journal of Biological Chemistry 278, 33540–33549. doi:10.1128/JVI.74.21.9916-9927.2000

Soto-Rifo, R., Rubilar, P.S., Ohlmann, T., 2013. The DEAD-box helicase DDX3 substitutes for the cap-binding protein eIF4E to promote compartmentalized translation initiation of the HIV-1 genomic RNA. Nucleic Acids Research 41, 6286–6299. doi:10.1093/nar/16.18.8953

Soulier, J., Grollet, L., Oksenhendler, E., Cacoub, P., Cazals-Hatem, D., Babinet, P., d'Agay, M.F., Clauvel, J.P., Raphael, M., Degos, L., 1995. Kaposi's Sarcoma-associated herpesvirus-like DNA sequences in multicentric Castleman's disease. Blood 86, 1276–1280.

Speck, S.H., Ganem, D., 2010. Viral latency and its Regulation: Lessons from the gamma-Herpesviruses. Cell Host Microbe 8, 100–115. doi:10.1016/j.chom.2010.06.014

Stallone, G., Stallone, G., Schena, A., Schena, A., Infante, B., Infante, B., Di Paolo, S., Di Paolo, S., Loverre, A., Loverre, A., Maggio, G., Maggio, G., Ranieri, E., Ranieri, E., Gesualdo, L., Gesualdo, L., Schena, F.P., Schena, F.P., Grandaliano, G., Grandaliano, G., 2005. Sirolimus for Kaposi's sarcoma in renal-transplant recipients. New England Journal of Medicine 352, 1317–1323. doi:10.1056/NEJMoa042831

Strahan, R.C., McDowell-Sargent, M., Uppal, T., Purushothaman, P., Verma, S.C., 2017. KSHV encoded ORF59 modulates histone arginine methylation of the viral genome to promote viral reactivation. PLoS Pathogens 13, e1006482. doi:10.1371/journal.ppat.1006482.s001

Sun, R., Lin, S.F., Gradoville, L., Yuan, Y., Zhu, F., Miller, G., 1998. A viral gene that activates lytic cycle expression of Kaposi's Sarcoma-associated herpesvirus. Proceedings of the National Academy of Sciences 95, 10866–10871.

Sun, S., Chen, S., Liu, F., Wu, H., McHugh, J., Bergin, I.L., Gupta, A., Adams, D., Guan, J.-L., 2015. Constitutive activation of mTORC1 in endothelial cells leads to the development and progression of lymphangiosarcoma through VEGF autocrine signaling. Cancer Cell 1–16. doi:10.1016/j.ccell.2015.10.004

Suzuki, K., Bose, P., Leong-Quong, R.Y., Fujita, D.J., Riabowol, K., 2010. REAP: A two minute cell fractionation method. BMC Research Notes 3, 294. doi:10.1186/1756-0500-3-294

Swanton, C., Mann, D.J., Fleckenstein, B., Neipel, F., Peters, G., Jones, N., 1997. Herpes viral cyclin/Cdk6 complexes evade inhibition by CDK inhibitor proteins. Nature 390, 184–187. doi:10.1038/36606

Tabtieng, T., Degterev, A., Gaglia, M.M., 2018. Caspase-dependent suppression of Type I Interferon signaling promotes Kaposi's Sarcoma-associated Herpesvirus lytic replication. Journal of Virology 92. doi:10.1128/JVI.00078-18

Tagawa, T., Gao, S., Koparde, V.N., Gonzalez, M., Spouge, J.L., Serquiña, A.P., Lurain, K., Ramaswami, R., Uldrick, T.S., Yarchoan, R., Ziegelbauer, J.M., 2018. Discovery of Kaposi's sarcoma herpesvirus-encoded circular RNAs and a human antiviral circular RNA. Proceedings of the National Academy of Sciences 115, 12805–12810. doi:10.1080/15476286.2015.1128065

Tan, B., Liu, H., Zhang, S., da Silva, S.R., Zhang, L., Meng, J., Cui, X., Yuan, H., Sorel, O., Zhang, S.-W., Huang, Y., Gao, S.-J., 2017. Viral and cellular N6-methyladenosin and N6,2'-0-dimethyladenosin epitranscriptomes in the KSH life cycle. Nature Microbiology 1–17. doi:10.1038/s41564-017-0056-8

Tang, S., Patel, A., Krause, P.R., 2016. Herpes simplex virus ICP27 regulates alternative pre-mRNA polyadenylation and splicing in a sequence-dependent manner. Proceedings of the National Academy of Sciences 113, 12256–12261. doi:10.1073/pnas.1609695113

Tcherkezian, J., Cargnello, M., Romeo, Y., Huttlin, E.L., Lavoie, G., Gygi, S.P., Roux, P.P., 2014. Proteomic analysis of cap-dependent translation identifies LARP1 as a key regulator of 5'TOP mRNA translation. Genes & Development 28, 357–371. doi:10.1101/gad.231407.113

Terenin, I.M., Smirnova, V.V., Andreev, D.E., Dmitriev, S.E., Shatsky, I.N., 2016. A researcher's guide to the galaxy of IRESs. Cellular and Molecular Life Sciences 1–25. doi:10.1007/s00018-016-2409-5

Thoreen, C.C., Chantranupong, L., Keys, H.R., Wang, T., Gray, N.S., Sabatini, D.M., 2012. A unifying model for mTORC1-mediated regulation of mRNA translation. Nature 486, 109–113. doi:10.1038/nature11083

Thoreen, C.C., Kang, S.A., Chang, J.W., Liu, Q., Zhang, J., Gao, Y., Reichling, L.J., Sim, T., Sabatini, D.M., Gray, N.S., 2009. An ATP-competitive mammalian target of rapamycin inhibitor reveals rapamycin-resistant functions of mTORC1. Journal of Biological Chemistry 284, 8023–8032. doi:10.1074/jbc.M900301200

Timpano, S., Uniacke, J., 2016. Human cells cultured under physiological oxygen utilize two cap-binding proteins to recruit distinct mRNAs for translation. Journal of Biological Chemistry jbc.M116.717363. doi:10.1074/jbc.M116.717363

Ting, L., Rad, R., Gygi, S.P., Haas, W., 2011. MS3 eliminates ratio distortion in isobaric multiplexed quantitative proteomics. Nature Methods 8, 937–940. doi:10.1016/1044-0305(94)80016-2

Toczyski, D.P., Matera, A.G., Ward, D.C., Steitz, J.A., 1994. The Epstein-Barr virus (EBV) small RNA EBER1 binds and relocalizes ribosomal protein L22 in EBV-infected human B lymphocytes. Proceedings of the National Academy of Sciences 91, 3463–3467.

Tomlinson, C.C., Damania, B., 2004. The K1 protein of Kaposi's Sarcoma-associated Herpesvirus activates the Akt signaling pathway. Journal of Virology 78, 1918–1927. doi:10.1128/JVI.78.4.1918-1927.2004

Toptan, T., Abere, B., Nalesnik, M.A., Swerdlow, S.H., Ranganathan, S., Lee, N., Shair, K.H., Moore, P.S., Chang, Y., 2018. Circular DNA tumor viruses make circular RNAs. Proceedings of the National Academy of Sciences 1, 201811728. doi:10.1145/2792745.2792775

Toro-Ascuy, D., Rojas-Araya, B., García-de-Gracia, F., Rojas-Fuentes, C., Pereira-Montecinos, C., Gaete-Argel, A., Valiente-Echeverría, F., Ohlmann, T., Soto-Rifo, R., 2018. A Rev–CBP80–eIF4AI complex drives Gag synthesis from the HIV-1 unspliced mRNA. Nucleic Acids Research 46, 11539–11552. doi:10.1093/nar/gky851

Toth, Z., Papp, B., Brulois, K., Choi, Y.J., Gao, S.-J., Jung, J.U., 2016. LANA-Mediated Recruitment of host Polycomb repressive complexes onto the KSHV genome during de novo infection. PLoS Pathogens 12, e1005878. doi:10.1371/journal.ppat.1005878.s009

Toth, Z., Toth, Z., Maglinte, D.T., Maglinte, D.T., Lee, S.H., Lee, S.H., Lee, H.-R., Lee, H.-R., Wong, L.-Y., Wong, L.-Y., Brulois, K.F., Brulois, K.F., Lee, S., Lee, S., Buckley, J.D., Buckley, J.D., Laird, P.W., Laird, P.W., Marquez, V.E., Marquez, V.E., Jung, J.U., Jung, J.U., 2010. Epigenetic analysis of KSHV latent and lytic genomes. PLoS Pathogens 6, e1001013. doi:10.1371/journal.ppat.1001013.g005

Tsai, K., Courtney, D.G., Cullen, B.R., 2018. Addition of m6A to SV40 late mRNAs enhances viral structural gene expression and replication. PLoS Pathogens 14, e1006919. doi:10.1371/journal.ppat.1006919.s007

Tsukumo, Y., Alain, T., Fonseca, B.D., Nadon, R., Sonenberg, N., 2016. Translation control during prolonged mTORC1 inhibition mediated by 4E-BP3. Nature Communications 7, 1–13. doi:10.1038/ncomms11776

Unal, A., Pray, T.R., Lagunoff, M., Pennington, M.W., Ganem, D., Craik, C.S., 1997. The protease and the assembly protein of Kaposi's Sarcoma-associated herpesvirus (human herpesvirus 8). Journal of Virology 71, 7030–7038.

Uniacke, J., Holterman, C.E., Lachance, G., Franovic, A., Jacob, M.D., Fabian, M.R., Payette, J., Holcik, M., Pause, A., Lee, S., 2013. An oxygen-regulated switch in the protein synthesis machinery. Nature 486, 126–129. doi:10.1038/nature11055

Uniacke, J., Kishan Perera, J., Lachance, G., Francisco, C.B., Lee, S., 2014. Cancer cells exploit eIF4E2-directed synthesis of hypoxia response proteins to drive tumor progression. Cancer Research. doi:10.1158/0008-5472.CAN-13-2278

Van Treeck, B., Protter, D.S.W., Matheny, T., Khong, A., Link, C.D., Parker, R., 2018. RNA self-assembly contributes to stress granule formation and defining the stress granule transcriptome. Proceedings of the National Academy of Sciences 115, 2734–2739. doi:10.1038/nmeth.2019

Veeranna, R.P., Haque, M., Davis, D.A., Yang, M., Yarchoan, R., 2011. Kaposi's Sarcoma-associated Herpesvirus Latency-Associated Nuclear Antigen induction by hypoxia and Hypoxia-Inducible Factors. Journal of Virology 86, 1097–1108. doi:10.1099/0022-1317-80-1-83

Verma, D., Li, D.-J., Krueger, B., Renne, R., Swaminathan, S., 2015. Identification of the physiological gene targets of the essential lytic replicative Kaposi's Sarcoma-associated herpesvirus ORF57 protein. Journal of Virology 89, 1688–1702. doi:10.1128/JVI.02663-14

Verschuren, E.W., Jones, N., Evan, G.I., 2004. The cell cycle and how it is steered by Kaposi's Sarcoma-associated herpesvirus cyclin. Journal of General Virology 85, 1347–1361. doi:10.1099/vir.0.79812-0

Vieira, J., O'Hearn, P.M., 2004. Use of the red fluorescent protein as a marker of Kaposi's Sarcoma-associated herpesvirus lytic gene expression. Virology 325, 225–240. doi:10.1016/j.virol.2004.03.049

Vink, E.I., Lee, S., Smiley, J.R., Mohr, I., 2018. Remodeling mTORC1 Responsiveness to Amino Acids by the Herpes Simplex Virus UL46 and Us3 Gene Products Supports Replication during Nutrient Insufficiency. Journal of Virology 92. doi:10.1128/JVI.01377-18

Vink, E.I., Smiley, J.R., Mohr, I., 2017. Subversion of host responses to energy insufficiency by Us3 supports HSV-1 replication during stress. Journal of Virology JVI.00295–17. doi:10.1128/JVI.00295-17

Virgin, H.W., Latreille, P., Wamsley, P., Hallsworth, K., Weck, K.E., Dal Canto, A.J., Speck, S.H., 1997. Complete sequence and genomic analysis of murine gammaherpesvirus 68. Journal of Virology 71, 5894–5904.

Wagner, S., Herrmannová, A., Šikrová, D., Valášek, L.S., 2016. Human eIF3b and eIF3a serve as the nucleation core for the assembly of eIF3 into two interconnected modules: the yeast-like core and the octamer. Nucleic Acids Research 44, 10772–10788. doi:10.1093/nar/gkw972

Walsh, D., 2004. Phosphorylation of eIF4E by Mnk-1 enhances HSV-1 translation and replication in quiescent cells. Genes & Development 18, 660–672. doi:10.1101/gad.1185304

Walsh, D., Mohr, I., 2006. Assembly of an active translation initiation factor complex by a viral protein. Genes & Development 20, 461–472. doi:10.1101/gad.1375006

Walsh, D., Perez, C., Notary, J., Mohr, I., 2005. Regulation of the translation initiation factor eIF4F by multiple mechanisms in Human Cytomegalovirus-infected cells. Journal of Virology 79, 8057–8064. doi:10.1128/JVI.79.13.8057-8064.2005

Wang, H.-W., Trotter, M.W.B., Lagos, D., Bourboulia, D., Henderson, S., Mäkinen, T., Elliman, S., Flanagan, A.M., Alitalo, K., Boshoff, C., 2004. Kaposi sarcoma herpesvirus–induced cellular reprogramming contributes to the lymphatic endothelial gene expression in Kaposi sarcoma. Nature Genetics 36, 687–693. doi:10.1007/BF02289565

Wang, L., Damania, B., 2008. Kaposi's Sarcoma-associated Herpesvirus confers a survival advantage to endothelial cells. Cancer Research 68, 4640–4648. doi:10.1158/0008-5472.CAN-07-5988

Wang, X., Lu, Z., Gomez, A., Hon, G.C., Yue, Y., Han, D., Fu, Y., Parisien, M., Dai, Q., Jia, G., Ren, B., Pan, T., He, C., 2013. N6-methyladenosine-dependent regulation of messenger RNA stability. Nature 505, 117–120. doi:10.1007/978-1-59745-033-1_8

Wang, X., Zhao, B.S., Roundtree, I.A., Lu, Z., Han, D., Ma, H., Weng, X., Chen, K., Shi, H., He, C., 2015. N6-methyladenosine modulates messenger RNA translation efficiency. Cell 161, 1388–1399. doi:10.1016/j.cell.2015.05.014

Weekes, M.P., Tomasec, P., Huttlin, E.L., Fielding, C.A., Nusinow, D., Stanton, R.J., Wang, E.C.Y., Aicheler, R., Murrell, I., Wilkinson, G.W.G., Lehner, P.J., Gygi, S.P., 2014. Quantitative Temporal Viromics: An approach to investigate host-pathogen interaction. Cell 157, 1460–1472. doi:10.1016/j.cell.2014.04.028

Welsch, S., Miller, S., Romero-Brey, I., Merz, A., Bleck, C.K.E., Walther, P., Fuller, S.D., Antony, C., Krijnse-Locker, J., Bartenschlager, R., 2009. Composition and three-dimensional architecture of the Dengue Virus replication and assembly sites. Cell Host Microbe 5, 365–375. doi:10.1016/j.chom.2009.03.007

Winkler, R., Gillis, E., Lasman, L., Safra, M., Geula, S., Soyris, C., Nachshon, A., Tai-Schmiedel, J., Friedman, N., Le-Trilling, V.T.K., Trilling, M., Mandelboim, M., Hanna, J.H., Schwartz, S., Stern-Ginossar, N., 2018. A modification controls the innate immune response to infection by targeting type I interferons. Nature Immunology 1–15. doi:10.1038/s41590-018-0275-z

Wu, J.-J., Li, W., Shao, Y., Avey, D., Fu, B., Gillen, J., Hand, T., Ma, S., Liu, X., Miley, W., Konrad, A., Neipel, F., Stürzl, M., Whitby, D., Li, H., Zhu, F., 2015. Inhibition of cGAS DNA Sensing by a Herpesvirus Virion Protein. Cell Host Microbe 18, 333–344. doi:10.1016/j.chom.2015.07.015

Wyant, G.A., Abu-Remaileh, M., Frenkel, E.M., Laqtom, N.N., Dharamdasani, V., Lewis, C.A., Chan, S.H., Heinze, I., Ori, A., Sabatini, D.M., 2018. NUFIP1 is a ribosome receptor for starvation-induced ribophagy. Science 360, 751–758. doi:10.1093/nar/gks1262

Yamashita, R., Suzuki, Y., Takeuchi, N., Wakaguri, H., Ueda, T., Sugano, S., Nakai, K., 2008. Comprehensive detection of human terminal oligo-pyrimidine (TOP) genes and analysis of their characteristics. Nucleic Acids Research 36, 3707–3715. doi:10.1074/jbc.M310574200

Yang, F., Shen, Y., Camp, D.G., Smith, R.D., 2012. High-pH reversed-phase chromatography with fraction concatenation for 2D proteomic analysis. Expert Review of Proteomics 9, 129–134. doi:10.1586/epr.12.15

Yang, X., Yang, Y., Sun, B.-F., Chen, Y.-S., Xu, J.-W., Lai, W.-Y., Li, A., Wang, X., Bhattarai, D.P., Xiao, W., Sun, H.-Y., Zhu, Q., Ma, H.-L., Adhikari, S., Sun, M., Hao, Y.-J., Zhang, B., Huang, C.-M., Huang, N., Jiang, G.-B., Zhao, Y.-L., Wang, H.-L., Sun, Y.-P., Yang, Y.-G., 2017. 5-methylcytosine promotes mRNA export — NSUN2 as the methyltransferase and ALYREF as an m5C reader. Cell Research 27, 606–625. doi:10.1038/cr.2017.55

Yang, Y., Fan, X., Mao, M., Song, X., Wu, P., Zhang, Y., Jin, Y., Yang, Y., Chen, L.-L., Wang, Y., Wong, C.C., Xiao, X., Wang, Z., 2017. Extensive translation of circular RNAs driven by N6-methyladenosine. Nature 27, 626–641. doi:10.1038/cr.2017.31

Ye, F., Chen, E.R., Nilsen, T.W., 2017. Kaposi's Sarcoma-associated Herpesvirus utilizes and manipulates RNA N6-adenosine methylation to promote lytic replication. Journal of Virology 91, JVI.00466–17. doi:10.1128/JVI.00466-17

Ye, L., Lee, J., Xu, L., Mohammed, A.-U.-R., Li, W., Hale, J.S., Tan, W.G., Wu, T., Davis, C.W., Ahmed, R., Araki, K., 2017. mTOR promotes anti-viral humoral immunity by differentially regulating CD4 helper T cell and B cell responses. Journal of Virology 91, e01653–16. doi:10.1128/JVI.01653-16

Yoo, S.-M., Ahn, A.-K., Seo, T., Hong, H.B., Chung, M.-A., Jung, S.-D., Cho, H., Lee, M.-S., 2008. Centrifugal enhancement of Kaposi's Sarcoma-associated virus infection of human endothelial cells in vitro. Journal of Virological Methods 154, 160–166. doi:10.1016/j.jviromet.2008.07.026

Young, S.K., Wek, R.C., 2016. Upstream open reading frames differentially regulate gene-specific translation in the integrated stress response. Journal of Biological Chemistry 291, 16927–16935. doi:10.1038/nature15377

Yu, L., McPhee, C.K., Zheng, L., Mardones, G.A., Rong, Y., Peng, J., Mi, N., Zhao, Y., Liu, Z., Wan, F., Hailey, D.W., Oorschot, V., Klumperman, J., Baehrecke, E.H., Lenardo, M.J., 2011. Termination of autophagy and reformation of lysosomes regulated by mTOR. Nature 465, 942–946. doi:10.1038/nature09076

Yu, Y., Wang, S.E., Hayward, G.S., 2005. The KSHV immediate-early transcription factor RTA encodes ubiquitin E3 ligase activity that targets IRF7 for proteosome-mediated degradation. Immunity 22, 59–70. doi:10.1016/j.immuni.2004.11.011

Zachari, M., Ganley, I.G., 2017. The mammalian ULK1 complex and autophagy initiation. Essays in Biochemistry 61, 585–596. doi:10.1042/EBC20170035

Zakaria, C., Sean, P., Hoang, H.-D., Leroux, L.-P., Watson, M., Workenhe, S.T., Hearnden, J., Pearl, D., Truong, V.T., Robichaud, N., Yanagiya, A., Tahmasebi, S., Jafarnejad, S.M., Jia, J.-J., Pelin, A., Diallo, J.-S., Le Boeuf, F., Bell, J.C., Mossman, K.L., Graber, T.E., Jaramillo, M., Sonenberg, N., Alain, T., 2018. Active-site mTOR inhibitors augment HSV1-dICP0 infection in cancer cells via dysregulated eIF4E/4E-BP axis. PLoS Pathogens 14, e1007264. doi:10.1371/journal.ppat.1007264.s006

Zhang, Y., Duc, A.-C.E., Rao, S., Sun, X.-L., Bilbee, A.N., Rhodes, M., Li, Q., Kappes, D.J., Rhodes, J., Wiest, D.L., 2013. Control of hematopoietic stem cell emergence by antagonistic functions of ribosomal protein paralogs. Developmental Cell 24, 411–425. doi:10.1016/j.devcel.2013.01.018

Zhang, Y., Wang, X., Zhang, X., Wang, J., Ma, Y., Zhang, L., Cao, X., 2018. RNA-binding protein YTHDF3 suppresses interferon-dependent antiviral responses by promoting FOXO3 translation. Proceedings of the National Academy of Sciences 18, 201812536. doi:10.1038/nature16998

Zhang, Z., Chen, W., Sanders, M.K., Brulois, K.F., Dittmer, D.P., Damania, B., 2016. The K1 protein of Kaposi's Sarcoma-associated Herpesvirus augments viral lytic replication. Journal of Virology 90, 7657–7666. doi:10.1128/JVI.03102-15

Zhao, Q., Liang, D., Sun, R., Jia, B., Xia, T., Xiao, H., Lan, K., 2015. Kaposi's Sarcoma-associated herpesvirus-encoded replication and transcription activator impairs innate immunity via ubiquitin-mediated degradation of myeloid differentiation factor 88. Journal of Virology 89, 415–427. doi:10.1128/JVI.02591-14

Zhao, Y., Ye, X., Dunker, W., Song, Y., Karijolich, J., 2018. RIG-I like receptor sensing of host RNAs facilitates the cell-intrinsic immune response to KSHV infection. Nature Communications 1–14. doi:10.1038/s41467-018-07314-7

Zheng, G., Dahl, J.A., Niu, Y., Fedorcsak, P., Huang, C.-M., Li, C.J., Vågbø, C.B., Shi, Y., Wang, W.-L., Song, S.-H., Lu, Z., Bosmans, R.P.G., Dai, Q., Hao, Y.-J., Yang, X., Zhao, W.-M., Tong, W.-M., Wang, X.-J., Bogdan, F., Furu, K., Fu, Y., Jia, G., Zhao, X., Liu, J., Krokan, H.E., Klungland, A., Yang, Y.-G., He, C., 2013. ALKBH5 is a mammalian RNA demethylase that impacts RNA metabolism and mouse fertility. Molecular Cell 49, 18–29. doi:10.1016/j.molcel.2012.10.015

Zhi, Y., Sandri-Goldin, R.M., 1999. Analysis of the phosphorylation sites of herpes simplex virus type 1 regulatory protein ICP27. Journal of Virology 73, 3246–3257.

Zhong, W., Wang, H., Herndier, B., Ganem, D., 1996. Restricted expression of Kaposi Sarcoma-associated herpesvirus (human herpesvirus 8) genes in Kaposi sarcoma. Proceedings of the National Academy of Sciences 93, 6641–6646.

Zhou, J., Wan, J., Shu, X.E., Mao, Y., Liu, X.-M., Yuan, X., Zhang, X., Hess, M.E., Brüning, J.C., Qian, S.-B., 2018. N6-methyladenosine guides mRNA alternative translation during integrated stress response. Molecular Cell 69, 636–647.e7. doi:10.1016/j.molcel.2018.01.019

Zhou, X., Liao, Q., Ricciardi, R.P., Peng, C., Chen, X., 2010. Kaposi's Sarcoma-associated Herpesvirus processivity factor-8 dimerizes in cytoplasm before being translocated to the nucleus. Biochemical and Biophysical Research Communications 397, 520–525. doi:10.1016/j.bbrc.2010.05.147

Zhu, F.X., Chong, J.M., Wu, L., Yuan, Y., 2004. Virion proteins of Kaposi's Sarcoma-associated Herpesvirus. Journal of Virology 79, 800–811. doi:10.1128/JVI.79.2.800-811.2005

Zhu, F.X., King, S.M., Smith, E.J., Levy, D.E., Yuan, Y., 2002. A Kaposi's Sarcoma-associated herpesviral protein inhibits virus-mediated induction of type I interferon by blocking IRF-7 phosphorylation and nuclear accumulation. Proceedings of the National Academy of Sciences 99, 5573–5578. doi:10.1073/pnas.082420599

Zhu, S., Romano, P.R., Wek, R.C., 1997. Ribosome targeting of PKR is mediated by two double-stranded RNA-binding domains and facilitates in vivo phosphorylation of eukaryotic initiation factor-2. Journal of Biological Chemistry 272, 14434–14441.

Zuberek, J., Kubacka, D., Jablonowska, A., Jemielity, J., Stepinski, J., Sonenberg, N., Darzynkiewicz, E., 2007. Weak binding affinity of human 4EHP for mRNA cap analogs. RNA 13, 691–697. doi:10.1261/rna.453107